YASHAVANTHI NIRANJAN

Functional Characterization of the Kinase and Pseudokinase Domains in the Janus Tyrosine Kinase (JAK) 2

ACADEMIC DISSERTATION
To be presented, with the permission of
the Board of the BioMediTech of the University of Tampere,
for public discussion in the Auditorium of Finn-Medi 5,
Biokatu 12, Tampere, on April 25th, 2014, at 12 o'clock.

UNIVERSITY OF TAMPERE

YASHAVANTHI NIRANJAN

Functional Characterization of the Kinase and Pseudokinase Domains in the Janus Tyrosine Kinase (JAK) 2

Acta Universitatis Tamperensis 1922
Tampere University Press
Tampere 2014

UNIVERSITY
OF TAMPERE

ACADEMIC DISSERTATION
University of Tampere, BioMediTech
Finland

Supervised by
Professor Olli Silvennoinen
University of Tampere
Finland

Reviewed by
Professor Gerhard Müller-Newen
Universitätsklinirum der RWTH Aachen
Germany
Professor Jari Yli-Kauhaluoma
University of Helsinki
Finland

Cover design by
Mikko Reinikka

Distributor:
kirjamyynti@juvenes.fi
http://granum.uta.fi

Acta Universitatis Tamperensis 1922
ISBN 978-951-44-9416-1 (print)
ISSN-L 1455-1616
ISSN 1455-1616

Acta Electronica Universitatis Tamperensis 1406
ISBN 978-951-44-9417-8 (pdf)
ISSN 1456-954X
http://tampub.uta.fi

Suomen Yliopistopaino Oy – Juvenes Print
Tampere 2014

This thesis is dedicated to my grandparents, beloved parents and my little sister

उत्साहो बलवानर्य नास्त्युत्साहात्परं बलम् |

सोत्साहस्य च लोकेषु न किञ्चिदपि दुर्लभम् ||

Nothing is unachievable for a person with enthusiasm and commitment

TABLE OF CONTENTS

1. LIST OF ORIGINAL COMMUNICATIONS

This thesis is based on the following Articles, which are referred to by their roman numerals I-III in the text.

I. Ungureanu D, Wu J, Pekkala T, **Niranjan Y**, Young C, Johnson ON, Xu CF, Neubert TA, Skoda RC, Hubbard SR and Silvennoinen O. The pseudokinase domain of JAK2 is a dual-specificity protein kinase that negatively regulates cytokine signaling. Nat Struct Mol Biol. 2011 Aug 14;18(9):971-6.

II. **Niranjan Y**, Ungureanu D, Hammarén H, Sanz-Sanz A, Westphal AH, Borst JW, Silvennoinen O, Hilhorst R. Analysis of steady-state Förster resonance energy transfer data by avoiding pitfalls: interaction of JAK2 tyrosine kinase with N-methylanthraniloyl nucleotides, Analytical Biochemistry, Vol 442, Issue 2, 213-222 (2013).

III. Sanz-Sanz A#, **Niranjan Y**#, Hammarén H , Ungureanu D, Ruijtenbeek R, Touw IP, Silvennoinen O, Hilhorst R. The JH2 domain and SH2-JH2 linker regulate JAK2 activity: a detailed kinetic analysis of wild type and V617F mutant kinase domains (submitted for publication).

#Equal contribution

2. LIST OF ABBREVIATIONS

ADP	Adenosine diphosphate
ADP-β-S	Adenosine diphosphate beta S
ALL	Acute lymphocytic leukemia
AMKL	Acute megakaryoblastic leukemia
AML	Acute myeloid leukemia
AMP	Adenosine monophosphate
AMP-PNP	Adenylyl imidodiphosphate
AT1	Angiotensin 1
ATP	Adenosine triphosphate
ATP-γ-S	Adenosine triphosphate gamma S
BCR	Breakpoint cluster region
BSF3	B-cell stimulating factor 3
CASK	Ca^{2+}/calmodulin-activated serine/threonine kinase
ch-B-ALL	Childhood B cell precussor acute lymphoblastic leukemia
CHD	Cytokine receptor homology domain
CML	Chronic myelogenous leukemia
CMN	Chronic myeloproliferative neoplasia
DTT	Dithiothreitol
EGF	Epidermal growth factor
Eph	Ephrin
EPO	Erythropoietin
ET	Essential thrombocythemia
FAK	Focal adhesion kinase
FDA	US Food and Drug Administration
FERM	Four point one, erzin, radixin, moesin
FGFR	Fibroblast growth factor
FRET	Fluorescence resonance energy transfer
GCN	General control non-derepressible
GH	Growth hormone
GM-CSF	Granulocyte macrophage colony stimulating factor
GST	Glutathione S-transferase
HA	Heme agglutinin

Haspin	Haploid germ cell-specific nuclear protein kinase
HEL	Human erythroleukemia
HER	Human epidermal growth receptor
His	Histidine
HSCs	Hematopoietic stem cells
IC50	Half maximal inhibitory concentration
IFN	Interferon
Ig	Immunoglobulin
IL	Interleukin
ILK	Integrin-linked kinase
IM	Idiopathic myelofibrosis
IPTG	Isopropyl β-D-1-thiogalactopyranoside
IRK	Insulin receptor kinase
JAK	Janus kinase
JH	Jak homology
K_a	K_m ATP
K_b	K_m peptide
K_{cat}	Catalytic constant
K_d	Equilibrium dissociation constant
kDa	Kilodalton
K_i	Inhibitory constant
K_m	Michaelis constant
KSR	Kinase suppressor of Ras 1
LB	Lineweaver-Burk
LB	Luria broth
MANT	2'/3'-*O*-(*N*-methylanthraniloyl)
MM	Michaelis-Menten
MPD	Myeloproliferative disorder
MPN	Myeloproliferative neoplasm
Ni-NTA	Nickel Nitrilotriacetic acid
NRTK	Non-receptor tyrosine kinase
PDB	Protein Data Bank
PDGFR	Platelet-derived growth factor
PH	Pleckstrin homology
PMF	Primary myelofibrosis
PRL	Prolactin

PRPK	p53-related protein kinase
PTK	Protein tyrosine kinase
PV	Polycythemia vera
RTK	Receptor tyrosine kinase
RYK	Wnt receptor tyrosine kinase
SDS-PAGE	Sodium dodecylsulphate polyacrylamide gel electrophoresis
*Sf*9	Spodoptera frugiperda 9
SH	Src homology
STAT	Signal transducer and activator of transcription
STRAD	Ste20-related adaptor proteins
TCEP	tris(2-carboxyethyl)phosphine
TPO	Thrombopoietin
TSLP	Thymic stromal lymphopoietin
TYK2	Tyrosine kinase 2
VEGFR	Vascular endothelial growth factor
VHR	Vaccinia H1-related phosphatase
V_{ini}	Initial velocity
V_{max}	Maximum velocity
WNK	With No Lysine
VRK	Vaccinia-related kinase
WT	Wild type
γ 2 A	Human fibrosarcoma

3. ABSTRACT

Hematopoiesis requires the controlled coordination of cell proliferation and differentiation through the action of soluble cytokines. The JAK/STAT signaling pathway, which is activated by cytokines, is required for hematopoietic cell development. Cytokines are involved in the growth, survival, development and differentiation of immune cells. The binding of cytokines to transmembrane cell surface receptors results in receptor oligomerization and activation of JAKs. Activated JAKs phosphorylate specific tyrosine residues on the receptor and create docking sites for STATs. STATs bind to these receptors and are phosphorylated by JAKs. Phosphorylated STATs dissociate from the receptor, dimerize and translocate to the nucleus to induce the transcription of their target genes. Thus JAKs, together with STATs, provide a rapid signaling pathway for cytokines. JAKs have a characteristic domain architecture consisting of a C-terminal catalytically active kinase domain, JH1, followed by a pseudokinase domain, JH2, whose function was, until now, unknown. The N-terminal half of the JAK protein contains the domains JH3-JH7 (collectively known as the FERM domain), which mediate the receptor-JAK interaction.

JAK2 is a critical molecule that has a significant and profound impact on mammalian development and diseases. JAK2 activity is stringently regulated at different levels in the pathway. The first level of regulation involves the interaction with SOCS (suppressors of cytokine signaling) and PTPs (protein tyrosine phosphatases). The second level of regulation includes post-translational modifications such as ubiquitination, sumoylation and phosphorylation. Thirdly, JH2 acts as a central regulator in cytokine mediated JAK2 signaling. The fourth and final level includes regulation through the involvement of the FERM domain.

The aim of this thesis study was to characterize the regulation of JAK2 at the second and third level. Phosphorylation of the activation loop is required for the catalytic activity of JAK2. This is achieved by the auto/transphosphorylation of tyrosine residues on two JAK kinases. The JH2 domain exhibits a strong sequence similarity with the neighboring JH1 kinase domain. However, certain amino acids in the JH2 domain that seem to be critical for its catalytic activity are either missing or altered. Importantly, JH2 has been found to be a hotspot for pathogenic mutations, including the $V^{617}F$ mutation, which is seen in 95% of polycythemia vera patients. The functional characterization of the JH2 domain has led to an unexpected discovery: in spite of lacking the conserved canonical residues, the JH2

domain is catalytically active and can phosphorylate two negative regulatory sites, S^{523} and Y^{570}. Thus, the JH2 domain can function as a kinase.

This thesis examined the ATP binding properties of both domains, JH1 and JH2. In spite of several studies on ATP binding, little was known about the affinity of the JAK2 domains towards ATP. Nucleotide binding was investigated with *N*-methylanthraniloyl (MANT) nucleotide analogs using fluorescence resonance energy transfer (FRET). We detected very tight binding between JH1 and the nucleotide analogs. And with further analyses with higher nucleotide concentrations we were able to determine the K_d for the binding. We describe a method for analyzing the binding parameters of any kinase-ATP combination.

The mechanism of action of JH2 domain mutants in disease pathogenesis is unknown. In order to understand the regulation of JAK2 activation, an in-depth biochemical characterization of the JAK2 kinase domains was done. Initial phosphorylation rates and the peptide substrate preferences for JH1 and JH1JH2 of JAK2 were determined using the novel platform of PamChip® peptide microarrays. We characterized the reaction mechanism of phosphorylation catalyzed by these domains using an inhibitor profiling approach. The presence of JH2 decreased JH1JH2's affinity for ATP up to ten fold. We report that the SH2-JH2 linker region participates in JAK2 inhibition by reducing its affinity for ATP. The $V^{617}F$ mutation increases the V_{max} possibly by affecting the activation loop conformation.

The results described in this thesis will help in understanding the mechanisms of regulating JAK2 activity at the molecular level and provide a functional and biochemical basis for designing strategies and methodologies for the screening and development of therapeutic compounds targeted to the ATP binding site in the JH2 domain.

4. INTRODUCTION

Signal transduction occurs when extracellular signaling molecules, such as hormones, neurotransmitters, antigens and growth factors, bind to extracellular receptors. Many of these molecules are soluble protein factors necessary for initiating signaling cascades, and are called cytokines. The signaling process transmits a signal from the cell surface receptors to specific gene promoters in the nucleus, through a series of sequential biochemical events, which further determine the physiological response. Such intracellular communication from the cell surface to the nucleus is mediated by several signaling pathways that involve protein kinases, regulatory signaling proteins and activators of transcription.

One well-defined ligand-specific cell signaling pathway is the JAK/STAT pathway. It involves various combinations of four different types of cytoplasmic tyrosine kinases called Janus Kinases (JAKs) and seven transcription factors of the Signal Transducer and Activator of Transcription (STAT) family to initiate responses in the nucleus. The binding of cytokines to their receptors is the first step in the JAK/STAT pathway. Cytokine binding leads to the oligomerization of the receptor molecule, which further sequesters JAK molecules to the cytoplasmic tail of the receptor or remains associated with the receptors followed by the transphosphorylation of JAKs. Activated JAKs then phosphorylate specific sites on the receptor, which creates docking sites for STATs, which in turn get phosphorylated, dimerize, dissociate and translocate to the nucleus to initiate the transcription of target genes. Thus JAKs, together with STATs, initiate signal transduction and induce gene expression.

Molecules in the JAK/STAT pathway are critical for the development and function of the hematopoietic system, and disturbances in this pathway lead to diseases such as autoimmune disorders, immune deficiencies, myeloproliferative disorders and cancer. In addition, gain-of-function and loss-of-function mutations are found in all of the characteristic seven JAK homology (JH) regions that each have a specific functional role. These result in the dysregulation of cytokine signaling, which can lead to oncogenesis (as seen for example in the constitutively active JAK2 bearing the $V^{617}F$ mutation) and primary immunodeficiencies (for example in JAK3 bearing $V^{722}I$, which leads to Severe combined immunodeficiency disorder).

The crystal structures of the kinase domains of all of the JAKs have been solved to date. Pseudokinases, which were thought to be 'dead' protein kinases, have

drawn considerable attention recently due to their roles in regulation. Some have even been shown to possess a catalytic activity despite the lack of one or more catalytic residues. However, the roles and mechanisms of action of the pseudokinase domains in JAKs remain a mystery. This thesis aimed to functionally characterize the kinase and pseudokinase domains of JAK2. Also, the study explored the ATP binding properties of the kinase and pseudokinase domains of JAK2, with special emphasis on their enzymatic characterization using a peptide microarray and FRET measurements.

5. REVIEW OF LITERATURE

5.1 Cytokines and the cytokine receptor family

Cytokines are a group of more than 50 soluble and secreted glycoproteins. Different cell types that mediate various cellular functions such as growth, cell proliferation and differentiation are regulated by soluble cytokines (1). The biological effects of cytokines are predominantly seen in the immune and hematopoietic systems. Immune functions such as the generation of inflammatory responses are regulated by cytokines, which provide immune responses against practically all viral and bacterial infections. In addition, homeostasis during hematopoiesis requires cytokines for the formation and differentiation of hematopoietic stem cells. Cytokines are signaling molecules which orchestrate cell-to-cell communication and function through specific transmembrane cell receptors. Cellular responses triggered upon the binding of a cytokine to its matching cell receptor are varied and diverse (2), (3). Binding of a cytokine to its cognate receptor initiates a series of intracellular signaling events that leads to modulated gene expression. This way, all the essential cellular mechanisms of hematopoiesis, embryogenesis, apoptosis, growth and differentiation are regulated by cytokines (4).

Cytokine nomenclature has been changed, improved and updated ever since interferons were described as the founding members of the cytokine family (5). After 50 years, significant studies have enhanced our understanding of cytokines and their complex functions in the cell. Initially, cytokines were classified based on their 'cell of secretion' or 'target of action' (examples include lymphokines and chemokines). However, most stringent classifications are based on either structural or functional features. Based on structural homology studies, a subfamily of cytokines are grouped as proteins (molecules) with four alpha-helix bundles. However, cytokine classification has been reviewed over several years, and advances in structurally characterizing cytokine receptors have facilitated the establishment of a seemingly well accepted classification based on three-dimensional structures.

The type I cytokine receptor family, also known as the hematopoietic growth factor family, the type II cytokine receptor family, the tumor necrosis factor (type

III) family, the IL-1 or immunoglobulin (Ig) -like receptor family and the seven transmembrane helix family are the five groups of cytokine receptors.

Members of the hematopoietic growth factor family or Type I receptor family, sometimes exemplified as interleukin receptors, possess an extracellular immunoglobulin (Ig)-like domain, a conserved extracellular region comprising of the cytokine receptor homology domain (CHD) and a fibronectin type III-like domain, a transmembrane domain and an intracellular homology domain. This family of receptors takes part exclusively in hematopoietic signaling, and the majority of these receptors aid the activation of the JAK/STAT pathway. Members of the type I family are composed of two pairs of positionally conserved cysteines, linked via disulfide bonds in the amino (N)-terminal region, and a carboxy (C)-terminal WSXWS motif within the CHD. This family is subdivided into four groups based on the receptor chains' involvement and the binding cytokine (Figure 1). Single-chain receptors form a small subgroup within Type-I receptors. Cytokines that utilize single-chain receptors include growth hormone, erythropoietin, thrombopoietin and prolactin (GH, EPO, TPO, PRL) (Yoshimura and Misawa, 1998). The second subgroup includes receptors, whose common feature is the βc receptor subunit as their signaling chain and which bind the cytokines IL-3, IL-5 and colony stimulating factor for granulocyte-macrophages (GM-CSF) (6, 7), Receptors of the third subgroup share a common γ-chain, γc and bind IL-2, IL-4, IL-7, IL-9, IL-13*, IL-15, IL-21 and thymic stromal lymphopoietin (TSLP) (8-10). Even though IL2-R consists of a βc specific to IL-2, both IL-2 and IL-15 transmit signals via a third chain, and high affinity ligand binding is mediated through this α-chain.

* IL-13 does not signal through γ_c, but through IL-4Rα and IL-13R

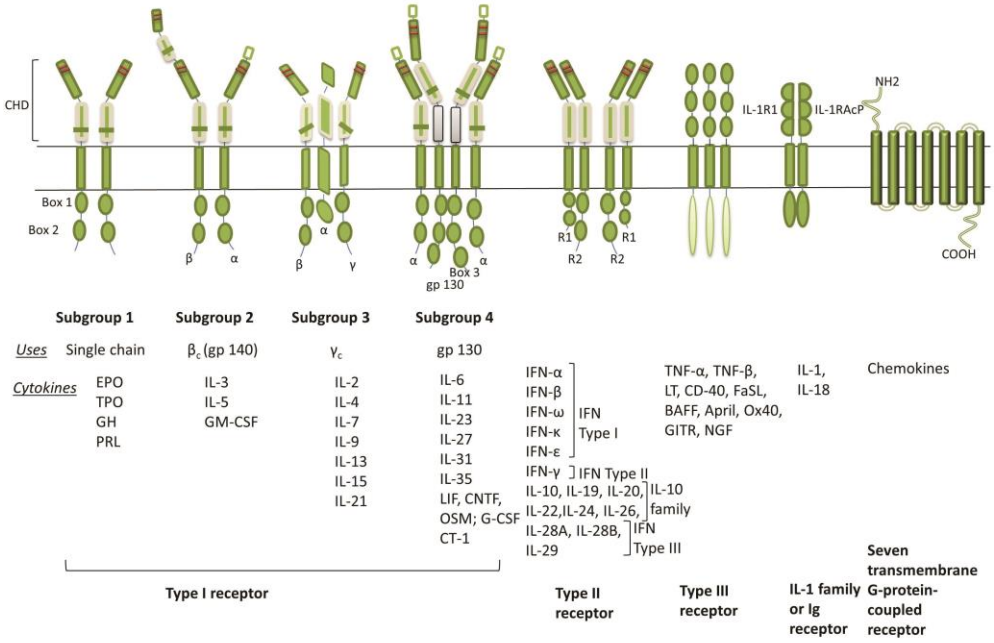

Figure 1. Five different cytokine receptor families; - Death domain, - Ig-like motif, - pair of cysteine residues, - WSXWS motif.

The type II receptor family is referred to as the interferon receptor family. Type II receptors have two extracellular domains with conserved cysteines but no WSXWS motif. Their ligands bind to only one polypeptide chain, but the signal is transduced through both chains (11). The type II family is divided into four subgroups based on the receptors' biological functions and usage: IFN type I receptors bind IFN-α, IFN-β, IFN-ω, IFN-ϰ and IFN-ε. All these ligands signal through IFNAR-1 and IFNAR-2, and exhibit their potent anti-viral activity as part of the innate and adaptive immunity. IFN-γ binds receptors of the second subgroup. It specifically utilizes IFNGR-1 and IFNGR-2 subunits and has a prominent role in protecting against mycobacterial infections in parallel with antiviral defense. The third subgroup, the IL-10 family receptors, includes IL-10 and IL-10 related receptors (IL-19, IL-20, IL-22, IL-24 and IL-26). The fourth subgroup is the IFN-λ or IL-28/29 family, which mediates signals from IL-28 A,

IL-28 B and IL-29, also known as IFN-λ2, λ3 and λ1, respectively. These cytokines transmit signals through a heterodimeric IFN-λ receptor complex composed of IFN-λR1 and the IL-10 R2 chain of the third subgroup (11-14).

The type III family is the TNF superfamily, which is the largest known family of cytokine receptors. Its cytokines include TNF-α, TNF-β, lymphotoxin (LT), nerve growth factor (NGF), B-cell activating factor (BAFF), CD 40 ligand (CD40L), OX 40 ligand (OX40L), FAS ligand (FASL), TNF-related apoptosis-inducing ligand (TRAIL), a proliferation inducing ligand (APRIL) and glucocorticoid induced TNFR-related protein(GITR). All type II receptor proteins have 1-6 cysteine-rich domains and type III receptor proteins may contain a death domain. The binding of a ligand to its receptor initiates intracellular signaling and triggers specific cellular events (cell death, NFKB activation, necroptosis) depending on the adaptor proteins involved (TRAF, TRADD) (15, 16).

The immunoglobulin (Ig) –like receptor family binds IL-1 and IL-18 cytokines, which are responsible for the activation of intracellular signaling pathways. There are more than the 10 molecules in the IL-1 family alone, which signal through IL1R1 and IL-1 receptor accessory protein (IL-1RAcP) (17). These cytokines act mainly in host defense and inflammation. IL-18 is an immune stimulatory cytokine and has a role in anti-tumor activity. Even though cytokines are many and varied, they are still able to work in a harmony, by using different signaling pathways to regulate different types of immune and hematopoietic cells. The detailed interplay between the different types of JAKs and STATs and their specific sets of cytokines is discussed in section 5.4.4 (Table 3).

The last group of the cytokine receptor family is the seven-transmembrane helix family. This family forms the most diverse group of proteins that are involved in neuronal transmission and other processes transmitted by hormones and chemokines.

5.2 Protein kinases

5.2.1 Classification

Eukaryotic protein kinases are a group of diverse enzymes, which are key regulators of cellular functions. Protein kinases play a critical role in cell signaling by catalyzing the transfer of the γ-phosphoryl group of the ATP (or GTP)

molecule to specific hydroxyl groups in serine, threonine or tyrosine containing protein substrates. This process of adding a phosphate group is called phosphorylation, and constitutes one of the major post-translational modification events involved in cell regulation. Phosphorylation affects cell stability and biological activity, and forms the basis for processes like cell differentiation, proliferation and migration. The addition of phosphate groups is balanced by group of proteins called phosphatases, which remove phosphate groups from proteins. Thus, kinases and phosphatases maintain cell function and regulation through the reversible processes of phosphorylation and dephosphorylation (18, 19).

Approximately 2% of the human genes encode the 518 known kinases, out of which 430 are predicted to be catalytically active and 48 have been classified as pseudokinases (20-22). Protein kinases are classified into two major groups based on their mechanism of substrate recognition. The serine/threonine kinases catalyze the transfer of a γ-phosphoryl group to a serine or threonine hydroxyl group on their substrate. The best examples of serine/threonine protein kinases are protein kinase A (PKA), mitogen-activated protein kinase (MAPK), protein kinase B (or Akt) and proviral integration of Moloney virus kinase (PIM).

Protein tyrosine kinases (PTKs) transfer the phosphate group only to a tyrosine hydroxyl group. The known tyrosine kinases (91 proteins) are subdivided into 59 receptor tyrosine kinases (RTKs) and 32 non-receptor tyrosine kinases (NRTKs) (23). RTKs and NRTKs both possess an intrinsic kinase (catalytic) activity. The extracellular ligand binding domain and cytoplasmic domain are connected by a single transmembrane helix. The cytoplasmic domain has a PTK core that is involved in phosphorylation events. The major RTKs are epidermal growth factor (EGF), fibroblast growth factor (FGFR), insulin receptor kinase (IRK), vascular endothelial growth factor (VEGFR), ephrin receptor (Eph), platelet-derived growth factor (PDGFR) and c-kit receptor. NRTKs exhibit structural variability compared with RTKs as they possess modular SH2/SH3 domains (Src homology domains) that facilitate the subcellular localization, or a pleckstrin homology (PH) domain that is involved in protein-lipid interactions (24, 25). In addition, they also lack transmembrane receptor-like domains and are predominantly found in the cytoplasm (26). In some cases, NRTKs are associated with the membrane through a membrane targeted amino terminal post-translational modification like palmitoylation or myristoylation. The best known examples of NRTKs are the Src family kinases (such as Yes, Fyn, Hck, Lck, Frk), Abl, Fes, ZAP-70 and JAKs (27-29). Protein kinases in *Arabidopsis thaliana*, *Saccharomyces cerevisiae*, *Caenorhabditis*

elegans, and *Dictyostelium* have also been extensively studied (20). Additionally, studies on PTKs in bacteria have provided a different understanding of their requirement in exopolysaccharide production and stress responses, contrary to the initial belief that PTKs were not present in prokaryotes (30).

5.2.2 Structural features of protein kinases

The overall structure of most protein kinases is conserved, and the first solved crystal structure of a kinase was that of the cyclic AMP-dependent kinase (cAPK or PKA) (31). All kinases maintain a balance between their active and inactive conformations, and a self-inhibitory role is known to play a crucial role in kinase activation. The Protein Data Bank (PDB) includes kinases solved in both conformations, and the structures differ from each other significantly. Nevertheless, the key structural elements that play a crucial role in activation (phosphorylation) are more or less similar.

The typical kinase fold is composed of two lobes, the amino and carboxy terminal lobes (an example of cAPK kinase lobes is shown in Figure 2), and is often referred to as the bi-lobed structure. The kinase domain has three distinct and separate roles. The first step towards phosphorylation is the binding and orientation of ATP (or GTP) along with a divalent cation (Mg^{2+} or Mn^{2+}). Secondly, the kinase binds and orientates an external protein substrate or residues within itself, and lastly transfers the phosphate group of ATP to the hydroxyl groups of the substrates. The catalytic or kinase domain is further sub-divided into twelve subdomains and, depending on the kinase family, can consist of up to 300 amino acids (22). The N-terminal lobe includes subdomains I – IV, and is composed of five β-strands, and one α-helix called the αC helix. The αC helix is primarily involved in anchoring and orienting ATP. The larger C-terminal lobe (subdomains VIa - XI) is responsible for substrate binding and phosphotransfer and is composed of α-helices. Flexibility between these two lobes is facilitated by a single polypeptide strand (the linker region) in response to substrate binding. Substrate binding leads to the transition from the open (inactive) to the closed (active) conformation (32). The deep region between these domains is the active site and this cleft is responsible for the catalysis.

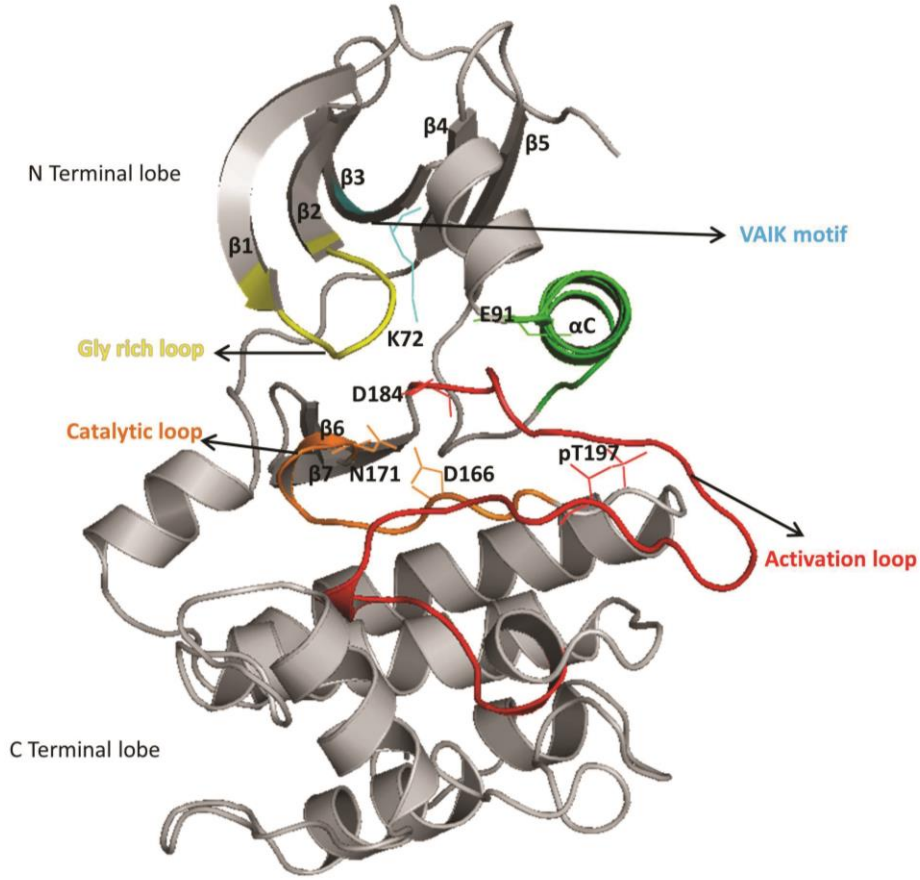

Figure 2. Structural features of a kinase are shown with an example of cAPK (or PKA) (PDB 2cpk). The kinase fold includes the N-terminal and C-terminal lobes. Conserved motifs in both lobes are depicted in the cartoon: the VAIK motif (and K^{72} in PKA) (in cyan), the αC helix (E^{91}) (in green), the glycine-rich loop between β1-β2 strands (in yellow), the catalytic loop harboring invariant the asparagine (N^{171}) that facilitates orientation of the aspartate in the HRD motif (D^{166}) (in orange), the activation loop (T^{197}) with aspartate D^{184}, the main chelator of Mg^{2+}, (in red). The other helices in the C-lobe are not shown in this cartoon.

The twelve subdomains are depicted in Figure 3 and the conserved loops/motifs in Figure 2, and their characteristic functions are explained below.

N-lobe

Glycine-rich loop (Nucleotide-binding loop) – The phosphate binding loop, or P loop, is situated between the β1 and β2 strands of subdomain I and it has a consensus sequence motif of six amino acids: GXGXϕG, where G is glycine, X is any amino acid and ϕ is phenylalanine or tyrosine. The glycine-rich loop is involved in stabilizing the transition state during a phosphotransfer reaction (33, 34).

VAI(V)K motif – Valine, alanine, isoleucine (valine) and lysine constitute this motif, which is found in the β3 strand (subdomain II) of the N-terminal lobe. The role of the lysine residue is to create an interaction between α- and β-phosphates of an ATP molecule by orienting ATP favorably. The interaction with ATP is seen only when the glutamate (E) in subdomain III (αC helix) forms a salt bridge with the lysine. The correct orienting of the αC helix is crucial for this interaction, as an inactive kinase does not project its αC helix in an angle that favors the formation of the Glu-Lys ion pair. In this way, the αC helix plays the role of mediator in all the conformational variations that take place in a kinase in its 'ON' and 'OFF' states ((35-37)).

C-lobe

The C-lobe forms the larger region of the two lobes in a kinase.

Catalytic loop – Subdomain IV and V are less important, but help in retaining the bi-lobed structure of a kinase. The catalytic loop is 10 – 12 residues long and is present in subdomain VIb, where it joins β strands 6 and 7. Although the specific role of subdomain VIa is not known, it is thought to mainly act as a support structure that is necessary for catalysis. Aspartic acid (D) residue in the conserved HRDLRXXN motif (for protein serine/threonine kinases) at the very base of the active site helps as a proton acceptor for hydroxyl groups of the substrates allowing the phosphoryl transfer to take place. The name catalytic loop comes from the obvious reason that the glutamate residue acts as a catalytic base. In some traditional kinases such as cyclin dependent kinase (CDK) 2, the second arginine (R) is substituted by a lysine (K) (HRDLKPQN) that neutralizes the negative charge of the γ-phosphate during transfer. This motif also has an invariant asparagine (N) at the end of the loop that forms a hydrogen bond with the carbonyl group of aspartate (D), and is where chelation of a secondary metal ion takes place (38, 39). The first known mutation in the HRD motif was found is in the *Drosophila melanogaster* src64 gene, where all the three amino acids in the HRD trio peptide sequence were mutated. The importance of the residues was evidenced by reduced fertility, and when the aspartate was mutated to asparagine (N) cytoskeletal processes were eliminated (40).

Activation loop – The most essential motif of the 'catalytic core' is the activation loop that resides in subdomain VII between the β strands 8 and 9. The loop has 20 – 30 residues and on one side a DFG (aspartate, phenylalanine and glycine), and on the other side a APE (alanine, phenylalanine and glutamate) motif, where APE is in subdomain VIII. The kinase is said to be active when one or more tyrosine or serine/threonine residues in this loop are phosphorylated. The most crucial step of phosphorylation is when the aspartate from the DFG motif aids in binding two divalent cations (Mg^{2+} in JAKs) and the ATP γ-phosphate is aligned for phosphotransfer. This further coordinates the β- and α-phosphates of ATP in the nucleotide binding cleft. Transformational changes occur during the transition between the active and inactive state (39, 41). Phosphorylation sites vary within kinases: in JAK2, the tyrosines at 1007 and 1008 get phosphorylated, after which JAK2 adopts a conformation favorable for binding and catalysis of its substrate. Usually the arginine in the HRD motif coordinates the γ-phosphate. The DFG motif swings away in an unphosphorylated kinase preventing the formation of the cation-ATP complex. It is believed that oligomerization or homodimerization of a kinase takes place upon the phosphorylation of critical residues in the activation loop. For example, in the mitogen-activated protein (MAP) kinase ERK2, dual phosphorylation of threonine and tyrosine residues induces conformational changes and exposes a hydrophobic surface, which favors homodimerization (42).

Other subdomains that are part of the C lobe are IX, X and XI (see Figure 3). Subdomain IX contains a DXWXXG consensus motif, and here an aspartate stabilizes the catalytic loop. Subdomains X and XI are less conserved and form the C-terminal end of the kinase domain. The glutamate in the APE motif forms an ion pair with arginine (R) in subdomain XI and stabilizes the C-lobe.

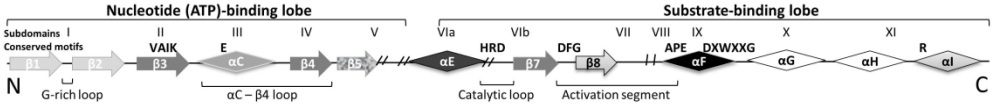

Figure 3. Twelve subdomains and catalytic residues are depicted as a linear diagram. Block arrows represent β-sheets (β1–5, β7 and β8) and diamonds represent the α-helices (αC and αE–I). β6, β9 and αD are very short and not depicted in this diagram. The image is modified from (43).

5.2.3 Common regulatory mechanisms in tyrosine kinases

Regulatory mechanisms govern the catalytic activity of a kinase. An example of an RTK and an NRTK are discussed below.

Cis/*Trans* Phosphorylation and dimerization

As discussed above, coupling of the αC helix with the activation loop provides the best conformational regulation of the catalytic activity in kinases. This is achieved through the phosphorylation steps that take place in the activation loop. The driving forces for activation are the conformational change that allow phosphorylation within the receptor and is called *cis* phosphorylation of the receptor. The other form of receptor phosphorylation is called *trans* phosphorylation, which takes place when two receptors are already aligned as a dimer (in close proximity). Ligand binding initiates this process and tyrosine residues are cross phosphorylated on both receptor chains. The best known example of a RTK is the insulin receptor kinase (IRK). However, since the IRK does not exist as monomers, left panel of Fig. 4a is of a regular RTK and tyrosines residues depicted in the right panel of Fig.4a is of IRK (see Fig.4 legend for more details). Three tyrosine residues (Y^{1158}, Y^{1162} and Y^{1163}) in the activation loop are phosphorylated in *trans* (Fig. 4a, right panel), and Y^{1162} connects with an aspartate in HRD and blocks the substrate. The DFG motif in turn blocks ATP binding. The result of this is an autoinhibited, inactive form of IRK, although not as monomers (Fig. 4a, left panel). The activation loop harboring Y^{1162} is situated in the active site and switches between active and inactive states. When Y^{1162} is engaged in the active site both the substrate- and the ATP-binding sites are inaccessible and Mg^{2+} cannot bind. Inhibition in *cis* and activation (phosphorylation) in *trans* will bring about a classic auto-inhibitory mechanism of an unphosphorylated (inactive) kinase (44).

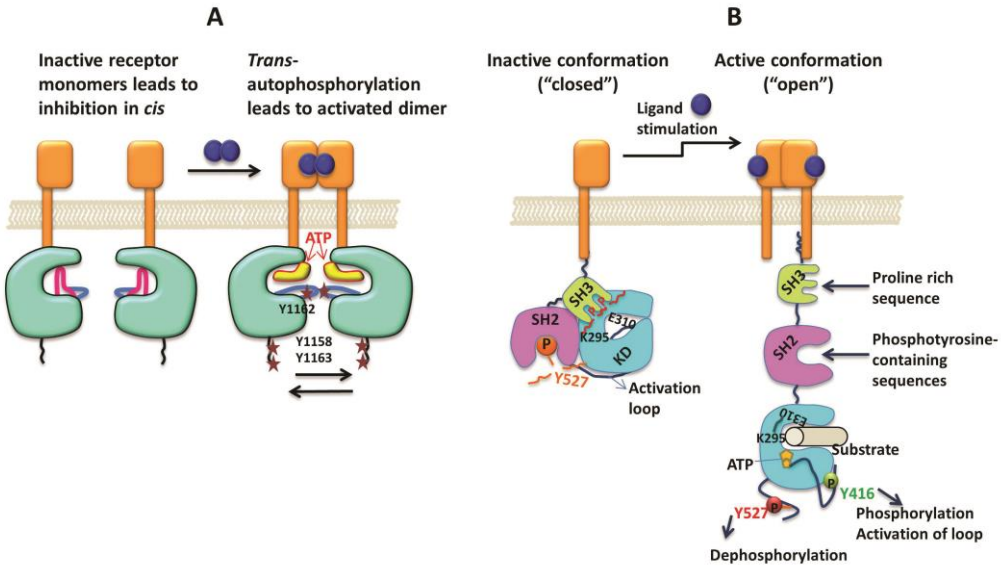

Figure 4. Regulatory mechanism of RTK and NRTK (Src) kinases: A) The left panel of the cartoon shows the cis inhibition by A-loop of RTKs. IRK is a preformed, disulfide-bridged dimer and monomers do not exist. In the picture, one of the numerous A-loop conformations in RTKs is shown. The activation loop changes its conformation and blocks binding of ATP. The right panel shows how the binding of the ligand leads to the activation of the receptor through dimerization, and leads to transphosphorylation of the tyrosine residues in the activation loop (tyrosine residues shown are with respect to the IRK). B) Regulation by the adjacent domains leads to the 'closed' and 'open' conformation of the Src kinase. In the closed conformation, the SH2 and SH3 domains interact with the kinase domain (KD) to stabilize the inactive 'closed' conformation (left panel). Dephosphorylation of an SH2 tyrosine may be an intermediate step between inactive forms. This accounts for phosphorylation of only available tyrosines in the activation loop. The C-helix is repositioned, and this leads to a formation of a hydrogen bond between glutamate-310 and lysine-295, which is required for ATP binding [modified from (41)].

In NRTKs, adjacent domains, such as SH2 and SH3, play a crucial role in phosphorylation/dephosphorylation and the kinases are subject to both intermolecular and intramolecular regulation. One such example is the Src family of tyrosine kinases. In c-Src, a polyproline sequence segment (PXXP) mediates a strong interaction between the SH2-kinase linker and the SH3 domain (Fig. 4b). The SH2 domain comes in close contact with Y^{527} in the C terminal domain, which further prompts the SH3 domain to form polyproline type II helices, by interacting with the SH2 domain, which is in contact with the C-terminal domain (45-47). This

interaction suppresses the kinase activity, because the αC helix (E^{310}) is not able to couple with the lysine in the VAIK motif (K^{295}). Since there is no room for flexibility between the lobes, the C-helix is displaced far from its active position, and ATP binding is restricted. This demonstrates that c-Src is a dynamic molecule subject to complex regulatory mechanisms. A similar interaction between adjacent domains in the phosphorylation of the kinase activation loop is seen in JAKs. This is discussed further in sections 5.4.2 and 5.4.3.

Non-requirement of phosphorylation of activation loop tyrosines

Not all tyrosine kinases follow the conventional phosphorylation/dephosphorylation followed by dimerization mechanism of regulation. Src regulatory protein kinases, such as Csk, display a different kind of regulatory behavior. The SH3-SH2 linker and the SH2-kinase linker form a hinge-like structure and make contact with the N-lobe. The αC helix orients itself in a way that it can interact with the linkers and stabilizes the activation loop. The phosphorylation step is left out, since the critical tyrosine residue is missing from the Csk activation loop (48).

5.3 Family of pseudokinases

5.3.1 History, evolution and properties of pseudokinases

The term 'pseudokinase' is loosely defined. Pseudokinases are supposed to be catalytically inactive kinases and lack at least one of the key residues required for catalysis. The whole catalytic motif or part of the motif essential for nucleotide binding and/or phosphoryl transfer activity is missing or altered. Pseudokinases were seen as the lost cousins of active protein kinases and were thought to have no signaling or regulatory function. The other commonly known term for pseudokinase is kinase-like domain, which was previously mentioned in the description of JAKs (49).

When the human kinome was systematically catalogued, a total of 50 listed kinases were found to lack catalytic residues and were assumed to have no kinase activity. This alleged lack of phosphoryl transfer activity was linked to the absence of Lys residue (in VAIK), Asp residue (in HRD) or Asp residue (in DFG) (20). Thus, this classification of 50 kinase-like proteins sums up to a surprising 10% of

518 (478 eukaryotic + 40 atypical) protein kinases (20). Pseudokinases are also conserved through metazoans, and 28 of the known pseudokinases have homologs in mouse, nematodes, worms, yeast and flies (all lack the catalytic residues).

Within the evolutionary timescale, the exact number of pseudokinases has changed, and currently 48 pseudokinases stand true. Apparently, apart from a few reports on atypical protein kinases and Manning's human kinome phylogeny, not many studies have explored these 'dead kinases' , until a comprehensive review on these 48 pseudokinases including one from an atypical protein kinase family, was published (50). In all known kinases, ATP binding has a regulatory role, and pseudokinases have probably arisen multiple times in evolution from nucleotide-binding proteins or corresponding active kinases. The pseudokinases of the human kinome are quite diverse and scattered throughout the evolutionary tree. They are present in almost all single and multi-domain protein kinase families. The phylogenetic tree of all 48 pseudokinases is shown in Figure 5. Since the sequences and structural folds of pseudokinases appear to be similar to those of classic kinases, they might have been "dead" proteins to start with or they may have once been active kinases and over successive evolution lost their activity. Based on a recent classification, all of the 48 pseudokinases, whose catalytic residues are missing or altered, can be divided mainly into 7 groups (Table 1) (50).

The properties of pseudokinases have not been distinctively reported. The classification of pseudokinases cannot be subjugated to just the absence of catalytic motifs. Each pseudokinase possesses special biochemical properties, which are worth mentioning. Several recent studies have shown that pseudokinases exhibit low levels of catalytic activity and have diverse roles in regulating signaling cascades. However, the significance and biological role of this low level activity remains a mystery. Detailed studies on structure and nucleotide binding properties revealed that in a handful of kinases, which were initially thought to be pseudokinases, missing motifs or residues were compensated for by neighboring residues. Some examples of such mis-categorised pseudokinases are the With No Lysine (WNK) family of kinases, the Haploid germ cell-specific nuclear protein kinase (Haspin) and the Human cardiac Titin kinase (more in detail in 5.3.3).

The list of kinases, which were previously thought to be pseudokinases, continues to grow with several other proteins such as the Wnt receptor tyrosine kinase (Ryk) (51) and the p53-related protein kinase (PRPK) (52). They also lack some of the critical residues required for catalysis, but these are compensated for or possess altered regulatory properties. Hence, classifying 10% of the kinome into 'pseudokinases' could be an over-statement. All the examples discussed above

deviate from the general requirements for a pseudokinase and add to the complexity of the biochemical properties that define an actual pseudokinase.

5.3.2 Structural insights into pseudokinases

In view of the accumulating evidence that supports the growing number of pseudokinases that possess a catalytic activity, some of the proteins in Table 1 can no longer be called pseudokinases. Some examples of pseudokinases which are catalytically active and whose crystal structure has been solved are discussed below.

Ca^{2+}/calmodulin-activated serine/threonine kinase (CASK) – CASK belongs to the membrane-associated guanylate kinases (MAGUK) superfamily of proteins, which are characterized by the presence of PDZ†, SH3 and GUK (or GK)‡ domains. In addition to these domains, CASK has a kinase domain called Ca^{2+}/calmodulin-dependent kinase (CaMK). Since CASK did not fulfill all the requirements for an active kinase, it was thought to be a catalytically inactive protein. For example as seen in Table 1, CASK comes under the group A, which possesses an altered DFG motif. There is a glycine residue in place of the aspartate (DFG to GFG). There is no change in just HRD motif, but when the full eight-residue motif (HRDLAXXN) is considered, CASK displays a modified version (HRDVKPHC), where the asparagine is replaced with a cysteine at the end of the motif. All other essential motifs such as the glycine-rich loop and the APE motif are intact and show no alterations.

† PDZ - Post synaptic density protein (PSD95), *Drosophila* disc large tumor suppressor (Dlg1), and zonula occludens-1 protein (zo-1)

‡ GUK - Guanylate kinase

Group	A	B	C	D	E	F	G
Missing motifs	**DFG**	**HRD**	**DFG, HRD**	**VAIK**	**DFG, VAIK**	**HRD, VAIK**	**DFG, HRD, VAIK**
Pseudo kinases	CASK	ANPα	ILK	KSR1	ULK4	GCN2	EphA10
	CCK4	ANPβ	IRAK2	KSR2	RSKL1		EPhB6
	SgK223	CYGD	MLKL		RSKL2		NRBP1
	SgK269	CYGF	SgK307				NRBP2
	SgK495	HER3	STRADβ				SCYL1
	SuRTK 106	HSER					SCYL2
	Trb1	JAK1					SCYL3
	Trb2	JAK2					SgK196
	Trb3	JAK3					SgK424
		PSKH2					Slob
		SgK071					STRADα
		SgK396					TRCK
		TYK2					TRRAP
		VACAMKL					VRK3

Table 1. Grouping of pseudokinases based on the motifs they lack [modified from (50)].

A high resolution crystal structure of CASK with a 5'-AMPPNP (and displaced with 3'-AMP) in the nucleotide-binding pocket was solved in 2008. CASK adopts a typical kinase fold, which contains five β-stranded sheets and a single α-helix, when it is in its active state. The C-terminus of the lobe demonstrates a fully ordered activation loop and a Mg^{2+} binding loop. However, the β- and γ-phosphates of ATP were found to be severly distorted, and the binding pocket cannot accommodate a Mg^{2+} ion.

This structural study was further supported by nucleotide-binding experiments, where it was shown that CASK is able to catalyze phosphotransfer without the presence of a Mg^{2+} ion. The study further elucidated that presence of Mg^{2+} hinders the catalytic activity. Another important observation is that the CASK kinase is not regulated by the auto-inhibitory helix (αR1), unlike other CaM kinases. The helix does not block the ATP-binding cleft. CASK is regulated only by the phosphorylation of its substrate protein neurexin-1 (53).

The Ste20-related adaptor (STRAD) proteins – STRADα and STRADβ are two isoforms that belong to the serine/threonine protein kinase STE20 subfamily. They are activators of the LKB1 heterotrimeric tumour suppressor complex (54). STRADs were previously recognized as catalytically active proteins (55). Further characterization has placed STRADα and STRADβ into group G and C respectively in Table 1, since crucial motifs are altered. The Lys in the VAIK motif is missing, the third glycine in the Gly-rich loop is replaced by methionine, the HRD motif is distorted as the catalytic aspartate is replaced and the DFG is entirely missing (56). Despite lacking these residues, STRADα binds ATP and activates LKB1 without the requirement of the activation loop (57). It activates LKB1 through an adaptor protein called MO25 (58).

Interestingly, STRADα acquires a typical kinase fold while adopting the conformations that may be required for phosphotransfer. A remarkable feature is that STRADα utilizes the absence of the DFG motif to its benefit by employing Gly-Leu-Arg instead to coordinate the β-phosphate of ATP so that Mg^{2+} is positioned properly. Also, the αC helix rotates itself to bridge the gap between the N-terminus and C-terminus of the helix. Studies show that on its own STRADα is inactive. It demonstrates no detectable autophosphorylation or phosphorylation of other substrates, but folds into an ATP-bound, closed conformation when the STRADα/MO25α heterodimer is formed. Since STRADα is incapable of being active; nature has made room for this allosteric 'pseudosubstrate' regulation that drives STRADα to bind ATP and activate LKB1 (56, 59).

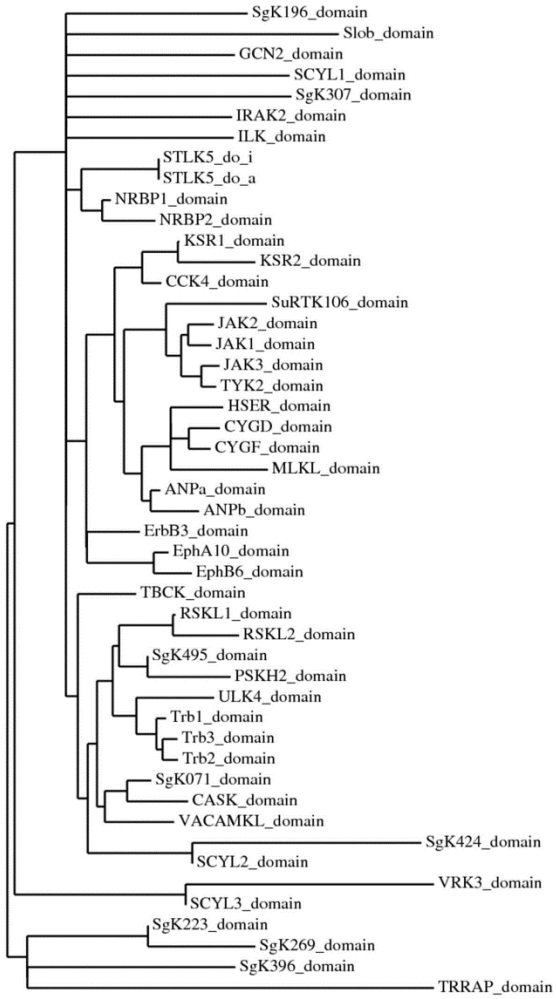

Figure 5. Phylogenetic tree of human pseudokinases generated by www.kinase.com and www.phylogeny.fr. The grouping was created using pseudokinase or kinase domain (FASTA format) sequences which were analyzed automatically using the MUSCLE software for alignment, PhyML for creating the phylogeny and TreeDyn for tree rendering as described on the web page.

Vaccinia-related kinase (VRK) 3 – VRK3 is a member of the Vaccinia-related kinase (VRK) family of serine/threonine protein kinases. The structures of both VRK3 and its close sibling VRK2 were solved recently (60). The only difference between them is that the former is a pseudokinase and the latter a *bona fide* kinase.

VRK3, similar to other pseudokinases discussed so far, lacks important residues and is placed into group G in Table 1. The second glycine in the glycine-rich loop is modified to an aspartate and the loop is severely altered TRD^{175}NQ^{177}G, the HRD motif is compromised as HGN and DFG motif is replaced by GFG. These alterations render the protein unable to bind ATP (60, 61). Q^{177} and D^{175} in the G-loop are negatively charged and mimic the ATP phosphate in the ATP binding site (otherwise seen in an ATP bound state). This gives the ATP binding pocket a double negative charge making ATP binding unfavorable. The key interactions that take place in an active site, such as hydroxyl group orientation of the substrate by the aspartate in HRD and steric clashes between ATP and the Q^{177} in G-loop, make VRK3 an 'inactive' pseudokinase. However, a fascinating feature of this protein is the formation of an intact ionic bond between αC and β3. This interaction is highly conserved and favors the formation of the kinase-like fold. It could thus act as a support base for activating the vaccinia-related H1 phosphatase (VHR) (62). Thus, VRK3 need not be an active kinase, but might play a regulatory role.

Integrin-linked kinase (ILK) – Since integrins lack an intrinsic catalytic activity, a serine/threonine protein adaptor kinase called ILK carries out the signaling reaction. Similar to other pseudokinases, ILK features structural variations in critical motifs and placed in group C. The crystal structure of ILK bound to α-parvin uncovers the reasons why ILK does not phosphorylate its substrates (63). However, there are discrepancies in this report, which states that despite the lack of a catalytic base (a lysine residue in the catalytic loop) and a cation binding residue (asparagine), ILK is capable of phosphorylating its substrates (integrin β1 CT, myosin light chain kinase LC20, β-parvin, cell survival kinase AKT/PKB, glycogen synthase kinase-3β) and is catalytically active (64-72). However, a recent study by the same group contradicts the previous report by stating that ILK is not active (73). The ATP molecule is lodged into the nucleotide binding pocket helped by substitutions from the glycine in the DFG motif, and the γ-phosphate of ATP is correctly oriented by the lysine residue. This pseudokinase also demonstrates 'pseudosubstrate' regulation similar to STRADα, as binding of α-parvin to ILK will not activate it.

5.3.3 Structural variation in non-pseudokinases

Below are some examples of kinases that were previously thought to be pseudokinases because of obvious missing or altered critical residues required for phosphotransfer activity. However, these proteins demonstrate distinctive structural variations, and this discovery has resulted in their removal from the pseudokinase family after re-classification.

With No Lysine (WNK) family of kinases – WNK kinases were first classified as pseudokinases since they lack the invariant catalytic lysine (K) residue in subdomain II (VAIK motif). However, it was shown that that a lysine in the subdomain I (K^{233}) compensated for this loss and phosphorylated WNKs exogenous substrate, myelin basic protein (74).

Haploid germ cell-specific nuclear protein kinase (Haspin) – Haspin also falls under the mis-categorized group of pseudokinases, once called ePKs due to their structural diversity uncommon to most conventional kinases (75). The crucial HRDLR/KXXN motif is altered and the conserved lysine is displaced by a histidine in subdomain VIb. Additionally, subdomains IV- XI have no consensus sequence. For example, the conserved DFG and APE motifs are missing. In spite of this lack of conservation in residues, Haspin still assumes a catalytic bi-lobed fold. Several studies have demonstrated that Haspin possess an *in vitro* catalytic activity and gets autophosphorylated through an intrinsic serine/threonine kinase activity (76).

Human cardiac titin kinase – Titin proteins are striated muscle sarcomeres that display a remarkable 'always open' conformation, as opposed to the conventional balance between 'open' and 'closed' conformations, which are controlled by the phosphorylation of conserved tyrosine/serine residues. The Y^{170} at the P + 1 position (not in the activation loop) is phosphorylated and aids in Ca^{2+}/calmodulin binding. The HRDL**K** motif is replaced by HFDI**R** and the DFG by the EFG motif. Once the catalytic base D in HRD forms a hydrogen bond with R (two residues downstream), the Q^{150} and Y^{170} active sites are blocked and no catalysis is seen. This auto-inhibited conformation maintained by titin facilitates the phosphorylation of the muscle protein telethonin, and promotes its activation in differentiating myocytes (77).

5.3.4 Determining the ATP binding characteristics and roles of pseudokinases

ATP binding and ATP catalysis are two distinct steps required to generate a catalytically active protein kinase. ATP binding is the process, where an ATP molecule is bound to the ATP binding pocket in a kinase. Catalysis, in turn, is defined by the transfer of the γ-phosphate group of the bound ATP to pre-designated tyrosine/serine-threonine residues. A pseudokinase can be a protein, which is incapable of performing either one of the above described steps.

The characteristics of ATP binding (together with catalysis) vary among the pseudokinases listed in Table 1. Quoting Zeqiraj *et al.,* they could be 'inactive pseudokinases or simply unusual active kinases' (78). There are several ways of investigating ATP binding characteristics. Though this helps in understanding the diversity in pseudokinase function, regulation and modulatory effects, uncovering the significance of the physiological role of these proteins is challenging. Yet, several studies have aimed at unraveling the mystery of pseudokinases. Differences in ATP binding can be investigated by employing some of the currently available methods. Radiolabelled [γ-^{32}P] ATP is used in kinase assays for measuring autophosphorylation (53, 56, 57, 63, 73, 79-81). An increase in activity is measured by autoradiography with or without substrates. This is a straightforward method. However, the downside of the technique is that a contaminating kinase in the pool of recombinant protein can influence the assay and thereby compromise the interpretation of the results. An alternative approach is to *in vitro* translate the domain or construct of interest and demonstrate its phosphorylation (79). But this also involves autoradiography, and demonstrating the phosphorylation of different substrates can be time-consuming.

Recently, a method based on fluorescence spectroscopy was described. It uses labeled nucleotide analogs such as TNP [2', 3' –*O*-(2, 4, 6-trinitrophenyl)] and MANT [2' (3')-*O*-(*N*-methylanthraniloyl)] to mimic ATP (53, 56, 57, 78, 79). The affinity of the nucleotide to a protein (K_d) is measured by exciting the sample at certain wavelengths and collecting the emission spectrum in a range of wavelengths. However, the K_d values for the modified analogs differ greatly from those of ATP. The modified nucleotides have been reported to bind tighter to proteins than does ATP. So although the approach can give an idea of the level of a ATP binding, it cannot be used to say how tight the binding actually is. Additionally, the method does not provide information about phosphotransfer activity to other substrates.

Kinase-affinity chromatography using immobilized ATP-mimetics, fluorescence polarization (82), isothermal titration calorimetry (ITC) (73), nuclear magnetic resonance (NMR) spectroscopy and X-ray crystallography are some of the other methods that can be used to study ATP binding. The experiments can be, however, complicated and may require large amounts of recombinant purified protein. Currently, thermodynamic methods such as the thermal shift assay (TSA), which is based on fluorescence, are being developed (60, 83, 84). In TSA the test protein, together with a nucleotide and a fluorescent dye, is subjected to thermal denaturation. The dye binds to the exposed hydrophobic residues and ligand binding to the protein enhances the melting temperature of the protein (T_m). This is seen as an increase in the thermal stability of the protein. This method is insensitive to impurities, independent of protein function, highly reproducible and provides information on protein stability. It is better to take a safe approach of characterizing proteins from a multidisciplinary angle, employing two or more methods. A recent thorough study, which covered three layers of ligand binding - a) binding of nucleotides b) binding of cations and c) binding of both nucleotides and cations revealed remarkable properties of pseudokinases (85). This study led to an altogether different classification of pseudokinases into proteins such as those (i) devoid of nucleotide/cation binding (ii) devoid of cation binding only (iii) devoid of nucleotide binding and (iv) devoid of both nucleotide and cation binding. To conclude, there is no established way of classifying pseudokinases yet, but as further studies keep revealing more about the function and features of these proteins, we will eventually be able to agree on a common classification.

The pseudokinase family has received much interest lately, and ways for classifying pseudokinases based on their ATP binding and catalysis characteristics have been introduced. Table 2 is a comprehensive list of pseudokinases, whose structures have been solved, and whose proposed function is supported by data from *in vitro* studies.

Conserved motifs	Glycine rich loop	β3-VAIK motif	HRD	DFG	Finding
Subdomains	I	II	VI	VII	
DEAD PSEUDOKINASES					
VRK3	TRDNQG	FSLK	HGN	GYG	No nucleotide binding, severely degraded G-loop
ROP2	GQEDPY	FEVH	HTY	GFE	No nucleotide binding
BubR1	CEDYKLF	TVIK	HGD	DFS	No catalytic activity
LOW ACTIVITY KINASES					
JAK2 JH2	GQGTFT	VLLK	HGN	DPG	Binds MANT-ATP-Mg^{2+}, shows catalytic activity
HER3	GSGVFG	VCIK	HRN	DFG	Binds MANT-ATP-Mg^{2+}, shows catalytic activity
CASK	GKGPFS	FACK	HRD	GFG	Shows catalytic activity, binds TNP-ATP
IRAK2	SQGTFA	FVFK	HSN	HPM	
NOT ANYMORE PSEUDOKINASES					
WNK1	GRGSFK	VAWC	HRD	DLG	Catalytically active
Titin	GRGEFG	YMAK	HFD	EFG	Catalytically active
Haspin	GVFGEV	VAIK	HRD	DYT	Catalytically active
SELECTIVE PSEUDOKINASES					
STRADα	GKGFEM	VTVR	HRS	GLR	Binds ATP- Mg^{2+}, binds TNP-ATP, shows no phosphorylation and no hydrolysis of ATP
ILK	NENHSG	IVVK	RHA	DVK	Binds ATP (?), does not regulate PINCH-ILK-parvin complex.

Table 2. Possible classification of pseudokinases based on their physiological role. Details on variations in key motifs in the respective pseudokinases are listed. The structures of all the pseudokinases in the table have been solved [modified from (60, 78, 84, 86, 87)].

Besides ATP binding and catalytic phosphotransfer, pseudokinases can perform other functions, which have caught the attention of researchers. Some

pseudokinases are known to regulate complexes (STRADα-MO25-LKB1 and PINCH-ILK-Parvin). Others have a specific role in scaffolding (KSR; Trb3). The Kinase suppressor of Ras 1 (KSR) proteins (KSR 1 and KSR 2) are mediators of the ERFR-Ras-Raf1-ERK/MAPK signaling pathway. Both KSR and Raf1 proteins have conserved kinase domains. But KSR proteins have a putative kinase domain that binds both MEK and Raf, whereas Raf has a functional kinase domain that binds only MEK. Some studies have reported a kinase activity in KSR, and this activity apparently promotes anti-apoptotic protective behavior in the intestinal epithelium in inflammatory bowel disease. Studies also show that KSR transphosphorylates and transactivates Raf1 on T^{269} (88-93). All these reports are based on *in vitro* data only, and since no *in vivo* validation was done, the role of KSR as an actual active kinase was questioned. A major breakthrough was made when both KSRs were found to act as scaffolds in the MAP pathway (94-96). Many kinases are regulated by allosteric activation, and KSR was also shown to exhibit dimerization driven regulation through the formation of heterodimers with Raf or via Raf/Raf homodimerization (97). However, the crystal structure of KSR revealed a new form of regulation. The structure shows that KSR2 does indeed get phosphorylated and acquires a catalytic activity towards MEK1 as shown by *in vitro* ATP binding assays. However, KSR still acts as a scaffold to pair up with BRAF to promote MEK phosphorylation. KSR switches between two conformations with Raf and promotes phosphorylation both in *cis* and in *trans* (98).

5.3.5 Regulation of catalytically active pseudokinases – intra/inter domain regulation

HER3 is involved in the regulation of the active HER2 kinase and provides the best example of inter domain regulation. HER3/ErbB3 is one of the four members (HER1, HER2 and HER4) of the human epidermal growth factor family of tyrosine kinase receptors. All members, except HER3, are kinases. HER3 lacks important residues including the HRD and DFG motifs (Table 2). HER3 was regarded as a pseudokinase until it was recently found to possess low kinase activity. HER3 was able to bind ATP at a 1.1 μM affinity; however, according to another report HER3 does not phosphorylate peptide substrates and retains an inactive kinase conformation (99, 100). Neuregulin is a growth factor that initiates the heterodimerization of HER2/HER3, where the HER3 pseudokinase domain activates the HER2 kinase domain. This further allows the autophosphorylation of

HER2 and initiates the recruitment of the SH2 and PTB domains to the receptor complex-induced PI3K and ERK pathways. During this process, HER3 is also phosphorylated by HER2 (101, 102). Additionally, in the absence of neuregulin, HER2 is maintained in an auto-inhibited monomeric state and can get activated only when HER3 forms a heterodimer with it (103). This is an excellent example of allosteric regulation between an active HER2 and an inactive HER3 domain. The mechanism keeps the activity of HER2 at check, and makes HER2 an attractive anti-cancer target.

Erythropoietin producing hepatocyte (Eph) kinases are receptor tyrosine kinases that lack the DFG, HRD and VAIK motifs. For example, EphB6 lacks tyrosine kinase activity. Nevertheless, it still activates ZAP-70 once ephrin is bound. EphB6 might also form heterodimers with Eph receptors; however the exact mechanism of the activation is not known (104).

General control non-derepressible (GCN) 2 also regulates its counterpart kinase domain. GCN2 has a pseudokinase domain adjacent to its kinase domain within the same molecule like JAK2 (and other JAKs). The pseudokinase domain is thought to balance the hyperactive kinase domain through an inter domain interaction in *trans* (105). An inter domain interaction in JAK2 performs a similar regulatory mechanism, which is discussed in section 5.5.2.

5.4 JAK tyrosine kinases

5.4.1 General overview of JAK kinases

The discovery of interferons began to unravel the events of cytokine mediated signal transduction via the JAK (Janus Kinase) / STAT (Signal Transducer and Activators of Transcription) pathway. JAKs are evolutionarily conserved from non-vertebrate chordates such as *Ciona intestinalis* (sea squirt), and insects to humans. The JAK family is one of the ten major families of non-receptor protein tyrosine kinases. It comprises four mammalian members: JAK1, JAK2, JAK3 and TYK2. The first member to be discovered was TYK2 (106), and this was followed by JAK2, JAK1 (107-109) and finally JAK3 (110). JAKs are distinguished from other protein kinases by the presence of a unique protein sequence that features two tandem kinase domains (where the second kinase domain is called the pseudokinase domain) adjacent to each other. However, on careful inspection the

two were found to resemble to each other, but one of them was inactive. Hence the protein was coined 'Janus' because of its resemblance to the two-faced Roman god. All JAKs, except JAK3, are ubiquitously expressed. JAK3 is restricted more to cells of hematopoietic origin (111-114). JAK homologs have also been identified in zebrafish (115) and *Drosophila melanogaster* (116). Two kinases were also cloned from *Dictyostelium* (slime mold) (117), however, they shared little homology with JAKs, and thus the presence of JAKs in molds was ruled out.

5.4.2 Domain organization of JAKs

Like most kinases, JAKs are relatively large proteins of over 1100 amino acids, with molecular masses of about 120 – 140 kDa. The recombinant purification of these large kinases is challenging and as of now, the crystal structure of a full length JAK is not available. The JAK domain structures are conserved between mammals, insects, flies and fish. The most intriguing feature of the JAK domain architecture, which distinguishes it from other kinases, is the presence of two domains (with extensive homology to each other): The C-terminal catalytically active kinase domain [referred to as JAK homology (JH) 1] and the pseudokinase (JH2) domain. The N-terminal half of JAKs contains an SH2-like domain (encompassing the JH3-JH4 regions) and the FERM domain - band 4.1, ezrin, radixin, moeisin (encompassing the JH5-JH7 regions). Lately, these regions have been spuriously referred as the seven JH domains instead of the four major domains (Figure 6).

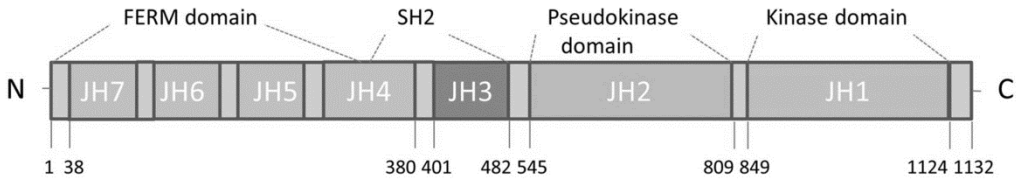

Figure 6. Schematic domain architecture of JAK kinases. The amino acid numbering displayed in the figure corresponds to JAK2.

Tyrosine kinase domain – The tyrosine kinase domain in JAKs has all the features of a conventional kinase domain and is approximately 300 amino acids long. The first glimpse demonstrating catalytic activity came when a mutation in the lysine residue in subdomain II led to abrogation of the kinetic activity (118), and later to a

kinase dead JAK2 mouse model (119). Additionally, the presence of two tyrosine residues needed for the activation of all JAKs was declared a hallmark of this family. The phosphorylation level and status of these residues vary between JAKs. The phosphorylation of the tyrosine residues could indicate - a) that they are required for optimal activity, b) catalytic activity or c) maximal kinase activity. It was shown that Y^{1007} was the critical residue for phosphorylation during phosphotransfer and is required for the regulation and function of JAK2. Unlike changes to Y^{1007}, mutagenesis studies on Y^{1008} showed no difference in catalytic activity (120). This holds true also with JAK1 and TYK2 proteins in which the tyrosine kinase activity is dependent on the first tyrosine (121, 122). However, between the two tyrosines in JAK3 (Y^{980}, Y^{981}), a mutation to Y^{981} led to a dramatic increase in catalytic activity (123).

The first structure of a kinase domain in the JAK family was solved in 2005 when the JAK3 JH1 domain was crystallized with a staurosporine analog (124). This was soon followed by the kinase domain structure of JAK2 (explained in section 5.4.3). By now, the structures of the kinase domains of all JAKs have been solved (125, 126). They all have the characteristic five β-strands and a single α-helix in the N-lobe. In addition to this, there is a striking additional helix in the C-lobe of all the JAKs. This kinase insertion loop was called the 'FG helix' in the JAK3 structure.

Pseudokinase domain – Like the kinase domain, the pseudokinase domain is also conserved in all four members of the JAK family. Clearly, a lack of activation loop tyrosines and other canonical motifs required for catalytic activity distinguishes this domain from the adjacent kinase domain. Few initial studies on the deletion of the JH2 domain in JAK2 and TYK2 mediated IFN-α and GH signaling resolved several unanswered questions in JAK biology (127, 128). Apart from a study by Wilks *et al.,* which described alterations in residues in the JH2 domain, and one other modeling study, where the JH2 and JH1 kinase domains showed a bi-lobal conformation in JAK3 (118, 129), no significant findings were reported in the JAK pseudokinase field. A major breakthrough was made when three studies from our laboratory discovered the importance of an intact pseudokinase domain in JAK2 (130-132) (see 5.4.3). Later, it was also shown by another group that the intact pseudokinase domain in TYK2 was responsible for the intrinsic catalytic activity of TYK2, and four specific mutants in TYK2 could not restore the binding of IFN-α to the IFNR (133). Recent studies have made huge progress in solving the three-dimensional structure of the pseudokinase domain of JAKs. The crystal structures of the pseudokinase domains of all JAKs

except JAK3 have been solved and they suggests approximately 30% identity to classic kinase domains (134, 135) and to the pseudokinase structure of TYK2 (PDB code 3ZON) (http://www.rcsb.org/pdb/explore/explore.do?structureId=3ZON). All the JAK pseudokinase domains also have a similar bi-lobed fold. The role of the pseudokinase domain in JAK2 function, and the phosphorylation sites in JAK2, are described in section 5.4.3.

SH2-like domain (JH3-JH4) – The Src homology domain 2 was originally discovered in v-Src. It is a non-catalytic motif of about 70-100 amino acids known to specifically bind phosphotyrosines. The initial two studies on JAKs reported no resemblance of the JH3-JH4 region to any known SH2 domains (106, 108). The first report on a weak resemblance came through a TYK2 study, which showed the existence of a SH2-like putative regulatory domain (136). Multiple sequence alignments and homology modeling studies revealed that the SH2-like domain is present with an invariant arginine residue in the core sequence of all JAKs. However, it was later shown that the arginine in the βB5 position is substituted by a histidine (137). The SH2-like domain of chicken JAK3 was shown to bind phosphorylated proteins in an *in vitro* binding assay (138). A modeling study revealed a centrally located four-stranded β-sheet flanked by two α-helices on either side, and concluded that the SH2-like domain in JAK2 may not be fully functional (139). The precise function of this domain is not known for all JAKs. A study from 2005 sheds some light on the role of this domain in JAK1. Despite mutating arginine to lysine ($R^{466}K$), no change was seen in the subcellular distribution of JAK1, nor did this inactivating mutation has any effect on IL-6 or IFN-γ/IFN-α signaling. However, the SH2-domain was shown to play a structural role in the interaction with and the binding to the receptor subunits of gp130 (140). Despite the lack of knowledge on the regulatory functions of the SH2 -like domains in JAKs, mouse knockout studies show that the JAK1 SH2-/- mouse is perinatally lethal, the JAK2 SH2-/- mouse is embryonically lethal and the JAK3 SH2 -/- mouse is immunodeficient and suffers from lymphopenia (141).

FERM domain (JH5-JH7) – JAKs and focal adhesion kinases (FAKs) are the only two families in NRTKs that possess a FERM domain. The FERM domain, which was discovered in JAKs, spans from the middle of the JH4 to end of the JH7 region (142). This domain forms a clover shaped structure consisting of subdomains A, B and C (143). The structure has two poorly conserved additional loops found only in JAKs. The N-terminal end of the FERM domain (JH6-JH7 regions) is involved in binding to cytokine receptors (144-146). The boundaries

required for binding to receptors vary between JAKs. JAK2 and JAK3 require the JH7-JH6 regions to bind to EPOR and γ_c, respectively (147-149). Together with the JH7-JH6 region, specific regions within JH3-JH5 also aid in the formation of a protein-receptor complex in TYK2 (150). JAK1 binds to gp130 through subdomain A of the JH7 region in the FERM domain (151, 152). Initially, it was thought that the role of the FERM domain was restricted only to receptor-protein interactions. But then FERM was found to be involved in enhancing the cell surface expression of IFNαRI. An intact FERM-SH2 is necessary for stabilizing IFNαRI at the cell surface (153). Recently, studies on a mutant JAK2 ($Y^{119}E$) showed that the tyrosine is needed to regulate JAK2 activity and to initiate the dissociation of JAK2 from the receptor complex especially with EPOR, TPOR and GH (154). Phosphorylation of Y^{221} has also been shown to be involved in JAK2 regulation (155, 156). A mutation in the JAK1 kinase domain led to impaired binding to the IFNαRI. One can speculate that in addition to FERM (as seen from studies on mutations which impair FERM-receptor binding) (157), other domains are also required for a tight receptor-protein interaction and overall JAK regulation (158).

5.4.3 Wild type JAK2 - emphasis on the kinase and pseudokinase domains

Kinase domain of JAK2 – In addition to the activation loop tyrosines, 15 other tyrosine residues (159, 160) have been identified in the JH1 domain of JAK2. Mutating them to either phenylalanine or glutamic acid had no significant effect on downstream signaling, when JAK2 was activated by Epo or IFNγ. The only exception was the phosphorylation of Y^{813} and Y^{966}. While Y^{813} recruits SH2-Bβ and enhances the kinase activity of JAK2 (161) and in turn increases the phosphorylation of STAT5, Y^{966} recruits p70 and has no known function (162). Y^{868} and Y^{972} were the other phosphorylated tyrosines detected by mass spectrometry when JAK2 was activated by the erythropoietin-bound chimeric erythropoietin/leptin receptor (163). These tyrosine residues are required for maximal kinase activity, and mutations in them result in reduced JAK2 activity. However, co-expression of Src homology (SH) 2B1β restores the activity and might stabilize the mutant JAK in its active conformation (164). While phosphorylation of the activation loop tyrosines aids in the recruitment of regulatory proteins such as SOCS-1, JAB (165), post-phosphorylation events on other tyrosines becomes equally important. In addition, Y^{372} was also shown to be

critical for kinase activation (166). Another negative regulatory residue is Y^{913}, which is an autophosphorylation site in JAK2 (167).

The crystal structure of the JAK2 kinase domain (168) was solved with a bound pan-Janus kinase inhibitor (Figure 7). Deletion of the additional helix in the C-lobe or the 'JAK specific insertion loop (JSI)' as termed by Haan *et al.,* was shown to abrogate autophosphorylation in JAK2 (169). The role of this additional helix in other JAKs is unclear. However, one could speculate that it functions in intramolecular regulation. The DFG-in conformation is usually considered an active open conformation, where residues 994-996 in JAK2 are repositioned towards the active site, which shifts the αC helix. The activation loop (aa 994-1023) in JAK2 is expelled out of the active site and stabilized by two β sheets (β6/β9 and β10/β11) and two arginine residues (R^{971} and R^{975}) that interact with the base and tip of the A loop. Other lysine residues also stabilize the phosphorylated Y^{1007}. This facilitates the binding of inhibitors, the discovery of which led to the development of type I inhibitors that mimic the ATP binding site. The crystal structure of the JAK3 kinase domain is similar to the JAK2 domain, except for a more open conformation due the docking of a larger staurosporine in the ATP binding site (124, 168).

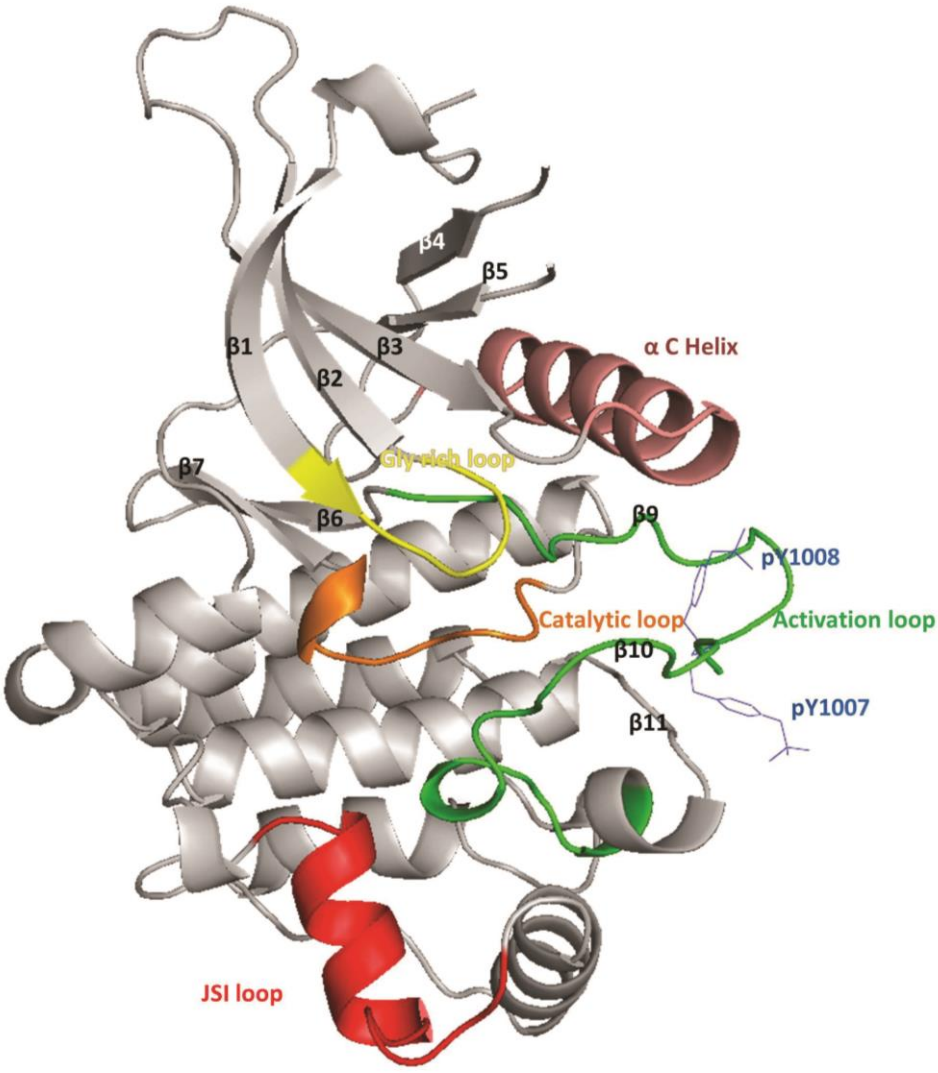

Figure 7. Structure of JAK2 kinase domain depicting its important features (PDB 2B7A). Structural elements are shown in different colors and the two tyrosines in the activation loop are shown as blue sticks. The main beta sheets, β6/β9 and β10/β11 are also shown in this cartoon.

Pseudokinase domain of JAK2 –Biochemical evidence gathered from three studies demonstrated the regulatory function of JAK2 kinase by its pseudokinase domain. The interaction between the two domains provided a model for the regulation of JAK activation in cytokine signaling (130). This was soon followed by the

discovery that the pseudokinase domain is needed to suppress the basal activity of the JAK2 and JAK3 kinases. JH2 was shown to negatively regulate JH1 activation and cytokine mediated JAK2 and JAK3 signaling. This study also pin-pointed specific inhibitory regions (IR1-3) in JH2, which are directly responsible for the inhibition of JH1 activity. Also modeling studies on JH2 showed that IR3 could form an α-helical fold and inhibit JH1 activity in JAK2 (131, 132).

A detailed study on transphosphorylation sites demonstrated that more than 40 tyrosine residues in JAK2 are conserved in mammals. The phosphorylation sites are depicted in Figure 8.

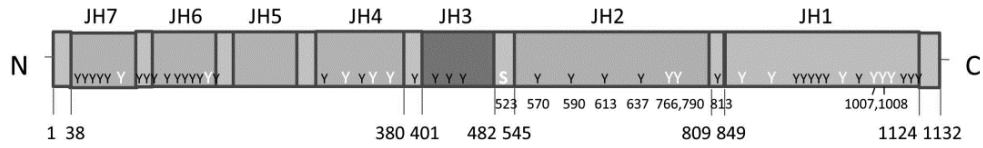

Figure 8. Schematic view of the phosphorylation sites in the JAK2 molecule. The tyrosines (Y) in white represent residues conserved throughout the JAK family, others are restricted to JAK2. Important phosphorylated sites in the JH1 and JH2 regions are mentioned in numbers [modified from (159)].

Y^{570} and Y^{637} were shown to be the target transphosphorylation sites in the JH2 domain (159). This study ruled out all possible serine/threonine phosphorylation. Further, Y^{570} was shown to inhibit JAK2 mediated signaling when phosphorylated (155, 156). However, other studies showed that phosphorylation of serine residues was involved in the regulation of JAK2 activity. In particular, serine 523 was shown to be a negative regulator of JAK2 activity in a manner that is dependent on GH and epidermal growth factor (170). In parallel, S^{523} was shown to inhibit leptin receptor signaling dependent JAK2 activity (171). However, this study revealed that the effect of S^{523} was independent of Y^{570} phosphorylation. This demonstrates that Y^{570} and S^{523} are negative regulators of JAK2 activity. The JAK2 JH2 structure is discussed in section 5.5.2.2.

5.4.4 JAK/STAT pathway – canonical and non-canonical functions

As mentioned earlier, JAKs combined with STATs provide a sequence of events that is known to induce the expression of specific genes. A schematic

representation of the JAK/STAT pathway, which is activated upon cytokine binding, is shown in Figure 9. A wide range of cytokines initiates the signaling cascade and induces receptor oligomerization. This result in the activation of JAKs that are non-covalently bound to the receptor chains. Further, this leads to the phosphorylation of specific tyrosine residues on the cytoplasmic tails of the receptors and creates docking sites for STATs. STATs get phosphorylated by JAKs upon binding to the receptors and eventually dissociate, dimerize and translocate to the nucleus to induce gene transcription (172-174). Thus, JAKs together with STATs provide a rapid signaling pathway for cytokines.

Specificity in the JAK/STAT pathway is achieved largely through different combinations of JAKs and STATs (STAT1, STAT2, STAT3, STAT4, STAT5A, STAT5B and STAT6) together with the ligands and their receptor chains. The specific sets of cytokines, JAKs and STATs are shown in Table 3. JAKs come into play mostly when receptors, which do not possess an intrinsic kinase activity, require a set of proteins that are bound to their cytoplasmic tails to initiate the signaling inside the cell. In its simplicity, the cascade requires only JAKs and STATs. However, the involvement of different adaptor proteins, negative regulators and other protein kinases make this pathway non-autonomous and increase the plasticity of its regulation. Single chain receptor families such as EPOR, GH and TPOR facilitate the binding of only one type of JAK i.e. JAK2 and feature homodimerization. Others, for example the IFN family and the IL family have two receptor subunits that bind two different JAKs which form heterodimers.

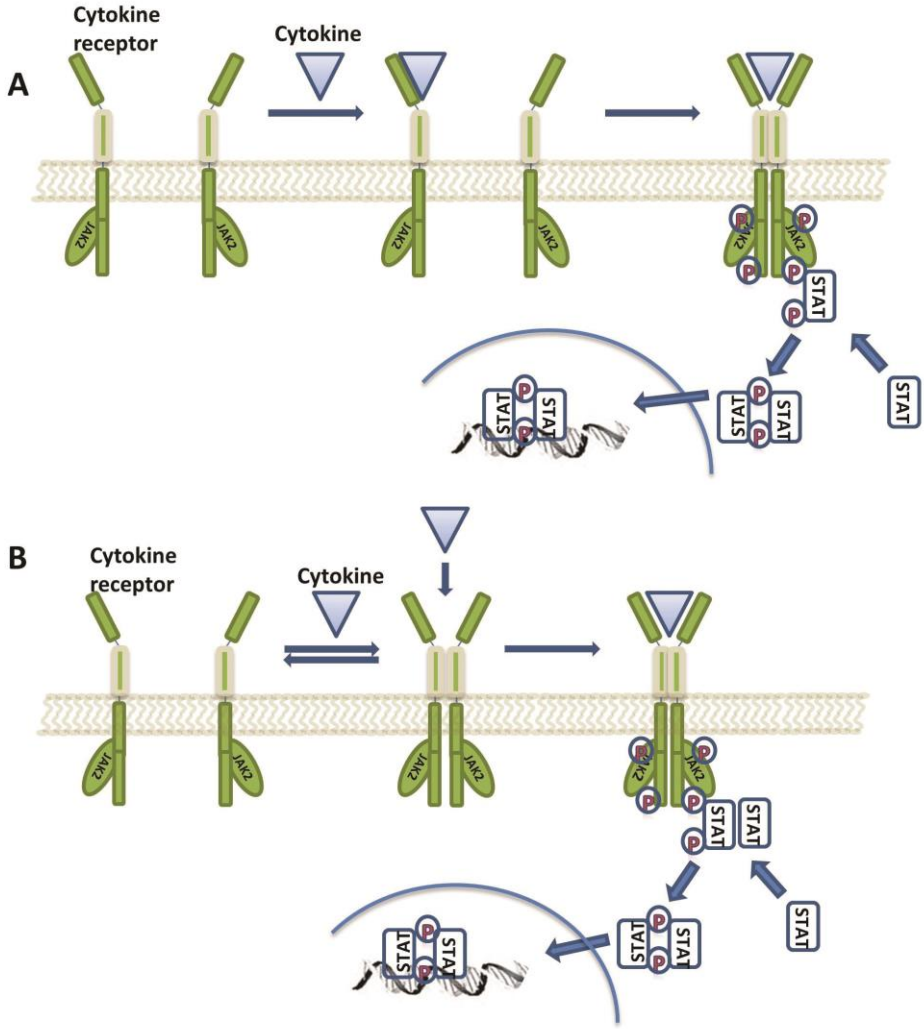

Figure 9. Canonical and non-canonical JAK/STAT pathways (A) The canonical signaling cascade starts with ligand binding to the extracellular domain of the receptor. This leads to the dimerization of two proximal monomeric receptors, which activates them. (B) In the non-canonical signaling cascade the receptor dimers are preformed or ligand binding induces an activating conformational change in the receptor. Both signaling cascades feature the formation of a distinct STAT dimer although cartoons of non-phosphorylated STATs translocating to the nucleus and other non-canonical functions of JAKs are not depicted here. This cartoon features the JAK2 molecule [adapted from (175)].

Cytokines	JAKs involved	STATs activated
Type I cytokines		
Cytokines with single chain receptors		
EPO, TPO	JAK2	STAT5A, STAT5B
PRL	JAK2	STAT5A, STAT5B
GH	JAK2	STAT5A, STATB, STAT3
Cytokines whose receptors share β_c		
IL-3, IL-5, GM-CSF	JAK2	STAT5A, STAT5B
Cytokines whose receptors share γ_c		
IL-2, IL-7, IL-9, IL-15, IL-21	JAK1, JAK3	With different combinations of STAT5A, STAT5B, STAT3 and STAT1
IL-13	JAK1, JAK2, TYK2	STAT3, STAT6
IL-4	JAK1, JAK3	STAT6, STAT5
Cytokines whose receptors share gp130		
IL-6, OSM, LIF, CNTF, BSF-3	JAK1, JAK2	STAT3, STAT1
IL-12	TYK2, JAK2	STAT4
IL-11	JAK1	STAT3, STAT1
Leptin	JAK1	STAT3
Type II cytokines		
IFN-α, IFN-β, IFN-γ	JAK1, TYK2	STAT1, STAT2
IFN-ω	JAK1, TYK2	STAT3-6
IL-10	JAK1, TYK2	STAT1, STAT3
IL-19, IL-20, IL-24	?	STAT1, STAT3
IL-22	JAK1, TYK2	STAT1, STAT3, STAT5
Receptor tyrosine kinase involving growth factors		
EGF, PDGF, CSF-1	JAK1, JAK2	STAT1, STAT3, STAT5-6
Insulin	JAK2	STAT1, STAT5B
G-protein coupled receptors		
Angiotensin (AT) 1	JAK2, TYK2	STAT1, STAT2

Table 3. Hematopoietins activate different combinations of JAKs and STATs [modified from (184-187)].

The whole signaling cascade from ligand binding at the receptors to gene expression in the nucleus is a mystery in itself. There are several questions in this process that remain unanswered despite several studies. Is the signaling pathway so straightforward? How are the choices between the receptor chains and the JAK/STAT molecules made? Does ligand binding initiate the JAK/STAT combination process or do the pre-determined homo/heterodimers sitting on the receptor tails choose the ligand? JAKs are outnumbered compared with receptors. This might be one reason for conservational evolvement of JAK/receptor pair.

Some studies have addressed these issues, and an intriguing discovery was made when EPOR dimers were crystallized in the absence of ligand. EPOR was found to exist as preformed homodimers in the membrane (176). This was supported by a structure of EPOR in the presence of EPO, which differed substantially from the previous structure of the unbound receptor (177). This opened up new aspects of non-canonical signaling, along with the generally accepted view of receptor activation in a canonical signaling pathway (Figure 9). Some studies on gp130 receptors revealed that the proper orientation of and conformational changes in juxta positioned domains facilitates the activation of cytokine receptors (178, 179).

Some other non-canonical functions of this set-up include the observation that a monomeric mutant EPO was unable to activate JAK2, but homodimerization of the same mutant restored its activity and induced proliferation (180). JAK2 has a previously unknown function in the nucleus where it phosphorylates Y^{41} on histone H3 in hematopoietic cells (181). When engineered chimeric GH receptors were intermixed with their intracellular and extracellular domains, and activated by extracellular ligands, we had a whole new understanding to the dynamics and diversity of signaling (182, 183).

5.5 Pathophysiology of JAK2

5.5.1 Mutational studies in JAK2, the discovery of the $V^{617}F$ pathogenic allele

The normal function of JAK2 is emphasized in its role in regulating the differentiation and proliferation of hematopoietic cells. Thus, it is no surprise that the constitutive and aberrant activation of JAK2 leads to pathological conditions and, in particular, hematopoietic malignancies. Chromosomal translocations and activating mutations are the primary cause for such malignancies, especially

myeloproliferative neoplasms (MPN) or myeloproliferative disorders (MPD). Myeloproliferative disorders are a heterogeneous group of diseases characterized by the excessive production of blood cells by hematopoietic precursors. Typically, myeloproliferative disorders encompass four related entities -- chronic myelogenous leukemia (CML), polycythemia vera (PV), essential thrombocythemia (ET), and idiopathic myelofibrosis (IM). These four groups were first classified as MPDs by Dr. William Dameshek in 1951 (188). Chromosomal translocations lead to the recombination of the JAK2 gene with parts of other genes like TEL or Breakpoint cluster region (BCR). JAK2 is hyperactivated in the resulting oncogenic fusion genes. The Tel-JAK2 fusion protein is the combination of the kinase domain of JAK2 and the N-terminal region of Tel, which results in constitutive signaling and eventually the uncontrolled production of blood cells independent of cytokines. As a consequence, this fusion protein is able to induce CML or acute lymphocytic leukemia (ALL) (189-191). The second cause for these pathological conditions is the presence of acquired somatic mutations in the JAK2 gene. Although it was known that such mutations could be responsible for MPDs, it took 40 years from the the first description a MPD to actually prove this.

Mutations in the JH2 domain – The indication of the existence of a JH2 domain mutation in JAK2 came from two simultaneous observations in Hopscotch, the JAK homologue in *Drosophila melanogaster*. Hopscotch tumour lethal (Hoptum-l), a prominent gain-of-function allele was found to be responsible for the hyperphosphorylation of Hop and resulted in melanotic tumors in flies due to its over-expression. This was because of a single amino acid substitution from glycine to glutamic acid ($G^{341}E$) (192, 193). Following this, the hallmark discovery of a point mutation from valine to phenylalanine at position 617 in the mammalian JAK2 by five independent groups marked the beginning of establishing a relationship between MPD and gain-of-function mutations (194-198). The JAK2 $V^{617}F$ mutation was found in patients with PV (incidence 97%), ET (incidence 50%) and primary myelofibrosis (PMF) (incidence 50%) all of which are characterized as BCR-ABL negative diseases (199). A striking observation made by one of the five groups was that erythroid colony formation in PV -hematopoietic stem cells (HSCs) was inhibited by the JAK kinase inhibitor AG490. This indicated that JAK2 is required for erythropoiesis (198).

The discovery of the $V^{617}F$ mutation was soon followed by several investigations, which led to the identification of other mutations in the pseudokinase domain. Recent clinical findings have established the JH2 domain as a mutational hotspot with a total of 32 different patient mutations shown to be

linked with haematological diseases (reviewed in (200, 201)). $V^{617}F$- negative PV patients have other mutations, which lead to the constitutive activation of JAK2. $K^{539}L$ is present in the SH2 domain (202). A study shows that there are 16 different insertions, deletions, mutations and substitutions that render JAK2 active (202). Other prominent mutations include $D^{620}E$ (203) and $C^{616}Y$ (204) in PV patients, $E^{627}E$ (203) in non-PV patients, a five amino acid deletion IREED in Down's syndrome (205), $R^{683}G$, $R^{683}S$, $R^{683}K$ in ALL patients associated with Down's syndrome (206), $L^{611}S$ in childhood ALL patients (207) and $K^{607}N$ in acute myeloid leukemia (208) (Table 4). The point mutation $E^{665}K$ and its homologous mutation $E^{695}K$ in *Drosophila melanogaster* also result in a constitutively activated JAK/STAT pathway (209). These observations and other studies (210) clearly state that mutations that activate JAK2 are present not only in exon 12 (del 537-543 and $K^{539}L$), but also in exons 13 ($R^{564}L$, $L^{579}F$, $S^{591}L$, $H^{587}N$), 14 (14-Del, $H^{606}Q$, $V^{617}I$, $C^{618}R$ and $V^{617}F$), 15 ($L^{624}P$) and 16 ($R^{683}X$). In addition to these, a functional screen of gain-of-function mutations in the pseudokinase domain and the SH2-pseudokinase linker yielded 13 mutations that induced the constitutive activation of JAK2 (211).

Mutations in the JH1 domain – Unlike in the other JAKs, disease causing mutations are only found in the pseudokinase and kinase domains of JAK2. The mutations that have been studied so far lie in the loop region between the β1 and β2 strands and are present in patients suffering from ch-B-ALL. The first mutation that was found was $T^{875}N$, which was characterized in an AMKL cell line, where it facilitated the constitutive activation of its downstream regulator STAT5 (212). Later on, three other mutations ($R^{867}Q$, $D^{873}N$ and $P^{933}R$) with similar effects were identified and characterized in pediatric ALL (213). Only one mutation in the FERM domain (exon 8) $R^{340}Q$ is seen in MPN patients (214). In addition, a random mutagenesis screen found several STAT5 activating and activity enhancing TEL-JAK2 mutants, which, could abolish the effects of a tyrosine kinase inhibitor (215).

EXON	DOMAIN	MUTATION	DISEASE
12	SH2-JH2 Linker	$T^{514}M$	CMN
		H^{531} (silent)	CMN
		$N^{533}Y$	CMN
		$M^{535}I$	ch-AMKL
		dupl/V^{536}-F^{547}	CMN, PV

		dupl/V^{536}-I^{546}	PV, IE	
		dupl/V^{536}-I^{546}+F^{547}L	PV, IE	
		F^{537}I	PV	
		del H^{538}	CMN	
		del/H^{538}-K^{539} ins/L	PV, IE, CMN	
		K^{539}L	PV, IE	
		del/F^{537}-K^{539} ins/L and ins/K	PV, IE	
		H^{538}Q + K^{539}L	PV, IE	
		H^{538}D + K^{539}L + I^{546}S	PV	
		del/^{N542}-E^{543}	PV, IE, CMN	
		del/N^{543}-D^{544}	PV, IE, CMN	
		del/I^{540}-E^{543} ins/MK	PV, IE	
		del/R^{541}-E^{543} ins/K	PV, IE	
		del/R^{541}-D^{544} ins/MK	CMN	
		del/N^{542}-D^{544} ins/N	CMN	
		del/D^{544}-L^{545}	PV	
		K^{539}L+L^{545}V	CMN	
		F^{547}L	CMN	
13	JH2	Y^{556} (silent)	CMN	
		G^{562} (silent)	CMN	
		Y^{570} (silent)	CMN	
		F^{557}L$^{\#}$	CMN	
		R^{564}L, R^{564}Q, V^{567}A, G^{571}S, G^{571}R, L^{579}F, H^{587}N, S^{591}L (all missense)	CMN	
		del/S^{593}-N^{622}	CMN	
14		H^{606}Q	CMN	
		K^{607}N	AML	
		H^{608}Y	CMN	
		L^{611}S	ch-B-ALL	
		L^{616}Y+V^{617}F	PV	
		V^{617}F	*MPN/MDS*	*Frequency (%)*
			PV	>90
			ET	~50
			PMF	≥50

			HES	<2
			CMML	<5
			aCML	<20
			JMML	<20
			AML*	≤50
			RARS, RA, RCMD, RAEB, CNL, IE, RARS-T, MDS/MPN-U, MPN-U, SM	-
		V617I	CMN	
		V617F+C618R	PV	
		C618R	CMN	
		D620E	PV, leukocytosis	
15		L624P	CMN	
		E627E	MPN	
		I645V	CMN	
Δexon15+16		ΔN622-D710	MDS/MPN-U	
16		**I682F**	ch-B-ALL	
		I682AQG	DS-B-ALL	
		R683G	ALL	
		R683S	DS-B-ALL, B-ALL	
		R683T, **R683K**	DS-B-ALL	
		del/I682-D686 (ΔIREED)	DS-B-ALL	
		del/I682 ins/MPAP	DS-B-ALL	
		L681+ del/I682_ins/TPYEGMPGH	DS-B-ALL	
20	JH1	R867Q	ch-B-ALL	
		D873N	ch-B-ALL	
		T875N	AMKL-cell line	
21		**P933R**	ch-B-ALL	

Table 4. Mutations in the JH2 and JH1 domain of JAK2 implicated in different forms of MPD diseases. Mutations in bold letters have been validated either by the monitoring of activated signaling with respect to the increased activity compared with the wild type JAK2 kinase or by monitoring the proliferation of hematopoietic cells. # This mutation leads to a frameshift and inserts ten residues, which leads to premature termination at 567th amino acid. * Arise from JAK2 associated with any other form of MPN, the de novo AML case frequency is 1. Abbreviations: CMN: Chronic myeloproliferative neoplasia, ALL: acute lymphoblastic leukemia, AMKL: acute megakaryoblastic leukemia, AML: acute myeloid leukemia, B-ALL: B cell precussor ALL, ch: childhood, CML: chronic myelogenous leukemia, CMML: chronic myelomonocytic leukemia, CNL: chronic neutrophilic leukemia, IE: idiopathic erythrocytosis, PV: polycythemia vera, MDS/MPN-U: non classified MPN, DS: Down syndrome, RARS: refractory anaemia and ringed sideroblasts, RA: refractory anaemia, RAEB: refractory anaemia with excess of blasts, JMML: juvenile myelomonocytic leukemia, HES: hypereosinophilic syndrome [modified from (200, 210, 216, 217)].

5.5.2 Regulation of JAK2

5.5.2.1 Mechanisms of JAK2 $V^{617}F$ activation

We know, at the moment, that the Y^{1007} residue in the activation loop is phosphorylated, and that this phosphorylation activates JAK2, when it takes place in *trans* between different JAK/JAK2 proteins. Phosphorylation on Y^{1008} did not affect the catalytic activity, as seen from mutation studies. Along with the discovery of the pathogenic $V^{617}F$ mutation, studies on an *in vitro* platform gave convincing proof for the constitutive activity of the JAK2 $V^{617}F$ molecule. It was shown that when JAK2 was overexpressed with EPOR in HeLa cells, the mutant JAK2 exhibited enhanced phosphorylation and this consequently resulted in the hyperactivation of downstream signaling components such as STAT5, Akt and ERK1/2 in the absence of EPO (196). Another study in JAK2 deficient human fibrosarcoma cells (γ2A) showed constitutive signaling by STAT5 and STAT3 with respect to IFN-alpha and IFN-gamma receptors (218). Studies in human erythroleukemia (HEL) and COS7 cell lines showed that hyperphosphorylation of JAK2 $V^{617}F$ was more pronounced at the Y^{1007} residue in the activation loop (219). Additional studies confirmed this hyperactivation in murine IL-3 dependent pro-B (BaF3) stably transfected cells, where the overexpressed mutant was able to enhance the basal kinase activity of a GST-fusion substrate containing the Y^{1007} residue (198, 220). It was initially proposed that the constitutive activity of the JAK2 $V^{617}F$ mutant requires a monomeric EPOR domain (since activation is

cytokine independent) (221). A later study by the same group showed that the cytokine-independent activation involved a second endogenous receptor. Thus, the authors concluded that a dimeric cytokine receptor may be needed to activate JAK $V^{617}F$ (222).

Experiments with a mutant ($Y^{114}A$) FERM domain of JAK2 showed that an intact FERM domain is required for JAK2 $V^{617}F$ to signal constitutively (160, 223). Biochemical studies have backed up the notion that the FERM domain regulates $V^{617}F$ activity (224).

5.5.2.2 Role of pseudokinase domain in JAK2 regulation

Saharinen *et al.,* (130-132) have described the functional role of the JH2 domain. The JH2 domain was found to negatively regulate JH1 activity (see section 5.4.3). After the discovery of $V^{617}F$, it was shown that the intrinsic inhibitory effect of JH2 on JH1 was cancelled out by the mere presence of the mutation. When the mechanism of activation was examined at the structural level, two significant studies revealed that the F^{595} residue aids in the activation of JAK2 $V^{617}F$. Molecular dynamics simulations and *in vitro* experiments showed that a pi-stacking mechanism between F^{595} and F^{617} is critical for the constitutive activation of the mutant JAK2. Inhibition and activation of the constitutively active $V^{617}F$ were seen when F^{595} was mutated to aliphatic and aromatic residues, respectively (225, 226). Additionally, mutating V^{617} to bulky non-polar residues (isoleucine, leucine, methionine and tryptophan) resulted in constitutive activity of the kinase. The $V^{617}W$ mutant displayed an activity that was comparable with $V^{617}F$. This indicated that $V^{617}W$ along with $V^{617}F$ could activate both the inactive and active conformations of the cytokine receptor dimer (227). A biochemical basis for the interaction of these two domains could be fathomed by investigating the biochemical parameters of the domains. One such study sheds light on the modulating role of the JH2 domain. JH2 decreased the activity of JH1 by decreasing its affinity for ATP (228). A major breakthrough came recently, when the pseudokinase domain of JAK2 (both wild type and $V^{617}F$ mutant) was crystallized. Although the exact mechanism for $V^{617}F$ activation and the inhibitory role of the pseudokinase domain are not known, the structure gave some directions towards solving the mystery. An aromatic environment is created in the $V^{617}F$ structure through interactions between F^{617}, F^{595} and F^{594} making the α-helix even more rigid than it is in the wild type protein. The structure indicates that the α-helix plays a crucial role in the aberrant activation of $V^{617}F$ (134).

5.5.2.3 Modeling studies on JH1JH2 regulation

Some of the questions on the regulation of JH2 in wild type and the $V^{617}F$ mutant JAK2 remain unanswered. The biological characterization of the JH2 domain has helped in understanding its functional role. However, investigating the structural aspects of JH2's negative regulation has been the focus of several aspiring laboratories. Everything began with the first hypothetical model, where two interaction interfaces between JH1 and JH2 were described based on the FGF receptor dimer. In addition, two residues from the catalytic loop, R^{971} and Y^{972}, were shown to interact with S^{599} and S^{605} in the α-helix of JH2. These interacting residues are present in the N-terminus of JH2 and are the most important feature of the domain. However, both of the modelled domains were in the inactive state (229).

When the crystal structure of two interacting domains is not available, structural models provide a basis for predicting possible regulatory mechanisms. One modeling study has specifically addressed the interaction of F^{595} and S^{591} with the activation loop, and F^{617} is predicted to inhibit this interaction, by making the loop move away from the JH2 domain and forcing it back into the activated form. In the wild type protein, the JH1 activation loop moves towards the JH2 domain and forms three interfaces, thus stabilizing the inactivated form of JH1 (230). This study provided the first glimpse of the interaction surface and a possible mechanism for JAK2 auto-inhibition and explanation for the constitutive activity of $V^{617}F$.

Later models, which were based on experimental evidence, provided further insights: In one model the regulation of JH2 is based on intra-molecular interactions similar to those found in asymmetric dimers. When the dimer is inactive, the authors describe JH2 as the 'receiver' and JH1 as the 'activator' in this JH1-JH2 interaction and when the dimer (JH1-JH2 or JH1-JH1) is active, JH2 as the 'activator' and JH1 as the 'receiver'. The model is fitted according to the inactive state based on the EGFR dimer. A specific interaction resulting in the orientation of the domains has been described, where the N- and C-lobes of JH1 make contact with the C- and N-lobes of JH2, respectively. Replacing valine with a bulky hydrophobic residue like phenylalanine disrupts this interaction, which possibly leads to the initiation of constitutive signaling in $V^{617}F$, featuring this disruption in inhibitory interaction as the first step in the process of activation (231). Another recent JH1-JH2 complex model offers two possibilities- one in the basal state and one in the activated state. A study, where V^{706} and L^{707}, in the so called JH2 activation loop, were mutated, supports the model where JH2 in its

active state interacts with an inactive JH1, and when this interaction (inhibition) is released, the above mentioned residues stabilize the inactive JH1 (232). However, one should keep in mind that an interaction between these two domains and the FERM domain is required for the full catalytic activity of JH1.

Two other possibilities for intra-domain interactions would be when 1) JH2 in one monomer inhibits JH1 in another monomer followed by the re-arrangement of two JAK2 molecules in such a way that the JH1 domains in both monomers reside next to each other and facilitate transphosphorylation (233) and 2) when activation is through the formation of a hydrophobic regulatory spine (R-spine) as seen in PKA (234). When such a spine comprised of four hydrophobic residues is formed in JH1 by F^{617} in JH2, it promotes the complete activation of the molecule (235).

5.5.3 JAK2 deficient mouse models

Long before the discovery of the $V^{617}F$ mutation, *in vivo* studies were carried out with JAK2-deficient mice. Although JAK2-deficient mouse embryos have primitive erythrocytes, the absence of enucleated erythrocytes at embryonic day 12.5 marks the complete absence of definitive erythropoiesis. The phenotype of JAK2 -/- compared with that of EPOR -/- mice was more severe and did not respond to IFNγ (236). JAK2 acts through multiple cytokine factors, and accordingly, it was shown that fetal liver myeloid progenitors failed to respond to EPO, TPO and IL-3. Reconstitution experiments were carried out using JAK2 expressing retroviral vectors, which were infected into fetal liver cells. This study led to the conclusion that the colony forming ability of hematopoietic progenitors could be rescued, and that JAK2 was not essential for the survival of lymphoid progenitors (237).

An in-depth study carried out by two groups on the expression of JAK2 $V^{617}F$ in murine bone marrow provided details on its *in vivo* effects. The pathological features in JAK2 $V^{617}F$ transduced mice were polycythemia vera-related including a striking elevation in the levels of hemoglobin, leukocytosis and reticulin fibrosis in the bone marrow. However, strain specific phenotypic differences were also seen when both Balb/c and C57BI/6 mice were used (238, 239). Later on, it was reported that the development of a particular phenotype is based on the gene dosage. Mice expressing the hematopoiesis specific Vav promoter, a transgene with an interferon-inducible MxCre and the retroviral transduced $V^{617}F$ gene gave lower, equal and higher levels of $V^{617}F$ JAK2, respectively compared with the endogenous

wild type JAK2. Concomitantly, the mice developed an essential thrombocythemia (ET) -resembling phenotype (higher platelet counts), a polycythemia vera (PV) phenotype (increased hemoglobin, thrombocytosis, neutrophilia) and a PV-phenotype with the absence of thrombocytosis in low, equal and high expressing JAK2 $V^{617}F$ mice, respectively. This study underlined the importance of the ratio of $V^{617}F$ to wild type JAK2 (240).

5.5.4 JAK2 and cancer

In addition to the JAK2 mutations that are involved in B-ALL, ch-ALL, AML and AMKL, the oncogenic potential of JAK2 is seen in several solid tumors. Since persistent activation of JAK2 leads to constitutive signaling through STAT partners, it will not be surprising if JAK2 is found to be involved in an aberrant IL-6/gp-130 pathway that leads to human lung adenocarcinoma. Constitutive STAT-3 activation and phosphorylation are directly related and dependent on this pathway. In addition, mutations in the EGFR kinase domain have been suggested to activate this pathway leading to lung cancer (241). Reduced expression of Suppressors of cytokine signaling (SOCS)-1, one of the negative regulators of the JAK/STAT pathway, led to over-expression of JAK2 in human hepatocarcinoma cells (242). A similar IL-6 mediated constitutive activation of STAT3 has been reported in both human and rat derived prostate cells, indicating the involvement of STAT3 in prostate cancers (243). BRCA 1 over-expression led to the constitutive activation of STAT3 in human prostate cancer cells (244). An analysis of head and neck cancer and breast cancer specimens revealed the constitutive activation of STAT3 by Src and JAK2 cooperatively. The kinase activity of EGFR is not required for this constitutive activation. However, stimulation by EGF increases the binding capacity of STAT3 to DNA (245). ErbB2 is involved in a variety of cancers. Autocrine secretion of prolactin leads to the activation of JAK2, which constitutively phosphorylates ErbB2 in human breast cancers (246). Another study showed cellular invasion in head and neck squamous cell carcinoma through EPO mediated activation of the JAK2/STAT5 pathway (247).

5.6 Biochemical properties of JAK2

5.6.1 Kinetic parameters

Enzyme kinetic assays, which determine the catalytic activity of the enzyme and the affinity of its substrates and inhibitors, have become important for functionally characterizing the biochemical properties of a kinase. These assays are time dependent and provide a measure of kinetic constants, which aid in elucidating the mechanisms of catalysis and regulation. In general, kinetic assays help in understanding the binding processes. An enzyme reaction starts with the binding of a substrate to an enzyme and ends with conversion into product. Binding is the first step to be examined when investigating the nature of the enzyme. This is followed by investigating the role of inhibitors and second substrates. The simplest kinetic reaction can be formulated as:

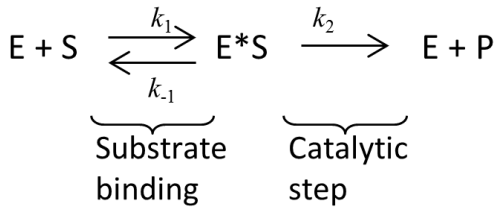

The first step in the reaction is described as substrate binding and is determined by two rate constants. k_1 is the second-order rate constant and k_{-1} is the first-order rate constant for the formation of ES. The second step of the reaction is described as the catalytic step and k_2 forms the rate constant. Sometimes, it is also referred to as k_{cat} (catalytic constant).

For kinases, the kinetic parameters are derived by measuring the initial rates of phosphorylation (when there is less than 10% product formation). This mainly depends on the amount of the catalytic enzyme [E] << [S] and usually requires high enzyme activity, with no impurities. The relationship between the substrate concentration and the reaction rate can be quantitatively expressed and is given by the Michaelis-Menten (MM) equation:

$$V_0 = \frac{V_{max}\,[S]}{K_m + [S]}$$

where K_m is the Michaelis constant, the substrate concentration when the reaction velocity is ½ V_{max}, V_{max} is the reaction velocity at the maximum substrate concentration and V_0 is the initial reaction rate. While V_{max} is used as an indicator of an enzymes' catalytic efficiency, K_m defines the rate limiting step that is useful for evaluating the effects mutations might have on a protein's function in some diseases. The two most common representations of the MM equation are the Michaelis-Menten representation and a linear graphical representation called the Lineweaver-Burk plot shown in Figure 10.

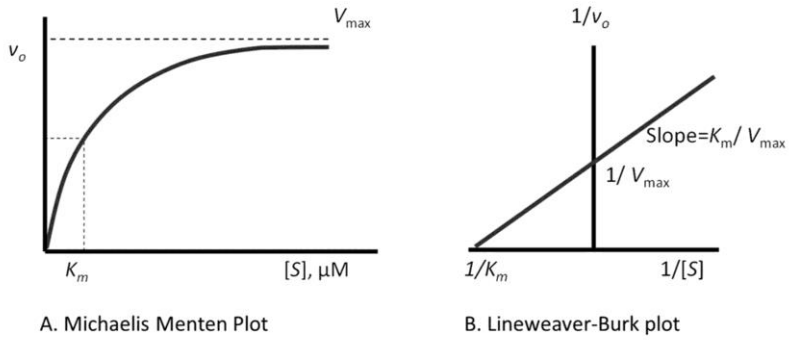

Figure 10. Representation of Michaelis-Menten plot (A) and linear Lineweaver-Burk plot (B).

The purification of the JAK2 protein has been a challenge ever since its discovery in 1992. Soluble forms of JAK2 are a prerequisite for detailed enzymatic characterization studies. At the beginning of the studies described here, the kinetic properties of JAK2 had been measured, but the influence of the JH2 domain on the kinetics was unclear. During the completion of this thesis, a couple of reports on the kinetics and the role of each domain in the regulation of JAK2 activity were published. These studies are reviewed in the Discussion.

The relative measure of the affinity of a compound/substrate for its enzyme is given by how strongly a compound binds to the enzyme. It is the equilibrium constant for the bound versus unbound ligand and is defined as the dissociation binding constant (K_d).

$$K_d = \frac{[E]*[S]}{[ES]}$$

The most commonly used methods for measuring affinity are radioligand labeling and fluorescence resonance energy transfer (FRET) using fluorescent analogs of the ATP. Both techniques have pitfalls and problems in measuring the amount of radioactivity that is removed can lead to an inaccurate K_d determination.

5.6.2 JAK2 inhibitors and their IC50 specificity

The concept of targeted therapies against diseases started with the discovery of inhibitors. Since protein phosphorylation is a key feature of cellular processes, the discovery of small molecule inhibitors against kinases has sparked interest in testing and approving several novel drugs. The selectivity and specificity of inhibitors is a challenge in drug design, not to mention the strong side effects. However, over the years efforts have been made to improve the inhibitors of JAKs, particularly of JAK2 and JAK3. JAK2 inhibitors show a specificity of < 200 nM and <500 nM in *in vitro* kinase assays and cell-based assays, respectively, when using cell lines that harbor the $V^{617}F$ mutation and hematopoietic progenitor cells from MPN patients. Similar effects are also seen in *in vivo* studies in murine models.

Several JAK2 inhibitors that are currently in different phases of clinical studies have specificities (in terms of IC50) ranging from 0.4 – 55 nM. Other non-selective JAK2 inhibitors have IC50 values of over 10 μM. One of these is WP.1066, which has not been used in clinical trials, even though it was the first JAK2 inhibitor to be identified in a high-throughput screen in 1995 (248). Subsequent research led to the discovery of more specific JAK2 inhibitors and these are grouped into two types. Type I inhibitors are competitors of ATP and bind to the active conformation of the kinase. Type II inhibitors bind and stabilize the inactive JAK2 kinase. There is also a third type of inhibitors called Type 1 ½ whose selectivity is based on the active conformation of the kinase, and the back pocket of ATP offers additional options for modulating selectivity (249, 250), since these can be targeting for both active and inactive kinases. Currently all of the JAK2 inhibitors in clinical studies are of type I, and improved efficacy within the other classes may be achieved in the future.

Name	IC50 (nM)	Company	Clinical trial stage	References
Ruxolitinib	0.036 – 4.5	Novartis	Approved, in market	(2-5)
TG101209	6	TargeGen		(6, 7)
TG101348	3	TargeGen	Phase II	(8-10)
INCB16562	2			(11)
Baricitinib (INCB028050)	5.7	Pfizer	Phase II/III	(12)
Pyridone 1	2.1			(13)
Pyridone 6	1			(14)
AZD1480	0.4	AstraZeneca	Phase II	(15)
XL019	2	Exelexis	Phase I	(16-18)
AT9283	1.2			(19, 20)
Lestauritinib (CEP-701)	1	Cephalon	Phase II	(21, 22)
CEP33779	1.8			(23, 24)
AZ960	3	AstraZeneca		(25)
R723	2			(26)
CYT387	18	TM Biosciences	Phase II	(27, 28)
BMS-911543	1.1	BMS	Phase I/II	(29)
NVP-BSK805	0.5			(30)
SGI1252	2-19			(31, 32)
Pacritinib	19-22	Onyx	Phase I/II	(33, 34)
LY2784544*	55	Eli Lilly & Co	Phase I	(35)
AC430	>1 μM	Ambit BioSciences	Phase I	reviewed in (36)
AEG41174	>1 μM	AEgera	Phase I	reviewed in (36)
WP-1066	2.3 μM			(37)
AG490/Tyrphostin B42	10 μM			(38)
Tofacitinib/CP690550#		Pfizer	Approved, in market for RA	(39)

Table 5. Detailed list of JAK2-targeting inhibitors that are currently under development [modified from (216, 250, 286, 289-292)]. *JAK2/Bcr-Abl, #Primarily for JAK3 with IC50 1nM, but 20-100-fold less potent versus JAK2/JAK1; RA: rheumatoid Arthritis

Some common Type I inhibitors of JAK2 are ruxolitinib, AZD1480, CYT387, pacritinib, CEP-701, LY2784544 and BMS-911543. To date, there is only one Type II inhibitor for JAK2 that is known to bind an inactive JAK2. NVP-BBT594 was shown to inhibit JAK2 activity (by abolishing the phosphorylation of the JAK2 activation-loop) and display an anti-proliferative effect in JAK2 $V^{617}F$ cells (251). A detailed list of the JAK2 inhibitors with their IC50 specificities is shown in Table 5.

Two random studies on phase III clinical trials made ruxolitinib the first small-molecule inhibitor of JAK2 to be approved by the FDA. It is currently administered for treating myelofibrosis, cancer and inflammatory diseases, and it was put on market in the USA in November 2011, followed by Europe in 2012. Another JAK (JAK3) inhibitor on the market is tofacitinib, which is currently the only available drug against rhematoid arthritis.

6. OBJECTIVES OF THE (PRESENT) STUDY

The discovery of the JAK/STAT pathway dates back twenty years, to when the first JAKs were cloned in 1990s. During the years that followed, scientists have succeeded in understanding the essential role of the JAK/STAT pathway in cytokine signaling, hematopoiesis, and its critical involvement in cell growth, survival and development, and in the differentiation of immune cells (293-295). JAK kinases form a very attractive target for therapeutic interventions in many disease states such as cancer, inflammation, autoimmune disorders and myeloproliferative disorders. Efforts have been made to address questions on the regulation of JAK and its relation to several diseases as a result of constitutive activation, uncontrolled growth and tumourigenesis. When I started my PhD project in 2008, the crystal structure of the JAK2 tyrosine kinase domain had been solved and questions regarding the intramolecular regulation between the kinase and pseudokinase domains were unanswered largely due to the difficulties in purifying these proteins. We have made major efforts towards developing methods to produce and purify recombinant JAK2 domains.

The role and mechanism of the JAK domains was a mystery, and our focus was on understanding the role of the JH2 and JH1 domains in regulating JAK2 activation.

The specific aims of this study were:

1) To analyze the function of the JH2 domain of JAK2 with special emphasis on its role in the regulation of JAK2 activity.

2) To characterize the kinetic properties of the JAK2 JH1 domain and its interaction with ATP and to understand this affinity using a FRET application and an *in vitro* filter binding assay.

3) To characterize the effects of the different domains of JAK2 on its kinetic parameters and to understand the role of the $V^{617}F$ mutation on the regulation of JAK2 activity using a peptide microarray analysis.

7. MATERIALS AND METHODS

7.1 DNA constructs and cloning

A schematic representation of the JAK2 protein and the positions of the point mutations that were incorporated are shown in Fig. 11.

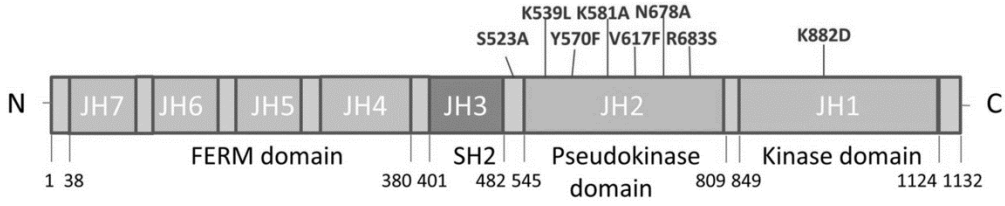

Figure 11. Diagram of the JAK2 domains with amino acid positions shown in the bottom. The point mutations described in Article I are shown above.

Human JAK2 (GenBank accession no. NM_004972.3) constructs with either a GST (glutathione S-transferase) or poly 6X Histidine tag containing a cleavable thrombin site comprising of different boundaries were cloned into the pBASTBAC1 vector (Invitrogen) for expression and recombinant purification in *Sf*9 cells using baculovirus mediated transfection. The Bac-to-Bac® Baculovirus expression system (Invitrogen, version D, 2004) was used for this purpose. The plasmids were transformed into DH10BacTM *E.coli* competent cells. Post-transformation, the cells were plated on LB plates containing 50 μg/ml kanamycin, 7 μg/ml gentamycin, 10 μg/ml tetracyclin, 100 μg/ml X-Gal and 40 μg/ml IPTG and incubated for 48 h at +37°C. The white colonies picked from a blue/white screening were restreaked onto LB plates. The plasmids were purified from the restreaked bacteria inoculated in LB media containing selective antibiotics. The plasmids are shown in Table 6. All of the mutant constructs made in this study were cloned in a similar manner (see section 7.2).

Baculovirus

PLASMID	BOUNDARIES	MUTATIONS	USED IN
JH2-GST	513-827	WT	I
JH1-GST	836-1132	WT	I
JH2-GST	513-827	$K^{581}A$	I
JH2-HIS	513-827	$S^{523}A$	I
JH2-HIS	513/536-827	$Y^{570}F$	I
JH2-HIS	513/536-827	WT	I, III
JH1-HIS	836-1132	WT	II
JH1JH2-HIS	513-1123	WT	III
JH1JH2-HIS	513-1123	$V^{617}F$	III
JH1JH2-HIS	536-1123	$V^{617}F$	III
JH1-HIS	836-1132	WT	III

Table 6. Expression plasmids used for recombinant protein purification.

Mammalian

The DNA constructs for mammalian expression cloned into the pCI-neo (Promega) vector are shown in Table 7.

PLASMID	BOUNDARIES	MUTATION	USED IN
Full length-HA	1-1132	WT	I
Full length-HA	1-1132	$Y^{570}F$	I
Full length-HA	1-1132	$S^{523}A$	I
Full length-HA	1-1132	$K^{581}A$	I
Full length-HA	1-1132	$K^{882}D$	I
Full length-HA	1-1132	$V^{617}F$	I
Full length-HA	1-1132	$K^{539}L$	I
Full length-HA	1-1132	$R^{683}S$	I
Full length-HA	1-1132	.del JH1, WT	I
Full length-HA	1-1132	$K^{581}R$	I
Full length-HA	1-1132	$N^{678}A$	I
JH2-HA	513/536-827	WT	I
JH2-HA	513/536-827	$K^{581}A$	I
JH2-HA	513/536-827	$V^{617}F$	I
STAT5 Full length	1-794	WT	I
STAT1 Full length	1-750	WT	I

Table 7. Expression plasmids used for mammalian cell culture.

Other general expression plasmids used in the study are presented in Table 8.

PLASMID	SOURCE/REFERENCE	MUTATION	USED IN
STAT5 Full length	Dr. Bernd Groner (40)	-	I
STAT1 Full length	David E. Levy, NYU	-	I
Gas Luciferase	Dr. Richard Pine (41)	-	I
Spi Luciferase	Dr. Timothy Wood (42)	-	I
pCi- Neo vector	Promega, Madison, WI	-	I
pFASTBac1	Invitrogen, CA	-	I, II, III
hJAK2	Dr. Stefan Constantinescu	-	I, II, III

Table 8. Original expression plasmids and their source/references.

7.2 Sequencing and sequence analysis

All the DNA clones were sequenced using Perkin Elmer's ABI 310 automatic DNA sequencers and the chromatograms were analyzed using an ABI sequence scanner. A multiple sequence alignment was created using the DNA STAR seq Man software. All the JAK2 mutants (shown in Fig.11) used in this study were generated using the QuikChange® Site-Directed Mutagenesis method (Stratagene) and verified by sequencing.

7.3 Cell culture

JAK2 deficient γ2A cells

HT-1080, a human fibrosarcoma cell line, ATCC CCL-121 derived from a JAK2 negative cell line which is resistant to the antibiotic geneticin (299) was cultured in Dulbecco's modified Eagle's medium (DMEM) (Sigma/Lonza, Basel, Switzerland) supplemented with 10% (vol/vol) FBS (Gibco), 2 mM L-glutamine (Sigma-Aldrich St. Louis, Mo, USA), 100U/ml penicillin and 100 μg/ml streptomycin (Lonza, Basel, Switzerland) at +37ºC in a humidified incubator containing 5% CO_2.

Sf9 insect cells

The *Spodoptera frugiperda* (*Sf9*) insect cells were cultured using the Hyclone SFX insect cell medium (Thermo Scientific) with no other supplements in a shaking incubator maintained at +27°C without any CO_2. The insect cells were derived as described elsewhere (300, 301). The cell density was always maintained at 2.0×10^6 cells/ml to obtain healthy viable cells. Cells that were at least 95% viable were used for further transfections.

7.4 Antibodies and cytokines

NAME	DETAILS	SOURCE/REFERENCE	USED IN
Anti-HA (anti-influenza virus hemagglutin epitope)	clone 16B12, mouse monoclonal	Covance, Princeton, NY, USA	I, III
Anti-phospho tyrosine	PY-20, mouse monoclonal, FITC conjugated	Exalpha Biologicals Inc, MA, USA	III
Anti-phospho tyrosine	PY-99, mouse monoclonal	Santa Cruz Biotechnology, Santa Cruz, CA, USA	III
Anti-phospho tyrosine	4G10, mouse monoclonal	Millipore	I
Anti-phospho JAK2 (1007, 1008)		Cell Signaling Technology,	I
Anti-phospho Serine (523) of hJAK2	Rabbit monoclonal	(43)	I
Anti-phospho tyrosine (570) of hJAK2		(44)	I
Anti-phospho STAT1 (Y^{701})	Rabbit polyclonal	Cell Signaling Technology	I
Anti-phospho STAT5 (Y^{694})	Rabbit polyclonal	Cell Signaling Technology	I

Anti-JAK2	Clone 1067, rabbit polyclonal	Silvennoinen *et al.*, 1993 (Made in Memphis, St. Jude Hospital, USA)	I
Anti-STAT5	Monoclonal, ST5a-2H2	Zymed Laboratories	I
Anti-GST	Rabbit monoclonal	Sigma Aldrich, Saint Louis, Missouri, USA	I
Biotinylated IgG	anti-mouse/anti-rabbit polyclonal	Dako A/S, Glostrup, Denmark	I, III
Horseradish peroxidase	Streptavidin biotinylated	GE Healthcare, Little Chalfont, UK	I, III
IFN-γ	Human recombinant IFN-γ	R&D Systems	I
Erythropoietin (Epo)	Human recombinant Epo	Janssen-Cilag Oy, Finland	I

Table 9. Antibodies and cytokines used in this study

7.5 Cell line transfections

γ2A cells

JAK2-deficient γ2A cells were plated in 6- or 12-well plates at a total amount of 2.0×10^5 cells/well in 1 ml of DMEM medium with 10% FBS together with antibiotics and glutamine before the day of transfection. Next day, the cells were transfected using the FuGeneTM6 transfection reagent (Roche Diagnostics, Indianapolis, IN) according to manufacturer's instructions. JAK2 wild type (1 μg), mutants (1 μg), STAT1 (0.2 μg) or STAT5 (0.2 μg) and human EpoR (0.5 μg) constructs were transfected at a 6: 1 FuGENE to DNA ratio. After 8 h, the cells were either harvested by cell lysis or were starved for 12 h in serum-free media followed by either treatment with either 100 U/ml of hIFN-γ or 50 U/ml of hEpo.

*Sf*9 cells

All of the *Sf*9 cell transfections were done using the Cellfectin® reagent (Invitrogen) according to the manufacturer's instructions. 1×10^6 cells/ml plated on 6-well plates were allowed to attach for 1 h at +27ºC and transfected with Cellfectin and 1 μg of Bacmid DNA mixture for 30 min, which was later replaced with 2 ml of Hyclone SFX cell media, after which the cells were for 6 h. Fresh

media was then added and the infected cells were incubated for 72 h. The P1 virus collected after 3 days transfection was used as initial inoculum for further stages of amplification.

7.6 Cell lysis, Immunoprecipitation and Immunoblotting

7.6.1 Cell lysis

γ2A cells were lysed for western blotting and immunoprecipitation. Cells on 6- or 12- well plates were washed with 1X ice cold PBS (pH 7.4) and harvested by scraping followed by lysis in Triton-X lysis buffer (50 mM Tris-HCl (pH 8.0), 150 mM NaCl, 100 mM NaF, 10% (v/v) glycerol, 1% (v/v) Triton-X and a protease inhibitor cocktail) for 30 minutes followed by centrifugation at 16000g for 20 minutes at 4ºC.

7.6.2 Immunoprecipitation

For the detection of protein phosphorylation, cells were transiently transfected as described in section 7.5. The cell lysates containing HA tagged JAK2 proteins were incubated with an anti-HA or an anti-JAK2 antibody for 2 h and then mixed and rotated gently with protein G sepharose beads (Sigma Aldrich) for an additional 1 h. All the immunoprecipitation steps were carried out at 4 ºC. The beads were washed twice with lysis buffer and the proteins were eluted with 2X or 4X SDS sample buffer by boiling for 5 min, and then centrifuged at 13000 g for 1 minute at room temperature.

7.6.3 Immunoblotting and analysis of protein phosphorylation

Analysis of JAK2 signaling in mammalian cells was done by subjecting the boiled and centrifuged lysates to western blotting. Equal amounts of lysates were run on 6% or 10% SDS-PAGE gels. The SDS-PAGE gels were transferred to a nitrocellulose membrane (WhatmanTM Protran BA85, 0.4 μm, GE Healthcare, Germany) and blocked with 5% non-fat dried milk in TBS 0.1% Tween 20 or in 5% BSA with 0.05% Tween 20. The membranes were incubated with specific

primary antibodies (anti-HA for STAT1, JAK2 proteins, anti-JAK2 antibody for JAK2 protein and anti-GST antibody for GST-tagged proteins or anti-phosphotyrosine and anti-phosphoserine antibodies) followed by incubation with secondary biotinylated antibodies and then incubating with a streptavidin-biotin horseradish peroxidase complex (see Table 9). Immunodetection was performed with an enhanced chemiluminescence (ECL) method (GE Healthcare, Little Chalfont, UK). When necessary, the membranes were stripped with stripping buffer (100 mM β-mercaptoethanol, 2% SDS, 62.5 mM Tris-HCl, pH 6.8) for 45 minutes at 56ºC shaking water bath. Stripped membranes were washed with TBS buffer 0.05%, 0.1% and 0.5% Tween 20 followed by blocking with 5% non-fat dried milk or 5% BSA.

7.7 Autophosphorylation studies and *in vitro* kinetic assay

For *in vitro* kinase assays, 1 μg of purified JAK2 per reaction was resuspended in kinase assay buffer together with 20 mM $MnCl_2$ or 20 mM $MgCl_2$ or both and 10 mM of unlabelled ATP or 10 μCi [γ ^{32}P]- ATP (Perkin Elmer). The reactions were incubated from 10 to 240 minutes at room temperature and stopped by adding EDTA to a final concentration of 100 mM or by adding 2X SDS loading buffer and separated on 7% or 10% SDS PAGE gel. Gels were dried for 45 minutes in a gel dryer (BioRad), exposed onto an X-ray film in an autoradiography cassette (BioRad) at -80ºC for 12–24 h and visualized by autoradiography. Alternatively, the phosphorylation states of JH2 from two different peaks post anion-exchange chromatography were run on a native PAGE (PhastGel System, GE Healthcare) and western blotted.

7.8 *In vitro* translation

A JH2 insert cloned into a T7 promoter containing pCI-neo vector was used as a template for an *in vitro* translation reaction using the TNT-reticulocyte lysate kit (Promega). The translation procedure was performed using a radioactive [^{35}S] methionine system. The standard reactions with and without insert were set up according to the manufacturer's instructions. The *in vitro* translated JH2 was subjected to an *in vitro* kinase reaction using 5 mM ATP and 10 mM $MnCl_2$ and the autophosphorylation of JH2 was analyzed by western blotting as described in

sections 7.7 and 7.6.3. Alternatively, an HA tagged wild type JH2 and a $K^{581}A$ JH2 cloned into pT7CEF1-CHis vector were used for protein purification and *in vitro* translation (Pierce *in vitro* translation kit). All the procedures were carried out according to the manufacturer's instructions. *In vitro* translated proteins were purified by making use of the His tag and further used in an *in vitro* kinase assay with labeled γ- ^{32}P- [ATP] for 30 minutes and run on SDS PAGE gels. JH2 phosphorylation was subsequently analyzed by autoradiography.

7.9 MANT-ATP direct binding studies

The fluorescent ATP analogs with a modified ribose hydroxyl group such as 2'/3'-*O*-(*N*-methylanthraniloyl) adenosine-5'-triphosphate (MANT-ATP) were used in this enzyme-ligand binding study in Article II. 0-88 μM of MANT-AXP (where X is adenosine-5'-triphosphate, adenosine-5'-diphosphate, adenosine-5'-monophosphate or adenosine-5'-thio-triphosphate) was incubated for 1 minute at 21ºC in a quartz cuvette (Perkin Elmer) with a buffer containing 10 mM $MnCl_2$, 20 mM Tris-HCl, pH 8.0, 200 mM NaCl, 10% glycerol, 1 mM TCEP and 1X PK buffer with or without 0.5 μM of the purified JH1. All of the measurements were collected at 300-500 nm after exciting at 280 nm or collected at 350-550 nm on exciting at 340 nm using a QuantaMaster spectrofluometer (Photon Technology International) equipped with PowerArc xenon lamp as an excitation source. Excitation and emission slit widths resulting in a band pass of 2 nm were chosen. The entire spectrum that was collected was corrected for the dilution of the added MANT nucleotides.

7.10 Protein expression and recombinant purification

The P1 virus (generated as described in section 7.5) was amplified by infecting insect cells at 1×10^6 /ml 1% (v/v) of the virus and grown at +27ºC in bottles in a shaking rotator spinning at 100 rpm. After 72 h the supernatant was collected and the procedure was repeated for the P2, P3 and P4 virus stages. Either the P3 or the P4 stage virus stock was used for protein expression. For the final recombinant purification, 3×10^6 /ml insect cells in bottles were infected with 10% (v/v) of the P4 virus stock and incubated for 48 h at +27ºC with continuous shaking. After the desired incubation time, the cells were collected by centrifugation at 2000g for 5

minutes at +4ºC and the cell pellets were either lysed or stored at -20ºC (short term) storage or at -80ºC (long term).

His- and GST-tagged JAK2 constructs were purified using Ni-NTA agarose (Qiagen) and Glutathione SepharoseTM 4B (GE Healthcare), respectively. Cell pellets were resuspended in lysis buffer (20 mM Tris-HCl, pH 8.5, 500 mM NaCl, 15% (v/v) glycerol, 0.5 mM TCEP). For His-tagged proteins 20 mM imidazole was added to the buffer. The resuspended cells were further supplemented with protease inhibitors (Roche) and incubated in ice or gently rotated at 4ºC for 30 min. The cells were lysed using a cell sonicator (SONICS or Avestin). The sonicated cell lysates were cleared by centrifugation for 1 h at 45000g or 14000g. The supernatant was incubated with the respective beads for 2 h at 4ºC with constant rotation. Post incubation, the beads were washed with wash buffer three times. The protein was eluted with 250 mM imidazole or with 10 mM glutathione, depending on the beads that were used for binding. The fractions were pooled and dialyzed in dialysis buffer (20 mM Tris-HCl, pH 8.5, 250 mM NaCl, 15% (v/v) glycerol and 0.5 mM TCEP) for 2 h at 4ºC using Slide-A-Lyser® dialysis cassettes (Thermo Scientific), in order to remove the imidazole or glutathione. When necessary, the buffer was changed at 1 h intervals. For the JH2-His, JH1-His, JH1JH2WT-His, JH1JH2V617F 510-His and JH1JH2V617F 536-His fusion protein, the samples were incubated with 10 U/ml of thrombin (Enzyme Research Laboratory) overnight after dialysis. When necessary, the samples were concentrated using an Amicon Ultra-4 centrifugal filter devise (Millipore) Ultracell-10k or a Micon Microcon® centrifugal filter devise (Millipore) Ultracell -YM-10 and centrifuge for for 5 minutes at 5000 g at 4ºC several times until a concentration of 0.5 mg/ml or 1 mg/ml was reached. Protein concentrations were measured using the Quick StartTM, Bradford Dye Reagent (BioRad Laboratories, Hecules, Ca, USA) based on the manufacturer's instructions.

To further purify the proteins, the pooled-concentrated protein fractions were subjected to anion exchange chromatography. A low salt buffer (20 mM Tris-HCl, pH 8.5, 25 mM NaCl, 15% (v/v) glycerol and 0.5 mM TCEP) was used to equilibrate the MonoQ 5/50 GL column (GE Healthcare) using an automated ÄKTA purifier system (GE Healthcare). Proteins were loaded onto the pre-equilibrated column and were eluted with a linear gradient of 1–200 mM NaCl. Differently phosphorylated forms of JH2 proteins were also eluted in a similar fashion, but using 1M NaCl. Fractions were pooled and the protein concentration was measured using the Bradford method. Fractions containing GST-JH2 were

also analyzed by Coomassie staining. For GST-JH1, the protein was purified as described (168).

7.11 PamChip® peptide microarrays

All the incubations and kinetic read outs from the PamChip® peptide microarrays, described in Article III, were performed on a PamStation 96 instrument® (PamGene International BV). PamChip arrays are based on porous three-dimensional layer of oxidized aluminium (Al_2O_3) called anapore. The branched Al_2O_3 used for these reactions has a solid, brittle large internal surface and up to 400 different peptides are covalently immobilized on each array by condensation process. The surface gets translucent when in contact with water which facilitates pumping up and down of sample (20-40 µl/array) actively through the pores allowing real-time detection of fluorescent signals. The continuous pumping of the sample through this 3D surface enables the test to be completed in less than an hour. Diffusion of the samples is not a rate-limiting factor in these reactions and incubation is homogenous. An additional benefit of this method is that a real-time kinetic readout is possible in relation to time and different peptide concentrations. This technology was utilized to perform the high-throughput kinetic analysis of different domains of JAK2 with different variables such as ATP (Sigma Aldrich), peptide and inhibitors as described elsewhere (302, 303). Depending on the experimental set up, the incubations were performed at 30ºC. Peptide microarrays were blocked with 2% (w/v) BSA (NEB) in water for 30 cycles and washed three times with a protein kinase (PK) buffer from NEB (50 mM Tris-HCl, pH 7.5, 10 mM $MgCl_2$, 0.1 mM EDTA, 2 mM DTT and 0.01% Brij-35). All the kinase reactions for JAK were 25 µl and included 1X PK buffer, 1X BSA, 12.5 µg/ml fluorescein-labeled PY20 antibody and varying concentrations of ATP. The reactions were incubated for 60 cycles of pumping up and down through the pores of the microarrays at a rate of 2 cycles per minute. Images of each array were taken after every second cycle by an integrated 12-bit charge couple device (CCD) -based optical system. The readout through PY20 antibody works as follows: excitation light required for detecting fluorescein dye is provided by light-emitting diode (LED). The excitation light is guided to a position above one array of the PamChip® through an angled mirror. The light of each LED is guided through appropriate FITC filter and this allow imaging in different wavelength ranges (excitation light at 460-490 nm and emission wavelength at 515-550 nm) suitable

for FITC fluorescence. The LED can detect fluorescein dye. A schematic representation of the PamChip array workflow is shown in Figure 12.

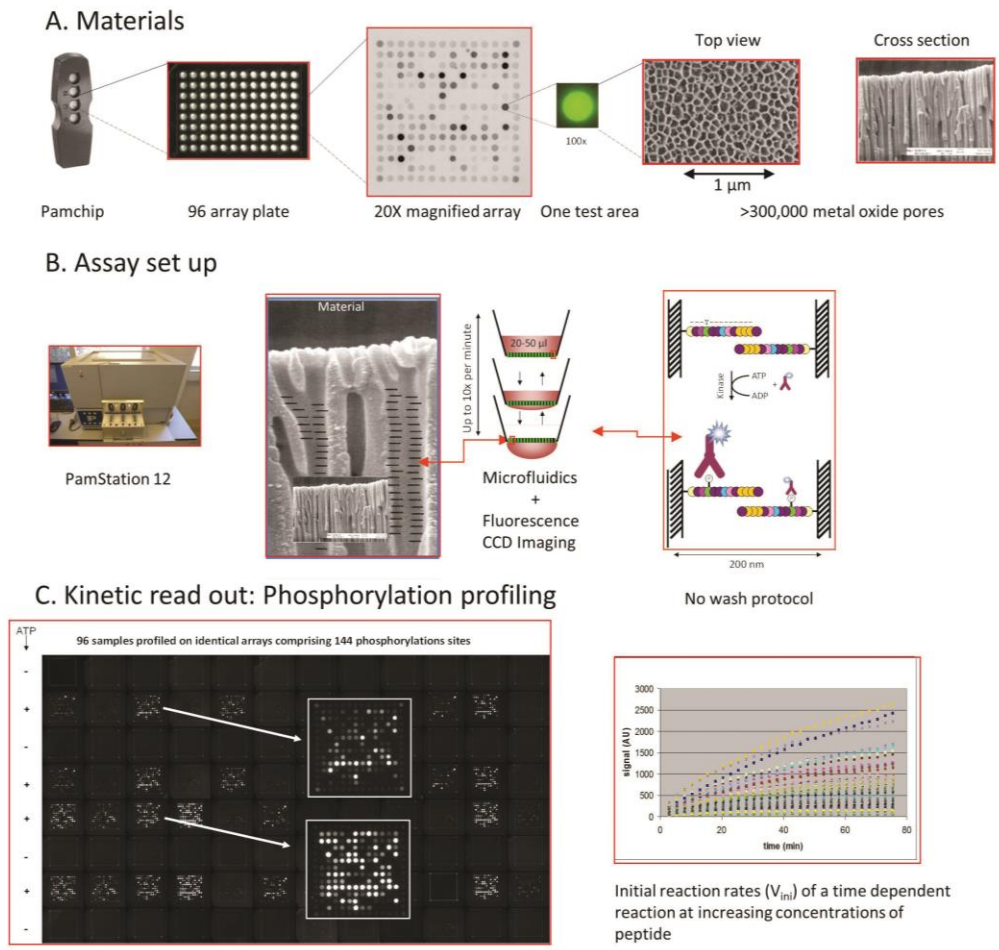

Figure 12. Schematic workflow of the PamChip® array experiment set-up. A. Arrays are positioned in the shape of a 96-well plate, with a 3-dimensional porous Aluminium oxide surface in each well. B. The fully integrated and automated PamStation® 96 enables the incubation of samples and also pumps the incubation mixture (JAK2 kinase, ATP and kinase buffer) up and down through the microarray. This microarray consists of up to 256 peptides, representing kinase substrates. C. Mixing and live monitoring of the assay takes place in real time and corresponds to the kinase reaction kinetics, in which the kinetic readout is peptide's phosphorylation.

Data generated from the PamChip peptide microarrays were analyzed with the Bionavigator® software. The signal intensity from each spot together with its background was quantified and signal minus background was calculated. The values were fitted against the time series representing different peptide concentrations using an equation for exponential association $y = y_0 + y_{max} (1 - e^{-kc)}$, where y is the signal intensity at each cycle of measurement, k is the reaction rate constant, and c is the cycle number when the image was recorded. The initial velocity of peptide phosphorylation (V_{ini}) was determined using the equation $V_{ini} = y_{max} * k * e^{-kc}$. Subsequently, the V_{ini} values were exported either to Microsoft excel or directly to the Sigma Plot® software for further data analysis to characterize the reaction mechanism that was followed by the different JAK2 proteins. Additionally, different phosphorylation patterns of peptides were monitored and changes in this phosphorylation were monitored together in the presence of ATP-competitive inhibitors such as AMP-PNP (Roche) and ADP-β-S to describe the inhibitory profile of the JAK2 protein.

7.12 Luciferase reporter gene assay

A luciferase assay was done using the γ2A cells. γ2A cells were transfected with either STAT1 or STAT5 together with other plasmids as described in section 7.5, and with β-galactosidase and other JAK2 constructs of interest. After transfection, starvation and stimulation for a given time (see section 7.5), the cells were lysed in 1X reporter lysis buffer (RLB) (Promega, Madison, WI, USA). The transcriptional activities of STAT1 and STAT5 with wild type and $K^{581}A$ JAK2 were measured using the GAS-luc STAT1 reporter or the SPI-luc2 STAT5A reporter according to the manufacturer's instructions. The luciferase activity was measured using Luciferase Assay Reagent (Promega, Madison, WI, USA) and normalized with the β-galactosidase activity of the lysates, determined using ONPG (*O*-nitrophenyl-β-D-galactopyranoside) as a substrate. The absorbance was measured at 420 nm using a Luminoscan Ascent 96-well plate luminometer (ThermoElectron Corporation, Finland).

8. RESULTS

8.1 Catalytic activity of the JAK2 pseudokinase domain (Article I)

8.1.1 Serine 523 and Tyrosine 570 are putative phosphorylation sites in JAK2JH2.

JH2 was previously shown to negatively regulate JAK2 signaling (130, 132). In addition, deletion of the JH2 domain was shown to increase the basal activity of JAK2 (131). Since JH2 negatively regulates JAK2 activity, we addressed the role of JH2 in JAK2 regulation in more detail. In order to find out precisely how JH2 regulates JAK2 activity, JH2 had to be purified by recombinant methods. The functional characterization of JAK2 has been compromised by difficulties in purification of JAK2 recombinant protein. Here, we have overcome these challenges and have successfully purified JAK2JH2 with both histidine and GST tags in insect cells (*Sf9*). Purified JAK2 JH2 proteins were used to further investigate the role of JH2.

In an *in vitro* kinase assay, wild type (WT) JH2 preferred Mn^{2+} and was phosphorylated in a time dependent manner unlike its kinase dead mutated JH2 ($K^{581}A$) (I, fig. 1a,b and fig. S3c). However, the activity of JH2 was very low compared with the active JH1 domain. To rule out contaminating kinases, *in vitro* translated JH2 WT and JH2 $K^{581}A$ were subjected to immuno blotting. This showed that the WT JH2 was phosphorylated on a tyrosine residue. Surprisingly, when purified by anion exchange chromatography JAK2 JH2 appeared as two peaks in the chromatogram. Further, an *in vitro* kinase assay run on fractions from the two peaks showed faster migration of peak 2 on a native gel (I, fig 2b, c). In order to further investigate possible differences in phosphorylation states, we subjected the Coomassie stained JH2 post kinase reactions to MS-MS spectrometry. This revealed two phosphorylation sites (S^{523}, Y^{570}) that were previously reported to negatively regulate JAK2 activity (155, 170). The difference in the phosphorylation states is attributed to S^{523}, which was phosphorylated from time zero (higher activity as shown by peak 2) compared with Y^{570} which was phosphorylated (low activity as shown by peak 1) over the time in the kinase reaction. Additionally, when S^{523} was mutated to alanine, phosphorylation at Y^{570}

was abolished (I, Fig. 3b), but the opposite did not hold true, indicating that S^{523} is the default phosphorylation site in JH2 and regulates the subsequent phosphorylation and activity of JH2.

In order to further characterize the binding affinity of JH2 to ATP, *in vitro* direct binding studies with MANT-ATP [2'/3'-*O*-(*N*-methylanthraniloyl) adenosine triphosphate] were done. The K_d of the binding was 1 μM. Put together, the findings suggest that the JH2 of JAK2 is catalytically active and is phosphorylated on two residues, Y^{570} and S^{523}. Thus, JH2 is not a tyrosine kinase but a dual-specificity kinase. This also suggest that JH2 can bind ATP with low affinity.

8.1.2 Phosphorylation of JH2 in JAK2 deficient γ2A fibrosarcoma cells

Phosphorylation is a post-translational modification that defines the catalytic activity of kinases. To confirm the results obtained in the *in vitro* set up, we carried out a series of experiments in JAK2-deficient γ2A cells using several constructs. The wild type JH2, the kinase-inactivating point mutation ($K^{581}A$), and mutations at phosphorylation sites $Y^{570}F$ and $S^{523}A$ in the JH2 domain all in the context of the full length JAK2 protein were overexpressed in fibrosarcoma cells. JAK2 phosphorylation was then analyzed by western blotting. All of the JAK2 constructs were immunoprecipitated from total cell lysates using an anti-hemagglutinin (HA) antibody and immunoblotted with anti-phospho ($Y^{1007, 1008}$), anti-phospho (Y^{570}) or anti-phospho (S^{523})antibodies. As expected, the mutations to S^{523} and Y^{570} resulted in increased JAK2 tyrosine phosphorylation compared with wild type as could be seen by the phosphorylation of the activation loop at $Y^{1007, 1008}$ (I, Fig.4a). The $K^{581}A$ JAK2 mutant was phosphorylated at a higher level than the wild type JAK2, but phosphorylation was completely abolished at the S^{523} and Y^{570} sites. This further validated our *in vitro* results and suggested that S^{523} phosphorylation regulates Y^{570} phosphorylation. However, the JH1 inactivating mutation $K^{882}D$ abolished JH1 activity, but showed phosphorylation on S^{523} and Y^{570} (I, Fig. 4c). These results suggest that phosphorylation of S^{523} is the first step in the activation of JH2, and that it further regulates the phosphorylation of Y^{570} over time.

8.1.3 Impact of JH2 activity on cytokine receptor-mediated signaling

In order to analyze the effects of JH2 activity on the transcriptional activity of STATs, luciferase reporter assay experiments were carried out in γ2A cells. Two

luciferase reporters, GAS-luc STAT1 and SPI-luc2 STAT5 were independently used to detect the activity of the JAK/STAT pathway in response to stimulation with hIFN-γ or hEpo. The $K^{581}A$ mutation bearing JAK2 displayed a significant increase in basal activity driven by both the STAT1 and STAT5 promoters, but this activity did not increase further upon cytokine-induction (I, Fig. 4f). Consistent with this, we also noticed increased basal phosphorylation of both STAT1 and STAT5 (I, Fig. 4d, e). These data suggest that the catalytic activity of JH2 plays a role in maintaining a low basal activity of JAK2, which implies the possible inhibition of JH1 by JH2 through a direct interaction.

8.1.4 Role of MPN-causing mutations on the catalytic activity of JH2

All the three tested MPN-causing mutations ($V^{617}F$, $K^{539}L$ and $R^{683}S$) showed increased phosphorylation at $Y^{1007, 1008}$ compared with wild type. However, S^{523} phosphorylation was markedly decreased indicating that these mutations abolished the catalytic activity of JH2 (I, Fig. 5a). The $V^{617}F$ mutation alone completely abolished phosphophorylation of S^{523} and Y^{570} in γ2A cells, similar to $K^{581}A$ (I, Fig. 5b). Taken together, these results show i) JH2 is catalytically active and autophosphorylates on S^{523} and Y^{570}, ii) JH2 activity is required for maintaining a basal activity of JAK2 and iii) the $V^{617}F$ mutation annuls the activity of JH2, which leads to an increase in the basal activity of JAK2.

8.2 Determination of the binding affinity of ATP to the JAK2 kinase domain (Article II)

8.2.1 Common factors that affect the intensity of fluorescence resonance energy transfer (FRET)

The most common method used for direct binding studies is fluorescence spectroscopy. In kinase-ATP interaction studies, *N*-methlyanthraniloyl (MANT) analogs of ATP are used to determine the equilibrium binding constant (K_d). However, common processes/factors that affect the determination of K_d cannot be ignored. Some of these factors are : a) absorbance of the donor fluorophore (MANT-ATP) both at the excitation (the primary inner filter effect) and emission

wavelength (the secondary inner filter effect), b) fluorescence contribution of an unbound fluorophore to the total fluorescence signal, c) quenching of tyrosines or tryptophans by the fluorophores, d) non-specific excitation of fluorophores at wavelengths that excite tryptophans/tyrosines in proteins e) fluorescence generated by a bound ligand-protein complex. All these complicate the K_d determination. If the absorbance of fluorescence starts to interfere by decreasing the actual fluorescence intensity, or if the actual final fluorescence signal is increased due to secondary fluorescence intensities, then its correction becomes absolutely necessary. These factors have been previously overlooked. In this study, we systematically analyze the interfering factors and provide correction procedures for nucleotide-kinase binding measurements using the JAK2 kinase domain as a model.

In general, when a solution containing the JAK2 protein and MANT-ATP is excited at 280 nm, the tryptophans in the protein absorb light and emit at 340 nm. However, the process is not always this simple. Rather, it is accompanied by residual fluorescence from tryptophans at 440 nm. In addition, the process of FRET also leads to energy transfer between the protein and bound MANT-ATP and increases the signal at 440 nm, by reducing the fluorescence at 340 nm. In addition, unbound MANT-ATP also gets excited at 280 nm, and emits at 440 nm. There is an additional process, which is often ignored, that adds secondary fluorescence factors. This is the generation of fluoresence when the MANT nucleotides in solution quench the tryptophans in a protein, which results in a decrease in the fluorescence at 340 nm. Thus, the seemingly simple excitation and emission process of the JAK2-ATP interaction has in fact additional fluorescent species that contribute to false fluorescence intensity (II, Fig. 1).

8.2.2 Determination of the instrument parameters l_p and l_y facilitates the correction of the primary and secondary inner filter effect

When a solution in the fluorescence cuvette is irradiated with a light intensity I_0, then the fluorophores in the solution (in this case MANT-ATP) get excited. On returning to the ground state the fluorophores emit fluorescence. The fluorescence that is generated in the cuvette is captured over a certain width of the cuvette after travelling a distance. l_p is the mean distance of the observed fluorescing sub-volume from the entry wall and l_y is the mean distance of the observed fluorescing sub-volume from the exit wall (II, Fig S2). Although a practical method for

correcting the primary inner filter effect has been developed, no correction protocol has been described for the correction of the secondary inner filter effect. l_p/l, (where l is the length of the excitation path in solution) was determined essentially from a plot of log(A280/F440) versus the absorbance of MANT-ATP at 280 nm and was found to be 0.39. log(A280/F440), when plotted against the absorbance of MANT-ATP at 340 nm yielded 0.46. The fluorescence generated in solution travels, on average, a distance of l_y to the wall of the cuvette and then to the detector (emission path length) and this is assumed to be linear for a short light path of 1 mm (which is otherwise 10 mm in excitation path length). Hence, a value of 0.046 is used for l_y/l to correct for the secondary inner filter effect.

8.2.3 Use of high concentrations of MANT-ATP is possible only when the primary inner filter effect is corrected

According to Beer-Lambert law, the relationship between MANT-ATP and the fluorescence intensity is normally expected to be linear. This, however, applies only at low MANT-ATP concentrations. The fluorescence emission at an observed wavelength shows a linear relation to the MANT-ATP concentration. However, at very high concentrations, the absorbance of incident light is non-linear and a decrease in fluorescence intensity is seen (II, Fig. S3). As a result the primary inner filter effect needs to be corrected for when using high concentrations of MANT-ATP.

8.2.4 Effect of protein fluorescence emission on MANT-ATP and *vice versa*

Two excitation wavelengths (ex 280 and ex 340) are used to study the effect of tyrosine/tryptophan fluorescence emission on MANT-ATP. All our fluorescence measurements showed that tyrosine does not contribute to the fluorescence at 440 nm when the sample is excited at 280 nm and neither tyrosine nor tryptophan affected the MANT-ATP fluorescence at 440 nm. However, when 50 μM MANT-ATP was titrated along with tyrosine, there was a clear shift in the fluorescence intensity. But, after the inner filter effect correction, the fluorescence intensity remained constant during titration with an increasing concentration of tyrosine (II, Fig. 2A). In contrast, when tryptophan was excited at 280 nm, a linear relation between the concentration and fluorescence at 440 nm was observed. When

tryptophan was further titrated with 50 μM MANT-ATP, the fluorescence signal increased, but was no longer linear at increasing tryptophan concentrations (II, Fig. 2B). However, when the fluorescence intensity was corrected for the primary inner filter effect, we could see a linear relation once again, but with increased fluorescence intensity. This suggests that MANT-ATP absorbs the fluorescence emitted by a protein at 340 nm. These results show that the primary inner filter effect correction is necessary, because MANT-ATP can absorb up to 5% of tryptophan's fluorescence.

Similarly, when increasing concentrations of MANT-ATP were used in measuring the fluorescence of tyrosine/tryptophan (ex 280 nm), a clear decrease in the signal was seen, due to increased absorbance at 280 nm. A decrease in the fluorescence was still evident even after the fluorescence intensity was corrected for the primary inner filter effect. This problem was overcome by introducing a correction for the secondary inner filter effect that starts to contribute at concentrations higher than 50 μM (II, Fig. 3).

8.2.5 Fluorescence measurement of nucleotide binding to the JAK2 kinase domain

Although it was known that JH1 binds ATP with a very tight affinity, the equilibrium constant had not been previously determined. A fixed amount of JAK2 JH1 was titrated with increasing concentrations of MANT-ATP, MANT-ADP and MANT-AMP. The fluorescence intensities were corrected for the inner filter effect, and the contribution of each species to F440 (as described in 8.2.1) was calculated for each concentration of MANT-nucleotide, and the K_d was calculated. These data showed that JH1 has a K_d of 15–25 nM and a K_d of 50–80 nM for MANT-ATP and MANT-ADP, respectively (II, Fig. 4). They also showed that MANT-AMP does not bind to JH1 and that JH1 has no additional binding sites.

This method was further extended to determine the binding of competitive inhibitors such as AMP-PNP. The result showed that MANT-ATP was chased from its binding site with increasing concentrations of AMP-PNP. This suggested that AMP-PNP displaced the MANT-ATP from the enzyme complex, as was seen by the decreased fluorescence intensity at 440 nm (II, Fig. 5).

To compare the FRET-MANT affinity measurements to another method, we measured the affinity of JH1 for ATP using a non-hydrolysable radioactive [^{35}S] ATP-γ-S. To do this, we used [^{35}S] ATP-γ-S in a filter binding assay at a starting

concentration of 5 μM, and diluted it serially to a lowest concentration of 100 pM. The final volume of the reaction mixture was 5 μl. 1 μl of the reaction mixture was spotted on to a 25 mm filter membrane (Nitrocellulose Whatman filter membrane, 0.45 μm pore size from GE Healthcare). A vacuum was briefly applied (< 5 s) followed by two washes with ice cold 1X PBS buffer (pH 7.4) and a vacuum was briefly applied to remove the liquid and air dry the membrane. The filter membrane was directly placed in 2 ml of of scintillation liquid (Perkin Elmer) in a 6 ml Pony Vial™ (Perkin Elmer) and counted in a Tri Carb 2910 TR counter (Perkin Elmer) as counts per minute (CPM). Figure 13 shows the average of four independent experiments with a K_d = 0.97 ± 0.33 μM. These results are in line with several earlier studies that have compared the affinities of unmodified ATP and MANT analogs, and found that the MANT analogs bind protein kinases with a higher affinity compared with unmodified nucleotides (304-310).

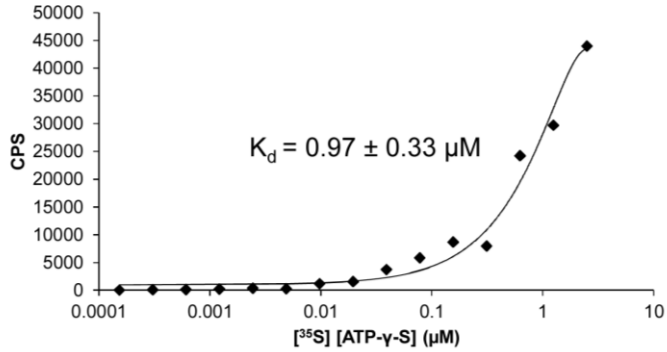

Figure 13. K_d determination using the non-hydrolysable [^{35}S] ATP-γ-S

Taken together, the results show that: a) a correction method for the primary and secondary inner filter effect has to be incorporated into the measurement of K_d, b) the correction method allows the use of high concentrations of MANT-ATP without compromising the method and the K_d determination, c) since MANT-ATP can absorb a fair amount of the tryptophan fluorescence, this has to be corrected for, d) JAK2 JH1 binds MANT-ATP at a K_d value of 15-25 nM depicting a very tight affinity and e) the improved FRET method is expected to help in determining the K_d for any protein-nucleotide complex more accurately.

8.3 Effect of JH2 and the SH2-JH2 linker on JAK2 activity (Article III)

8.3.1 JAK2 JH1 and the tandem JH1JH2 domains follow a random Bi-Bi mechanism

As previously described, the inability to produce JAK2 recombinant proteins has stalled its biochemical characterization. The effects of JH2 and the SH2-JH2 linker were studied using recombinant proteins containing JAK2 JH1 and the tandem JH1JH2 domain. The role of the JH2 domain in JAK2 activation and substrate specificity has been addressed previously (228). In the current study, we exploited PamChip® peptide microarrays to produce full kinetic analyses of the reaction mechanisms of the different JAK2 domains. The tyrosine kinase domain (JH1) and the tandem domains tyrosine kinase JH1 and the pseudokinase domain (JH2) in the wild type and $V^{617}F$ background were subjected to varying concentrations of dead-end inhibitors.

The protein concentration in the microarray was maintained at a range where the kinase activity was linear to the protein concentration. The phosphorylation kinetics of 144 peptide microarrays were monitored simultaneously using the binding of a fluorescent anti-phosphotyrosine antibody. The initial reaction rates for JAK2 catalyzed peptide phosphorylation as a function of varying ATP and peptide concentrations resulted in plots that showed a sequential reaction mechanism. The plot representations gave a series of lines intersecting above the X-axis, confirming a sequential mechanism. The lines intersecting above the X-axis demonstrate that binding of ATP increases the interaction with the peptides. Data for other peptides on the arrays confirmed this observation.

ADP-β-S, a competitive inhibitor of ATP, was used to further understand the kinetics of the JAK2 phosphorylation reaction. The effect of increasing the concentrations of ADP-β-S on JAK2 kinetics was investigated, while varying either the ATP or peptide concentration, with the fixed substrate present at saturating concentrations. Reciprocal plots of 1/V and 1/[peptide] show a non-competitive inhibition pattern for ADP-β-S with the JAK1_1015–1027 and JAK2_563–577 peptides and a competitive pattern with respect to ATP (III, Fig. 1C&D and Fig. 2C&D). Taken together, our results reveal that JAK2 follows a sequential random Bi-Bi mechanism through the formation of a ternary complex.

8.3.2 Kinetic properties of the JAK2 JH2 domain

Since the JH2 domain is able to phosphorylate two regulatory residues in JAK2, the catalytic activity of the JH2 domain alone was investigated on a peptide microarray comprising 256 different tyrosine containing peptides. Incubations were performed in a Mn^{2+} containing buffer, with an increasing ATP concentration (0 – 1000 μM). The peptide phosphorylation was monitored in real time by taking images with an integrated CCD-based optical system. Images were taken 1 minute after the start of the incubation with a JH2 protein assay mix on the PamChip® peptide microarray and every 2.5 minutes after the start of the incubation. The incubation lasted a total of 31 minutes. Images of these arrays with and without ATP are shown (Fig. 15). These arrays show the phosphorylation of several peptides, the most prominent signals are seen for the PHKA6_485–499 (pleckstrin homology domain-containing family A member 6, UniProt ID Q9Y2H5) and DCBD2_743–757 (Discoidin, CUB and LCCL domain-containing protein 2, UniProt ID Q96PD2) peptides (Fig. 14).

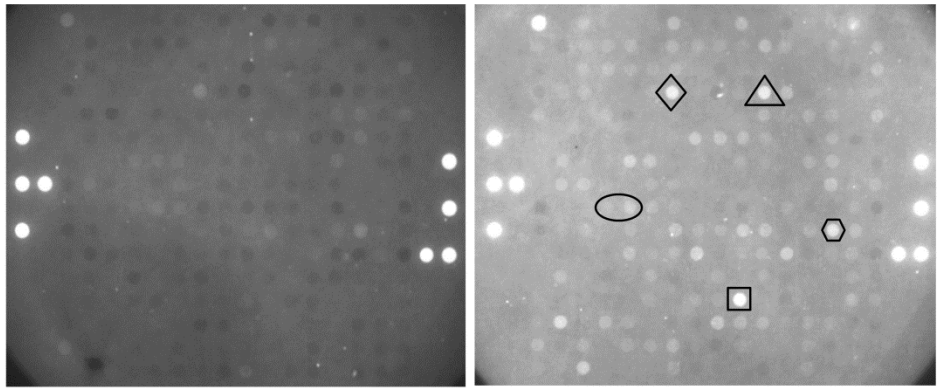

Figure 14. Arrays comprising 256 tyrosine containing peptides, one prephosphorylated peptide and 8 fluorescent gridding spots were incubated with JH2 at no ATP and 1000 μM ATP concentrations. The marked boxes are as follows: square-PKHA6, oval- left JAK1; right JAK2, triangle-DDR2, diamond-DCBD2_743–757, rhombus-MATR3_212–226 (Matrin-3, UniProt ID P43243).

To verify this finding, 5 μl of JH2 (at a concentration of 0.03 pmoles/μl) was incubated with increasing concentrations of ATP (0, 200, 400 and 1000 μM). The PKHA6_485–499 peptide showed neat kinetics with JAK2 JH2 for three ATP

concentrations (Fig. 15). However, V_{ini} did not increase with an increasing ATP concentration. There were many other peptides that showed binding type kinetics i.e the signal that is already relatively high at the start of the reaction and increased slowly in time or remained at a constant level. The peptide JAK2_563–577 (VRREVGDYGQLHETE) shows a comparably high signal at the start of the incubation that increases in time. This signal is absent in the absence of ATP. An example for the binding type kinetics is shown for the peptide ART_003_EAI (pY) AAPFAKKKXC, which is artifical sequence and not derived from any protein. This peptide contains a phosphotyrosine, so the antibody binds immediately. This acts as a positive control for the antibody presence and functionality, as the signal is high already at the first time point.

Although the results of incubations with the JH2 domain and with increasing concentrations of ATP imply that PKHA6 is a probable substrate, the kinetics shows a constant V_{ini} at all three ATP concentrations used. Additionally, the dependency of JH2 activity on the ATP concentration is very erratic: with increasing ATP concentrations the activity of some peptides increases [(for example DDR2_733–745 (Discoidin domain-containing receptor 2, UniProt ID Q16832]), while the activity of others decreases or remains constant (for example JAK2_563–577). Thus, it can be concluded that the signal did not meet the criteria for a *bona fide* kinase activity, i.e. a time-dependent increase in the signal and an increase in the initial reaction rate with an increasing concentration of ATP (Fig. 15). Additionally, the kinetic curves point more at binding than phosphorylation, except for the PKHA6 peptide.

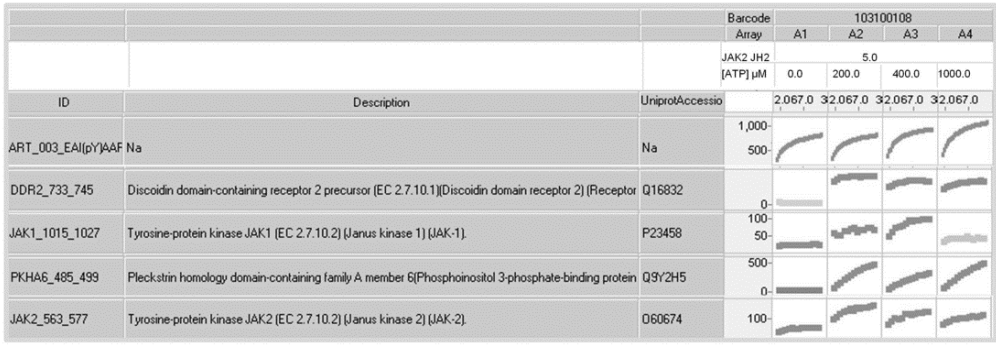

Figure 15. Representation of peptide phosphorylation and/or binding kinetics shown for pre phosphorylated peptide (ART_003) used as positive control, DDR2_733–745, JAK1_1015–1027, PKHA6_845–499 and JAK2_563–577. Peptides are denoted by the peptide ID, its abbreviated name, description and UniProt ID. The cycles representative of incubation time is shown on the X-axis, the signal intensity on the Y-axis.

Taken together, the results show that the catalytic activity of the isolated JH2 domain is low, which is consistent with regulatory phosphorylation of residues rather than phosphorylation of substrate proteins. However, further studies are required to identify potential substrates for JH2.

8.3.3 Effect of JH2 on JH1JH2 kinetics

Although JH2 did not have an effect on the JH1JH2 reaction mechanism, the determination of the kinetic parameters with and without the JH2 domain revealed significant differences between the different protein variants (III, Table 1 and Table S1). We used two different JH1JH2V617F recombinant proteins [JH1JH2VF 513-1132 (including the SH2-JH2 linker) and JH1JH2VF536-1132 (without the linker)] to analyze the effect of the JH2 domain in mutant form.

K_m : The effect of the JH2 domain on the affinity for ATP has not been reported before.

The K_a (K_m ATP) increased two-fold for JH1JH2V617F_536, four-fold for JH1JH2WT and six-fold for JH1JH2V617F_513 as compared with the affinity of JH1 for the best peptides. For the STAT5A peptide and other substrates with a lower catalytic efficiency (228), the increase was stronger. The presence of $V^{617}F$ decreased JAK2's affinity for ATP, but the mutant's catalytic activity increased

significantly compared with wildtype. This also demonstrated that the SH2-JH2 linker is involved in reducing JAK2's affinity for ATP.

The K_b (K_m peptide) is affected in a peptide dependent fashion by the construct used. Substrates with high catalytic efficiency such as EGFR_1190–1202, JH1JH2WT and JH1JH2V617F_536 showed similar K_b values, but the K_b increased by two-fold for JH1JH2V617F_513 as compared with JH1. However, the K_b of other peptides such as STAT5_687–699 showed no significant difference between the constructs containing the JH2 domain.

V_{max}: The JH2 domain imparts the inhibitory effect on the JH1 domain. A 15–20-fold reduction in V_{max} was seen with JH1JH2WT, as compared with JH1 alone. However, the presence of the $V^{617}F$ mutation (513_VF construct) cancelled out this inhibitory effect and V_{max} was reduced when compared with JH1. Removal of the amino acid sequence 513–536 from the $V^{617}F$ construct resulted in a six to ten-fold reduction in V_{max}.

Collectively, these results confirm that the JH2 domain restrains the activity of the JH1 domain, reduces JAK2s affinity for ATP and does not significantly affect its affinity for peptide substrates. This study also demonstrated the participation of the linker domain in the regulation of JAK2 activity.

8.3.4 Effect of inhibitors on JAK2 activity

ADP-β-S –inhibition constants for the three best peptides, JAK1_1015–1027, JAK2_563–577 and EGFR_1190–1202, were determined at a fixed peptide concentration of 2000 μM or at a fixed ATP concentration of 100 μM for JH1, and 400 μM for JH2 containing constructs. The presence of the JH2 domain reduced JAK2s affinity for ATP, which was reflected by the affinity constants for competitive inhibitors of ATP (III, Table 2). JH2 containing constructs had a K_i that was four to ten-fold higher than the K_i of JH1 alone. A significant difference was seen with the $V^{617}F$ construct where the SH2-JH2 linker was absent. These differences in K_i for ADP-β-S demonstrate the altered affinity for ATP and ADP-β-S in the presence of JH2 and the SH2-JH2 linker, confirming the inhibitory function of the linker in JAK2.

The inhibition studies were extended to other competitive inhibitors of ATP. In Figure 16, the increase in activity is represented by dark red squares and the maximum activity and low activity by blue and light blue squares, respectively. When using AMP-PNP, JH1 activity was unaffected upto high micromolar concentrations and was inhibited at concentrations above 100 μM. Surprisingly, the activity of the JH1JH2 constructs increased, until inhibition occurred at mM concentrations of AMP-PNP (seen as red squares even at 1 mM, and later as blue squares). This increase in activity was very obvious in the JH1JH2WT construct (Figure 16) and could be reproduced in independent experiments. To investigate whether this activation is a general effect of competitive ATP inhibitors, imatinib and erlotinib were also tested. While imatinib did not affect the activity at all, the presence of erlotinib resulted in a concentration dependent activation for JH1JH2WT, though not for JH1 (data not shown). Since the activation of JAK2 wild type is ATP dependent and linked to its kinase activity, these results point towards the binding of some inhibitors to ATP binding sites other than the JH1 site. These findings are preliminary and further studies to analyze the effects of different inhibitors on different JAK2 constructs should be undertaken to understand JAK2 regulation.

This observation may have clinical implications for patients treated with, for example, erlotinib, since this drug could activate JAK2 and thus cause unwanted side effects.

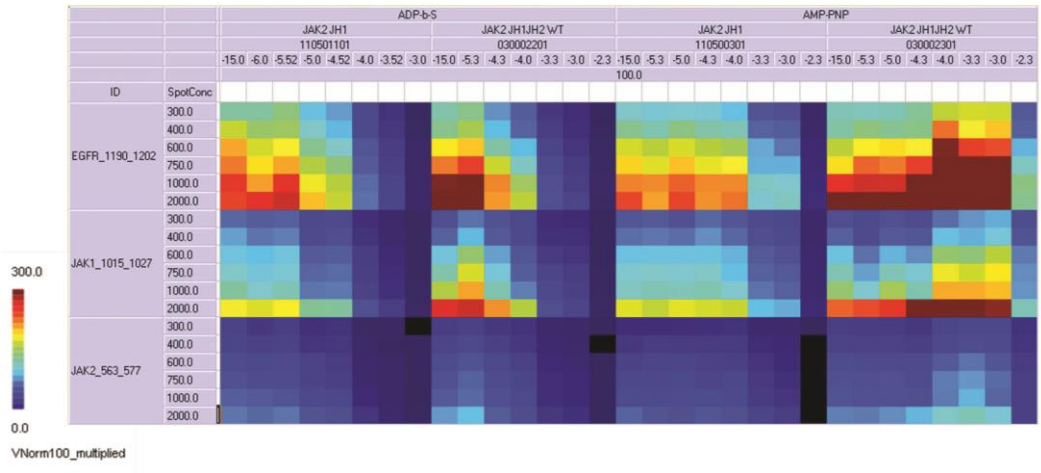

Figure 16. Each spot in the panel describes 6 different concentrations of the respective peptide substrate as seen in the second column (300, 400, 600, 750, 1000 and 2000 µM). Concentrations of inhibitors are represented as log [M] values as seen in fourth row from the top. V_{ini} at six different concentrations of three different peptides is shown at 100 µM ATP. Note that these are raw values and not expressed per pmol of enzyme. AMP-PNP mediated activation of JAK2 JH1JH2WT, but not JH1. This effect is absent in panels incubated with ADP-β-S. Bright red squares represent high activity and blue squares represent low activity.

9. DISCUSSION

The JAK/STAT pathway is important for maintaining cytokine-induced gene expression, which regulates cell proliferation, differentiation and survival. JAKs, together with STATs, are part of a complex pathway, whose canonical and non-canonical regulation has been studied. Advances have been made in describing the regulatory processes, which maintain the proper function of the pathway and coordinated expression of its target genes. Reversible protein phosphorylation plays a crucial role in regulating and monitoring JAK2 activity. JAK2 activation is tightly regulated and stimulated by cytokines that induce phosphorylation of JAK2 on $Y^{1007, 1008}$ in the activation loop. However, in addition to activation loop tyrosines, more than 20 other different tyrosine residues are known to be phosphorylated during JAK2 activation. While phosphorylation on some tyrosine residues such as Y^{637}, Y^{813}, Y^{868}, Y^{966} and Y^{972} is known to positively regulate JAK2 activity, phosphorylation on others like Y^{119}, Y^{221}, Y^{317}, Y^{570} and the serine residue, S^{523} negatively regulates JAK2 activity. The discovery of JAK2's critical role in cytokine dependent signaling based on its phosphorylation status is a key feature of the JAK/STAT pathway.

9.1 Phosphorylation of the JH2 domain in the negative regulation of cytokine signaling

A central finding in the field of cell signaling was the discovery that the pseudokinase, or JH2 domain in JAK2 negatively regulates JAK2 activity. The JH2 domain apparently keeps the activity of the JH1 domain suppressed by an auto-inhibitory action through an unknown mechanism. It was shown that the JH2 domain maintains the basal activity of JAK2 and is required for cytokine dependent activation of JAK2. However, understanding the exact mechanism of the JH2 mediated inhibitory function warrants further studies. Several key residues have been identified through their involvement in myeloproliferative disorders, where mutations to these amino acids compromise the inhibitory role of the JH2 domain. One hallmark mutation is $V^{617}F$, which is found in polycythemia vera patients and is situated between the β4-β5 loop in the N-terminal lobe of the JH2 domain. This mutation has been predicted to suppress the inhibitory interaction

between JH1 and JH2 leading to a hyperactive JAK2 and the constitutive activation of the JAK-STAT pathway.

Lately, studies have shed light on the regulatory properties of several pseudokinases. The functional properties of pseudokinases are being actively investigated and the current classification, which is based on the presence/absence of catalytic motifs (required for catalytic transfer) continues to evolve. Some pseudokinases such as WNK and Haspin have been removed from the list of 'pseudokinases' and others, such as CASK, have to be renamed based on new insight into their functions.

Two of the Articles (I & III) in this thesis attempt to address some open questions on the regulation of JAK2 activation based on the functional and enzymatic characterization of full length and tandem domains (JH1JH2) both *in vitro* and in cells.

The functional characterization of JAK2 domains was stalled by the inability to produce recombinant protein. In Article I, we show, for the first time, the purification of GST- and His-tagged JH2. When analysed by ion exchange chromatography, JH2 separated into two distinct peaks (peak 1 and peak 2) demonstrating differences in its phosphorylation status. Further, the differential migration of the two peaks in a native PAGE and the results of *in vitro* kinase assays showed that JH2 autophosphorylates two previously known residues Y^{570} and S^{523}. The activity of JH2 and its proposed role in the regulation of JAK2 activation were further studied in cells using Epo and IFN-γ stimulation. Surprisingly, S^{523} was phosphorylated in the absence of cytokine induction and this led to the phosphorylation of Y^{570} upon cytokine induction over time. This revealed a whole new regulatory feature of JH2: phosphorylation of S^{523} is the first event that takes place in the advent of JH2 phosphorylation. In this study we speculated that the phosphorylation of S^{523} and of Y^{570} takes place in *cis* and in *trans*, respectively. Further evidence was gathered upon solving the structure of JH2 to confirm the *cis* and *trans* phosphorylation of these residues (134).

The discovery of MPN mutations, along with $V^{617}F$, raised several questions pertaining to the mechanism of JAK2 activation. Although it was shown that the F^{595}-F^{617} interaction is essential for the constitutive activation of JAK2 $V^{617}F$, the precise mechanism of $V^{617}F$ activation remains elusive. This study marks the beginning of the characterization of the functional role of JH2. We described three hyperactivating mutations ($V^{617}F$, $K^{539}L$ and $R^{683}S$) involved in the abrogation of JH2 activity. The JH1-JH2 inhibitory regulation, which relies on the phosphorylation of S^{523} and Y^{570}, is completely abolished in MPN patient samples.

This study unravels the previously unknown regulatory mechanism of JH2 in JAK2.

9.2 Role of the low JH2 activity in phosphorylating external substrates

In light of the discovery presented in Article I, we continued to further investigate, whether JH2 activity is needed only to control the basal activity of JAK2 and JAK2 signaling. In the research related to Article III, we explored the possibility that a low JH2 activity could phosphorylate external substrates. Surprisingly, out of the PamChip array comprising 256 tyrosine containing peptides, only one peptide, named PKHA6_485-499, showed a signal that was above the standard deviation of the background and increased with time. However, the V_{ini} of this reaction did not increase with an increasing ATP concentration. Experiments carried out with increasing ATP amounts showed no robust activity. These results suggest that though some peptides may display binding kinetics indicative of increased ATP binding, this is not necessarily accompanied by an increase in peptide phosphorylation. The only peptide which met the criteria for a probable JAK2 JH2 substrate was PKHA6 peptide.

These results could mean that the low JH2 activity only plays a regulatory role in intramolecular phosphorylation events. The peptide substrate containing the Y^{570} residue showed a low level of phosphorylation but a very different ATP dependency compared to other peptides tested. Further peptide phosphorylation studies containing S^{523} could provide insights into the substrates of JH2. Since S^{523} is the default site of phosphorylation, the idea of its phosphorylation in an unstimulated situation makes more sense than the phosphorylation of an external or downstream substrate.

9.3 Role of the $V^{617}F$ mutation and the SH2-JH2 linker region in regulating JAK2 activity

Understanding the role of the JH2 domain at the molecular level requires its thorough enzymatic characterization. In order to understand the role of the $V^{617}F$ mutation in regulating JAK2, tandem domains of JH1JH2 with and without the pathogenic mutation were recombinantly purified for full kinetic analyses.

PamChip® 96 array plates, containing 21 different peptides at six different concentrations each, were used to incubate the kinases with ATP. This facilitated the simultaneous recording of kinetic readings from the arrays. All the JAK2 kinases incubated followed a random Bi-Bi reaction mechanism, where both substrates bound to the enzyme randomly. This is a completely novel finding, and did not differ between the different JAK2 constructs. Additionally, the presence of the $V^{617}F$ mutation both in its short (536–1132) and long (513–1132) forms, displayed no difference in the type of reaction mechanism they followed. However, when the kinetic parameters were determined, remarkable differences between the JH1 and JH1JH2 domains became apparent. Determining these kinetic parameters by extrapolation to an infinite concentration of substrates allows the accurate determination of K_m, since K_m is not a fixed value, but varies with concentration of the second substrate. Hence, by varying the amount of both the substrates, we can obtain near to accurate values. Previously, it was shown that when the JH1JH2 domains are together, the activity (V_{max}) was lower than when only JH1 was incubated with varying JAK2 activation loop peptide concentrations. The K_m for the peptide, however, remained unchanged (132). Two later studies also showed that JH2 lowered the V_{max} for JH1JH2WT drastically, but also decreased the K_m for peptide substrates for $V^{617}F$ (224, 228). In addition it was shown that JH2 increased the K_m for ATP. These differences suggest that, in addition to relieving the JH2 inhibitory interaction, $V^{617}F$ might also be involved in the activation of JAK2 through another, unknown mechanism.

In this study we resolve this issue, and show that both $V^{617}F$ and the SH2-JH2 linker affect the kinetic parameters of JAK2. Surprisingly, the increase in the V_{max} of $V^{617}F$ constructs could indicate that a conformational change takes place in the activation loop, especially since it is known that the interaction of F^{595} and S^{591} in JH2 with the activation loop results in an auto-inhibited conformation in JAK2WT. The central finding of Article III is the difference in the kinetics between the short and long forms of $V^{617}F$. The affinity of the V617F_536 form to ATP is stronger than that of of V617F_513 form as can be interpreted from the differences in the K_a values of the two $V^{617}F$ constructs tested (III, Table 1). However V_{max} is reduced. A previous molecular dynamics study demonstarted the role of the SH2-JH2 linker in maintaining the π-π interaction in $V^{617}F$ in a hyperactive conformation (232). Since other parts of JAK2, such as the FERM domain, are involved in regulating JAK2 activity (224), it is not hard to imagine that the SH2-JH2 linker can reduce the activity of JH1JH2WT.

Differences in these K_m values will have an impact on inhibitor design. In addition to affecting ATP binding, the SH2-JH2 linker also has a major role in binding to competitive ATP inhibitors. This was seen as differences between the inhibitory constant (K_i) values among the tested constructs. As expected, the presence of the JH2 domain resulted in higher values, but, surprisingly, the absence of the linker region in the $V^{617}F$ construct also led to increased K_i values. In conclusion, these results have identified an inhibitory role for the SH2-JH2 linker in regulating JAK2.

9.4 ATP and inhibitor binding properties of JAK2

Reports on JAK2 activity controlled both by inhibitors and activators have widened our knowledge of different levels of tight regulation in JAK/STAT signaling. In spite of this tight regulation, JAK2 signaling is altered in hematopoetic malignancies. The determination of the precise K_d and K_m values for ATP becomes a crucial factor when aiming at understanding the preferential binding of these molecules. In light of this, we made an effort to improve the JAK-FRET enzyme assay, which allows direct binding studies of ATP/ADP/AMP to the JAK2 tyrosine kinase domain. Incorporation of the correct excitation wavelength and correction for the inner filter effects minimized the error in the K_d determination of ligand binding to kinases. The binding of fluorescent analogs of ATP to the JH1 domain revealed a high affinity ranging from 15 to 25 nM. This was confirmed by a non-hydrolysable ATP analog MANT-ATP-γ-S. A difference in the K_d values for ATP and ATP analogs was observed. Often, the ATP analogs of ATP display an affinity that is three orders of magnitude higher than the actual binding of ATP. Of note, MANT nucleotides only mimic the binding characteristics of ATP, but not its affinity. Hence, comparing the FRET-MANT affinity measurements to another method might not point out the correct affinity. However, it should be noted that when employing FRET-MANT measurements, the corrections reported in Article II are necessary and will make the K_d analysis more accurate and help to extend titrations to higher ligand concentrations.

9.5 Physiological role of pseudokinases

Pseudokinases are the evolutionary cousins of kinases and it would not be a surprise to find them associated with a range of various diseases such as cancer, diabetes, bowel disease, cardiovascular disease and disorders of the extracellular matrix and in smooth muscle contraction.

Role in cancer – Almost all of the listed pseudokinases in Table 2 are involved in cancer when their activity is altered (hyperactivation). Studies from KSR1-/- knockout mice show defects in T-cell proliferation and disoriented hair follicles. Also, in a KSR -/- breast cancer model, the forming of a Raf/ERK/MEK complex is compromised. However, reports also suggest that the knockout mice are not susceptible to tumors, as KSR2 compensates for the loss of KSR1 (94, 311, 312). CASK studies related to cancer are sparse; however, squamous cell carcinoma and small cell lung cancer tissues show elevated levels of CASK gene expression. Similarly ILK levels are also increased in almost all forms of cancer (small lung, ovarian, colon, gastric thyroid, pancreatic). Peutz-Jeghers syndrome is a rare autosomal dominant disorder, which eventually progresses to colon, breast and pancreatic cancers. A single amino acid substitution in LKB1 prevents STRADα from forming a complex with LKB1, eventually curbing the G1 cell cycle arrest. Dysregulation of the cell cycle also contributes to different forms of cancer, because of the aberrant activity of LKB1 (312).

Role in cardiovascular diseases – JAK2 plays an important role in molecular processes that have been implicated in a variety of heart diseases. The earliest observation came from a study, where increased tyrosine phosphorylation of JAK1, 2 and TYK2 was seen in mechanically stretched cardiomyocytes (313). Since cardiotropin 1 is an activator of JAK2, links were drawn directly from JAK2 to cardiac hypertrophy, especially since the gp130 signaling pathway plays a pivotal role in this disease (314). Although the pseudokinase domains in the JAK family are not related to cardiovascular diseases, other proteins, which were previously thought to be pseudokinases, such as Tribbles and WNK1, have been linked with hypertension, Mendelian disease and high blood pressure. Trb-1 has been linked to elevated levels of low density lipoprotein and an increased risk of coronary heart disease in an Asian Malay population (315) and to ischemic heart disease and myocardial infarction (316). WNK1 gene polymorphisms are associated with variations in blood pressure in European families, since mutations in WNK1 and WNK4 cause monogenic hypertensive syndrome (317). Mutations and intronic

deletions cause increased WNK1 expression and are attractive targets for antihypertensive drugs (318).

Role in diabetes – *In vivo* studies in mouse β cells expressing a missense polymorphism in Trb3 (referred to as Trb3 $Q^{84}R$) linked Trb3 with reduced insulin exocytosis and a high risk of type 2 diabetes. This has been confirmed using the murine β cell line MIN6 and human islet cells (319). Diabetic nephropathy occurs due to angiopathy of the capillaries in the kidney glomeruli. Differences in the expression of ILK, as observed in normal and diabetic kidneys, link ILK to the pathogenesis of this progressive disease (320).

Why the kinetic profiling of JAK2 has clinical significance?

The JAK2 JH2 domain is a hotspot for mutations involved in myeloproliferative diseases. Currently all of the drugs in clinical trials target the JH1 domain, since its structure is available. The non-specific targeting of drugs to the JH1 domain leads to secondary unwanted clinical effects (in myelopoeisis and IFN responses). Persistent efforts to understand resistence to the inhibitor have been made. One of the most common forms of resistance due to long term exposure to a JAK2 inhibitor is seen in the presence of mutations in JH1 kinase domain (321). Other mutagenesis studies also showed the JAK2 gatekeeper mutation ($M^{929}I$) to be another cause for insensitivity. Studies in cells with JAK2 $V^{617}F$ and $R^{683}G$ mutations, showed additional three mutations, which were capable of inducing resistance to JAK2 inhibitors (322).

The preliminary result, which shows an increase in JAK2 activity caused by competitive ATP inhibitors (Figure 15), demonstrates the complexity of JAK2 autoregulation, which can further complicate and change therapeutic approaches. A similar compound mediated activation mechanism was shown recently for the Rapidly Accelerated Fibrosarcoma (RAF) kinase: RAF-inhibitors activated the MAPK pathway by relieving an inhibitory autophosphorylation mechanism on RAF (323). Another study showed that when cells are exposed to ruxolitinib, JAK2 pairs up with JAK1 and TYK2 and gets activated. The inhibitor stabilizes JAK2, but activates downstream signaling (324). This underpins the importance to understand the mechanism of action of inhibitors. Hence, the design of specific compounds that target the JH2 domain directly, or a JAK2 mutant with less side-effects, are a current priority. Now that the JH2 crystal structure has been solved and its enzymatic properties have been characterized, it would be interesting to screen and develop specific inhibitors for JH2.

10. CONCLUSIONS AND PERSPECTIVES

When I joined the host laboratory, the role of the pseudokinase domain and the involvement of the three regions within the domain that mediate the inhibitory function in JAK2, had been identified. With the advent of the discovery of the pathogenic mutation $V^{617}F$ in JH2 domain, further studies on how a single amino acid substitution can trigger the aberrant activation of JAK2 were carried out. In no time, JAK2 became the primary target for pharmacological intervention, and several inhibitors targeting JAK2 were developed.

Understanding the role of the kinase and pseudokinase domains in JAK2 regulation is of high importance, especially since the majority of activating mutations that are linked with myeloproliferative diseases, are located in this region. The present study functionally characterizes the kinase and pseudokinase domains in JAK2. Results from the current thesis work suggest that : (i) the pseudokinase domain of JAK2 is catalytically active and hyperactivating mutations in JH2 are involved in abolishing JH2 activity, (ii) JH2 phosphorylates two negative regulatory sites, S^{523} and Y^{570}, and the critical activity of JH2 plays a major role in maintaining a low basal activity of JAK2 (I), (iii) the tandem domains in JAK2 follow a random Bi-Bi reaction mechanism, and the addition of the JH2 domain does not necessarily have to change the type of reaction mechanism that JAK2 follows, (iv) the kinetic parameters of the $V^{617}F$ mutation vary significantly with and without the presence of the SH2-JH2 linker and this adds a new dimension to the already known role of the SH2-JH2 linker in wild type JAK2, (v) JH2 containing constructs show a 10-15-fold decrease in their affinity for ATP, compared with JH1 constructs which also indicates, that the SH2-JH2 linker participates in JAK2 inhibition by reducing its affinity for ATP (III), (vi) the kinase domain (JH1) binds ATP strongly and the accurate determination of dissociation constants with fluorescent analogs of ATP/ADP/AMP confirmed the preferential binding of these nucleotides. Moreover, this thesis describes an improved FRET binding method applicable to the study of any kinase-nucleotide pair. After the careful consideration of crucial factors that might affect the FRET measurements, such as inner filter effects, higher concentrations of nucleotides that lead to the absorption of fluorescence, we were able to conclude that the affinity of ATP for the JH1 domain is in the range of 15-25 nM, which is indicative of a very tight binding and rules out additional binding sites in the JH1 domain (II).

The current study also shed light to the probable role of peptide binding mediated regulation of JAK2 activity. The very strong affinity demonstrated by JH1JH2VF (the short form without the linker region) compared with other constructs, was specific for certain peptides only. This might be an indication of the modifying role of the peptides in the regulation of the activity in the presence of JH2 $V^{617}F$. This could mean that the FERM domain affects JAK2 JH1 kinetics in a way that is different from the effect of the JH2 domain. This might correlate with the fact that conformational changes together with the change in the phosphorylation status, might lead to differences in the K_m values between the proteins.

All these open ends could be satisfactorily answered with a three-dimensional structure of the JH1-JH2 tandem domains. The structure would definitively establish the interplay between the two domains. Further, with the increasing evidence that also other domains regulate JAK2 activity, solving the structure of the full length JAK2 can be expected to answer many of the burning questions on JAK2 activation and regulation.

11. ACKNOWLEDGEMENTS

This study was carried out in the Molecular Immunology Laboratory, Institute of Biomedical Technology (IBT), BioMediTech, University Of Tampere, Tampere, Finland.

I like to convey my heart felt gratitude to my mentor and supervisor Prof. Olli Silvennoinen (MD, PhD) for providing this excellent opportunity to work in his laboratory. I'm so blessed to have joined his group for both professional and personal reasons. He ensured that I had freedom to conduct research with the best facilities in place. And the continuous exchange of mails for scientific advice motivated me to carry out my doctoral thesis. His far sightedness towards various issues, including crisis management, and his words of wisdom has kept me from sinking into the scientific calamities. He is also thanked for his invaluable time when he was on his sabbatical in the United States of America during 2007-2008 and when he was the director of the institute during 2008-2010. Thank you, Olli, for believing me and guiding me all these years.

I wish to acknowledge Professor Yli-Kauhaluoma, Jari (PhD) and Professor Gerhard Müller-Newen (PhD. rer. nat) for reviewing my thesis manuscript and for their critical and explicit suggestions, which have produced a better manuscript. I am honored to have Professor Päivi Koskinen (PhD) as my thesis opponent and I thank her for accepting the invitation to act as my opponent. A special note of thanks goes to my thesis committee supervisors Professor Markku Kulomaa (PhD) and Docent Herma Renkema (PhD) for those intriguing sessions of annual thesis updates where I got ideas and comments on how to drive my project forward. I am also thankful to Dr. Helen Cooper (PhD) for the language revision of my thesis.

I wish to express my sincere thanks to Docent Daniela Ungureanu (PhD) for her constant guidance and support during most of my PhD studies. As a foreign student coming from a hot, tropical country I knew very little about the norms and culture in Finland. Her constant vigilance on my experiments and her help and expertise are appreciated. Her positive attitude and encouragement towards science helped me achieve my best in the lab. She always gave me a chance to learn from my mistakes in lab experiments and was generous with her time and efforts. I also gratefully appreciate every time you changed the media in the *Sf9* bottles during some late evenings and weekends or helped me in purifying those notorious JAK proteins. Thank you for introducing me to the world of 'veganism' where I learnt a lot about food alternatives to animal products. Even though I did not become a

vegan, our intense discussions on this subject opened me to a different world and made me conscious and precautious to be considerate towards people on special diets. I cherish every moment of time spent together.

I wish to warmly thank all my co-authors and collaborators who have contributed to this thesis. Dr. Riet Hilhorst (PhD) deserves a huge 'thanks' for collaborating with us in the JAK2 project. When I met her in the ReceptEUR meeting on JAKs and STATs in Rotterdam in 2009, little did I knew that this small meeting of two days would develop into a profound and strong collaboration that would lead us to address some of the intriguing questions in the field. Her knowledge, expertise, time, support and more importantly her patience for the project in all these years will always be remembered and appreciated. I wish to say that without Dr Riet, this thesis would have remained as a dream. Dr. Arturo Sanz Sanz (PhD) is acknowledged for his efforts and help in the JAK2 projects. The intense discussions that we had over Skype for months were worth the effort, as his knowledge in the area of kinetics is profound and I could get all the help and advice I needed from him. Dr. Adrie H. Westphal (PhD) and Dr. Jan William Borst (PhD) are sincerely thanked for their support and time invested in my second paper. I want to thank Dr. Rob Ruijtenbeek (PhD) and Dr. Ivo P. Touw (PhD) for their invaluable suggestions in completing the third paper. My sincere thanks go to Professor Steve Hubbard (PhD), NYU for those intellectual talks and discussions that we had during the preparation of my first paper. His immense expertise and ability to tackle issues logically and intellectually always left me in awe. I wish to thank Clifford Young for investing time on doing mass spectrometry for the JAK2 and JAK3 proteins.

All this would have gone in vain without current and past colleagues of my laboratory. I specially thank Dr. Astrid Murumägi (PhD) for very good, humorous company during the first year of my PhD. Our outing along with Daniela to Idea Park for shopping, brief jogging sessions (where I used to fall behind) and bird watching in Niihama bring me joy. I warmly thank Dr. Juha Saarikettu (PhD) (big Juha) for all the advice on technicalities, details on the experiments and discussions on general science matters. His basic science knowledge is so immensely good that he could always help me. Light hearted evening sessions with him were fun, when we had tiny but rewarding chats on protein shakes and dieting. He corrected my pronunciation on 'Yellow' and 'Yeast' when I used to pronounce them 'ellow' and 'east' which was so funny. Thank you for your friendship. Dr. Juha Grönholm (PhD) (small Juha) is thanked for his jovial and fun filled company and for being a good friend during all these years. Henrik Hammarén (MSc.) joined our group two

years ago and instantly I felt like he added a spark to our lab meetings and group discussions with his outspoken comments and questions. His invaluable inputs on data analysis, troubleshooting ideas and 'never say NO' attitude are worth mentioning as they completely changed my way of looking at things. He always had time for whatever I asked. Our informal chats on almost every topic from history and cooking to weird games, puzzles and podcasts kept me on right track in maintaining my confidence and energy. I thank you for your unconditional support and friendship. I wish to express my warm thanks to Dr. Tekele Fashe (DVM, PhD) for good moments and timely tips on writing my thesis and choosing reviewers on time. His laid back, relaxed, "no-tension" attitude surprised me until I started to know that stressing about things will not help. Thanks for showing me this side of life.

Tuija Pekkala (MSc.) joined our lab for her MSc thesis during 2009. We recognized each others' likes and interests and became good friends. The cycling sessions, parties at home, get -togethers at friends' places, playing and photo sessions with Elsa (an American pitbull terrier) were all fun and frolic. Fun had no limits when she invited me to her parent's home in Ylikiiminki for Juhannus 2010. I wish to thank her for her invaluable friendship. The two persons I will remember forever are lab technicians Paula Kosonen and Merja Lehtinen. They helped me in making buffers, media and constructs and in cell culture maintenance, whenever I asked for it and without any delay. Ordering items from companies and finding a solution for a practical problem has never been so easy before. Maintaining inventories, log books, reagents and data sheets were just so perfect that I never felt that I was lost. They are special !! I immensely thank you for running this lab smoothly. I also shared a special bond with Elina Koskenalho. Regular chats on techniques, solving mysteries and her general work attitude put me in the fast lane for finishing my thesis. Regular sauna meetings, swimming in lakes and baking sessions were specially required for surviving this PhD and I'm glad we did them together. Thank you for your friendship.

I wish to express my sincere thanks to other members of the lab: Dr. Jang Jie (PhD) (Sophie), Dr. Tuuli Valineva (PhD), Heidi Peussa, Docent Pia Isomäki (MD, PhD), Dr. Samuli Rounioja (MD, PhD). I wish to thank all the summer students Markus Ojanen, Meri Uusi Mäkelä and Miina Ojansivu for being nice colleagues all these years. All the members – Sanna Hämäläinen, Zuzet Martinez Cordova, Saara Aittomäki (PhD), Ortutay Zsuzsanna from the neighboring group 'Immunoregulation' are greatly acknowledged. Special thanks to Dr. Kaisa Teittinen (PhD) for making me feel comfortable in Finnish gatherings and her

candid thoughts on different matters gave me a new perspective on Finnish customs and Laura Airaksinen (MSc.) for her friendship.

I wish to express my warm thanks to our Institute's current director Dr. Hannu Hanijärvi (DDS, PhD) for providing excellent working facilities in the institute. I had the opportunity to meet some of the best secretaries in our institutes: the Late Pirjo Malmi, Kaarin Forsman, Erja Lassila, Jaana Anttila-Salmensivu, Merja Koivula (Human resource) and Riitta Aallos. They always had time to get me the correct official documents translated from Finnish to English, prepared my contract letters and carried out other administration task without delay. Thank you for that. A special thanks to Dr. Henna Mattila for managing my TGPBB records, meetings and credits. Nothing is possible without a computer connected to the internet. I wish to express my warmest gratitude to our 'computer experts' Toni Vormisto, Tomi Malmström and Heli Koivisto for fixing my hard drives and installing softwares during these years.

Maintaining a friendly atmosphere outside the lab is crucial for personal development. I've had the greatest opportunity to make friends with Indian and non-Indian communities in Tampere, Turku and Helsinki. My best friends Katri Suhonen and Mari Kentälä are warmly thanked for being my support and guide, for tackling issues (both social and cultural) and for helping me maintain my emotional intelligence. Amanpreet Kaur, Nagabhooshan Hegde, SriVani, Hasan Mohammad, Ravi Mysore Shantamurthy, Prabhakar Sharma (Prabhu), Prasanna Deshpande, Subash Tripathi, Himanshu Chedda, Jothi Anantharajan, Moutusi Manna, Rishi Mohanta and Maria Ojanen are thanked from the deepest of my heart for their friendship and all the support that I needed all these years. The board game sessions, trips to nearby towns in Finland, long trips to Lapland and abroad would not have been possible without you. This was a kind of a stress buster for me during these years. I wish to also express my warmest thanks to Indian communities in Tampere, Turku and Helsinki for making me part of Deepavali, Ganesha Chaturti, Holi, Dasara, Indian Independence day and other festive celebrations all these years.

Back in India, friends and family have waited for me to visit them every year. My role model icons are my aunt Sucheta (ate) and uncle Krishnamurthy (mava). They have taught me to have the endless fighting spirit. Thanks for all your support and love for these years. Special thanks to my best friends Manivannan S (Mani), Harish S (Hari), Shruthi Prasad (Shru), Vijayalakshmi (putti), Dr. Kajal Kanchan, Herojeet Salam (Hero), Chandrashekar (Chandru), Sumanth Kashyap, Rajaneesh, Sujay and Bopanna MP (Bops). My deepest gratitude to my

mentors/teachers Prof. Cletus D'Souza, Wesley Roy Balasubramaniam, Dr. Leena Khare Satyam and Dr. Murali Ramachandra for guiding me in the right path.

Words fall short, when I want to express my sincere gratitude to my beloved family. They have given me love and support beyond any boundaries for all these years. My parents Sujatha Niranjan (Amma) and Niranjan Anandakrishna (Pappa), my grandparents Yashodamma (Ajji) and the late Anandakrishna (Tata), Lakshamma (Ajji) and the late Nagaraj (Tata), my in-laws Nagarathnamma (atte) and Lingappa M.L (mava) mean everything to me. Thank you all for believing in me and waiting for me patiently until I finished my PhD. My little sweet sister Avanthi Rao Paplikar (Athu) has given me love, emotional and mental support for all these years. Thank you for that and I love you all.

Finally, I would like to express my deepest gratitude for my beloved husband Raghavendra Mysore (Raghu) for taking all the negative projectiles from me and filling me with positive energy, for being extremely patient and not losing hope in me (even when I sounded hopeless). I could not have done this without you.

This work was financially supported by the EU Research Training Network ReceptEUR Marie-Curie pre-seed exploratory fund, Sigrid Juselius Foundation, the Medical Research Council of the Academy of Finland, the Finnish Cancer Foundation, the Medical Research Fund of Tampere University Hospital, the Tampere Tuberculosis Foundation, University Of Tampere fund, Alfred Kordelinin Foundation and Tampere graduate program for Biomedicine and Biotechnology (TGPBB) graduate school fund.

Tampere, March 2014

Yashavanthi Niranjan

12. REFERENCES

1. O'shea J. Targeting the jak/STAT pathway for immunosuppression. Ann Rheum Dis. 2004;63(suppl 2):ii67-71.
2. Clark SC, Kamen R. The human hematopoietic colony-stimulating factors. Science. 1987;236(4806):1229-37.
3. Metcalf D. The molecular control of cell division, differentiation commitment and maturation in haemopoietic cells. Nature. 1989;339(6219):27-30.
4. Kishimoto T, Taga T, Akira S. Cytokine signal transduction. Cell. 1994;76(2):253-62.
5. Isaacs A, Lindenmann J. Virus interference. I. the interferon, Proc.R.Soc.Lond.B.Biol.Sci,. 1957(147):258-67.
6. Bagley CJ, Woodcock JM, Stomski FC, Lopez AF. The structural and functional basis of cytokine receptor activation: Lessons from the common β subunit of the granulocyte-macrophage colony-stimulating factor, interleukin-3 (IL-3), and IL-5 receptors. Blood. 1997;89(5):1471-82.
7. Miyajima A, Mui AL, Ogorochi T, and Sakamaki K. Receptors for granulocyte-macrophage colony-stimulating factor, interleukin-3, and interleukin-5, blood 82, 1960-1974. Blood. 1993(82):1960-74.
8. Leonard WJ, Shores EW, Love PE. Role of the common cytokine receptor γ chain in cytokine signaling and lymphoid development. Immunol Rev. 1995;148(1):97-114.
9. Murata T, Obiri N, Puri R. Structure of and signal transduction through interleukin-4 and interleukin-13 receptors (review). Int J Mol Med. 1998;1(3):551-8.
10. Demoulin JB, Renauld JC. Signalling by cytokines interacting with the interleukin-2 receptor gamma chain. Cytokines Cell Mol Ther. 1998 Dec;4(4):243-56.
11. Kotenko SV, Pestka S. Jak-stat signal transduction pathway through the eyes of cytokine class II receptor complexes. Oncogene. 2000;19(21):2557-65.
12. Kotenko SV. IFN-λs. Curr Opin Immunol. 2011;23(5):583-90.
13. Kotenko SV, Langer JA. Full house: 12 receptors for 27 cytokines. Int Immunopharmacol. 2004;4(5):593-608.
14. Langer JA, Cutrone EC, Kotenko S. The class II cytokine receptor (CRF2) family: Overview and patterns of receptor–ligand interactions. Cytokine Growth Factor Rev. 2004;15(1):33-48.
15. Cabal-Hierro L, Lazo PS. Signal transduction by tumor necrosis factor receptors. Cell Signal. 2012;24(6):1297-305.
16. Croft M, Benedict CA, Ware CF. Clinical targeting of the TNF and TNFR superfamilies. Nature Reviews Drug Discovery. 2013;12(2):147-68.
17. Allan SM, Tyrrell PJ, Rothwell NJ. Interleukin-1 and neuronal injury. Nature Reviews Immunology. 2005;5(8):629-40.
18. Sutherland EW, Wosilait WD. Inactivation and activation of liver phosphorylase. Nature. 1955; 22 Jan; 175(4447):169-70.
19. Fischer EH, Krebs ED. Conversion of phosphorylase b to phosphorylase a in muscle extracts. Journal of Biological Chemistry. 1955;216(1):121-32.
20. Manning G, Whyte DB, Martinez R, Hunter T, Sudarsanam S. The protein kinase complement of the human genome. Science. 2002;298(5600):1912-34.
21. Hanks SK. Genomic analysis of the eukaryotic protein kinase superfamily: A perspective. Genome Biol. 2003;4(5):111.
22. Hanks SK, Hunter T. Protein kinases 6. the eukaryotic protein kinase superfamily: Kinase (catalytic) domain structure and classification. The FASEB Journal. 1995;9(8):576-96.
23. Robinson DR, Wu YM, Lin SF. The protein tyrosine kinase family of the human genome. Oncogene. 2000 Nov 20;19(49):5548-57.
24. Kuriyan J, Cowburn D. Modular peptide recognition domains in eukaryotic signaling. Annu Rev Biophys Biomol Struct. 1997;26(1):259-88.
25. Lemmon M, Ferguson K. Pleckstrin homology domains. In: Protein modules in signal transduction. Springer; 1998. p. 39-74.

26. Neet K, Hunter T. Vertebrate non-receptor protein–tyrosine kinase families. Genes to Cells. 1996;1(2):147-69.
27. Hubbard SR. Protein tyrosine kinases: Autoregulation and small-molecule inhibition. Curr Opin Struct Biol. 2002;12(6):735-41.
28. Hubbard SR, Till JH. Protein tyrosine kinase structure and function. Annu Rev Biochem. 2000;69(1):373-98.
29. Lemmon MA, Schlessinger J. Cell signaling by receptor tyrosine kinases. Cell. 2010;141(7):1117-34.
30. Grangeasse C, Nessler S, Mijakovic I. Bacterial tyrosine kinases: Evolution, biological function and structural insights. Philosophical Transactions of the Royal Society Lon, Series B: Biological Sciences. 2012 Sep;367(1602):2640-55.
31. Knighton DR, Zheng J, Ten Eyck LF, Xuong N, Taylor SS, Sowadski JM. Structure of a peptide inhibitor bound to the catalytic subunit of cyclic adenosine monophosphate-dependent protein kinase. Science. 1991;253(5018):414-20.
32. Johnson LN, Noble ME, Owen DJ. Active and inactive protein kinases: Structural basis for regulation. Cell. 1996;85(2):149-58.
33. Cowan-Jacob SW. Structural biology of protein tyrosine kinases. Cellular and Molecular Life Sciences CMLS. 2006;63(22):2608-25.
34. Scapin G. Structural biology in drug design: Selective protein kinase inhibitors. Drug Discov Today. 2002;7(11):601-11.
35. Huse M, Kuriyan J. The conformational plasticity of protein kinases. Cell. 2002;109(3):275-82.
36. Johnson LN, Lowe ED, Noble ME, Owen DJ. The structural basis for substrate recognition and control by protein kinases. FEBS Lett. 1998;430(1):1-11.
37. Kornev AP, Taylor SS, Ten Eyck LF. A helix scaffold for the assembly of active protein kinases. Proceedings of the National Academy of Sciences. 2008;105(38):14377-82.
38. Endicott JA, Noble ME, Johnson LN. The structural basis for control of eukaryotic protein kinases. Annu Rev Biochem. 2012;81:587-613.
39. Taylor SS, Kornev AP. Protein kinases: Evolution of dynamic regulatory proteins. Trends Biochem Sci. 2011;36(2):65-77.
40. Strong TC, Kaur G, Thomas JH. Mutations in the catalytic loop HRD motif alter the activity and function of drosophila Src64. PloS one. 2011;6(11):e28100.
41. Hubbard SR, Mohammadi M, Schlessinger J. Autoregulatory mechanisms in protein-tyrosine kinases. J Biol Chem. 1998;273(20):11987-90.
42. Canagarajah BJ, Khokhlatchev A, Cobb MH, Goldsmith EJ. Activation mechanism of the MAP kinase ERK2 by dual phosphorylation. Cell. 1997;90(5):859-69.
43. Lahiry P, Torkamani A, Schork NJ, Hegele RA. Kinase mutations in human disease: Interpreting genotype–phenotype relationships. Nature Reviews Genetics. 2010;11(1):60-74.
44. Hubbard SR, Wei L, Ellis L, Hendrickson W. Crystal structure of the tyrosine kinase domain of the human insulin receptor. Nature. 1993;372(6508):746-54.
45. Wenqing X, Harrison S, Eck M. Three-dimensional structure of the tyrosine kinase c-src. Nature. 1997;385:595-602.
46. Williams JC, Weijland A, Gonfloni S, Thompson A, Courtneidge SA, Superti-Furga G, et al. The 2.35 Å crystal structure of the inactivated form of chicken src: A dynamic molecule with multiple regulatory interactions. J Mol Biol. 1997;274(5):757-75.
47. Feng S, Chen JK, Yu H, Simon JA, Schreiber SL. Two binding orientations for peptides to the src SH3 domain: Development of a general model for SH3-ligand interactions. Science. 1994;266(5188):1241-7.
48. Ogawa A, Takayama Y, Sakai H, Chong KT, Takeuchi S, Nakagawa A, et al. Structure of the carboxyl-terminal src kinase, csk. J Biol Chem. 2002;277(17):14351-4.
49. Riedy M, Dutra AS, Blake TB, Modi W, Lal B, Davis J, et al. Genomic sequence, organization, and chromosomal localization of human JAK3. Genomics. 1996;37(1):57-61.
50. Boudeau J, Miranda-Saavedra D, Barton GJ, Alessi DR. Emerging roles of pseudokinases. Trends Cell Biol. 2006;16(9):443-52.
51. Katso R, Russell R, Ganesan T. Functional analysis of H-ryk, an atypical member of the receptor tyrosine kinase family. Mol Cell Biol. 1999;19(9):6427-40.

52. Abe Y, Matsumoto S, Wei S, Nezu K, Miyoshi A, Kito K, et al. Cloning and characterization of a p53-related protein kinase expressed in interleukin-2-activated cytotoxic T-cells, epithelial tumor cell lines, and the testes. J Biol Chem. 2001;276(47):44003-11.
53. Mukherjee K, Sharma M, Urlaub H, Bourenkov GP, Jahn R, Südhof TC, et al. CASK functions as a Mg2+ -independent neurexin kinase. Cell. 2008;133(2):328-39.
54. Baas A, Boudeau J, Sapkota G, Smit L, Medema R, Morrice N, et al. Activation of the tumour suppressor kinase LKB1 by the STE20-like pseudokinase STRAD. EMBO J. 2003;22(12):3062-72.
55. Dan I, Watanabe NM, Kusumi A. The Ste20 group kinases as regulators of MAP kinase cascades. Trends Cell Biol. 2001;11(5):220-30.
56. Zeqiraj E, Filippi BM, Goldie S, Navratilova I, Boudeau J, Deak M, et al. ATP and MO25α regulate the conformational state of the STRADα pseudokinase and activation of the LKB1 tumour suppressor. PLoS biology. 2009 June;7(6):e1000126.
57. Zeqiraj E, Filippi BM, Deak M, Alessi DR, van Aalten DM. Structure of the LKB1-STRAD-MO25 complex reveals an allosteric mechanism of kinase activation. Science. 2009;326(5960):1707-11.
58. Boudeau J, Baas AF, Deak M, Morrice NA, Kieloch A, Schutkowski M, et al. MO25α/β interact with STRADα/β enhancing their ability to bind, activate and localize LKB1 in the cytoplasm. EMBO J. 2003;22(19):5102-14.
59. Rajakulendran T, Sicheri F. Allosteric protein kinase regulation by pseudokinases: Insights from STRAD. Science Signaling. 2010 Mar;3(111):pe8.doi:10.1126/scisignal.3111pe8.
60. Scheeff ED, Eswaran J, Bunkoczi G, Knapp S, Manning G. Structure of the pseudokinase VRK3 reveals a degraded catalytic site, a highly conserved kinase fold, and a putative regulatory binding site. Structure. 2009;17(1):128-38.
61. Nichols RJ, Traktman P. Characterization of three paralogous members of the mammalian vaccinia related kinase family. J Biol Chem. 2004;279(9):7934-46.
62. Kang T, Kim K. VRK3-mediated inactivation of ERK signaling in adult and embryonic rodent tissues. Biochimica et Biophysica Acta (BBA)-Molecular Cell Research. 2008;1783(1):49-58.
63. Fukuda K, Gupta S, Chen K, Wu C, Qin J. The pseudoactive site of ILK is essential for its binding to α-parvin and localization to focal adhesions. Mol Cell. 2009;36(5):819-30.
64. Maydan M, McDonald PC, Sanghera J, Yan J, Rallis C, Pinchin S, et al. Integrin-linked kinase is a functional Mn2 -dependent protein kinase that regulates glycogen synthase kinase-3β (GSK-3β) phosphorylation. PLoS One. 2010;5(8):e12356.
65. Persad S, Attwell S, Gray V, Mawji N, Deng JT, Leung D, et al. Regulation of protein kinase B/akt-serine 473 phosphorylation by integrin-linked kinase critical roles for kinase activity and amino acids arginine 211 and serine 343. J Biol Chem. 2001;276(29):27462-9.
66. Legate KR, Montañez E, Kudlacek O, Füssler R. ILK, PINCH and parvin: The tIPP of integrin signalling. Nature Reviews Molecular Cell Biology. 2005;7(1):20-31.
67. Wickström SA, Lange A, Montanez E, Fässler R. The ILK/PINCH/parvin complex: The kinase is dead, long live the pseudokinase! EMBO J. 2009;29(2):281-91.
68. Hannigan G, Leung-Hagesteijn C, Fitz-Gibbon L, Coppolino M, Dedhar S, Hannigan G, et al. Regulation of cell adhesion and anchorage-dependent growth by a new. Nature. 1996;379(6560):91-6.
69. Deng JT, Van Lierop JE, Sutherland C, Walsh MP. Ca2 -independent smooth muscle contraction A NOVEL FUNCTION FOR INTEGRIN-LINKED KINASE. J Biol Chem. 2001;276(19):16365-73.
70. Yamaji S, Suzuki A, Sugiyama Y, Koide Y, Yoshida M, Kanamori H, et al. A novel integrin-linked Kinase–Binding protein, affixin, is involved in the early stage of Cell–Substrate interaction. J Cell Biol. 2001;153(6):1251-64.
71. Delcommenne M, Tan C, Gray V, Rue L, Woodgett J, Dedhar S. Phosphoinositide-3-OH kinase-dependent regulation of glycogen synthase kinase 3 and protein kinase B/AKT by the integrin-linked kinase. Proceedings of the National Academy of Sciences. 1998;95(19):11211-6.
72. McDonald PC, Fielding AB, Dedhar S. Integrin-linked kinase–essential roles in physiology and cancer biology. J Cell Sci. 2008;121(19):3121-32.
73. Fukuda K, Knight JD, Piszczek G, Kothary R, Qin J. Biochemical, proteomic, structural, and thermodynamic characterizations of integrin-linked kinase (ILK) CROSS-VALIDATION OF THE PSEUDOKINASE. J Biol Chem. 2011;286(24):21886-95.

74. Xu B, English JM, Wilsbacher JL, Stippec S, Goldsmith EJ, Cobb MH. WNK1, a novel mammalian serine/threonine protein kinase lacking the catalytic lysine in subdomain II. Science Signaling. 2000;275(22):16795.
75. Higgins JM. Haspin-like proteins: A new family of evolutionarily conserved putative eukaryotic protein kinases. Protein Science. 2001;10(8):1677-84.
76. Tanaka H, Yoshimura Y, Nozaki M, Yomogida K, Tsuchida J, Tosaka Y, et al. Identification and characterization of a haploid germ cell-specific nuclear ProteinKinase (haspin) in spermatid nuclei and its effects on somatic cells. J Biol Chem. 1999;274(24):17049-57.
77. Mayans O, van der Ven, Peter FM, Wilm M, Mues A, Young P, Fürst DO, et al. Structural basis for activation of the titin kinase domain during myofibrillogenesis. Nature. 1998;395(6705):863-9.
78. Zeqiraj E, van Aalten DM. Pseudokinases-remnants of evolution or key allosteric regulators? Curr Opin Struct Biol. 2010;20(6):772-81.
79. Ungureanu D, Wu J, Pekkala T, Niranjan Y, Young C, Jensen ON, et al. The pseudokinase domain of JAK2 is a dual-specificity protein kinase that negatively regulates cytokine signaling. Nature structural & molecular biology. 2011;18(9):971-6.
80. Kawagoe T, Sato S, Matsushita K, Kato H, Matsui K, Kumagai Y, et al. Sequential control of toll-like receptor–dependent responses by IRAK1 and IRAK2. Nat Immunol. 2008;9(6):684-91.
81. Suijkerbuijk SJ, van Dam TJ, Karagöz GE, von Castelmur E, Hubner NC, Duarte A, et al. The vertebrate mitotic checkpoint protein BUBR1 is an unusual pseudokinase. Developmental cell. 2012;22(6):1321-9.
82. Gee CL, Papavinasasundaram KG, Blair SR, Baer CE, Falick AM, King DS, et al. A phosphorylated pseudokinase complex controls cell wall synthesis in mycobacteria. Science signaling. 2012;5(208):ra7.
83. Murphy JM, Czabotar PE, Hildebrand JM, Lucet IS, Zhang J, Alvarez-Diaz S, et al. The pseudokinase MLKL mediates necroptosis via a molecular switch mechanism. Immunity. 2013.
84. Lucet IS, Babon JJ, Murphy JM. Techniques to examine nucleotide binding by pseudokinases. Biochem Soc Trans. 2013;41:975-80.
85. James MM, Qingwei Z, Samuel NY, Michael LR, Fiona PB, Patrick AE, et al. A robust methodology to subclassify pseudokinases based on their nucleotide binding properties. Biochem J. 2013.
86. Dar AC. A pickup in pseudokinase activity. Biochem Soc Trans. 2013;41(part 4).
87. Eyers PA, Murphy JM. Dawn of the dead: Protein pseudokinases signal new adventures in cell biology. Biochem Soc Trans. 2013;41(4):969-74.
88. Kolesnick R, Xing HR. Inflammatory bowel disease reveals the kinase activity of KSR1. J Clin Invest. 2004;114(9):1233-7.
89. Therrien M, Chang HC, Solomon NM, Karim FD, Wassarman DA, Rubin GM. KSR, a novel protein kinase required for RAS signal transduction. Cell. 1995;83(6):879-88.
90. Xing HR, Lozano J, Kolesnick R. Epidermal growth factor treatment enhances the kinase activity of kinase suppressor of ras. J Biol Chem. 2000;275(23):17276-80.
91. Xing HR, Kolesnick R. Kinase suppressor of ras signals through Thr269 of c-raf-1. J Biol Chem. 2001;276(13):9733-41.
92. Zafrullah M, Yin X, Haimovitz-Friedman A, Fuks Z, Kolesnick R. Kinase suppressor of ras transphosphorylates c-raf-1. Biochem Biophys Res Commun. 2009;390(3):434-40.
93. Zhang Y, Yao B, Delikat S, Bayoumy S, Lin X, Basu S, et al. Kinase suppressor of ras is ceramide-activated protein kinase. Cell. 1997;89(1):63-72.
94. Kolch W. Coordinating ERK/MAPK signalling through scaffolds and inhibitors. Nature Reviews Molecular Cell Biology. 2005;6(11):827-37.
95. McKay MM, Ritt DA, Morrison DK. Signaling dynamics of the KSR1 scaffold complex. Proceedings of the National Academy of Sciences. 2009;106(27):11022-7.
96. Dougherty MK, Ritt DA, Zhou M, Specht SI, Monson DM, Veenstra TD, et al. KSR2 is a calcineurin substrate that promotes ERK cascade activation in response to calcium signals. Mol Cell. 2009;34(6):652-62.
97. Rajakulendran T, Sahmi M, Lefrançois M, Sicheri F, Therrien M. A dimerization-dependent mechanism drives RAF catalytic activation. Nature. 2009;461(7263):542-5.
98. Brennan DF, Dar AC, Hertz NT, Chao WC, Burlingame AL, Shokat KM, et al. A raf-induced allosteric transition of KSR stimulates phosphorylation of MEK. Nature. 2011;472(7343):366-9.

99. Shi F, Telesco SE, Liu Y, Radhakrishnan R, Lemmon MA. ErbB3/HER3 intracellular domain is competent to bind ATP and catalyze autophosphorylation. Proceedings of the National Academy of Sciences. 2010;107(17):7692-7.
100. Jura N, Shan Y, Cao X, Shaw DE, Kuriyan J. Structural analysis of the catalytically inactive kinase domain of the human EGF receptor 3. Proceedings of the National Academy of Sciences. 2009;106(51):21608-13.
101. Holbro T, Beerli RR, Maurer F, Koziczak M, Barbas CF, Hynes NE. The ErbB2/ErbB3 heterodimer functions as an oncogenic unit: ErbB2 requires ErbB3 to drive breast tumor cell proliferation. Proceedings of the National Academy of Sciences. 2003;100(15):8933-8.
102. Berger MB, Mendrola JM, Lemmon MA. ErbB3/HER3 does not homodimerize upon neuregulin binding at the cell surface. FEBS Lett. 2004;569(1):332-6.
103. Zhang X, Gureasko J, Shen K, Cole PA, Kuriyan J. An allosteric mechanism for activation of the kinase domain of epidermal growth factor receptor. Cell. 2006;125(6):1137-49.
104. Luo H, Yu G, Tremblay J, Wu J. EphB6-null mutation results in compromised T cell function. J Clin Invest. 2004;114(12):1762-73.
105. Wek RC, Ramirez M, Jackson BM, Hinnebusch AG. Identification of positive-acting domains in GCN2 protein kinase required for translational activation of GCN4 expression. Mol Cell Biol. 1990;10(6):2820-31.
106. Firmbach-Kraft I, Byers M, Shows T, Dalla-Favera R, Krolewski J. Tyk2, prototype of a novel class of non-receptor tyrosine kinase genes. Oncogene. 1990;5(9):1329-36.
107. Wilks AF. Two putative protein-tyrosine kinases identified by application of the polymerase chain reaction. Proceedings of the National Academy of Sciences. 1989;86(5):1603-7.
108. Wilks A, Harpur A, Kurban R, Ralph S, Zürcher G, Ziemiecki A. Two novel protein-tyrosine kinases, each with a second phosphotransferase-related catalytic domain, define a new class of protein kinase. Mol Cell Biol. 1991;11(4):2057-65.
109. Fwilks AF, Cloning members of protein-tyrosine kinase family using polymerase chain reaction. Meth Enzymol. 1991;200:533-46.
110. Kawamura M, McVicar DW, Johnston JA, Blake TB, Chen Y, Lal BK, et al. Molecular cloning of L-JAK, a janus family protein-tyrosine kinase expressed in natural killer cells and activated leukocytes. Proceedings of the National Academy of Sciences. 1994;91(14):6374-8.
111. Witthuhn BA, Silvennoinen O, Miura O, Lai KS, Cwik C, Liu ET, et al. Involvement of the jak-3 janus kinase in signalling by interleukins 2 and 4 in lymphoid and myeloid cells. Nature, 1994; 370, pg:153-157.
112. Takahashi T, Shirasaw T. Molecular cloning of rat JAK3, a novel member of the JAK family of protein tyrosine kinases. FEBS Lett. 1994;342(2):124-8.
113. Rane SG, Reddy EP. JAK3: A novel JAK kinase associated with terminal differentiation of hematopoietic cells. Oncogene. 1994;9(8):2415-23.
114. Johnston JA, Kawamura M, Kirken RA, Chen Y, Blake TB, Shibuya K, et al. Phosphorylation and activation of the jak-3 janus kinase in response to interleukin-2. Nature. 1994 Jul; 370(6385): 153-157.
115. Conway G, Margoliath A, Wong-Madden S, Roberts RJ, Gilbert W. Jak1 kinase is required for cell migrations and anterior specification in zebrafish embryos. Proceedings of the National Academy of Sciences. 1997;94(7):3082-7.
116. Binari R, Perrimon N. Stripe-specific regulation of pair-rule genes by hopscotch, a putative jak family tyrosine kinase in drosophila. Genes Dev. 1994;8(3):300-12.
117. Adler K, Gerisch G, von Hugo U, Lupas A, Schweiger A. Classification of tyrosine kinases from< i> dictyostelium discoideum with two distinct, complete or incomplete catalytic domains. FEBS Lett. 1996;395(2):286-92.
118. Briscoe J, Rogers N, Witthuhn B, Watling D, Harpur A, Wilks A, et al. Kinase-negative mutants of JAK1 can sustain interferon-gamma-inducible gene expression but not an antiviral state. EMBO J. 1996;15(4):799.
119. Frenzel K, Wallace TA, McDoom I, Xiao HD, Capecchi MR, Bernstein KE, et al. A functional Jak2 tyrosine kinase domain is essential for mouse development. Exp Cell Res. 2006;312(15):2735-44.
120. Feng J, Witthuhn BA, Matsuda T, Kohlhuber F, Kerr IM, Ihle JN. Activation of Jak2 catalytic activity requires phosphorylation of Y1007 in the kinase activation loop. Mol Cell Biol. 1997;17(5):2497-501.

121. Liu KD, Gaffen SL, Goldsmith MA, Greene WC. Janus kinases in interleukin-2-mediated signaling: JAK1 and JAK3 are differentially regulated by tyrosine phosphorylation. Current Biology. 1997;7(11):817-26.
122. Gauzzi M, Velazquez L, McKendry R, Mogensen K, Fellous M, Pellegrini S. Interferon-alpha dependent activation of Tyk2 requires phosphorylation of positive regulatory tyrosines by another kinase. J.Biol.Chem. 1996;271(34):20494-500.
123. Zhou Y, Hanson EP, Chen Y, Magnuson K, Chen M, Swann PG, et al. Distinct tyrosine phosphorylation sites in JAK3 kinase domain positively and negatively regulate its enzymatic activity. Proceedings of the National Academy of Sciences. 1997;94(25):13850-5.
124. Boggon TJ, Li Y, Manley PW, Eck MJ. Crystal structure of the Jak3 kinase domain in complex with a staurosporine analog. Blood. 2005;106(3):996-1002.
125. Williams NK, Bamert RS, Patel O, Wang C, Walden PM, Wilks AF, et al. Dissecting specificity in the janus kinases: The structures of JAK-specific inhibitors complexed to the JAK1 and JAK2 protein tyrosine kinase domains. J Mol Biol. 2009;387(1):219-32.
126. Chrencik JE, Patny A, Leung IK, Korniski B, Emmons TL, Hall T, et al. Structural and thermodynamic characterization of the TYK2 and JAK3 kinase domains in complex with CP-690550 and CMP-6. J Mol Biol. 2010;400(3):413-33.
127. Frank SJ, Yi W, Zhao Y, Goldsmith JF, Gilliland G, Jiang J, et al. Regions of the JAK2 tyrosine kinase required for coupling to the growth hormone receptor. J Biol Chem. 1995;270(24):14776-85.
128. Velazquez L, Mogensen K, Barbieri G, Fellous M, Uzé G, Pellegrini S. Distinct domains of the protein tyrosine kinase tyk2 required for binding of interferon-alpha/beta and for signal transduction. J.Biol.Chem. 1995;270((7)):3327-34.
129. Vihinen M, Villa A, Mella P, Schumacher RF, Savoldi G, O'Shea JJ, et al. Molecular modeling of the Jak3 kinase domains and structural basis for severe combined immunodeficiency. Clinical Immunology. 2000;96(2):108-18.
130. Saharinen P, Takaluoma K, Silvennoinen O. Regulation of the Jak2 tyrosine kinase by its pseudokinase domain. Mol Cell Biol. 2000;20(10):3387-95.
131. Saharinen P, Silvennoinen O. The pseudokinase domain is required for suppression of basal activity of Jak2 and Jak3 tyrosine kinases and for cytokine-inducible activation of signal transduction. J Biol Chem. 2002;277(49):47954-63.
132. Saharinen P, Vihinen M, Silvennoinen O. Autoinhibition of Jak2 tyrosine kinase is dependent on specific regions in its pseudokinase domain. Mol Biol Cell. 2003;14(4):1448-59.
133. Yeh T, Dondi E, Uze G, Pellegrini S. A dual role for the kinase-like domain of the tyrosine kinase Tyk2 in interferon-alpha signaling. Proceedings of the National Academy of Sciences. 2000;97((16)):8991-6.
134. Bandaranayake RM, Ungureanu D, Shan Y, Shaw DE, Silvennoinen O, Hubbard SR. Crystal structures of the JAK2 pseudokinase domain and the pathogenic mutant V617F. Nature structural & molecular biology. 2012 Aug; 19(8):754-9.
135. Toms AV, Deshpande A, McNally R, Jeong Y, Rogers JM, Kim CU, et al. Structure of a pseudokinase-domain switch that controls oncogenic activation of jak kinases. Nature structural & molecular biology. 2013;20(10):1221-3.
136. Bernards A. Predicted tyk2 protein contains two tandem protein kinase domains. Oncogene. 1991 Jul;6(7):1185-7.
137. Al-Lazikani B, Sheinerman FB, Honig B. Combining multiple structure and sequence alignments to improve sequence detection and alignment: Application to the SH2 domains of janus kinases. Proceedings of the National Academy of Sciences. 2001;98(26):14796-801.
138. Kampa D, Burnside J. Computational and functional analysis of the putative SH2 domain in janus kinases. Biochem Biophys Res Commun. 2000;278(1):175-82.
139. Giordanetto F, Kroemer RT. Prediction of the structure of human janus kinase 2 (JAK2) comprising JAK homology domains 1 through 7. Protein Eng. 2002;15(9):727-37.
140. Radtke S, Haan S, Jörissen A, Hermanns HM, Diefenbach S, Smyczek T, et al. The Jak1 SH2 domain does not fulfill a classical SH2 function in jak/STAT signaling but plays a structural role for receptor interaction and up-regulation of receptor surface expression. J Biol Chem. 2005;280(27):25760-8.

141. Liu BA, Jablonowski K, Raina M, Arcé M, Pawson T, Nash PD. The human and mouse complement of SH2 domain proteins—establishing the boundaries of phosphotyrosine signaling. Mol Cell. 2006;22(6):851-68.
142. Girault J, Labesse G, Mornon J, Callebaut I. Janus kinases and focal adhesion kinases play in the 4.1 band: A superfamily of band 4.1 domains important for cell structure and signal transduction. Molecular Medicine. 1998;4(12):751.
143. Pearson MA, Reczek D, Bretscher A, Karplus PA. Structure of the ERM protein moesin reveals the FERM domain fold masked by an extended actin binding tail domain. Cell. 2000;101(3):259-70.
144. Lebrun J, Ali S, Ullrich A, Kelly PA. Proline-rich sequence-mediated Jak2 association to the prolactin receptor is required but not sufficient for signal transduction. J Biol Chem. 1995;270(18):10664-70.
145. Frank DA, Robertson MJ, Bonni A, Ritz J, Greenberg ME. Interleukin 2 signaling involves the phosphorylation of stat proteins. Proceedings of the National Academy of Sciences. 1995;92(17):7779-83.
146. Tanner JW, Chen W, Young RL, Longmore GD, Shaw AS. The conserved box 1 motif of cytokine receptors is required for association with JAK kinases. J Biol Chem. 1995;270(12):6523-30.
147. Chen M, Cheng A, Chen Y, Hymel A, Hanson EP, Kimmel L, et al. The amino terminus of JAK3 is necessary and sufficient for binding to the common γ chain and confers the ability to transmit interleukin 2-mediated signals. Proceedings of the National Academy of Sciences. 1997;94(13):6910-5.
148. Cacalano NA, Migone T, Bazan F, Hanson EP, Chen M, Candotti F, et al. Autosomal SCID caused by a point mutation in the N-terminus of Jak3: Mapping of the Jak3–receptor interaction domain. EMBO J. 1999;18(6):1549-58.
149. Huang LJ, Constantinescu SN, Lodish HF. The N-terminal domain of janus kinase 2 is required for golgi processing and cell surface expression of erythropoietin receptor. Mol Cell. 2001;8(6):1327-38.
150. Richter MF, Duménil G, Uzé G, Fellous M, Pellegrini S. Specific contribution of Tyk2 JH regions to the binding and the expression of the interferon α/β receptor component IFNAR1. J Biol Chem. 1998;273(38):24723-9.
151. Haan C, Is' harc H, Hermanns HM, Schmitz-Van de Leur H, Kerr IM, Heinrich PC, et al. Mapping of a region within the N terminus of Jak1 involved in cytokine receptor interaction. J Biol Chem. 2001;276(40):37451-8.
152. Hilkens CM, Is'harc H, Lillemeier BF, Strobl B, Bates PA, Behrmann I, et al. A region encompassing the FERM domain of Jak1 is necessary for binding to the cytokine receptor gp130. FEBS Lett. 2001;505(1):87-91.
153. Ragimbeau J, Dondi E, Alcover A, Eid P, Uzé G, Pellegrini S. The tyrosine kinase Tyk2 controls IFNAR1 cell surface expression. EMBO J. 2003;22(3):537-47.
154. Funakoshi-Tago M, Pelletier S, Matsuda T, Parganas E, Ihle JN. Receptor specific downregulation of cytokine signaling by autophosphorylation in the FERM domain of Jak2. EMBO J. 2006;25(20):4763-72.
155. Argetsinger LS, Kouadio JK, Steen H, Stensballe A, Jensen ON, Carter-Su C. Autophosphorylation of JAK2 on tyrosines 221 and 570 regulates its activity. Mol Cell Biol. 2004;24(11):4955-67.
156. Feener EP, Rosario F, Dunn SL, Stancheva Z, Myers MG. Tyrosine phosphorylation of Jak2 in the JH2 domain inhibits cytokine signaling. Mol Cell Biol. 2004;24(11):4968-78.
157. Zhou Y, Chen M, Cusack NA, Kimmel LH, Magnuson KS, Boyd JG, et al. Unexpected effects of FERM domain mutations on catalytic activity of Jak3: Structural implication for janus kinases. Mol Cell. 2001;8(5):959-69.
158. Haan S, Margue C, Engrand A, Rolvering C, Schmitz-Van de Leur H, Heinrich PC, et al. Dual role of the Jak1 FERM and kinase domains in cytokine receptor binding and in stimulation-dependent jak activation. The Journal of Immunology. 2008;180(2):998-1007.
159. Matsuda T, Feng J, Witthuhn BA, Sekine Y, Ihle JN. Determination of the transphosphorylation sites of Jak2 kinase. Biochem Biophys Res Commun. 2004;325(2):586-94.
160. Funakoshi-Tago M, Pelletier S, Moritake H, Parganas E, Ihle JN. Jak2 FERM domain interaction with the erythropoietin receptor regulates Jak2 kinase activity. Mol Cell Biol. 2008;28(5):1792-801.

161. Kurzer J, Argetsinger L, Zhou Y, Kouadio J, O'Shea J, Carter-Su C. Tyrosine 813 is a site of JAK2 autophosphorylation critical for activation of JAK2 by SH2-B beta. Mol.Cell.Biol. 2004;24(10):4557-70.
162. Carpino N, Kobayashi R, Zang H, Takahashi Y, Jou S, Feng J, et al. Identification, cDNA cloning, and targeted deletion of p70, a novel, ubiquitously expressed SH3 domain-containing protein. Mol Cell Biol. 2002;22(21):7491-500.
163. McDoom I, Ma X, Kirabo A, Lee K, Ostrov DA, Sayeski PP. Identification of tyrosine 972 as a novel site of Jak2 tyrosine kinase phosphorylation and its role in Jak2 activation†. Biochemistry (N Y). 2008;47(32):8326-34.
164. Argetsinger LS, Stuckey JA, Robertson SA, Koleva RI, Cline JM, Marto JA, et al. Tyrosines 868, 966, and 972 in the kinase domain of JAK2 are autophosphorylated and required for maximal JAK2 kinase activity. Molecular Endocrinology. 2010;24(5):1062-76.
165. Yasukawa H, Misawa H, Sakamoto H, Masuhara M, Sasaki A, Wakioka T, et al. The JAK-binding protein JAB inhibits janus tyrosine kinase activity through binding in the activation loop. EMBO J. 1999;18(5):1309-20.
166. Sayyah J, Gnanasambandan K, Kamarajugadda S, Tsuda S, Caldwell-Busby J, Sayeski PP. Phosphorylation of Y372 is critical for Jak2 tyrosine kinase activation. Cell Signal. 2011;23(11):1806-15.
167. Funakoshi-Tago M, Tago K, Kasahara T, Parganas E, Ihle JN. Negative regulation of Jak2 by its auto-phosphorylation at tyrosine 913 via the epo signaling pathway. Cell Signal. 2008;20(11):1995-2001.
168. Lucet IS, Fantino E, Styles M, Bamert R, Patel O, Broughton SE, et al. The structural basis of janus kinase 2 inhibition by a potent and specific pan-janus kinase inhibitor. Blood. 2006;107(1):176-83.
169. Haan C, Kroy DC, Wüller S, Sommer U, Nöcker T, Rolvering C, et al. An unusual insertion in Jak2 is crucial for kinase activity and differentially affects cytokine responses. The Journal of Immunology. 2009;182(5):2969-77.
170. Mazurkiewicz-Munoz AM, Argetsinger LS, Kouadio JK, Stensballe A, Jensen ON, Cline JM, et al. Phosphorylation of JAK2 at serine 523: A negative regulator of JAK2 that is stimulated by growth hormone and epidermal growth factor. Mol Cell Biol. 2006;26(11):4052-62.
171. Ishida-Takahashi R, Rosario F, Gong Y, Kopp K, Stancheva Z, Chen X, et al. Phosphorylation of Jak2 on Ser523 inhibits Jak2-dependent leptin receptor signaling. Mol Cell Biol. 2006;26(11):4063-73.
172. Aaronson DS, Horvath CM. A road map for those who don't know JAK-STAT. Science. 2002;296(5573):1653-5.
173. O'Shea JJ, Gadina M, Schreiber RD. Cytokine signaling in 2002: New surprises in the jak/stat pathway. Cell. 2002;109(2):S121-31.
174. Rawlings JS, Rosler KM, Harrison DA. The JAK/STAT signaling pathway. J Cell Sci. 2004;117(8):1281-3.
175. Mohr A, Chatain N, Domoszlai T, Rinis N, Sommerauer M, Vogt M, et al. Dynamics and non-canonical aspects of JAK/STAT signalling. Eur J Cell Biol. 2012;91(6):524-32.
176. Livnah O, Stura EA, Middleton SA, Johnson DL, Jolliffe LK, Wilson IA. Crystallographic evidence for preformed dimers of erythropoietin receptor before ligand activation. Science. 1999;283(5404):987-90.
177. Syed RS, Reid SW, Li C, Cheetham JC, Aoki KH, Liu B, et al. Efficiency of signalling through cytokine receptors depends critically on receptor orientation. Nature. 1998;395(6701):511-6.
178. Constantinescu SN, Huang LJ, Nam H, Lodish HF. The erythropoietin receptor cytosolic juxtamembrane domain contains an essential, precisely oriented, hydrophobic motif. Mol Cell. 2001;7(2):377-85.
179. Greiser JS, Stross C, Heinrich PC, Behrmann I, Hermanns HM. Orientational constraints of the gp130 intracellular juxtamembrane domain for signaling. J Biol Chem. 2002;277(30):26959-65.
180. Qiu H, Belanger A, Yoon HP, Bunn HF. Homodimerization restores biological activity to an inactive erythropoietin mutant. J Biol Chem. 1998;273(18):11173-6.
181. Dawson MA, Bannister AJ, Göttgens B, Foster SD, Bartke T, Green AR, et al. JAK2 phosphorylates histone H3Y41 and excludes HP1&agr; from chromatin. Nature. 2009;461(7265):819-22.
182. Fuh G, Cunningham BC, Fukunaga R, Nagata S, Goeddel DV, Wells JA. Rational design of potent antagonists to the human growth hormone receptor. Science. 1992;256(5064):1677-80.

183. Ballinger MD, Wells JA. Will any dimer do? Nature Structural & Molecular Biology. 1998;5(11):938-40.
184. Schindler CW. Series introduction: JAK-STAT signaling in human disease. J Clin Invest. 2002;109(9):1133-7.
185. Gadina M, Hilton D, Johnston JA, Morinobu A, Lighvani A, Zhou Y, et al. Signaling by type I and II cytokine receptors: Ten years after. Curr Opin Immunol. 2001;13(3):363-73.
186. Rane SG, Reddy EP. Janus kinases: Components of multiple signaling pathways. Oncogene. 2000;19(49):5662.
187. Kisseleva T, Bhattacharya S, Braunstein J, Schindler C. Signaling through the JAK/STAT pathway, recent advances and future challenges. Gene. 2002;285(1):1-24.
188. DAMESHEK W. Editorial: Some speculations on the myeloproliferative syndromes. Blood. 1951;6(4):372-5.
189. Lacronique V, Boureux A, Della Valle V, Poirel H, Quang CT, Mauchauffé M, et al. A TEL-JAK2 fusion protein with constitutive kinase activity in human leukemia. Science. 1997;278(5341):1309-12.
190. Lacronique V, Boureux A, Monni R, Dumon S, Mauchauffé M, Mayeux P, et al. Transforming properties of chimeric TEL-JAK proteins in ba/F3 cells. Blood. 2000;95(6):2076-83.
191. Carron C, Cormier F, Janin A, Lacronique V, Giovannini M, Daniel M, et al. TEL-JAK2 transgenic mice develop T-cell leukemia. Blood. 2000;95(12):3891-9.
192. Harrison DA, Binari R, Nahreini TS, Gilman M, Perrimon N. Activation of a drosophila janus kinase (JAK) causes hematopoietic neoplasia and developmental defects. EMBO J. 1995;14(12):2857.
193. Luo H, Hanratty W, Dearolf C. An amino acid substitution in the drosophila hopTum-l jak kinase causes leukemia-like hematopoietic defects. EMBO J. 1995;14(7):1412.
194. Baxter EJ, Scott LM, Campbell PJ, East C, Fourouclas N, Swanton S, et al. Acquired mutation of the tyrosine kinase JAK2 in human myeloproliferative disorders. The Lancet. 2005;365(9464):1054-61.
195. Levine RL, Wadleigh M, Cools J, Ebert BL, Wernig G, Huntly BJ, et al. Activating mutation in the tyrosine kinase JAK2 in polycythemia vera, essential thrombocythemia, and myeloid metaplasia with myelofibrosis. Cancer cell. 2005;7(4):387-97.
196. Zhao R, Xing S, Li Z, Fu X, Li Q, Krantz SB, et al. Identification of an acquired JAK2 mutation in polycythemia vera. J Biol Chem. 2005;280(24):22788-92.
197. Kralovics R, Passamonti F, Buser AS, Teo S, Tiedt R, Passweg JR, et al. A gain-of-function mutation of JAK2 in myeloproliferative disorders. N Engl J Med. 2005;352(17):1779-90.
198. James C, Ugo V, Le Couédic J, Staerk J, Delhommeau F, Lacout C, et al. A unique clonal JAK2 mutation leading to constitutive signalling causes polycythaemia vera. Nature. 2005;434(7037):1144-8.
199. Campbell PJ, Green AR. The myeloproliferative disorders. N Engl J Med. 2006;355(23):2452-66.
200. Smith CA, Fan G. The saga of JAK2 mutations and translocations in hematologic disorders: Pathogenesis, diagnostic and therapeutic prospects, and revised world health organization diagnostic criteria for myeloproliferative neoplasms. Hum Pathol. 2008;39(6):795-810.
201. Levine RL. Janus kinase mutations. Seminars in oncology; Elsevier; 2009.
202. Scott LM, Tong W, Levine RL, Scott MA, Beer PA, Stratton MR, et al. JAK2 exon 12 mutations in polycythemia vera and idiopathic erythrocytosis. N Engl J Med. 2007;356(5):459-68.
203. Schnittger S, Bacher U, Kern W, Schröder M, Haferlach T, Schoch C. Report on two novel nucleotide exchanges in the JAK2 pseudokinase domain: D620E and E627E. Leukemia. 2006;20(12):2195-7.
204. Zhang S, Li J, Li W, Song J, Xu W, Qiu H. The investigation of JAK2 mutation in chinese myeloproliferative diseases-identification of a novel C616Y point mutation in a PV patient. International journal of laboratory hematology. 2007;29(1):71-2.
205. Malinge S, Ragu C, Della-Valle V, Pisani D, Constantinescu SN, Perez C, et al. Activating mutations in human acute megakaryoblastic leukemia. Blood. 2008;112(10):4220-6.
206. Bercovich D, Ganmore I, Scott LM, Wainreb G, Birger Y, Elimelech A, et al. Mutations of< i> JAK2 in acute lymphoblastic leukaemias associated with down's syndrome. The Lancet. 2008;372(9648):1484-92.
207. Kratz C, Böll S, Kontny U, Schrappe M, Niemeyer C, Stanulla M. Mutational screen reveals a novel JAK2 mutation, L611S, in a child with acute lymphoblastic leukemia. Leukemia. 2005;20(2):381-3.

208. Lee J, Kim Y, Soung Y, Han K, Kim S, Rhim H, et al. The JAK2 V617F mutation in de novo acute myelogenous leukemias. Oncogene. 2005;25(9):1434-6.
209. Luo H, Rose P, Barber D, Hanratty WP, Lee S, Roberts TM, et al. Mutation in the jak kinase JH2 domain hyperactivates drosophila and mammalian jak-stat pathways. Mol Cell Biol. 1997;17(3):1562-71.
210. Ma W, Kantarjian H, Zhang X, Yeh C, Zhang ZJ, Verstovsek S, et al. Mutation profile of JAK2 transcripts in patients with chronic myeloproliferative neoplasias. The Journal of Molecular Diagnostics. 2009;11(1):49-53.
211. Zhao L, Dong H, Zhang CC, Kinch L, Osawa M, Iacovino M, et al. A JAK2 interdomain linker relays epo receptor engagement signals to kinase activation. J Biol Chem. 2009;284(39):26988-98.
212. Mercher T, Wernig G, Moore SA, Levine RL, Gu T, Fröhling S, et al. JAK2T875N is a novel activating mutation that results in myeloproliferative disease with features of megakaryoblastic leukemia in a murine bone marrow transplantation model. Blood. 2006;108(8):2770-9.
213. Mullighan CG, Zhang J, Harvey RC, Collins-Underwood JR, Schulman BA, Phillips LA, et al. JAK mutations in high-risk childhood acute lymphoblastic leukemia. Proceedings of the National Academy of Sciences. 2009;106(23):9414-8.
214. Aranaz P, Ormazábal C, Hurtado C, Erquiaga I, Calasanz MJ, García-Delgado M, et al. A new potential oncogenic mutation in the FERM domain of< i> JAK2 in< i> BCR/< i> ABL1-negative and V617F-negative chronic myeloproliferative neoplasms revealed by a comprehensive screening of 17 tyrosine kinase coding genes. Cancer Genet Cytogenet. 2010;199(1):1-8.
215. Marit MR, Chohan M, Matthew N, Huang K, Kuntz DA, Rose DR, et al. Random mutagenesis reveals residues of JAK2 critical in evading inhibition by a tyrosine kinase inhibitor. PloS one. 2012;7(8):e43437.
216. Haan C, Behrmann I, Haan S. Perspectives for the use of structural information and chemical genetics to develop inhibitors of janus kinases. J Cell Mol Med. 2010;14(3):504-27.
217. Gnanasambandan K, Sayeski P. A structure-function perspective of jak2 mutations and implications for alternate drug design strategies: The road not taken. Curr Med Chem. 2011;18(30):4659-73.
218. Kohlhuber F, Rogers NC, Watling D, Feng J, Guschin D, Briscoe J, et al. A JAK1/JAK2 chimera can sustain alpha and gamma interferon responses. Mol Cell Biol. 1997;17(2):695-706.
219. Li Z, Xu M, Xing S, Ho WT, Ishii T, Li Q, et al. Erlotinib effectively inhibits JAK2V617F activity and polycythemia vera cell growth. J Biol Chem. 2007;282(6):3428-32.
220. Staerk J, Kallin A, Demoulin J, Vainchenker W, Constantinescu SN. JAK1 and Tyk2 activation by the homologous polycythemia vera JAK2 V617F mutation cross-talk with IGF1 receptor. J Biol Chem. 2005;280(51):41893-9.
221. Lu X, Levine R, Tong W, Wernig G, Pikman Y, Zarnegar S, et al. Expression of a homodimeric type I cytokine receptor is required for JAK2V617F-mediated transformation. Proc Natl Acad Sci U S A. 2005;102(52):18962-7.
222. Lu X, Huang LJ, Lodish HF. Dimerization by a cytokine receptor is necessary for constitutive activation of JAK2V617F. J Biol Chem. 2008;283(9):5258-66.
223. Wernig G, Gonneville JR, Crowley BJ, Rodrigues MS, Reddy MM, Hudon HE, et al. The Jak2V617F oncogene associated with myeloproliferative diseases requires a functional FERM domain for transformation and for expression of the myc and pim proto-oncogenes. Blood. 2008;111(7):3751-9.
224. Zhao L, Ma Y, Seemann J, Huang L. A regulating role of the JAK2 FERM domain in hyperactivation of JAK2 (V617F). Biochem J. 2010;426:91-8.
225. Dusa A, Mouton C, Pecquet C, Herman M, Constantinescu SN. JAK2 V617F constitutive activation requires JH2 residue F595: A pseudokinase domain target for specific inhibitors. PLoS One. 2010;5(6):e11157.
226. Gnanasambandan K, Magis A, Sayeski PP. The constitutive activation of Jak2-V617F is mediated by a π stacking mechanism involving phenylalanines 595 and 617. Biochemistry (N Y). 2010;49(46):9972-84.
227. Dusa A, Staerk J, Elliott J, Pecquet C, Poirel HA, Johnston JA, et al. Substitution of pseudokinase domain residue val-617 by large non-polar amino acids causes activation of JAK2. J Biol Chem. 2008;283(19):12941-8.

228. Sanz A, Ungureanu D, Pekkala T, Ruijtenbeek R, Touw IP, Hilhorst R, et al. Analysis of Jak2 catalytic function by peptide microarrays: The role of the JH2 domain and V617F mutation. PloS one. 2011;6(4):e18522.
229. Lindauer K, Loerting T, Liedl KR, Kroemer RT. Prediction of the structure of human janus kinase 2 (JAK2) comprising the two carboxy-terminal domains reveals a mechanism for autoregulation. Protein Eng. 2001;14(1):27-37.
230. Lee T, Ma W, Zhang X, Giles F, Kantarjian H, Albitar M. Mechanisms of constitutive activation of janus kinase 2-V617F revealed at the atomic level through molecular dynamics simulations. Cancer. 2009;115(8):1692-700.
231. Wan S, Coveney PV. Regulation of JAK2 activation by janus homology 2: Evidence from molecular dynamics simulations. Journal of chemical information and modeling. 2012;52(11):2992-3000.
232. Wan X, Ma Y, McClendon CL, Huang LJ, Huang N. Ab initio modeling and experimental assessment of janus kinase 2 (JAK2) kinase-pseudokinase complex structure. PLoS computational biology. 2013;9(4):e1003022.
233. Lee T. On the negative regulation and activation of JAK2: A novel hypothetical model. Molecular Cancer Research. 2013 April, 11(8);811-4.
234. Kornev AP, Haste NM, Taylor SS, Ten Eyck LF. Surface comparison of active and inactive protein kinases identifies a conserved activation mechanism. Proceedings of the National Academy of Sciences. 2006;103(47):17783-8.
235. Constantinescu SN, Leroy E, Gryshkova V, Pecquet C, Dusa A. Activating janus kinase pseudokinase domain mutations in myeloproliferative and other blood cancers. Biochem Soc Trans. 2013;41(part 4):1048-54.
236. Parganas E, Wang D, Stravopodis D, Topham DJ, Marine J, Teglund S, et al. Jak2 is essential for signaling through a variety of cytokine receptors. Cell. 1998;93(3):385-95.
237. Neubauer H, Cumano A, Müller M, Wu H, Huffstadt U, Pfeffer K. Jak2 deficiency defines an EssentialDevelopmental checkpoint in DefinitiveHematopoiesis. Cell. 1998;93(3):397-409.
238. Wernig G, Mercher T, Okabe R, Levine RL, Lee BH, Gilliland DG. Expression of Jak2V617F causes a polycythemia vera–like disease with associated myelofibrosis in a murine bone marrow transplant model. Blood. 2006;107(11):4274-81.
239. Lacout C, Pisani DF, Tulliez M, Gachelin FM, Vainchenker W, Villeval J. JAK2V617F expression in murine hematopoietic cells leads to MPD mimicking human PV with secondary myelofibrosis. Blood. 2006;108(5):1652-60.
240. Tiedt R, Hao-Shen H, Sobas MA, Looser R, Dirnhofer S, Schwaller J, et al. Ratio of mutant JAK2-V617F to wild-type Jak2 determines the MPD phenotypes in transgenic mice. Blood. 2008;111(8):3931-40.
241. Gao SP, Mark KG, Leslie K, Pao W, Motoi N, Gerald WL, et al. Mutations in the EGFR kinase domain mediate STAT3 activation via IL-6 production in human lung adenocarcinomas. J Clin Invest. 2007;117(12):3846-56.
242. Yoshikawa H, Matsubara K, Qian G, Jackson P, Groopman JD, Manning JE, et al. SOCS-1, a negative regulator of the JAK/STAT pathway, is silenced by methylation in human hepatocellular carcinoma and shows growth-suppression activity. Nat Genet. 2001;28(1):29-35.
243. Ni Z, Lou W, Leman ES, Gao AC. Inhibition of constitutively activated Stat3 signaling pathway suppresses growth of prostate cancer cells. Cancer Res. 2000;60(5):1225-8.
244. Gao B, Shen X, Kunos G, Meng Q, Goldberg ID, Rosen EM, et al. Constitutive activation of JAK–STAT3 signaling by BRCA1 in human prostate cancer cells. FEBS Lett. 2001;488(3):179-84.
245. Garcia R, Bowman TL, GUILLIAN N, HUA Y, Minton S, Muro-Cacho CA, et al. Constitutive activation of Stat3 by the src and JAK tyrosine kinases participates in growth regulation of human breast carcinoma cells. Oncogene. 2001;20(20):2499-513.
246. Yamauchi T, Yamauchi N, Ueki K, Sugiyama T, Waki H, Miki H, et al. Constitutive tyrosine phosphorylation of ErbB-2 via Jak2 by autocrine secretion of prolactin in human breast cancer. J Biol Chem. 2000;275(43):33937-44.
247. Lai SY, Childs EE, Xi S, Coppelli FM, Gooding WE, Wells A, et al. Erythropoietin-mediated activation of JAK-STAT signaling contributes to cellular invasion in head and neck squamous cell carcinoma. Oncogene. 2005;24(27):4442-9.

248. Meydan N, Grunberger T, Dadi H, Shahar M, Arpaia E, Lapidot Z, et al. Inhibition of acute lymphoblastic leukaemia by a jak-2 inhibitor. Nature. 1996 Feb; 379(6566):645-8.
249. Zuccotto F, Ardini E, Casale E, Angiolini M. Through the "gatekeeper door": Exploiting the active kinase conformation. J Med Chem. 2009;53(7):2681-94.
250. LaFave LM, Levine RL. JAK2 the future: Therapeutic strategies for JAK-dependent malignancies. Trends Pharmacol Sci. 2012.
251. Andraos R, Qian Z, Bonenfant D, Rubert J, Vangrevelinghe E, Scheufler C, et al. Modulation of activation-loop phosphorylation by JAK inhibitors is binding mode dependent. Cancer Discovery. 2012;2(6):512-23.
252. Verstovsek S, Kantarjian HM, Pardanani AD, Thomas D, Cortes J, Mesa RA, et al. The JAK inhibitor, INCB018424, demonstrates durable and marked clinical responses in primary myelofibrosis (PMF) and post-polycythemia/essential thrombocythemia myelofibrosis (post-PV/ET-MF). 50th American society of hematology (ASH) annual meeting and exposition; 2008.
253. Mesa R, Friedman S, Newton R, Erickson-Viitanen S, Yeleswaram S, Hunter D, et al. INCB018424, a selective JAK1/2 inhibitor, significantly improves the compromised nutritional status and frank cachexia in patients with myelofibrosis (MF). Body Image. 2008;2(3):4.
254. Verstovsek S, Kantarjian HM, Pardanani AD, Burn T, Vaddi K, Redman J, et al. Characterization of JAK2 V617F allele burden in advanced myelofibrosis (MF) patients: No change in V617F: WT JAK2 ratio in patients with high allele burdens despite profound clinical improvement following treatment with the JAK inhibitor, INCB018424. Blood. 2008;112(11).
255. Quintás-Cardama A, Vaddi K, Liu P, Manshouri T, Li J, Scherle PA, et al. Preclinical characterization of the selective JAK1/2 inhibitor INCB018424: Therapeutic implications for the treatment of myeloproliferative neoplasms. Blood. 2010;115(15):3109-17.
256. Wang Y, Fiskus W, Chong DG, Buckley KM, Natarajan K, Rao R, et al. Cotreatment with panobinostat and JAK2 inhibitor TG101209 attenuates JAK2V617F levels and signaling and exerts synergistic cytotoxic effects against human myeloproliferative neoplastic cells. Blood. 2009;114(24):5024-33.
257. Pardanani A, Hood J, Lasho T, Levine R, Martin M, Noronha G, et al. TG101209, a small molecule JAK2-selective kinase inhibitor potently inhibits myeloproliferative disorder-associated JAK2V617F and MPLW515L/K mutations. Leukemia. 2007;21(8):1658-68.
258. Geron I, Abrahamsson AE, Barroga CF, Kavalerchik E, Gotlib J, Hood JD, et al. Selective inhibition of JAK2-driven erythroid differentiation of polycythemia vera progenitors. Cancer cell. 2008;13(4):321-30.
259. Lasho T, Tefferi A, Hood J, Verstovsek S, Gilliland D, Pardanani A. TG101348, a JAK2-selective antagonist, inhibits primary hematopoietic cells derived from myeloproliferative disorder patients with JAK2V617F, MPLW515K or JAK2 exon 12 mutations as well as mutation negative patients. Leukemia. 2008;22(9):1790-2.
260. Wernig G, Kharas MG, Okabe R, Moore SA, Leeman DS, Cullen DE, et al. Efficacy of TG101348, a selective JAK2 inhibitor, in treatment of a murine model of JAK2V617F-induced polycythemia vera. Cancer cell. 2008;13(4):311-20.
261. Liu PC, Caulder E, Li J, Waeltz P, Margulis A, Wynn R, et al. Combined inhibition of janus kinase 1/2 for the treatment of JAK2V617F-driven neoplasms: Selective effects on mutant cells and improvements in measures of disease severity. Clinical Cancer Research. 2009;15(22):6891-900.
262. Fridman JS, Scherle PA, Collins R, Burn TC, Li Y, Li J, et al. Selective inhibition of JAK1 and JAK2 is efficacious in rodent models of arthritis: Preclinical characterization of INCB028050. The Journal of Immunology. 2010;184(9):5298-307.
263. Mathur A, Mo J, Kraus M, O'Hare E, Sinclair P, Young J, et al. An inhibitor of janus kinase 2 prevents polycythemia in mice. Biochem Pharmacol. 2009;78(4):382-9.
264. Thompson JE, Cubbon RM, Cummings RT, Wicker LS, Frankshun R, Cunningham BR, et al. Photochemical preparation of a pyridone containing tetracycle: A jak protein kinase inhibitor. Bioorg Med Chem Lett. 2002;12(8):1219-23.
265. Hedvat M, Huszar D, Herrmann A, Gozgit JM, Schroeder A, Sheehy A, et al. The JAK2 inhibitor AZD1480 potently blocks Stat3 signaling and oncogenesis in solid tumors. Cancer cell. 2009;16(6):487-97.

266. Shah NP, Olszynski P, Sokol L, Verstovsek S, Hoffman R, List AF. A phase I study of XL019, a selective JAK2 inhibitor, in patients with primary myelofibrosis, post-polycythemia vera, or post-essential thrombocythemia myelofibrosis. Blood. 2008;112(11):98.
267. Paquette R, Sokol L, Shah NP, Silver RT, List AF, Clary DO, et al. A phase I study of XL019, a selective JAK2 inhibitor, in patients with polycythemia vera. Blood; AMER SOC HEMATOLOGY 1900 M STREET. NW SUITE 200, WASHINGTON, DC 20036 USA; 2008.
268. Verstovsek S, Pardanani AD, Shah NP, Sokol L, Wadleigh M, Gilliland DG, et al. A phase 1 study of XL019 a selective JAK2 inhibitor, in patients with primary myelofibrosis and, post-polycythemia vera/essential thrombocythemia myelofibrosis. Blood; AMER SOC HEMATOLOGY 1900 M STREET. NW SUITE 200, WASHINGTON, DC 20036 USA; 2007.
269. Lyons J, Curry J, Mallet K, Miller D, Reule M, Sevears L, et al. JAK2 and T315I abl activity of clinical candidate, AT9283. Proc am assoc cancer res; ; 2007.
270. Squires MS, Cuny JE, Dawson MA, Scott MA, Barber K, Reule M, et al. AT9283, a potent inhibitor of JAK2, is active in JAK2 V617F myeloproliferative disease models. Blood; AMER SOC HEMATOLOGY 1900 M STREET. NW SUITE 200, WASHINGTON, DC 20036 USA; 2007.
271. Dobrzanski P, Hexner E, Serdikoff C, Jan M, Swider C, Robinson C, et al. CEP-701 is a JAK2 inhibitor which attenuates JAK2/STAT5 signaling pathway and the proliferation of primary cells from patients with myeloproliferative disorders. Blood; AMER SOC HEMATOLOGY 1900 M STREET. NW SUITE 200, WASHINGTON, DC 20036 USA; 2006.
272. Hexner EO, Serdikoff C, Jan M, Swider CR, Robinson C, Yang S, et al. Lestaurtinib (CEP701) is a JAK2 inhibitor that suppresses JAK2/STAT5 signaling and the proliferation of primary erythroid cells from patients with myeloproliferative disorders. Blood. 2008;111(12):5663-71.
273. Lu LD, Stump KL, Wallace NH, Dobrzanski P, Serdikoff C, Gingrich DE, et al. Depletion of autoreactive plasma cells and treatment of lupus nephritis in mice using CEP-33779, a novel, orally active, selective inhibitor of JAK2. The Journal of Immunology. 2011;187(7):3840-53.
274. Stump KL, Lu LD, Dobrzanski P, Serdikoff C, Gingrich DE, Dugan BJ, et al. A highly selective, orally active inhibitor of janus kinase 2, CEP-33779, ablates disease in two mouse models of rheumatoid arthritis. Arthritis Res Ther. 2011;13(2):R68.
275. Gozgit JM, Bebernitz G, Patil P, Ye M, Parmentier J, Wu J, et al. Effects of the JAK2 inhibitor, AZ960, on pim/BAD/BCL-xL survival signaling in the human JAK2 V617F cell line SET-2. J Biol Chem. 2008;283(47):32334-43.
276. Shide K, Kameda T, Markovtsov V, Shimoda HK, Tonkin E, Fang S, et al. R723, a selective JAK2 inhibitor, effectively treats JAK2V617F-induced murine myeloproliferative neoplasm. Blood. 2011;117(25):6866-75.
277. Tyner JW, Bumm TG, Deininger J, Wood L, Aichberger KJ, Loriaux MM, et al. CYT387, a novel JAK2 inhibitor, induces hematologic responses and normalizes inflammatory cytokines in murine myeloproliferative neoplasms. Blood. 2010;115(25):5232-40.
278. Pardanani A, Lasho T, Smith G, Burns C, Fantino E, Tefferi A. CYT387, a selective JAK1/JAK2 inhibitor: In vitro assessment of kinase selectivity and preclinical studies using cell lines and primary cells from polycythemia vera patients. Leukemia. 2009;23(8):1441-5.
279. Purandare A, McDevitt T, Wan H, You D, Penhallow B, Han X, et al. Characterization of BMS-911543, a functionally selective small-molecule inhibitor of JAK2. Leukemia. 2011;26(2):280-8.
280. Baffert F, Régnier CH, De Pover A, Pissot-Soldermann C, Tavares GA, Blasco F, et al. Potent and selective inhibition of polycythemia by the quinoxaline JAK2 inhibitor NVP-BSK805. Molecular cancer therapeutics. 2010;9(7):1945-55.
281. Ahmed K, Nussenzveig R, Chen A, Prchal J, Parker C, Gourley E, et al. Preclinical characterization of the JAK-2 inhibitor, SGI-1252. Blood [50th Annu Meet Am Soc Hematol (Dec 6-9, San Francisco) 2008]. 2008;112(11).
282. Riaz Ahmed KB, Warner SL, Chen A, Gourley ES, Liu X, Vankayalapati H, et al. In vitro and in vivo characterization of SGI-1252, a small molecule inhibitor of JAK2. Exp Hematol. 2011;39(1):14-25.
283. Younes A, Romaguera J, Fanale M, McLaughlin P, Hagemeister F, Copeland A, et al. Phase I study of a novel oral janus kinase 2 inhibitor, SB1518, in patients with relapsed lymphoma: Evidence of clinical and biologic activity in multiple lymphoma subtypes. Journal of Clinical Oncology. 2012;30(33):4161-7.

284. Novotny-Diermayr V, Hart S, Goh K, Cheong A, Ong L, Hentze H, et al. The oral HDAC inhibitor pracinostat (SB939) is efficacious and synergistic with the JAK2 inhibitor pacritinib (SB1518) in preclinical models of AML. Blood cancer journal. 2012;2(5):e69.
285. Ma L, Clayton J, Walgren R, Zhao B, Evans R, Smith M, et al. Discovery and characterization of LY2784544, a small-molecule tyrosine kinase inhibitor of JAK2V617F. Blood cancer journal. 2013;3(4):e109.
286. Seavey MM, Dobrzanski P. The many faces of janus kinase. Biochem Pharmacol. 2012;83(9):1136-45.
287. Verstovsek S, Manshouri T, Quintás-Cardama A, Harris D, Cortes J, Giles FJ, et al. WP1066, a novel JAK2 inhibitor, suppresses proliferation and induces apoptosis in erythroid human cells carrying the JAK2 V617F mutation. Clinical Cancer Research. 2008;14(3):788-96.
288. Manshouri T, Quintás-Cardama A, Nussenzveig RH, Gaikwad A, Estrov Z, Prchal J, et al. The JAK kinase inhibitor CP-690,550 supresses the growth of human polycythemia vera cells carrying the JAK2V617F mutation. Cancer science. 2008;99(6):1265-73.
289. Pardanani A. JAK2 inhibitor therapy in myeloproliferative disorders: Rationale, preclinical studies and ongoing clinical trials. Leukemia. 2007;22(1):23-30.
290. Stein BL, Crispino JD, Moliterno AR. Janus kinase inhibitors: An update on the progress and promise of targeted therapy in the myeloproliferative neoplasms. Curr Opin Oncol. 2011;23(6):609-16.
291. Sayyah J, Sayeski PP. Jak2 inhibitors: Rationale and role as therapeutic agents in hematologic malignancies. Curr Oncol Rep. 2009;11(2):117-24.
292. Quintás-Cardama A. The role of janus kinase 2 (JAK2) in myeloproliferative neoplasms: Therapeutic implications. Leuk Res. 2013 Apr; 37(4):465-72.
293. Haan C, Kreis S, Margue C, Behrmann I. Jaks and cytokine receptors—an intimate relationship. Biochem Pharmacol. 2006;72(11):1538-46.
294. Yamaoka K, Saharinen P, Pesu M, Holt 3rd V, Silvennoinen O, O'Shea JJ. The janus kinases (jaks). Genome Biol. 2004;5(12):253.
295. Ghoreschi K, Laurence A, O'Shea JJ. Janus kinases in immune cell signaling. Immunol Rev. 2009;228(1):273-87.
296. Wakao H, Gouilleux F, Groner B. Mammary gland factor (MGF) is a novel member of the cytokine regulated transcription factor gene family and confers the prolactin response. EMBO J. 1994;13(9):2182.
297. Pine R, Canova A, Schindler C. Tyrosine phosphorylated p91 binds to a single element in the ISGF2/IRF-1 promoter to mediate induction by IFN alpha and IFN gamma, and is likely to autoregulate the p91 gene. EMBO J. 1994;13(1):158.
298. Wood TJ, Sliva D, Lobie PE, Goullieux F, Mui AL, Groner B, et al. Specificity of transcription enhancement via the STAT responsive element in the serine protease inhibitor 2.1 promoter. Mol Cell Endocrinol. 1997;130(1):69-81.
299. Watling D, Guschin D, Müller M, Silvennoinen O, Witthuhn BA, Quelle FW, et al. Complementation by the protein tyrosine kinase JAK2 of a mutant cell line defective in the interferon-& gamma; signal transduction pathway. Nature. 1993 Nov; 366(6451):166-70.
300. Smith GE, Summers M, Fraser M. Production of human beta interferon in insect cells infected with a baculovirus expression vector. Mol Cell Biol. 1983;3(12):2156-65.
301. Smith GE, Ju G, Ericson BL, Moschera J, Lahm H, Chizzonite R, et al. Modification and secretion of human interleukin 2 produced in insect cells by a baculovirus expression vector. Proceedings of the National Academy of Sciences. 1985;82(24):8404-8.
302. Hilhorst R, Houkes L, van den Berg A, Ruijtenbeek R. Peptide microarrays for detailed, high-throughput substrate identification, kinetic characterization, and inhibition studies on protein kinase A. Anal Biochem. 2009;387(2):150-61.
303. Lemeer S, Ruijtenbeek R, Pinkse MW, Jopling C, Heck AJ, den Hertog J, et al. Endogenous phosphotyrosine signaling in zebrafish embryos. Molecular & Cellular Proteomics. 2007;6(12):2088-99.
304. Divita G, Goody R, Gautheron D, Di Pietro A. Structural mapping of catalytic site with respect to alpha-subunit and noncatalytic site in yeast mitochondrial F1-ATPase using fluorescence resonance energy transfer. J Biol Chem. 1993;268(18):13178-86.

305. Falson P, Penin F, Divita G, Lavergne JP, Di Pietro A, Goody RS, et al. Functional nucleotide-binding domain in the F0F1-ATP synthase. alpha. subunit from the yeast schizosaccharomyces pombe. Biochemistry (N Y). 1993;32(39):10387-97.
306. Jault J, Divita G, Allison W, Di Pietro A. Glutamine 170 to tyrosine substitution in yeast mitochondrial F1 beta-subunit increases catalytic site interaction with GDP and IDP and produces negative cooperativity of GTP and ITP hydrolysis. J Biol Chem. 1993;268(28):20762-7.
307. Moore KJ, Lohman TM. Kinetic mechanism of adenine nucleotide binding to and hydrolysis by the escherichia coli rep monomer. 1. use of fluorescent nucleotide analogs. Biochemistry (N Y). 1994;33(48):14550-64.
308. Vertommen D, Bertrand L, Sontag B, Di Pietro A, Louckx MP, Vidal H, et al. The ATP-binding site in the 2-kinase domain of liver 6-phosphofructo-2-kinase/fructose-2, 6-bisphosphatase STUDY OF THE ROLE OF lys-54 AND thr-55 BY SITE-DIRECTED MUTAGENESIS. J Biol Chem. 1996;271(30):17875-80.
309. Woodward SK, Eccleston JF, Geeves MA. Kinetics of the interaction of 2'(3')-O-(N-methylanthraniloyl)-ATP with myosin subfragment 1 and actomyosin subfragment 1: Characterization of two acto-S1-ADP complexes. Biochemistry 1991 Jan;30(2):422-30.
310. Stewart RC, VanBruggen R, Ellefson DD, Wolfe AJ. TNP-ATP and TNP-ADP as probes of the nucleotide binding site of CheA, the histidine protein kinase in the chemotaxis signal transduction pathway of escherichia coli. Biochemistry (N Y). 1998;37(35):12269-79.
311. Pérez-Rivas LG, Prieto S, Lozano J. 1. modulation of ras signaling by the KSR family of molecular scaffolds. Emerging Signaling Pathways in Tumor Biology:1.
312. Zhang H, Photiou A, Grothey A, Stebbing J, Giamas G. The role of pseudokinases in cancer. Cell Signal. 2012;24(6):1173-84.
313. Pan J, Fukuda K, Saito M, Matsuzaki J, Kodama H, Sano M, et al. Mechanical stretch activates the JAK/STAT pathway in rat cardiomyocytes. Circ Res. 1999;84(10):1127-36.
314. Pennica D, King KL, Shaw KJ, Luis E, Rullamas J, Luoh S, et al. Expression cloning of cardiotrophin 1, a cytokine that induces cardiac myocyte hypertrophy. Proceedings of the National Academy of Sciences. 1995;92(4):1142-6.
315. Tai ES, Sim XL, Ong TH, Wong TY, Saw SM, Aung T, et al. Polymorphisms at newly identified lipid-associated loci are associated with blood lipids and cardiovascular disease in an asian malay population. J Lipid Res. 2009;50(3):514-20.
316. Varbo A, Benn M, Tybjærg-Hansen A, Grande P, Nordestgaard BG. TRIB1 and GCKR polymorphisms, lipid levels, and risk of ischemic heart disease in the general population. Arterioscler Thromb Vasc Biol. 2011;31(2):451-7.
317. Tobin MD, Raleigh SM, Newhouse S, Braund P, Bodycote C, Ogleby J, et al. Association of WNK1 gene polymorphisms and haplotypes with ambulatory blood pressure in the general population. Circulation. 2005;112(22):3423-9.
318. Wilson FH, Disse-Nicodeme S, Choate KA, Ishikawa K, Nelson-Williams C, Desitter I, et al. Human hypertension caused by mutations in WNK kinases. Science. 2001;293(5532):1107-12.
319. Liew CW, Bochenski J, Kawamori D, Hu J, Leech CA, Wanic K, et al. The pseudokinase tribbles homolog 3 interacts with ATF4 to negatively regulate insulin exocytosis in human and mouse β cells. J Clin Invest. 2010;120(8):2876.
320. Guo L, Sanders PW, Woods A, Wu C. The distribution and regulation of integrin-linked kinase in normal and diabetic kidneys. The American journal of pathology. 2001;159(5):1735-42.
321. Deshpande A, Reddy M, Schade G, Ray A, Chowdary T, Griffin J, et al. Kinase domain mutations confer resistance to novel inhibitors targeting JAK2V617F in myeloproliferative neoplasms. Leukemia. 2011;26(4):708-15.
322. Weigert O, Lane AA, Bird L, Kopp N, Chapuy B, van Bodegom D, et al. Genetic resistance to JAK2 enzymatic inhibitors is overcome by HSP90 inhibition. J Exp Med. 2012;209(2):259-73.
323. Holderfield M, Merritt H, Chan J, Wallroth M, Tandeske L, Zhai H, et al. RAF inhibitors activate the MAPK pathway by relieving inhibitory autophosphorylation. Cancer cell. 2013;23(5):594-602.
324. Koppikar P, Bhagwat N, Kilpivaara O, Manshouri T, Adli M, Hricik T, et al. Heterodimeric JAK-STAT activation as a mechanism of persistence to JAK2 inhibitor therapy. Nature. 2012;489(7414):155-9.

13. ORIGINAL COMMUNICATIONS

http://www.nature.com/nsmb/journal/v18/n9/full/nsmb.2099.html

The pseudokinase domain of JAK2 is a dual-specificity protein kinase that negatively regulates cytokine signaling

Daniela Ungureanu[1], Jinhua Wu[2,6], Tuija Pekkala[1], Yashavanthi Niranjan[1], Clifford Young[3,6], Ole N Jensen[3], Chong-Feng Xu[2,6], Thomas A Neubert[2], Radek C Skoda[4], Stevan R Hubbard[2] & Olli Silvennoinen[1,5]

Human JAK2 tyrosine kinase mediates signaling through numerous cytokine receptors. The JAK2 JH2 domain functions as a negative regulator and is presumed to be a catalytically inactive pseudokinase, but the mechanism(s) for its inhibition of JAK2 remains unknown. Mutations in JH2 lead to increased JAK2 activity, contributing to myeloproliferative neoplasms (MPNs). Here we show that JH2 is a dual-specificity protein kinase that phosphorylates two negative regulatory sites in JAK2: Ser523 and Tyr570. Inactivation of JH2 catalytic activity increased JAK2 basal activity and downstream signaling. Notably, different MPN mutations abrogated JH2 activity in cells, and in MPN (V617F) patient cells phosphorylation of Tyr570 was reduced, suggesting that loss of JH2 activity contributes to the pathogenesis of MPNs. These results identify the catalytic activity of JH2 as a previously unrecognized mechanism to control basal activity and signaling of JAK2.

JAK2 belongs to the Janus family of cytoplasmic tyrosine kinases (JAK1–JAK3, TYK2) and functions as a crucial mediator of signaling for hematopoietic cytokines and hormones such as erythropoietin (Epo), thrombopoietin (Tpo), interferon-γ (IFN-γ), several interleukins, growth hormone, prolactin, leptin and granulocyte-macrophage colony-stimulating factor (GM-CSF)[1,2]. JAK2 serves as a triggering kinase for cytokine receptors, and phosphorylation and activation of downstream signaling proteins and the progression of signal transduction are dependent on its activity. JAK2 associates with the cytoplasmic domains of cytokine or hormone receptors, and ligand-induced receptor rearrangement facilitates JAK2 *trans*-phosphorylation of activation-loop Tyr1007 and Tyr1008 in JH1 (the tyrosine kinase domain), leading to its activation. Subsequent phosphorylation by JAK2 of tyrosine residues in the receptors creates docking sites for SH2-containing signaling proteins such as the signal transducer and activator of transcription (STAT) proteins[3,4].

Phosphorylation is important in the regulation of JAK2, both positively and negatively. In the absence of cytokine stimulation, JAK2 is constitutively phosphorylated on Ser523 (ref. 5); however, upon activation, JAK2 becomes phosphorylated on as many as 20 tyrosine residues. In addition to Tyr1007 and Tyr1008, phosphorylation of Tyr637, Tyr813, Tyr868, Tyr966 and Tyr972 potentiate JAK2 activity, whereas phosphorylation of Ser523, Tyr119, Tyr221, Tyr317, Tyr570 and Tyr913 negatively regulate JAK2 (refs. 6–11). Because JAK2 mediates crucial physiological functions such as cell proliferation, the kinase activity of JAK2 is tightly regulated through various means, including *trans*-acting proteins (tyrosine phosphatases, SOCS (suppressor of cytokine signaling) proteins) and JH2 (pseudokinase domain)[12–15].

Both biochemical and clinical evidence have demonstrated an important regulatory function for JH2 in JAKs. At present, 32 different mutations in JH2 of JAK2 have been shown to cause, or are linked to, hematological diseases[16]. The most frequent somatic mutation, V617F, results in constitutively active JAK2 and is responsible for >95% of cases of polycythemia vera and ~50% of cases of essential thrombocythemia and primary myelofibrosis[17–19]. The mechanism(s) by which JH2 negatively regulates the tyrosine kinase activity of JH1 is currently unknown, but it is likely to involve an intramolecular interaction between JH2 and JH1 (ref. 13). In JAK2 and JAK3, deletion of JH2 increases basal JAK activity, and the JH2 domain has been shown to co-immunoprecipitate with the JH1 domain (in *trans*)[14,20]. Currently, crystal structures are available for only JH1 of JAKs[21,22]. JH2 is predicted to adopt a canonical protein kinase fold but to be catalytically inactive owing to amino acid substitutions of key catalytic residues that are conserved in active protein kinases—in particular, an aspartate residue in the catalytic loop (HRD motif). Therefore, JH2 in JAKs has been classified as a pseudokinase. Pseudokinases make up ~10% of the kinome and have been implicated in the regulation of various cellular functions, including tumorigenesis[23].

The understanding of JAK kinase function, regulation and structure has been hampered by the difficulty of producing and purifying recombinant, soluble JAKs and their domains. This holds true also for JH2, and production and purification of JH2 has not been previously reported. We have now produced recombinant JAK2 JH2

[1]Institute of Biomedical Technology, University of Tampere, Tampere, Finland. [2]Structural Biology Program, Kimmel Center for Biology and Medicine of the Skirball Institute, New York University School of Medicine, New York, New York, USA. [3]Department of Biochemistry and Molecular Biology, University of Southern Denmark, Odense, Denmark. [4]Department of Biomedicine, University Hospital Basel, Basel, Switzerland. [5]Tampere University Hospital, Tampere, Finland. [6]Present addresses: Fox Chase Cancer Center, Philadelphia, Pennsylvania, USA (J.W.); Analytical Development, Biogen Idec, Cambridge, Massachusetts, USA (C.-F.X.); Novo Nordisk Foundation Center for Protein Research, University of Copenhagen, Copenhagen, Denmark (C.Y.). Correspondence should be addressed to O.S. (olli.silvennoinen@uta.fi).

Received 17 January; accepted 14 June; published online 14 August 2011; doi:10.1038/nsmb.2099

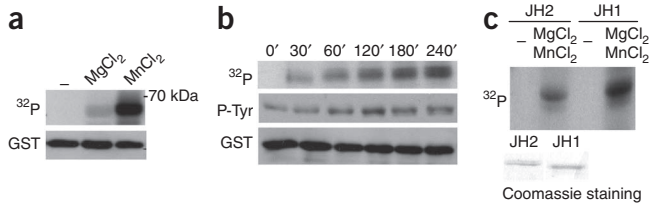

Figure 1 Identification of JAK2 JH2 catalytic activity *in vitro*. (**a**) *In vitro* kinase assay with purified JAK2 GST-JH2 with [^{32}P-γ]ATP in the absence or presence of divalent cations. (**b**) Time-course kinase assay with purified JAK2 GST-JH2 in the presence of [γ-^{32}P]ATP or unlabeled ATP. (**c**) Autoradiography of kinase assay (30 min) using purified JAK2 JH2 and JH1 domain and [γ-^{32}P]ATP, in the absence or presence of cations. Coomassie staining shows the protein levels of JH1 and JH2.

domain using a baculovirus expression system, allowing us to address questions about the function of the JAK2 pseudokinase domain. We show that, contrary to the generally accepted belief, JH2 is an active protein kinase that phosphorylates two sites in JAK2—Ser523 and Tyr570—in a process that serves to maintain a low basal level of JAK2 activity. Moreover, JAK2 mutations that cause MPNs were found to abrogate JH2 activity. These results identify a previously unrecognized mechanism in the regulation of normal and pathogenic JAK2 and cytokine signaling.

RESULTS

Phosphorylation of purified JAK2 JH2 *in vitro*

We used insect cells (*Sf*9) to express JH2 as a glutathione *S*-transferase (GST) fusion protein (**Supplementary Figs. 1** and **2**). We used the purified GST-JH2 in an *in vitro* kinase assay, which showed a time-dependent phosphorylation of JH2 with a strong preference for Mn^{2+} as divalent cation (**Fig. 1a**,**b**). A comparison of the autophosphorylation activity of purified JH1 versus JH2 of JAK2 indicated that JH2's activity is ~10% of that of JH1 (**Fig. 1c**), which could explain why JH2 activity has previously gone unnoticed. To verify the autophosphorylation activity of JH2, we introduced a kinase-inactivating mutation, K581A, into JH2. This lysine (in β-strand 3 of the JH2 N-lobe) serves to coordinate the α- and β-phosphates of ATP in active protein kinases[24]. We produced and purified GST-JH2 (wild type) and the GST-K581A mutant side by side from insect cells. An *in vitro* kinase assay (**Supplementary Fig. 3a**) showed that the kinase-inactive JH2 mutant is devoid of autophosphorylation activity.

To further confirm that the observed kinase activity was due to JH2 autophosphorylation and not to phosphorylation by a contaminating protein kinase, we analyzed *in vitro*—translated JH2 (**Supplementary Methods**) using a kinase assay. Western blotting showed that *in vitro*–translated JH2 of JAK2 is autophosphorylated on tyrosine (**Supplementary Fig. 3b**). Next, we carried out *in vitro* translation of wild-type JH2 and JH2 K581A, followed by His-tag purification, and subjected the proteins to an *in vitro* kinase assay in the presence of [γ-^{32}P]ATP. We detected autophosphorylation in the JH2 domain but not in the JH2 K581A mutant (**Supplementary Fig. 3c**). Taken together, these results demonstrate that JH2 has autophosphorylation activity.

JAK2 JH2 is autophosphorylated on Ser523 and Tyr570

To study the kinase activity of the JAK2 pseudokinase domain in more detail, we expressed His-tagged JH2 in insect cells and purified it using Ni-NTA affinity and anion-exchange chromatography. JH2 eluted in two closely spaced peaks on an anion-exchange column (**Fig. 2a** and **Supplementary Fig. 4**). During native PAGE, JH2 in peak 2 (JH2-peak2) migrated faster than JH2-peak1 (**Fig. 2b**). The chromatography and electrophoresis data are suggestive of a higher phosphorylation state for JH2-peak2 than for JH2-peak1. We analyzed the autophosphorylation activities of the two JH2 samples in an *in vitro* kinase assay. Native PAGE showed the appearance of a faster-migrating band for both samples at later time points of the reaction, consistent with an increase in phosphorylation state (**Fig. 2c**). We used LC-ESI-MS and LTQ-Orbitrap MS to identify the phosphorylated residues in JH2. JH2-peak1 was unphosphorylated at time zero and underwent autophosphorylation on Ser523 during the kinase reaction (data not shown). In contrast, JH2-peak2 was robustly (stoichiometrically) phosphorylated on Ser523 at time zero (thus explaining the migration difference between the proteins in the two peaks) and became phosphorylated additionally on Tyr570 during the kinase reaction (**Fig. 2d**).

Further analysis of the JH2 autophosphorylation activity in kinase assays showed that JH2-peak2 has substantially higher tyrosine

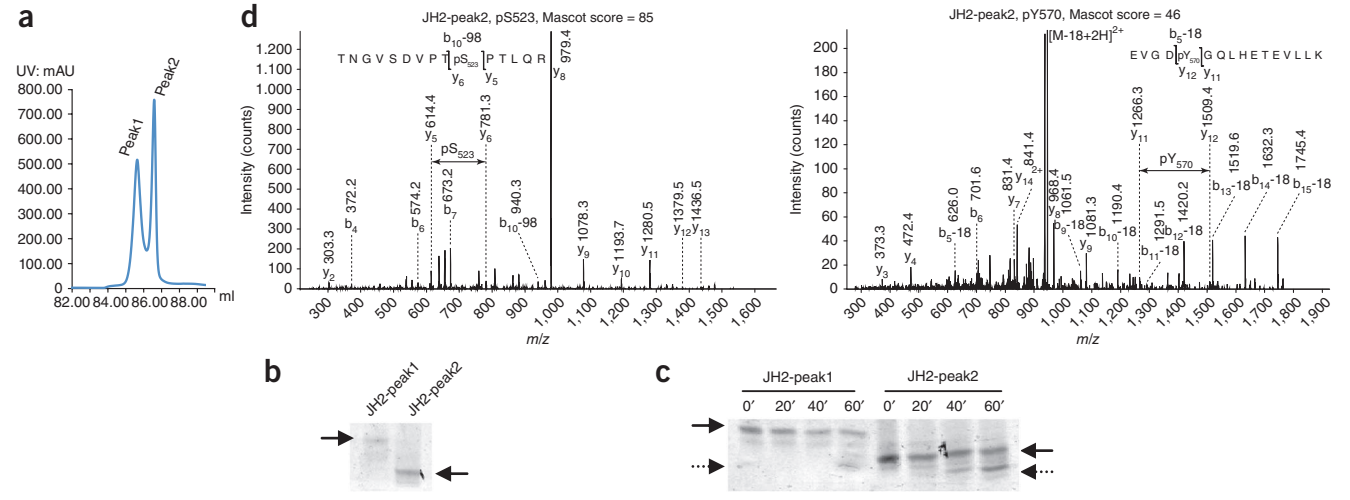

Figure 2 Identification of phosphorylated residues in JAK2 JH2. (**a**) Chromatogram of JAK2 JH2 purification showing the peaks from anion-exchange chromatography. (**b**) Coomassie staining of a native gel of JH2-peak1 and JH2-peak2 proteins. (**c**) Coomassie staining of a native gel of purified JH2-peak1 and JH2-peak2 after a kinase reaction. (**d**) MS-MS spectra of the phosphorylated residues in a JAK2 JH2-peak2 4-h kinase assay. Left, JH2-peak2 is stoichiometrically phosphorylated at Ser523. Right, JH2-peak2 is partially phosphorylated at Tyr570.

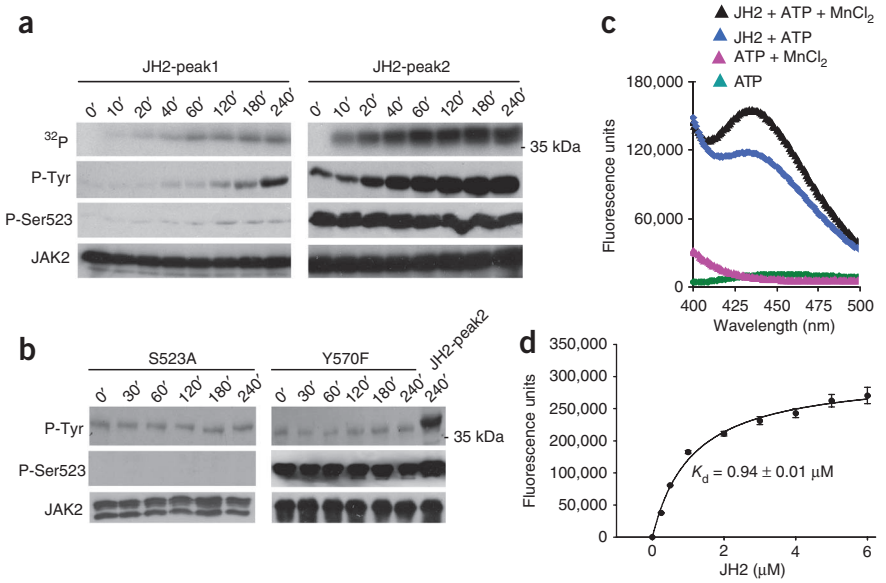

Figure 3 Analysis of JAK2 JH2 autophosphorylation and ATP-binding activity. (**a**) Time-course kinase assay of purified JH2-peak1 and JH2-peak2. (**b**) Time-course kinase assay of purified JH2 S523A and Y570F mutants compared to JH2-peak2. (**c**) Fluorescence measurement of an ATP-binding assay of JAK2 JH2-peak2. (**d**) K_d measurement of mant-ATP binding to JH2-peak2. Graph shows mean ± s.d. of three independent experiments.

kinase activity than does JH2-peak1 (**Fig. 3a**). To investigate the basis for this difference, we monitored the phosphorylation state of Ser523 by western blotting using an anti-pSer523 specific antibody[5]. Consistent with the MS results, Ser523 phosphorylation increased in JH2-peak1 during the kinase reaction, whereas JH2-peak2 was fully phosphorylated already at time zero, and the phosphorylation level of Ser523 remained constant during the reaction (**Fig. 3a**). Moreover, the GST-JH2 K581A mutant purified from insect cells showed no phosphorylation on Ser523 (**Supplementary Fig. 5**), demonstrating that Ser523 is the *de facto* autophosphorylation site of JH2. These results, together with the results presented in **Figure 2c**, suggest that phosphorylation of Ser523 regulates the tyrosine kinase activity of JH2.

To address this possibility, we mutated Ser523 to alanine. Consistent with the hypothesis, S523A did not undergo tyrosine phosphorylation during an *in vitro* kinase assay (**Fig. 3b**). Mutation of Tyr570 to phenylalanine did not affect Ser523 phosphorylation, but abolished tyrosine phosphorylation. These phosphospecific antibody data also confirm the MS identification of the two autophosphorylated residues in JH2: Ser523 and Tyr570. Notably, these two residues have previously been identified as negative regulatory sites in JAK2 (refs. 5,7,9,10).

If the pseudokinase domain of JAK2 is an active protein kinase, using ATP as a phosphate donor, it should bind ATP with a physiological K_d value. We evaluated the binding of ATP to JH2 of JAK2 using the fluorescent ATP analog 2′-(3′)-*O*-(*N*-methylanthraniloyl)-ATP (mant-ATP). The fluorescence emission scan showed a peak at ~440 nm only when $MnCl_2$ and JH2 were present along with mant-ATP (**Fig. 3c**). Mant-ATP bound to JH2 with a K_d of ~1 μM (**Fig. 3d**), which is ~10% of the reported K_d for JH1 of JAK2 (ref. 25). Taken together, the *in vitro* data demonstrate that the pseudokinase domain of JAK2 is a dual-specificity serine and tyrosine kinase. Autophosphorylation of Ser523 is the primary event in JH2 activation, which enhances subsequent autophosphorylation of Tyr570.

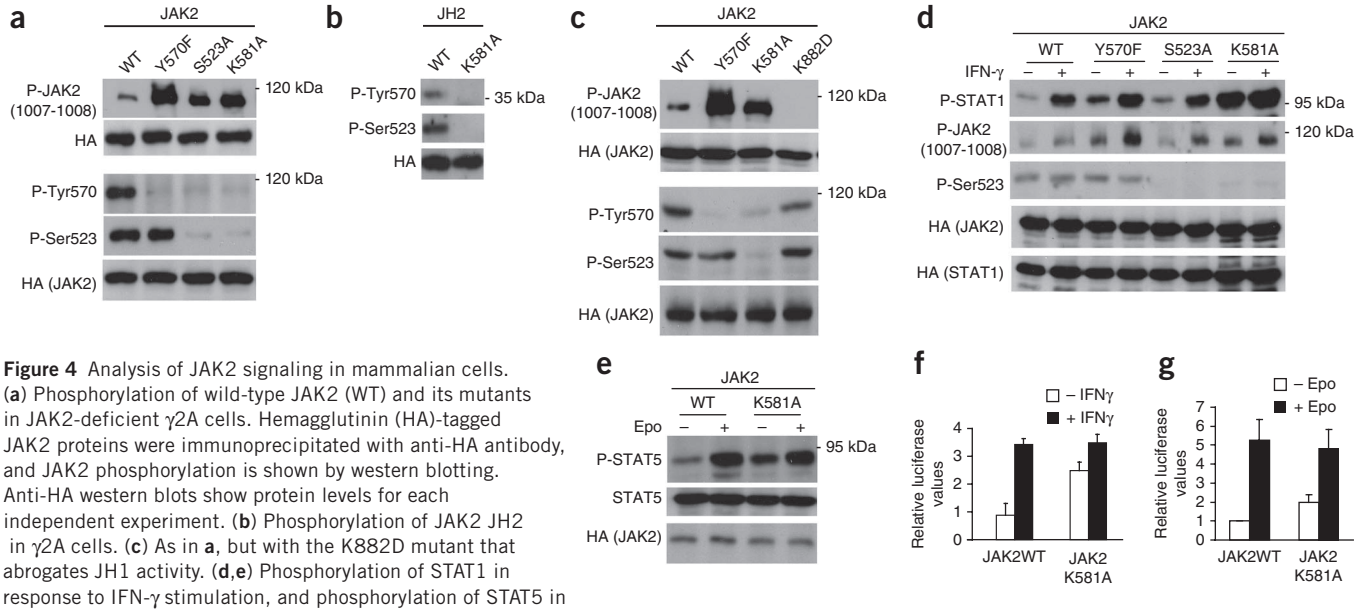

Figure 4 Analysis of JAK2 signaling in mammalian cells. (**a**) Phosphorylation of wild-type JAK2 (WT) and its mutants in JAK2-deficient γ2A cells. Hemagglutinin (HA)-tagged JAK2 proteins were immunoprecipitated with anti-HA antibody, and JAK2 phosphorylation is shown by western blotting. Anti-HA western blots show protein levels for each independent experiment. (**b**) Phosphorylation of JAK2 JH2 in γ2A cells. (**c**) As in **a**, but with the K882D mutant that abrogates JH1 activity. (**d**,**e**) Phosphorylation of STAT1 in response to IFN-γ stimulation, and phosphorylation of STAT5 in response to Epo stimulation in γ2A cells. (**f**) Effect of JAK2 K581A mutation on STAT1 transcription activation using an IFN–γ—dependent *GAS* luciferase reporter. Graph shows mean ± s.d. of three independent experiments ($P < 0.05$). (**g**) Effect of the JAK2 K581A mutation on STAT5 transcription activation using an SPI-*Luc2* luciferase reporter. The basal wild-type JAK2 activity was set to 1 for all experiments. Graph shows mean ± s.d. of six independent experiments ($P < 0.05$).

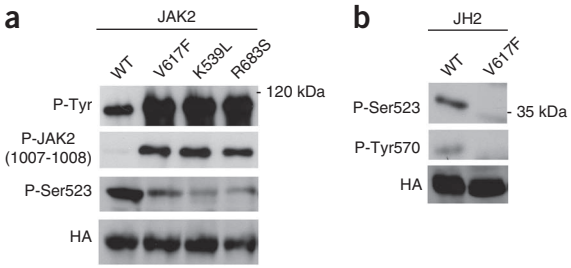

Figure 5 Phosphorylation of different JAK2 MPN mutants. (**a**) Phosphorylation of wild-type JAK2 (WT) and MPN mutants in JAK2-deficient γ2A cells. (**b**) Phosphorylation of JAK2 JH2 in γ2A cells.

Analysis of JAK2 JH2 in mammalian cells

To analyze the function of the catalytic activity of JH2 in a cellular context, we introduced the kinase-inactivating point mutation in JH2, K581A, into JAK2. We carried out expression of various JAK2 constructs in JAK2-deficient γ2A cells and analyzed JAK2 phosphorylation by western blotting. Wild-type JAK2 was tyrosine phosphorylated at a low level and, consistent with previous studies[5,7,9,10], mutation of either Ser523 or Tyr570 increased JAK2 tyrosine phosphorylation of the JH1 activation loop (Tyr1007-Tyr1008), an indicator of JAK2 activation. Similar to the data for JAK2 S523A and JAK2 Y570F, JAK2 K581A showed a higher level of tyrosine phosphorylation than did wild-type JAK2 and, notably, Ser523 and Tyr570 sites were not phosphorylated in K581A (**Fig. 4a**). In addition, these results corroborate the *in vitro* results (**Fig. 3b**) and show that, in cells, phosphorylation of Tyr570 is dependent on Ser523 phosphorylation of JH2.

To confirm the role of JH2 catalytic activity in phosphorylation of Ser523 and Tyr570, we expressed JH2 alone, wild-type JAK2 or the K581A mutant in γ2A cells. For wild-type JH2, both Ser523 and Tyr570 were phosphorylated, and the K581A mutation abolished their phosphorylation (**Fig. 4b**). Moreover, in the context of full-length JAK2 bearing a point mutation that abrogates JH1 activity (K882D), phosphorylation of Ser523 occurred to the same extent as in wild-type JAK2, and the K882D mutation did not markedly affect phosphorylation of Tyr570 (**Fig. 4c**). Finally, in JAK2 constructs lacking the entire JH1 domain (JAK2del.JH1), phosphorylation of Ser523 and Tyr570 occurred to the same level as in wild-type JAK2 (**Supplementary Fig. 6**).

Last, we wanted to verify that the effects of the K581A mutation were due to abrogation of JH2 catalytic activity and minimize the possibility that they were caused by secondary conformational alterations in JH2. To this end, we introduced a more conservative mutation, K581R, and, separately, a distinct inactivating mutation, N678A (catalytic loop), into the full-length protein. The K581R mutant showed clear decreases in Ser523 and Tyr570 phosphorylation and an increase in JAK2 Tyr1007-Tyr1008 phosphorylation. We observed similar effects, albeit less pronounced, with the N678A mutant (**Supplementary Fig. 7**). These in-cell data substantiate the conclusion that JH2 is a dual-specificity protein kinase that autophosphorylates Ser523 and Tyr570.

JH2 catalytic activity maintains low JAK2 basal activity

We investigated JH2 activity in cytokine receptor–mediated signaling by analyzing STAT activation in γ2A cells in response to cytokine stimulation. Compared to wild-type JAK2, the JAK2 mutants S523A, Y570F and K581A showed increased basal phosphorylation of STAT1, but the mutations did not influence the IFN-γ-induced STAT1 phosphorylation (**Fig. 4d**). There was some variation in the level of STAT1 phosphorylation between the experiments (**Fig. 4d** and **Supplementary Fig. 8**), but we consistently saw increased basal phosphorylation of STAT1, which was also observed with the K581A mutant in erythropoietin receptor (EpoR)-induced STAT5 phosphorylation (**Fig. 4e**). We investigated the JH2 activity in the cytokine-induced transcriptional response by using reporter-gene analysis. Introduction of the K581A mutation into JAK2 increased the basal STAT1- and STAT5-dependent reporter-gene activation, but did not affect the IFN-γ or Epo-induced responses (**Fig. 4f,g**). Taken together, these results indicate that JH2 catalytic activity is required to maintain a low basal level of JAK2 (JH1) activity.

JAK2 MPN-causing mutations affect JH2 catalytic activity

Our results showing that the catalytic activity of JH2 regulates the basal activity of JAK2 raises the question of the possible connection of this activity to human JAK2 mutants and disease pathogenesis. We were interested in understanding whether the catalytic activity of JH2 was involved in the pathogenesis of JAK2 MPN mutants. For this analysis, we chose three distinct MPN-causing JH2 mutants: V617F (exon 14, the predominant MPN-causing mutation), K539L (exon 12)[26] and R683S (exon 16)[27].

Consistent with previous studies, the analyzed mutants showed high levels of tyrosine phosphorylation and activation of JAK2 in γ2A cells when compared to wild-type JAK2 (**Fig. 5a**). Notably, all three mutants showed substantially decreased Ser523 phosphorylation. These results suggest that the JH2 mutations that cause MPN reduce or abrogate JH2 catalytic activity. To test this hypothesis directly, we analyzed JH2 alone and its V617F counterpart in γ2A cells. The results show that V617F, similar to K581A, abrogates Ser523 and Tyr570 phosphorylation (**Fig. 5b**).

To determine whether altered JH2 function is also observed in clinical samples from MPN patients, and thus could be a causative mechanism for the disease, we isolated platelets from three MPN patients carrying the V617F mutation and from a healthy control and subjected them to Tpo stimulation (**Supplementary Methods**). As a readout for JH2 activity, we analyzed the phosphorylation of JAK2 Tyr570. Tpo stimulation readily induced Tyr570 phosphorylation in control cells, but in patient samples Tyr570 phosphorylation was substantially reduced, and this reduction correlated with the V617F allelic burden of the patient cells (**Supplementary Fig. 9**). Taken together, these results show that MPN-causing mutations disturb the catalytic activity of JH2 and abrogate phosphorylation of negative regulatory residues that lead to increased basal activation of JAK2.

DISCUSSION

Protein kinases have been classified as pseudokinases if they lack conserved residues that are thought to be required for phosphoryl transfer, and if catalytic activity has not been detected[23,28]. Recent studies have provided important new information and insights into the functions of this protein family. An example is provided by the structural characterization of VRK3, which is unable to bind ATP and obtains a pseudoactive conformation by filling the ATP-binding pocket by hydrophobic residues, thus retaining the pseudokinase status[29]. However, for several other proteins the functional status has been overturned, and proteins including CASK, haspin, WNK1, HER3(ErbB3) and STRADα have ATP-binding and (or) catalytic activity that can be achieved through noncanonical mechanisms[30–34]. Each of these pseudokinases uses a distinct mechanism to carry out its cellular functions. For example, WNK1 compensates for the missing ATP-binding lysine in β-strand 3 by instead using a lysine residue in the nucleotide-binding loop[32].

The calcium- and calmodulin-activated serine-threonine kinase CASK displays atypical catalytic activity in that Mg^{2+} inhibits its activity[30]. HER3 lacks the catalytic base aspartate, and the crystal structure revealed that it assumes an atypical conformation for active kinases, particularly in the αC helix and activation segment[33,35]. However, HER3 was found to retain low-level kinase activity and phosphorylate its intracellular region *in vitro*, but the physiological role of this activity remains to be determined[33]. These results argue that each alleged pseudokinase needs to be functionally analyzed and scrutinized for possible catalytic activity. In this study, we have shown that, both *in vitro* and in cells, the pseudokinase domain of JAK2 is an active dual-specificity protein kinase that phosphorylates two previously identified negative regulatory sites in JAK2: Ser523 and Tyr570. Phosphorylation of these sites is required to maintain low basal activity of JAK2.

Our results on the catalytic activity of JH2 provide new insights into the regulation of JAK activation in signaling by various cytokines such as Epo, Tpo, IFN-γ, growth hormone, prolactin, interleukin-3 (IL-3), IL-5 and GM-CSF. In unstimulated cells, Ser523 is the only constitutively phosphorylated residue in JAK2 (ref. 5), and phosphorylation of other sites, including Tyr570, occurs only upon cytokine stimulation and activation of JAK2 (refs. 9,10). The kinases responsible for phosphorylation of Ser523 and Tyr570 have not been identified, but the activity of JH1 was not required for these phosphorylation events[5,7,9,10]. We show here that JH2 phosphorylates Ser523 and Tyr570, that autophosphorylation of Ser523 is the primary event in JH2 activation, and that it is observed in unstimulated conditions (**Fig. 4d**). Cytokine-induced receptor dimerization and juxtaposition of the JAKs lead to other regulatory *trans*-phosphorylation events, including phosphorylation of Tyr570. Ser523 resides in the linker region between the SH2-like domain of JAK2 and JH2 (**Supplementary Fig. 10**), and steric considerations indicate that it could be phosphorylated in *cis*. Tyr570, predicted to be in the β2-β3 loop of JH2, is distal to the JH2 active site and is presumed to be phosphorylated in *trans* by JH2 in another JAK2 molecule. A crystal structure of JH1-JH2 will be required to understand the mechanisms by which JH2 sterically inhibits JH1 and by which JH2-mediated phosphorylation of Ser523 and Tyr570 suppresses JH1 activity. Our results are consistent with a model whereby phosphorylation of Ser523 and Tyr570 strengthens the JH1-JH2 autoinhibitory interaction. The relatively low catalytic activity of JH2 is in accordance with autophosphorylation of regulatory residues as a physiological function for JH2, whereas JH1 is mainly responsible for phosphorylation of substrate proteins. The low catalytic activity, together with the crucial regulatory role of Ser523 and the atypical requirement for Mn^{2+} for catalysis, has probably hampered the detection of JH2 activity.

The discovery of somatic mutations in JH2 of JAK2 in most Philadelphia chromosome–negative MPNs and other hematological malignancies have focused attention on the functional role of JH2 and implicated JAKs as important therapeutic targets. However, the underlying mechanisms for JAK2 hyperactivation in MPNs have remained obscure. Currently, several inhibitors targeting the JAK2 tyrosine kinase domain are in clinical trials for MPNs[36]. The JAK2 inhibitors show beneficial clinical effects and alleviate symptoms, but they do not substantially reduce the JAK2 mutant tumor load, and the inhibitors do not discriminate between normal and mutated JAK2. We show that MPN-causing JAK2 mutations disturb JH2 catalytic activity and remove the negative regulatory effects of Ser523 and Tyr570 phosphorylation in cell lines and in primary cells from MPN patients. These results identify a molecular pathogenic mechanism in MPNs and suggest that loss of JH2 function is involved in the hyperactive JAK2 MPN phenotype.

In conclusion, these studies have identified an unexpected regulatory mechanism for JH2 in JAK2. JH2 is an active protein kinase that autophosphorylates two negative regulatory residues, which is required to maintain low-level activity of JAK2 in the absence of cytokine stimulation. The discovery of JH2 catalytic activity and its connection to MPNs may also afford new approaches for the development of targeted therapies to combat JAK-mediated diseases.

METHODS

Methods and any associated references are available in the online version of the paper at http://www.nature.com/nsmb/.

Note: Supplementary information is available on the Nature Structural & Molecular Biology website.

ACKNOWLEDGMENTS

We thank M. Myers (University of Michigan Medical School) for reagents (anti-pSer523 and anti-pTyr570 specific antibodies), E. Koskenalho, P. Kosonen and M. Lehtinen for technical assistance, and the Biocenter Finland protein production platform (V. Hytönen and U. Kiiskinen) for technological support. This study was supported by the Medical Research Council of Academy of Finland (O.S.), the Sigrid Juselius Foundation (O.S.), the Finnish Cancer Foundation (O.S.), the EU Research Training Network ReceptEur (O.S.), Science Center, Competitive Research Funding and Centre of Laboratory Medicine of the Tampere University Hospital (O.S.), the Tampere Tuberculosis Foundation (O.S.), US National Institutes of Health core grant CA016087 (T.A.N.), the Danish Research Agency and the Danish National Research Foundation (Centre for Epigenetics) (C.Y. and O.N.J.).

AUTHOR CONTRIBUTIONS

D.U. performed the experiments and wrote the paper. O.S. and S.R.H. designed the experiments and wrote the paper. J.W. performed the *in vitro* experiments with recombinant proteins. T.P. and Y.N. performed the mutagenesis experiments in mammalian cells. C.Y., O.N.J., T.A.N. and C.-F.X. performed the experiments for MS analysis. R.C.S. performed the experiments for clinical sample analysis.

COMPETING FINANCIAL INTERESTS

The authors declare no competing financial interests.

Published online at http://www.nature.com/nsmb/.
Reprints and permissions information is available online at http://www.nature.com/reprints/index.html.

1. Gadina, M. *et al.* Signaling by type I and II cytokine receptors: ten years after. *Curr. Opin. Immunol.* **13**, 363–373 (2001).
2. Imada, K. & Leonard, W.J. The Jak-STAT pathway. *Mol. Immunol.* **37**, 1–11 (2000).
3. Silvennoinen, O. *et al.* Structure of the murine Jak2 protein-tyrosine kinase and its role in interleukin 3 signal transduction. *Proc. Natl. Acad. Sci. USA* **90**, 8429–8433 (1993).
4. Yamaoka, K. *et al.* The Janus kinases (Jaks). *Genome Biol.* **5**, 253 (2004).
5. Ishida-Takahashi, R. *et al.* Phosphorylation of Jak2 on Ser(523) inhibits Jak2-dependent leptin receptor signaling. *Mol. Cell. Biol.* **26**, 4063–4073 (2006).
6. Matsuda, T., Feng, J., Witthuhn, B.A., Sekine, Y. & Ihle, J.N. Determination of the transphosphorylation sites of Jak2 kinase. *Biochem. Biophys. Res. Commun.* **325**, 586–594 (2004).
7. Mazurkiewicz-Munoz, A.M. *et al.* Phosphorylation of JAK2 at serine 523: a negative regulator of JAK2 that is stimulated by growth hormone and epidermal growth factor. *Mol. Cell. Biol.* **26**, 4052–4062 (2006).
8. Robertson, S.A. *et al.* Regulation of Jak2 function by phosphorylation of Tyr317 and Tyr637 during cytokine signaling. *Mol. Cell. Biol.* **29**, 3367–3378 (2009).
9. Feener, E.P., Rosario, F., Dunn, S.L., Stancheva, Z. & Myers, M.G. Jr. Tyrosine phosphorylation of Jak2 in the JH2 domain inhibits cytokine signaling. *Mol. Cell. Biol.* **24**, 4968–4978 (2004).
10. Argetsinger, L.S. *et al.* Autophosphorylation of JAK2 on tyrosines 221 and 570 regulates its activity. *Mol. Cell. Biol.* **24**, 4955–4967 (2004).
11. Argetsinger, L.S. *et al.* Tyrosines 868, 966, and 972 in the kinase domain of JAK2 are autophosphorylated and required for maximal JAK2 kinase activity. *Mol. Endocrinol.* **24**, 1062–1076 (2010).
12. Shuai, K. & Liu, B. Regulation of JAK-STAT signalling in the immune system. *Nat. Rev. Immunol.* **3**, 900–911 (2003).

13. Saharinen, P., Takaluoma, K. & Silvennoinen, O. Regulation of the Jak2 tyrosine kinase by its pseudokinase domain. *Mol. Cell. Biol.* **20**, 3387–3395 (2000).
14. Saharinen, P. & Silvennoinen, O. The pseudokinase domain is required for suppression of basal activity of Jak2 and Jak3 tyrosine kinases and for cytokine-inducible activation of signal transduction. *J. Biol. Chem.* **277**, 47954–47963 (2002).
15. Saharinen, P., Vihinen, M. & Silvennoinen, O. Autoinhibition of Jak2 tyrosine kinase is dependent on specific regions in its pseudokinase domain. *Mol. Biol. Cell* **14**, 1448–1459 (2003).
16. Haan, C., Behrmann, I. & Haan, S. Perspectives for the use of structural information and chemical genetics to develop inhibitors of Janus kinases. *J. Cell. Mol. Med.* **14**, 504–527 (2010).
17. Baxter, E.J. *et al.* Acquired mutation of the tyrosine kinase JAK2 in human myeloproliferative disorders. *Lancet* **365**, 1054–1061 (2005).
18. James, C. *et al.* A unique clonal JAK2 mutation leading to constitutive signalling causes polycythaemia vera. *Nature* **434**, 1144–1148 (2005).
19. Kralovics, R. *et al.* A gain-of-function mutation of JAK2 in myeloproliferative disorders. *N. Engl. J. Med.* **352**, 1779–1790 (2005).
20. Chen, M. *et al.* Complex effects of naturally occurring mutations in the JAK3 pseudokinase domain: evidence for interactions between the kinase and pseudokinase domains. *Mol. Cell. Biol.* **20**, 947–956 (2000).
21. Lucet, I.S. *et al.* The structural basis of Janus kinase 2 inhibition by a potent and specific pan-Janus kinase inhibitor. *Blood* **107**, 176–183 (2006).
22. Boggon, T.J., Li, Y., Manley, P.W. & Eck, M.J. Crystal structure of the Jak3 kinase domain in complex with a staurosporine analog. *Blood* **106**, 996–1002 (2005).
23. Boudeau, J., Miranda-Saavedra, D., Barton, G.J. & Alessi, D.R. Emerging roles of pseudokinases. *Trends Cell Biol.* **16**, 443–452 (2006).
24. Hubbard, S.R. & Till, J.H. Protein tyrosine kinase structure and function. *Annu. Rev. Biochem.* **69**, 373–398 (2000).
25. Hall, T. *et al.* Expression, purification, characterization and crystallization of non- and phosphorylated states of JAK2 and JAK3 kinase domain. *Protein Expr. Purif.* **69**, 54–63 (2010).
26. Scott, L.M. *et al.* JAK2 exon 12 mutations in polycythemia vera and idiopathic erythrocytosis. *N. Engl. J. Med.* **356**, 459–468 (2007).
27. Bercovich, D. *et al.* Mutations of JAK2 in acute lymphoblastic leukaemias associated with Down's syndrome. *Lancet* **372**, 1484–1492 (2008).
28. Zeqiraj, E. & van Aalten, D.M. Pseudokinases-remnants of evolution or key allosteric regulators? *Curr. Opin. Struct. Biol.* **20**, 772–781 (2010).
29. Scheeff, E.D., Eswaran, J., Bunkoczi, G., Knapp, S. & Manning, G. Structure of the pseudokinase VRK3 reveals a degraded catalytic site, a highly conserved kinase fold, and a putative regulatory binding site. *Structure* **17**, 128–138 (2009).
30. Mukherjee, K. *et al.* CASK functions as a Mg^{2+}-independent neurexin kinase. *Cell* **133**, 328–339 (2008).
31. Eswaran, J. *et al.* Structure and functional characterization of the atypical human kinase haspin. *Proc. Natl. Acad. Sci. USA* **106**, 20198–20203 (2009).
32. Min, X., Lee, B.H., Cobb, M.H. & Goldsmith, E.J. Crystal structure of the kinase domain of WNK1, a kinase that causes a hereditary form of hypertension. *Structure* **12**, 1303–1311 (2004).
33. Shi, F., Telesco, S.E., Liu, Y., Radhakrishnan, R. & Lemmon, M.A. ErbB3/HER3 intracellular domain is competent to bind ATP and catalyze autophosphorylation. *Proc. Natl. Acad. Sci. USA* **107**, 7692–7697 (2010).
34. Zeqiraj, E., Filippi, B.M., Deak, M., Alessi, D.R. & van Aalten, D.M. Structure of the LKB1-STRAD-MO25 complex reveals an allosteric mechanism of kinase activation. *Science* **326**, 1707–1711 (2009).
35. Jura, N., Shan, Y., Cao, X., Shaw, D.E. & Kuriyan, J. Structural analysis of the catalytically inactive kinase domain of the human EGF receptor 3. *Proc. Natl. Acad. Sci. USA* **106**, 21608–21613 (2009).
36. Santos, F.P. & Verstovsek, S. JAK2 inhibitors: what's the true therapeutic potential? *Blood Rev.* **25**, 53–63 (2011).

ONLINE METHODS

Protein expression and purification. JH2 from JAK2 was amplified and cloned into the pFASTBAC1 vector (Invitrogen) with a thrombin-cleavable N-terminal GST tag or a C-terminus His_6 tag and expressed as a fusion protein in insect cells (*Sf*9). For protein expression, cells were infected with 10% (v/v) virus supernatant, grown for 48 h and collected by centrifugation. Cell pellets containing GST-JH2 or JH2-His fusion protein were resuspended in lysis buffer containing 20 mM Tris-HCl (pH 8.5), 500 mM NaCl, 15% (v/v) glycerol, 0.5 mM TCEP and 20 mM imidazole (for JH2-His protein only), supplemented with protease inhibitors cocktail (Roche), lysed using a cell disruptor (Avestin) and clarified by centrifugation for 1 h at 45,000*g*. The supernatant was incubated for 2 h with prewashed GST beads (GE Healthcare) or Ni-NTA beads (Qiagen) with gentle rotation at 4 °C. The beads were extensively washed, and the fusion protein was eluted with 10 mM glutathione (Sigma-Aldrich) for GST-JH2, or 250 mM imidazole (Fluka) for the JH2-His protein. Fractions containing the fusion protein were pooled and dialyzed for 2 h at 4 °C in buffer (20 mM Tris-HCl (pH 8.5), 250 mM NaCl, 15% (v/v) glycerol and 0.5 mM TCEP). For the JH2-His fusion protein, after dialysis samples were incubated with 10 U ml^{-1} thrombin (Enzyme Research Laboratory) overnight. Proteins were loaded onto a MonoQ column (GE Healthcare) equilibrated with 20 mM Tris-HCl (pH 8.5), 25 mM NaCl, 15% (v/v) glycerol and 0.5 mM TCEP and eluted with a linear gradient of 1–200 mM NaCl. Fractions containing purified GST-JH2 or JH2 were analyzed by Coomassie staining and pooled and concentrated to 1 mg ml^{-1} for further use. The JAK2 JH1 kinase domain (residues 836–1132) was cloned by PCR amplification into the pFASTBAC1 plasmid with an N-terminal GST tag and purified as described[21].

Autophosphorylation reaction. The autophosphorylation reactions were carried out using 1 μg $μl^{-1}$ of JH2, 10 mM ATP (Sigma-Aldrich) or 10 μCi [γ-^{32}P]ATP (PerkinElmer), 20 mM $MnCl_2$, 300 mM NaCl, 10% (v/v) glycerol, 0.5 mM TCEP and 20 mM Tris-HCl (pH 8.0) at room temperature (25 °C). The reactions were stopped by adding EDTA to a final concentration of 100 mM. The phosphorylation states of JH2 were monitored by autoradiography as well as native PAGE (PhastGel System, GE Healthcare) and western blotting.

Mass spectrometry. JAK2 gel bands were processed for in-gel digestion as described[37]. Phosphopeptide enrichment was performed with titanium dioxide microcolumns, with eluates desalted with Poros R3 microcolumns as described[38]. LC-MS-MS was conducted on an EASY-nLC system (Thermo Fisher Scientific) coupled to an LTQ-Orbitrap XL mass spectrometer (Thermo Fisher Scientific) as reported[39], except that chromatography was conducted with a 30-min gradient. Raw data files were submitted for Mascot searches (Matrix Science) using Proteome Discoverer 1.1 software (Thermo Fisher Scientific). Databases containing the human JAK2 protein sequence were searched with the following parameters: ESI-TRAP was selected as the instrument setting, with specified mass tolerances of 10 p.p.m. (precursor) and 0.6 Da (fragment). Serine, threonine and tyrosine phosphorylation, along with methionine oxidation, were set as variable modifications. Cysteine carbamidomethylation was included as a fixed modification and Trypsin-P specified with a maximum of two missed cleavages. Only MS-MS spectra from JAK2 phosphopeptides possessing Mascot ion scores above 20 were manually validated for the sites of phosphorylation.

Mant-ATP binding assay. The fluorescence intensity of mant-ATP (Invitrogen) complex with JH2 was measured using a FluoroMax-2 spectrofluorometer. Mant-ATP (1 μM) was added to a buffer solution (20mM Tris-HCl (pH 8.0), 200 mM NaCl, 10% (v/v) glycerol and 0.5 mM TCEP) along with 5 mM $MnCl_2$ and 1 μM JH2 (from the peak 2 fraction). The excitation and emission wavelengths were 280 nm and 440 nm, respectively, and emission was scanned from 400 nm to 500 nm. For K_d measurements, increased concentration of purified JH2 (0.25 μM to 6 μM) was added to buffer solution with 5 mM $MnCl_2$ and 1 μM mant-ATP.

Transfection, western blotting and luciferase assay. Wild-type human JAK2, JAK2 JH2 domain and human EpoR were obtained by PCR amplification and cloned with a C-terminal HA-tag into the pCI-neo mammalian expression plasmid (Promega). JAK2 mutations were done using the QuikChange Site-Directed Mutagenesis method (Stratagene) and verified by sequencing. STAT1 and STAT5 plasmids were as described[14]. JAK2-deficient γ2A cells (fibrosarcoma cells) were transfected with different JAK2 mutants using Fugene (Roche) according to manufacturer's instructions. After 8 h, cells were lysed in lysis buffer (50 mM Tris-HCl (pH 8.0), 150 mM NaCl, 100 mM NaF, 10% (v/v) glycerol, 1% (v/v) Triton-X and protease inhibitors cocktail), and protein phosphorylation was analyzed by immunoprecipitation and western blotting with anti-phosphotyrosine (4G10) antibody (Millipore), anti-pJAK2 1007-1008 (Cell Signaling Technology), anti-pSer523 (ref. 5), anti-pTyr570 (ref. 9) and anti-HA (Covance) antibody. Phosphorylation of STAT1 and STAT5 was analyzed in γ2A cells transfected with different JAK2 constructs together with STAT1 or STAT5 as indicated, and after 8 h cells were starved for 12 h in serum-free media, followed by stimulation with hIFN-γ (100 U ml^{-1}; R&D Systems) or hEpo (50 U ml^{-1}; Janssen-Cilag). After cell lysis, STAT1 phosphorylation was analyzed by western blotting with anti-pSTAT1 antibody or anti-pSTAT5 antibody (Cell Signaling Technology). STAT1 and STAT5 transcriptional activities of wild-type JAK2 and the K581A mutant were measured in γ2A cells using the *GAS*-luc STAT1 reporter or the SPI-*luc2* STAT5 reporter as described[14]. After stimulations, cells were lysed in 1× reporter lysis buffer (Promega). Luminescence was recorded using Luminoscan Ascent 96-well plate luminometer (Thermo Labsystem), and the transfection efficiency was normalized using β-GAL values.

37. Shevchenko, A., Tomas, H., Havlis, J., Olsen, J.V. & Mann, M. In-gel digestion for mass spectrometric characterization of proteins and proteomes. *Nat. Protoc.* **1**, 2856–2860 (2006).
38. Thingholm, T.E., Jorgensen, T.J., Jensen, O.N. & Larsen, M.R. Highly selective enrichment of phosphorylated peptides using titanium dioxide. *Nat. Protoc.* **1**, 1929–1935 (2006).
39. Ye, J. *et al.* Optimized IMAC-IMAC protocol for phosphopeptide recovery from complex biological samples. *J. Proteome Res.* **9**, 3561–3573 (2010).

Analytical Biochemistry 442 (2013) 213–222

Contents lists available at ScienceDirect

Analytical Biochemistry

journal homepage: www.elsevier.com/locate/yabio

Analysis of steady-state Förster resonance energy transfer data by avoiding pitfalls: Interaction of JAK2 tyrosine kinase with *N*-methylanthraniloyl nucleotides

Yashavanthi Niranjan [a], Daniela Ungureanu [a], Henrik Hammarén [a], Arturo Sanz-Sanz [b], Adrie H. Westphal [c], Jan Willem Borst [c], Olli Silvennoinen [a,d], Riet Hilhorst [e,*]

[a] Institute of Biomedical Technology, University of Tampere, FI-33014 Tampere, Finland
[b] Department of Hematology, Erasmus MC, 3015 CE Rotterdam, The Netherlands
[c] Department of Biochemistry, Wageningen University, 6700 ET Wageningen, The Netherlands
[d] School of Medicine, Tampere University Hospital, FI-33014 Tampere, Finland
[e] PamGene International, 5211 HH 's-Hertogenbosch, The Netherlands

ARTICLE INFO

Article history:
Received 12 April 2013
Received in revised form 10 July 2013
Accepted 14 July 2013
Available online 23 July 2013

Keywords:
MANT nucleotide
FRET
JAK2
Primary inner filter effect
Secondary inner filter effect
Ligand binding

ABSTRACT

Förster resonance energy transfer (FRET) between the fluorescent ATP analogue 2′/3′-(*N*-methyl-anthraniloyl)-adenosine-5′-triphosphate (MANT–ATP) and enzymes is widely used to determine affinities for ATP–protein binding. However, in analysis of FRET fluorescence data, several important parameters are often ignored, resulting in poor accuracy of the calculated dissociation constant (K_d). In this study, we systematically analyze factors that interfere with K_d determination and describe methods for correction of primary and secondary inner filter effects that extend the use of the FRET method to higher MANT nucleotide concentrations. The interactions of the fluorescent nucleotide analogues MANT–ATP, MANT–ADP [2′/3′-*O*-(*N*-methylanthraniloyl) adenosine diphosphate], and MANT–AMP [2′/3′-*O*-(*N*-methylanthraniloyl) adenosine monophosphate] with the JAK2 tyrosine kinase domain are characterized. Taking all interfering factors into consideration, we found that JAK2 binds MANT–ATP tightly with a K_d of 15 to 25 nM and excluded the presence of a second binding site. The affinity for MANT–ADP is also tight with a K_d of 50 to 80 nM, whereas MANT–AMP does not bind. Titrations of JAK2 JH1 with nonhydrolyzable ATP analogue MANT–ATP-γ-S [2′/3′-*O*-(*N*-methylanthraniloyl) adenosine-5′-(thio)- triphosphate] yielded a K_d of 30 to 50 nM. The methods demonstrated here are applicable to other enzyme–fluorophore combinations and are expected to help improve the analysis of steady-state FRET data in MANT nucleotide binding studies and to obtain more accurate results for the affinities of nucleotide binding proteins.

Fluorescence spectroscopy is a widely used technique to analyze protein–ligand interactions. One method is the use of Förster resonance energy transfer (FRET),[1] which results in the appearance of acceptor fluorescence on excitation of the donor fluorophore(s) of the protein [1] and has become the method of choice for binding studies. In such studies, *N*-methylanthraniloyl (MANT) ligands are often used as fluorescent analogues. Over the past years, several fluorescent nucleotide analogues with modifications in the phosphate or ribose groups have been developed. Metal substitutes with Co(III) or Cr(III) have been developed to stabilize ATP [2]. Fluorescent ATP analogues with modified ribose hydroxyl groups such as 2′,3′-*O*-(2, 4, 6-trinitrocyclohexadienylidene) adenosine 5′-triphosphate (TNP–ATP), *N*-methyl-anthraniloyl-amide-ethyl triphosphate (MANT–TP), and 2′/3′-(*N*-methyl-anthraniloyl)-adenosine-5′-triphosphate (MANT–ATP) have often been used to study ATP binding to proteins [3–5], to determine the role of lysine and threonine residues in ATP binding in protein kinases [6], and to determine the binding of MANT derivatives to kinases [7]. In addition, nonhydrolyzable forms of ATP have been used successfully [8].

The use of fluorescence spectroscopy in binding studies with ATP analogues has become common because of the sensitivity and ease of this technique. However, a number of experimental pitfalls challenge precise determination of equilibrium binding constants. Parameters that complicate the analysis include the absorbance of MANT–ATP (and other MANT forms) at both

* Corresponding author. Fax: +31 73 615 8081.
E-mail address: rhilhorst@pamgene.com (R. Hilhorst).

[1] *Abbreviations used:* FRET, Förster resonance energy transfer; MANT, *N*-methylanthraniloyl; TNP–ATP, 2′,3′-*O*-(2, 4, 6-trinitrocyclohexadienylidene) adenosine 5′-triphosphate; MANT–TP, *N*-methyl-anthraniloyl-amide-ethyl triphosphate; MANT–ATP, 2′/3′-(*N*-methyl-anthraniloyl)-adenosine-5′-triphosphate; JH, JAK homology; MANT–ATP-γ-S, 2′/3′-*O*-(*N*-methylanthraniloyl) adenosine-5′-(thio)- triphosphate; MANT–ADP, 2′/3′-*O*-(*N*-methylanthraniloyl) adenosine diphosphate; MANT–AMP, 2′/3′-*O*-(*N*-methylanthraniloyl) adenosine monophosphate; MANT–AXP, MANT–ATP, –ATP-γ-S, –ADP, or –AMP; AMP–PNP, adenylyl-imidodiphosphate; TCEP, tris(2-carboxyethyl)phosphine; SD, standard deviation; PKA, protein kinase A.

0003-2697/$ - see front matter © 2013 Elsevier Inc. All rights reserved.
http://dx.doi.org/10.1016/j.ab.2013.07.020

excitation and emission wavelengths and the fluorescence contribution of free MANT–ATP to the total fluorescence signal at 440 nm (which is the FRET detection window). Furthermore, the assumption that the concentration of free MANT–ATP is equal to the total MANT–ATP concentration (i.e., assuming that the fraction of bound MANT–ATP is negligible) is not always valid. Most studies using MANT–ATP in FRET measurements have not taken these factors into account in the analysis of FRET data, leading to erroneous results.

JAK2 belongs to the Janus kinase family of tyrosine kinases (JAK1–3 and Tyk2), which are critical mediators in cytokine-dependent signal transduction [9,10]. JAKs are characterized by the presence of seven JAK homology (JH) domains. The N terminal of JAK2 (JH domains 7–3) consists of a FERM domain that mediates the receptor–JAK interaction [11]. The C terminus harbors the tyrosine kinase domain, JH1, which is connected through a short hinge region to the JH2 (or pseudokinase) domain. The JH2 domain shows a strong structural similarity to the neighboring JH1 domain and for a long time was considered to be catalytically inactive [12]. Although it lacks the highly conserved residues required for phospho transfer reaction, it was recently shown to possess dual specific catalytic activity [13]. Binding of cytokines to members of the hematopoietin family of transmembrane cell surface receptors leads to receptor oligomerization and transphosphorylation of specific tyrosine residues in the activation loop of the JH1 domain of JAK2. Activated JAK2 catalyzes ATP-dependent phosphorylation of tyrosine residues in substrates and also undergoes autophosphorylation [14]. Deregulation of JAK kinases severely distorts normal cellular processes such as hematopoietic cell development, blood cell formation, and cell signaling. Compelling evidence has linked deregulated cytokine signaling with cellular transformation and human cancer, and aberrantly activated JAK2 has been shown to cause myeloproliferative neoplasms and different types of leukemia. These findings have made JAK2 an actively pursued target for drug development and have turned significant interest toward the kinetic characteristics of the JH1 domain.

The nucleotide binding properties of JH1 of JAK2 have previously been studied using γ-ATP binding and kinase activity assays [15–17]. The kinetic parameters (K_m and k_{cat}) were determined by Hall and coworkers using a caliper-based microfluidics assay and high-performance liquid chromatography (HPLC) for different phosphorylation states of the JH1 domain using fluorescein isothiocyanate (FITC)-conjugated peptides [18]. Sanz and coworkers used peptide microarrays to analyze the catalytic activity of JAK2 and found that the K_m for ATP of the JAK2 tyrosine kinase domain increased 2-fold to approximately 100 μM in the presence of the pseudokinase domain [15]. The ATP binding affinity of the JAK2 kinase domain has not been determined. Fluorescent analogues of ATP such as TNP–ATP [19–21] and MANT–ATP [4,7,13,22,23] have been used extensively to determine the nucleotide binding properties and stoichiometric determinants of various kinase domains and pseudokinases, but not for determining the affinity of kinase domains of JAKs for ATP. In the current work, steady-state FRET was employed to determine the affinity of nucleotides for the active site of recombinant tyrosine kinase domain (JH1) of JAK2 using MANT nucleotides with concentrations up to and above the K_m values [15] so as to establish a highly accurate assay for MANT–ATP binding to JH1.

The analysis methods and correction procedures used to interpret FRET data vary a lot between publications, illustrating that commonly used methods are vulnerable to pitfalls. In this study, we have systemically analyzed the contribution of different variables to the FRET signal and determined the relevant corrections needed to obtain reliable values for K_d, thereby providing a concise method of analyses that shows considerably less variation compared with previously described methods.

Theory

Primary inner filter effect

Fluorescence intensity is a function of the following parameters: the intensity of the excitation light (I_0), the concentration of the fluorophore (C), the molar extinction coefficient (ε_{ex}) at the excitation wavelength, the length of the excitation light path through the solution (l), the quantum yield (φ), and the instrument parameters (k_{in}), which include the optical configuration of the instrument and the bandwidth of the monochromators. This relationship can be written as:

$$F_{em,obs} = I_0 * C * \varepsilon_{ex} * l * \varphi * k_{in}. \quad (1)$$

This equation shows that fluorescence is linear with the concentration of the fluorophore and with the absorbance at the excitation wavelength A_{ex} because $A_{ex} = C * \varepsilon * l$.

This relation is valid only at low concentrations of fluorophores. At high concentrations, deviation from linearity occurs due to nonhomogeneous excitation throughout the cuvette. This effect is called the primary inner filter effect. If the absorbance of the solution (A_{ex}) surpasses an optical density of approximately 0.06, the inner filter effect starts to noticeably contribute to the decrease in fluorescence [24]. At this optical density, 7% of the incident light is absorbed at a distance of 0.5 cm from the entry of the excitation light into the cuvette, that is, the distance where fluorescence generally is measured. If more than one component in the solution absorbs the excitation light, the components' contributions to the absorbance are additive.

In a recent review, several pitfalls in the analysis of fluorescence measurements were described, including inner filter effects [25]. Several correction procedures for inner filter effects have been published [24,26–29], some more sophisticated than others (see Refs. 7–11 in Ref. [24]). Kubista and coworkers provided a practical correction method for the primary inner filter effect for fluorometers with right angle detection geometry [24] and derived the formula:

$$F_{em,corr} = F_{em,\,obs} * 10^{(A_{ex} * l_p / l)}, \quad (2)$$

where $F_{em,obs}$ is the observed fluorescence intensity, $F_{em,corr}$ is the fluorescence corrected for the primary inner filter effect, A_{ex} is the absorbance of the solution at the excitation wavelength, l is the length of the excitation light path in solution, and l_p is the mean distance of the observed fluorescing subvolume from the entry wall. It has been shown that using the fluorescence intensity at the mean distance instead of the average integrated intensity is accurate with errors of less than 0.6% even in extreme conditions [26]. l_p can be determined experimentally [24].

Secondary inner filter effect

Absorption of fluorescence occurs when the optical density of a solution at the emission wavelength is high. This effect is called the secondary inner filter effect. It can be caused by self-absorption by the fluorophore or by the presence of other absorbing compounds in the solution. Because the path length of fluorescence leaving the solution is usually shorter than the path length of the excitation light, the contribution of this effect is small but cannot always be neglected. No practical approach to correct for this effect has been described in the literature. Applying the same analysis as for the primary inner filter effect to the secondary inner filter effect, the correction can be described by Eq. (3):

$$F_{em,corr} = F_{em,obs} * 10^{(A_{em} * l_y / l)}, \quad (3)$$

where $F_{em,obs}$ is the observed fluorescence intensity, $F_{em,corr}$ is the fluorescence corrected for the secondary inner filter effect, A_{em} is

the absorbance of the solution at the emission wavelength, l is the length of the excitation light path in solution, and l_y is the mean distance of the observed fluorescing subvolume from the exit wall. l_y cannot easily be determined experimentally, but it can be estimated from the experimentally determined value for l_p at the excitation wavelength and from geometric considerations. In most experimental configurations, the path length that the fluorescence traverses before leaving the sample solution is 1 to 2 mm. In analogy to the analysis for the primary inner filter effect, the secondary inner filter effect is expected to start contributing when approximately 7% of the light has been absorbed, that is, when the absorbance surpasses a value of approximately 0.3 for a light path of 1 mm.

Corrections for primary and secondary inner filter effects can be treated independently [24], resulting in a function where the primary and secondary inner filter corrections are multiplied, as shown in Eq. (4):

$$F_{\mathrm{em,corr}} = F_{\mathrm{em,obs}} * 10^{(A_{\mathrm{ex}} * l_p/l)} * 10^{(A_{\mathrm{em}} * l_y/l)}. \quad (4)$$

Processes affecting FRET fluorescence intensity

In methods using FRET as readout in binding studies, one usually measures the fluorescence intensity of an acceptor fluorophore. This acceptor emission is the result of energy transfer from excited tryptophan and/or tyrosine residues of a protein to the bound fluorophore. FRET intensity depends not only on factors that affect the primary fluorescence (Eq. (1)) but also on the efficiency of energy transfer (governed mainly by the distance between tryptophans and the bound fluorophore, the orientation of the donor–acceptor pair [κ^2], and their spectral overlap) and the contribution of absorbance of emitted light by the components in the solution (secondary inner filter effect). Fig. 1 gives an overview of the processes that can take place in an experimental setup with excitation at 280 or 340 nm, using the FRET between the JAK2 JH1 domain and MANT nucleotides as an example. The fluorescence intensity for each process can be described by Eq. (1). Determination of fluorescence intensity with a given concentration of a solute under identical experimental conditions results in fluorescence intensity per concentration (defined as f) that is dependent on the molar extinction coefficient ($\varepsilon_{\mathrm{ex}}$) at the excitation wavelength and the quantum yield (φ).

Excitation at 280 nm, mainly tryptophan but also tyrosine residues in the protein (JAK2 JH1), absorb the light, resulting in fluorescence emission with a maximum at around 340 nm (*F340*) (process 1). Some residual tryptophan fluorescence is observed at 440 nm (*F440*) (process 2). Because the protein emission spectrum and the MANT–AXP (MANT–ATP, MANT–ATP-γ-S [2′/3′-*O*-(*N*-methylanthraniloyl) adenosine-5′-(thio)- triphosphate], MANT–ADP [2′/3′-*O*-(*N*-methylanthraniloyl) adenosine diphosphate], or MANT–AMP [2′/3′-*O*-(*N*-methylanthraniloyl) adenosine monophosphate] absorption spectrum have a large overlap, energy transfer between protein and bound MANT nucleotides can take place, resulting in a FRET signal at 440 nm (process 3). The f factor for this process, f_{FRET}, not only depends on the $\varepsilon_{\mathrm{ex}}$ and φ for MANT–AXP but also depends on f_p and the efficiency of energy transfer. The free (unbound) MANT nucleotides in solution can absorb excitation light, contributing to the primary inner filter effect, or can lead to absorption of the protein fluorescence (secondary inner filter effect), resulting in reduction of fluorescence at 340 nm and an increase of fluorescence at 440 nm (process 4). In addition, direct quenching of tyrosines or tryptophans by MANT nucleotides (leading to nonradiative decay of the excited state) can decrease fluorescence at 340 nm. MANT nucleotides that are directly excited at 280 nm (process 5) fluoresce at 440 nm. The fluorescence due to the direct excitation of bound protein (with factor f_{Pc}) and bound MANT–AXP (with factor f_{Lc}) are not depicted separately in Fig. 1.

The fluorescence detected at 440 nm on excitation at 280 nm is the sum of the contributions of all species present, each having its own f factor that relates fluorescence intensity to the concentration of the species. The fluorescence measured at 440 nm can be described by Eq. (5):

$$F440_{\mathrm{ex\_280nm}} = L * f_{\mathrm{L}} + PL * f_{\mathrm{Lc}} + PL * f_{\mathrm{FRET}} + PL * f_{\mathrm{Pc}} + P * f_{\mathrm{P}} + F_{\mathrm{sec}}. \quad (5)$$

The concentration of free MANT–AXP is represented by L, protein–MANT–AXP complex is represented by PL, and free protein is represented by P. f_{Lc} is the factor of MANT–AXP emission of bound MANT–AXP, f_{FRET} is the factor of FRET emission of bound MANT–AXP, and f_{Pc} is the factor of protein emission of bound protein. The term F_{sec} represents the contribution of process (4), that is, protein fluorescence at 340 nm that is absorbed by free MANT–AXP resulting in fluorescence at 440 nm. The secondary emission F_{sec} depends on the concentrations of both protein and ligand.

On excitation at 340 nm, both free MANT nucleotides (process 6) and bound MANT nucleotides (process 7) absorb excitation light and fluoresce at 440 nm. The protein does not absorb at 340 nm and so does not contribute to *F440*.

The fluorescence emission at 440 nm on excitation at 340 nm is described as follows:

$$F440_{\mathrm{ex\_340nm}} = L * f_{\mathrm{L}^{340}} + PL * f_{\mathrm{Lc}^{340}}. \quad (6)$$

This implies that the fluorescence at 440 nm depends on the fluorescence of all MANT–AXP species in solution. When $f_{\mathrm{L}^{340}}$ and $f_{\mathrm{Lc}^{340}}$ are (near) identical, $F440_{\mathrm{ex\_340nm}}$ is linearly related to the total MANT–AXP concentration and bound and free MANT–AXP cannot be distinguished from each other.

Calculation of concentration of protein–ligand complex

The dissociation constant is defined as the concentration of free ligand at which half of the number of binding sites on a protein (assuming a single binding site for JAK2 JH1) is occupied and is given by Eq. (7):

$$K_{\mathrm{d}} = \frac{[P] * [L]}{[PL]}, \quad (7)$$

where $[P]$ represents the concentration of free protein, $[L]$ represents the concentration of free ligand, and $[PL]$ represents the concentration of complex.

Using the mass balance equations, K_{d} can be expressed in terms of concentrations of total ligand and protein:

$$K_{\mathrm{d}} = \frac{([L_{\mathrm{total}}] - [PL]) * ([P_{\mathrm{total}}] - [PL])}{[PL]}. \quad (8)$$

The concentration of bound ligand can be calculated from the solution of a quadratic equation of the type $ax^2 + bx + c = 0$, resulting in the following equation:

$$[PL] = \frac{([P_{\mathrm{total}}] + [L_{\mathrm{total}}] + K_{\mathrm{d}}) - \sqrt{([P_{\mathrm{total}}] + [L_{\mathrm{total}}] + K_{\mathrm{d}})2 - 4 * [P_{\mathrm{total}}][L_{\mathrm{total}}]}}{2} \quad (9)$$

Combining Eqs. (5) and (9), and using $L = L_{\mathrm{total}} - PL$ and $P = P_{\mathrm{total}} - PL$, Eq. (5) can be rewritten as:

$$F440_{\mathrm{ex\_280nm}} = PL * (f_{\mathrm{Lc}} + f_{\mathrm{FRET}} + f_{\mathrm{Pc}} - f_{\mathrm{L}} - f_{\mathrm{P}}) + L_{\mathrm{total}} * f_{\mathrm{L}} + P_{\mathrm{total}} * f_{\mathrm{p}} + F_{\mathrm{sec}}. \quad (10)$$

The f factors that relate the fluorescence to the concentration of free or bound MANT–AXP or protein were determined experimentally.

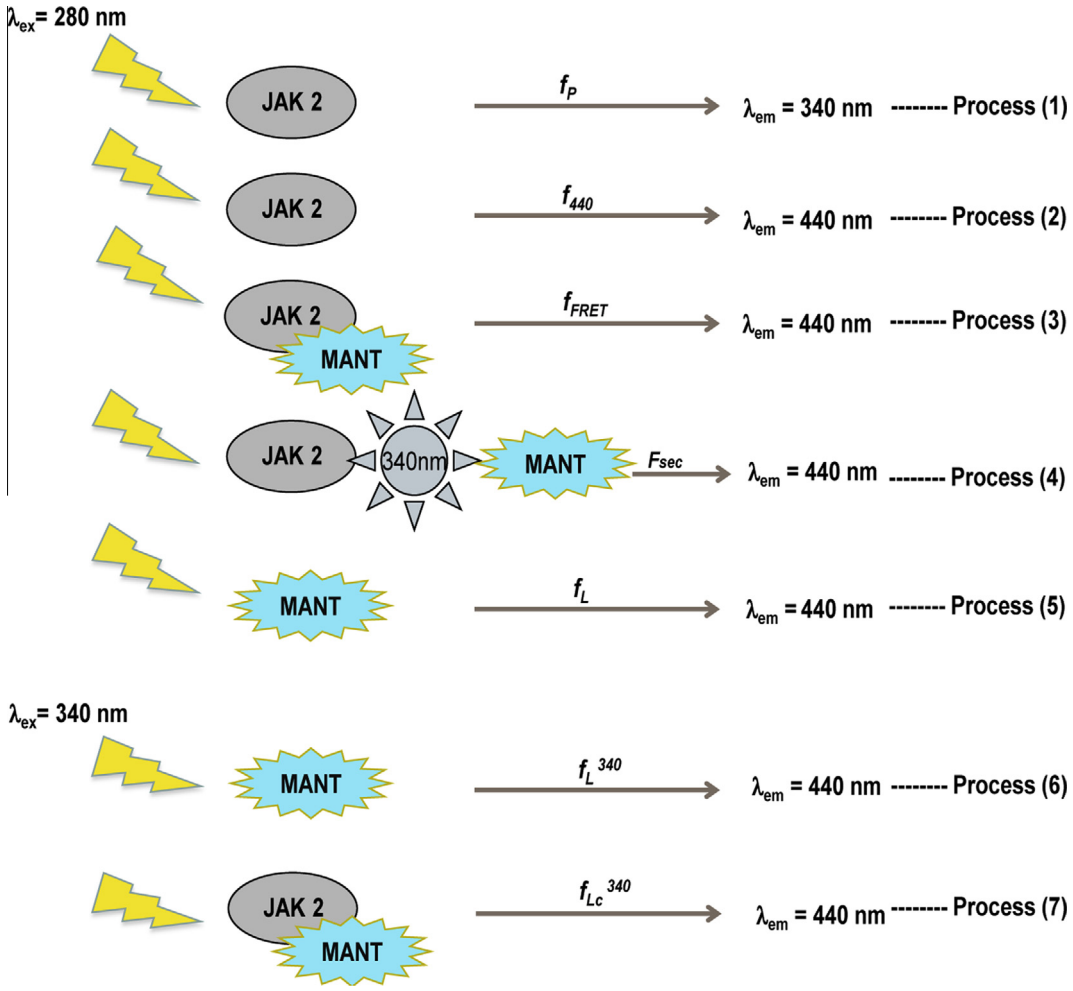

Fig.1. Overview of mechanisms that contribute to fluorescence. A schematic representation of processes yielding fluorescence that take place in a solution containing protein and MANT–AXP (AXP can be ATP, ATP-γ-S, ADP, or AMP) on excitation at 280 or 340 nm is shown.

Materials and methods

Plasmid constructs and reagents

The human JAK2 (GenBank accession no. NM_004972.3) JH1 construct was cloned into the pFASTBac1 vector, allowing for recombinant protein expression and purification using the C-terminal polyhistidine tag and thrombin cleavage site. The part of the gene coding for the JH1 domain (aa 810–1113) was cloned into the vector.

MANT–ATP, MANT–ATP-γ-S, MANT–ADP, and MANT–AMP were obtained from Jena Biosciences. PK buffer (10×) was obtained from New England Biolabs, ATP was obtained from Fermentas, adenylyl-imidodiphosphate (AMP–PNP) was obtained from Roche Applied Science, and tris(2-carboxyethyl)phosphine (TCEP) was purchased from Calbiochem.

Protein expression and purification

Spodoptera fugiperda (Sf9) insect cells (1×10^6 cells/ml) were transfected with the recombinant JH1 JAK2 pFASTBac1–6×His construct, and virus amplification was carried out until the P3 stage at the same cell count. For protein production, 3×10^6 cells/ml were infected with 10% P3 virus and incubated for 48 h at 27 °C in a shaking incubator. After 48 h, the cells were harvested and lysed in buffer containing 20 mM Tris–HCl (pH 8.0) (Sigma Life Science), 500 mM NaCl (Sigma–Aldrich), 20% (v/v) glycerol (Sigma Life Science), 20 mM imidazole (Fluka), and protease inhibitor cocktail (Roche Diagnostics) for 30 min on ice, followed by sonication and centrifugation for 1 h at 4 °C and 14,000*g*. The supernatant was mixed with previously washed and equilibrated with Ni–NTA (nickel–nitrilotriacetic acid) beads (Macherey–Nagel) and incubated at 4 °C for 2 h with gentle rotation. The protein was eluted with 250 mM imidazole. Fractions containing JAK2 JH1 were pooled and dialyzed for 2 h in 20 mM Tris–HCl (pH 8.0), 500 mM NaCl, and 20% glycerol with a buffer change after 1 h. The protein was concentrated with Amicon Ultra centrifugal units from Millipore and injected onto a Superdex 75 gel filtration column previously equilibrated with the same buffer. The monomeric protein fractions obtained were used for direct binding studies. A detailed purification protocol is described in Ref. [13].

MANT nucleotide binding assay

Purified JAK2 JH1 (0.5 μM) was incubated for 1 min at 21 °C in a quartz cuvette with light path of 10 × 2 mm (product no. B0631124, PerkinElmer) filled with a buffer containing 10 mM $MnCl_2$ (Sigma–Aldrich), 20 mM Tris–HCl (pH 8.0), 200 mM NaCl, 10% glycerol, 1 mM TCEP, and 1× PK buffer (New England Biolabs), with or without the addition of MANT–AXP, at concentrations ranging from 0 to 88 μM. As control, the fluorescence of a concentration series of MANT–AXP without protein was measured. All

concentrations were corrected for dilution brought about by the addition of ligand. A QuantaMaster spectrofluorometer (Photon Technology International) equipped with a PowerArc xenon arc lamp as an excitation source and excitation and emission channel monochromators was used to measure the steady-state fluorescence of MANT-labeled nucleotides. MANT nucleotides were excited at 280 or 340 nm, and emission spectra were collected from 300 to 500 nm or from 350 to 500 nm, with both excitation and emission slit widths resulting in a bandpass of 2 nm.

Determination of extinction coefficients

The extinction coefficient for the JAK2 JH1 domain was calculated with the method given by Shi and coworkers [23] and was verified experimentally. Extinction coefficients for AMP–PNP and MANT–AXP at 280, 340, and 440 nm were determined from a concentration series of AMP–PNP or MANT–AXP. For MANT–AXP, the published values for ε_{255nm} and ε_{356nm} were used to determine the exact concentration. For tyrosine and tryptophan, absorbances of a concentration series were used to verify the reported extinction coefficients.

Determination of instrument factors

The instrument parameter l_p was determined as described by Kubista and coworkers [24]. Whereas in their study a single solution was scanned to vary the optical density, assuming a wavelength independent quantum yield, we measured the increase in absorption (A) and in fluorescent signal (F) at fixed wavelengths with different MANT–ATP concentrations. l_p was calculated from a plot of $\log(A_{280}/F_{440})$ as a function of A_{280}, with MANT–ATP ranging from 0 to 500 μM. Concentration series of MANT–ADP and MANT–AMP and tyrosine and tryptophan were used to verify the value of l_p. To determine l_p for excitation at 340 nm and emission at 440 nm, $\log(A_{340}/F_{440})$ was plotted as function of A_{340} for MANT–ATP concentrations ranging from 0 to 500 μM.

Validation of correction for inner filter effects and study of interactions between free tyrosine and tryptophan and MANT–ATP

Solutions of tyrosine (0.275 and 0.55 mM) or tryptophan (61, 122, and 244 μM) in buffer containing 20 mM Tris–HCl (pH 8.0), 200 mM NaCl, 10% glycerol, and 1 mM TCEP were titrated with increasing concentrations of MANT–ATP (0–150 μM), and steady-state fluorescence spectra were recorded. Fluorescence intensities at 340 nm (*F340*) and 440 nm (*F440*) were corrected for the primary inner filter effect with Eq. (2). Eq. (4) was applied to correct *F440* for both primary and secondary inner filter effects.

Calculation of K_d

The average value of fluorescence intensity between 430 and 440 nm ($F_{430–440,obs}$) was used for calculations. This approach improves the signal-to-noise ratio of the measurements. $F_{430–440,obs}$ was corrected for primary inner filter effects with Eq. (2). The values for f_L were determined individually for each experiment. Dilution of the protein due to the addition of ligand stocks was taken into account, and the $F_{430–440,obs}$ data were fitted with GraphPad Prism software (http://www.graphpad.com) using the quadratic Eq. (9) for tight binding interactions with ligand depletion with free parameters K_d by minimization of the weighted sum of squares. 1/*F440* was used as a weighting factor based on analysis of residuals. The experiments were repeated five times, from which average values of K_d were calculated. The K_d (without correction for the inner filter effect incorporated) was calculated by nonlinear regression analysis in GraphPad Prism using the equation for one-site specific binding $y = B_{max} * x/(K_d + x)$, where y is the measured fluorescence, B_{max} is the maximum fluorescence, x is the concentration of the ligand, and K_d is obtained in the same units as x. The experiments were repeated at least five times and represented with standard deviation (SD) values.

Results

Determination of extinction coefficients for MANT–ATP and protein

To correct for inner filter effects on fluorescence intensities, the molar extinction coefficients for the JAK2 JH1 protein, AMP–PNP, and MANT–ATP at 280 and 340 nm were determined. At 280 nm, values of 38,850, 3800, and 3003 M^{-1} cm^{-1}, respectively, were obtained. At 340 and 440 nm, the absorbance of JAK2 JH1 was negligible. For MANT–AXP, a molar extinction coefficient of 5160 M^{-1} cm^{-1} was obtained at 340 nm, whereas the value was less than 50 M^{-1} cm^{-1} at 440 nm. The different MANT nucleotides had identical extinction coefficients. Literature values of the molar extinction coefficients for tyrosine and tryptophan (1490 and 5500 M^{-1} cm^{-1} at 280 nm, negligible at 340 nm) were confirmed experimentally.

Determination of instrument parameters l_p and l_y

The values for l_p were determined essentially as described in Ref. [24]. The l_p value for excitation at 280 nm (A_{280}) and fluorescence emission detection at 440 nm (F_{440}) was determined from a plot of $\log(A_{280}/F_{440})$ versus the absorbance of MANT–ATP at 280 nm, with [MANT–ATP] ranging from 0 to 500 μM. A value for l_p/l of 0.39 was calculated (see Supplementary Fig. 1A in supplementary material). Using the same MANT–ATP solutions, applying excitation at 340 nm and emission at 440 nm yielded an l_p/l of 0.46 (Supplementary Fig. 1B). Performing the same analysis with a concentration series of tryptophan or tyrosine (excitation at 280 nm and emission at 340 nm) yielded an l_p/l value of 0.4 for both compounds. The excitation wavelength used for K_d determination was 280 nm; thus, a value for l_p/l of 0.4 was used to correct for the primary inner filter effect.

A practical method for correction for secondary inner filter effects caused by absorption of fluorescence at 340 nm by components in solution has not been described in the literature. Fluorescence is generated over the full length of the light path of the cuvette and usually is detected in a limited window. Absorption of emitted light takes place along the path from the origin of fluorescence to the wall of the cuvette (l_y). For the fluorescence cuvettes used here, the distance between the source of fluorescence and the cuvette wall is relatively small, on average 1 mm. Assuming that the secondary inner filter effect is independent of the primary inner filter effect, the same processes take place as for the primary inner filter effect. Therefore, the factor l_p, obtained with excitation at 340 nm (A_{340nm}) and fluorescence emission detection at 440 nm (F_{440}) that was determined from a plot of $\log(A_{340}/F_{440})$ versus A_{340nm}, was used as the starting point. Assuming linear behavior of absorption over short distances, the value for l_p was corrected for the short light path of 1 mm (instead of 10 mm for the excitation path length), resulting in a value of 0.046 for l_y/l (see Supplementary Fig. 2 in supplementary material).

Correction of MANT–ATP fluorescence for inner filter effect

At low concentrations of MANT–ATP, $F_{em,obs}$ (excitation at 280 nm, detection at 440 nm) shows a linear relation with concentration, but at higher concentrations the absorbance of the incident light results in deviation from linearity (see Supplementary Fig. 3

in supplementary material) and at high concentrations even results in a decrease in fluorescence. Correction for the primary inner filter effect using Eq. (2) results in a linear relation between fluorescence values and MANT–ATP concentration up to an optical density of 2.5. The slope of this curve is factor f_L (process 5 in Fig. 1). Application of this correction allows the use of high concentrations of MANT–ATP in the titrations.

Performing the same experiment with excitation at 340 nm yields a higher fluorescence intensity because $f_{L^{340}} = 17 * f_L$ due to a higher excitation intensity at 340 nm (data not shown).

Effect of tyrosine or tryptophan on fluorescence of MANT–ATP at 440 nm (λ_{ex} = 280 nm)

Tryptophan and tyrosine fluorescence emission from proteins at 340 nm can be absorbed by MANT–AXP in solution (process 4 in Fig. 1). The contribution of this process to the MANT nucleotide fluorescence intensity at 440 nm was investigated by titration of a solution containing 50 μM MANT–ATP with tyrosine or tryptophan. These molecules have similar fluorescence characteristics as tyrosine and tryptophan in a protein but do not bind MANT–ATP.

Fluorescence spectra were recorded with excitation at 280 nm and fluorescence emission detected from 400 to 500 nm. The average fluorescence intensity values between 430 and 440 nm were corrected for the primary inner filter effect. Fig. 2A shows that tyrosine does not contribute to the fluorescence at 440 nm. After correction for the primary inner filter effect, the MANT–ATP fluorescence at 440 nm remains constant on titration with tyrosine. This indicates that the emission of tyrosine is low at 340 nm.

Fig. 2B shows a titration of MANT–ATP with tryptophan. A solution containing only tryptophan shows a linear relation between concentration and fluorescence at 440 nm. In the presence of 50 μM MANT–ATP, the fluorescence signal increases slightly more than in a solution containing tryptophan only. The ratio of the slopes is 1.5. The fluorescence intensity is composed of contributions of tryptophan, MANT–ATP, and absorbance of tryptophan fluorescence by MANT–ATP. MANT–ATP (50 μM) has absorption at 340 nm of 0.26 and so absorbs 5% of the tryptophan fluorescence over a path length of 1 mm. This implies that MANT–AXP in solution can reabsorb fluorescence emitted by the protein (process 4 in Fig. 1).

Effect of tyrosine or tryptophan on fluorescence of MANT–ATP at 440 nm (λ_{ex} = 340 nm)

Excitation at 340 nm of a solution of MANT–ATP with or without tryptophan (range of 0–2.44 mM) in solution did not affect MANT–ATP fluorescence at 440 nm (data not shown). Tryptophan and tyrosine do not absorb light at 340 nm and so do not contribute to an inner filter effect. These results confirm that excitation at 340 nm can be used to measure both bound and free MANT–ATP in solution and are in agreement with previous findings [4].

Effect of MANT–ATP on tyrosine or tryptophan fluorescence at 340 nm (λ_{ex} = 280 nm)

The fluorescence at 340 nm of tyrosine or tryptophan (excitation at 280 nm) was measured in the presence of increasing concentrations of MANT–ATP. As expected, the signal intensity decreased with increasing absorbance at 280 nm. When values were corrected for the primary inner filter effect, a slight decrease in fluorescence was still observed (Fig. 3). Correction for the absorbance of fluorescence by MANT–ATP was necessary because the A_{340} of MANT–ATP ranged from 0 to 0.77. Fig. 3 shows that the secondary inner filter effect starts to contribute if the A_{340} of the

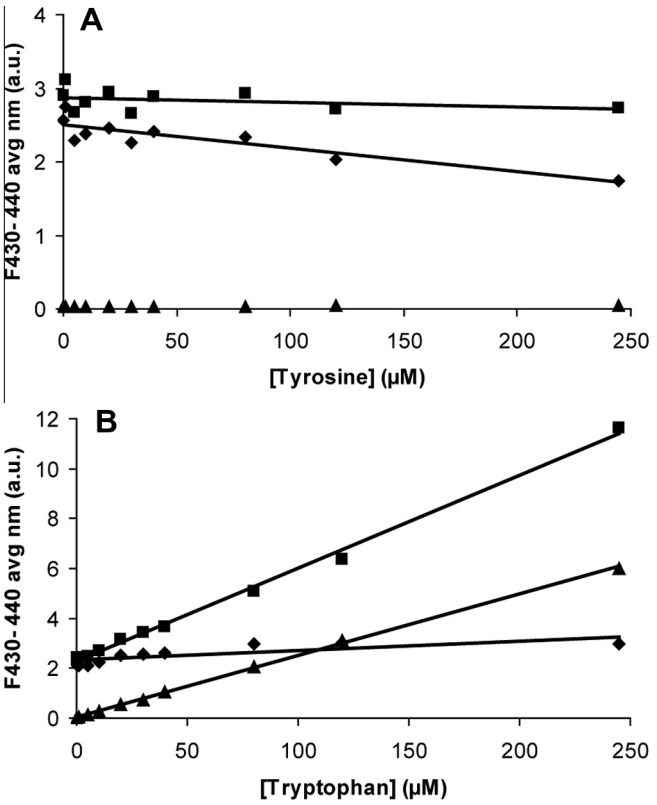

Fig.2. Effect of tyrosine or tryptophan on fluorescence of MANT–ATP at 440 nm (λ_{ex} = 280 nm). (A) Effect of increasing concentrations of tyrosine on MANT–ATP fluorescence at 430 to 440 nm. The excitation wavelength used was 280 nm. ▲, tyrosine; ♦, 50 μM MANT–ATP + tyrosine; ■, 50 μM MANT–ATP + tyrosine corrected for primary inner filter effect. The lines are the results of fitting the data to a linear model. (B) Effect of increasing concentrations of tryptophan on MANT–ATP fluorescence at 430 to 440 nm. The excitation wavelength used was 280 nm. ▲, tryptophan corrected for primary inner filter effect; ♦, 50 μM MANT–ATP + tryptophan; ■, 50 μM MANT–ATP + tryptophan corrected for primary inner filter effect. The lines are the results of fitting the data to a linear model.

MANT–ATP solution surpasses the value 0.3 (~50 μM MANT–ATP). After correction for the secondary inner filter effect, the fluorescence signal at 340 nm is not affected by the concentration of MANT–ATP. This indicates that MANT–ATP does not quench the fluorescence of tyrosine and tryptophan other than by absorbing a fraction of the emitted light.

The increase in MANT–ATP fluorescence by absorption of tryptophan emission (F_{sec}) was determined by measuring the *F440* of a concentration series of MANT–ATP in the presence of different concentrations of tryptophan. f_L increased to $(1 + 0.005 * [Trp]) * f_L$, with tryptophan concentration expressed in micromolar (μM).

Determination of f factors

To apply Eq. (10) for the calculation of K_d, the concentration of the components must be calculated with Eq. (9) and the values of the *f* factors must be assessed. For each species, the *f* factor units used here are μM^{-1}.

f_L was determined from a concentration series of MANT–AXP. Expression of other *f* factors in terms of f_L eliminates variation in instrument parameters such as lamp intensities. f_P was calculated from the ratio of *F440*/*F340* for incubations with protein only. This ratio of 0.026 was used to calculate the contribution of protein fluorescence at 440 nm in the titrations of protein with MANT–AXP. f_{FRET} was expressed in relation to f_L and used as a variable in the fit. The fluorescence factors of bound protein (f_{Pc}) and bound

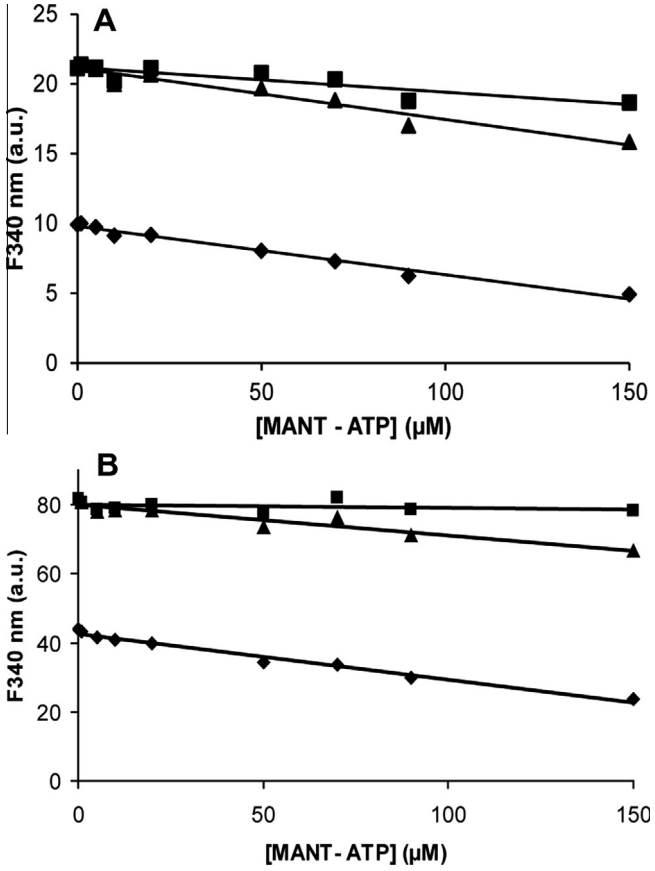

Fig.3. Effect of MANT–ATP on tyrosine or tryptophan fluorescence at 340 nm (λ_{ex} = 280 nm). (A) Effect of increasing concentrations of MANT–ATP on the fluorescence of 551 μM tyrosine (excitation at 280 nm, emission of 340 nm). ♦, uncorrected; ▲, corrected for primary inner filter effect; ■, corrected for primary and secondary inner filter effects. The lines are the results of fitting the data to a linear model. (B) Effect of increasing concentrations of MANT–ATP on the fluorescence of 122 μM tryptophan (excitation at 280 nm, emission at 340 nm). ♦, uncorrected; ▲, corrected for primary inner filter effect; ■, corrected for primary and secondary inner filter effects. The lines are the results of fitting the data to a linear model.

MANT–AXP (f_{Lc}) cannot be measured experimentally but are assumed to be similar to the f factors of free protein or MANT nucleotides. Eq. (10) also contains the contribution of emitted protein fluorescence absorbed by MANT–AXP, which results in 0.5% additional fluorescence signal per tryptophan in the protein at 440 nm (F_{sec}). Because JAK2 JH1 contains three tryptophans, this would result in an effective increase of f_L of only 1.5%. Assuming that $f_{Lc} = f_L$ and $f_{Pc} = f_P$ and that F_{sec} can be neglected below 50 μM MANT–AXP, Eq. (10) simplifies to:

$$F440_{ex\_280nm} = PL * f_{FRET} + L_{total} * f_L + P_{total} * f_P. \quad (11)$$

The factors $f_{L^{340}}$ and $f_{Lc^{340}}$ that describe the fluorescence on excitation at 340 nm were determined for free MANT–AXP and for MANT–AXP in complex with protein (0.2 μM MANT nucleotide with 0.5 μM protein). No clear blue shift due to binding was seen in the spectrum. Binding to protein resulted in 6% higher fluorescence for bound MANT–ATP and 10% higher fluorescence for bound MANT–ATP-γ-S, indicating that the quantum yield of MANT nucleotide fluorescence hardly changes on binding.

Determination of K_d for JAK2 JH1

The K_d of JAK2 JH1 for MANT–ATP can be determined either by titration of a fixed amount of MANT–ATP with protein or by titration of a fixed amount of protein with MANT–ATP. Although the result obtained from titrating a fixed concentration of MANT–ATP with protein is easier to interpret, this method requires large amounts of protein. Therefore, a fixed amount of protein was titrated with MANT–AXP. First, the average fluorescence intensity from 430 to 440 nm was corrected for the primary inner filter effect. The concentration of the protein–MANT–AXP complex was calculated with Eq. (9). The contribution for each of the species to *F440* was calculated for each concentration of MANT–AXP, and K_d and f_{FRET} were determined from fitting the data to the model described by Eq. (11).

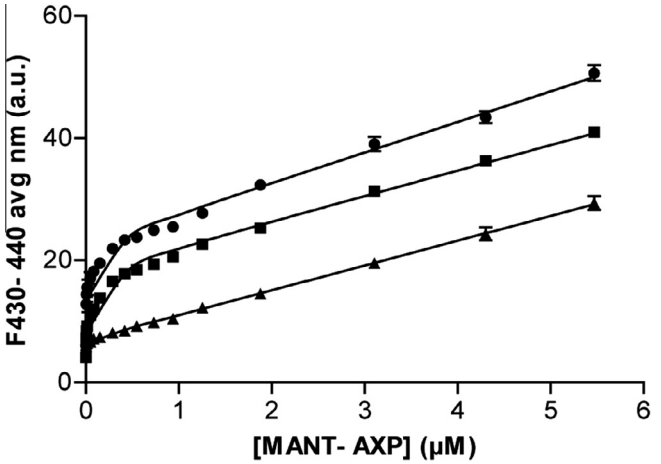

Fig.4. Titration of MANT nucleotides with JAK2 JH1. Determination of K_d of JAK2 JH1 with MANT–AXP is shown, with 0.5 μM JAK2 JH1 being titrated with increasing concentrations of MANT–AXP up to 88 μM. Average *F430* to *F440* values for MANT–ATP (●), MANT–ADP (■), and MANT–AMP (▲) are represented by points. The line is the result of fitting the data points to Eq. (11) as described in the text.

The analysis shows that JH1 has a K_d of 15 to 25 nM for MANT–ATP and a K_d of 50 to 80 nM for MANT–ADP (Fig. 4). f_{FRET} for MANT–ATP was found to be 8 * f_L and 5 * f_L for MANT–ADP. The results for MANT–AMP titrations reveal that MANT–AMP does not appreciably bind to JH1 (Fig. 4). On the addition of increasing concentrations of MANT–AMP, there was a slight increase in total fluorescence that might be due to absorption of protein fluorescence by MANT–AMP(F_{sec}).

Plots of the increase of fluorescence as a function of MANT–AMP concentrations up to 88 μM revealed that no additional binding sites are present in JH1 (data not shown). To investigate the impact of the corrections on the determination of the K_d values of JH1 for the MANT nucleotides, the K_d value for MANT–ATP was calculated using another method. If the observed MANT–ATP fluorescence at 430 to 440 nm in the presence of protein is corrected for the contribution of total MANT–ATP fluorescence and analyzed without taking ligand depletion into account, a K_d of 145 ± 30 nM is obtained (see Supplementary Fig. 4 in supplementary material), which is 10-fold higher than the 15 nM found after taking all appropriate corrections into account.

Determination of binding of nonfluorescent compounds by chasing MANT–ATP

As control for binding of MANT–ATP, the ligand was chased from the binding site by the addition of an excess of the nonfluorescent ATP analogue AMP–PNP, where an amine replaces the β-phosphate (Fig. 5). The fluorescence at each wavelength was corrected for the primary inner filter effect. Fig. 5 shows that the fluorescence of MANT–ATP increases dramatically after binding to the protein and is reduced on the addition of 10 μM AMP–PNP, indicating displacement of MANT–ATP by the inhibitor.

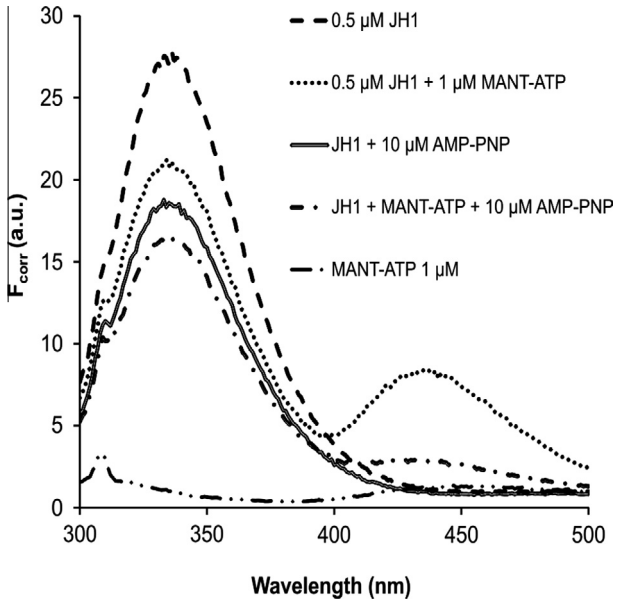

Fig.5. Chasing of MANT–ATP from JAK2 JH1 by AMP–PNP. The effect of the addition of an excess concentration of the nonfluorescent ATP competitive inhibitor on fluorescence spectra along with control incubations is shown. Here, 0.5 μM JAK2 JH1 alone, 1 μM MANT–ATP alone, JH1 with 1 μM MANT–ATP, JH1 with 1 μM MANT–ATP and 10 μM AMP–PNP, and JH1 with 10 μM AMP–PNP were excited at 280 nm. Fluorescence intensities have been corrected for the primary inner filter effect.

The binding affinity of inhibitors can be assessed using this setup. This also illustrates the advantage of using FRET over quenching of the protein fluorescence at 340 nm. FRET clearly shows the binding and release of MANT–ATP, whereas the fluorescence at 340 nm is still quenched when MANT–ATP has been chased by AMP–PNP.

Confirmation of K_d values for MANT–ATP

Although MANT–ATP is stable in solution under the conditions used in this assay, it might by hydrolyzed by kinases. Titrations of JAK2 JH1 with the nonhydrolyzable ATP analogue MANT–ATP-γ-S yielded a K_d value of 30 to 50 nM (see Supplementary Fig. 5 in supplementary material). f_{FRET} for MANT–ATP-γ-S was found to be 4.0 * f_L. The different geometry around the γ-phosphate might be responsible for the differences in K_d and f_{FRET} as compared with MANT–ATP.

Discussion

Choice of excitation wavelength

The most commonly used approach to determine the dissociation constant for ATP is by titration of a protein of interest in appropriate buffer with increasing concentrations of MANT nucleotides. In such experiments, the fluorescence excitation wavelength varies between 280 to 295 nm. The excitation wavelength can be chosen close to the absorption maximum of tryptophan to increase the FRET fluorescence, but another wavelength might be preferred depending on the spectral properties of the species in solution. If the fluorophore itself absorbs, its contribution should be minimized. For MANT nucleotides, changing the excitation wavelength from 280 to 295 nm reduces the absorbance by a factor of approximately 5 and so reduces the inner filter effect. On the other hand, this also reduces the absorbance of protein, and thus the FRET intensity, so a balance must be found between low MANT–AXP absorption and high protein absorption. The presence of more absorbing or fluorescing species in solution complicates the choice of the optimal excitation wavelength. Understanding the factors that interfere with fluorescence helps to apply appropriate correction factors.

In this study, we chose the excitation wavelength at 280 nm so as to allow a good visualization of the effects of the primary absorption and how the correction procedures affect the outcome.

Corrections for the inner filter effect

The most important pitfalls encountered in the analysis of FRET data are the contribution of inner filter effects. In the current study, we extend the corrections for the primary inner filter effect, which should be applied when the absorbance at the excitation wavelength is above 0.06, to the secondary inner filter effect. We provide an experimental method to determine the instrument correction factor and show that above an optical density of 0.3 at 340 nm the secondary inner filter effect begins to contribute. Furthermore, we quantitate the absorption of protein fluorescence by the ligand in solution and its contribution to the observed fluorescence at 440 nm as well as the contribution of the protein to fluorescence at 440 nm. Absorption of fluorescence by other species in solution that absorb at 440 nm may also contribute and can be accounted for with the analysis provided here. Understanding of these factors makes it possible to avoid conditions where they play a role or to better analyze the data in such a way that these factors are taken into account.

Determination of binding of ligands using ATP analogues is not only complicated with several factors that need to be taken into consideration but also challenging if the binding is very tight, so the precise K_d values cannot be resolved. The affinity of JAK2 JH1 for MANT–ATP is high, with K_d values ranging from 15 to 25 nM. The high affinity was confirmed using the nonhydrolyzable ATP analogue MANT–ATP-γ-S. The data show that replacement of oxygen by a larger sulfur atom reduces the affinity slightly. A comparable high affinity for ATP has been found for 6-phosphofructo-2-kinase [6] and for members of the CDK family. The affinities ranged from 50 to 90 nM for CDK2 + cyclin A, CDK7 + cyclin H, and CDC2 + cyclin A as determined from direct titration using the enhancement of the MANT–ATP fluorescence [7]. The affinity of JAK2 JH1 for MANT–ADP is tighter than for the CDK proteins that have a K_d for ADP of 1.0 to 3.1 μM.

The difference in FRET efficiency between MANT–ATP and MANT–ADP could indicate a different orientation of the two nucleotides provided that the orientation factor κ^2 is identical for both species. Although κ^2 may range from 0 to 4, its most likely value is 2/3 for most proteins [30]. MANT–AMP shows no FRET at all but quenches the protein fluorescence in the same way as the other MANT nucleotides. This illustrates the advantage of FRET by monitoring acceptor fluorescence compared with fluorescence quenching experiments.

Because K_d values for dissociation of substrates or cofactors from enzymes are often in the same range as K_m values, the K_d value for MANT–ATP for JAK2 JH1 was much lower than expected based on the previously published K_m value (10–20 μM) [15,18]. Ni and coworkers [4] and Cheng and Koland [21] also reported much lower K_d values than the reported K_m values for protein kinase A (PKA) and epidermal growth factor receptor (EGFR), respectively. Part of this discrepancy can be explained by the fact that for many proteins the affinity for ATP was reported to be lower by 3 orders of magnitude than for MANT–ATP [6]. In-depth analysis of the fluorescence data provided no evidence for the presence of a second binding site with affinities in this concentration range.

Screening of the literature, where FRET fluorescence between a protein and MANT–ATP was used to determine affinities, revealed that in most cases limited or no corrections were applied—even under conditions where their use is advised based on the analysis

presented here. As an illustration, two cases are discussed here. In a recent article, Rivas-Pardo and coworkers [31] used fluorescence spectroscopy to investigate the metal ion requirements of phosphofructokinase-2. The authors titrated a solution of the enzyme with MANT–ATP (0–250 μM). The excitation wavelength was adjusted to minimize the inner filter effects, but at the highest concentration the absorbance of MANT–ATP at 295 nm was approximately 0.1. Correction for the inner filter effect becomes necessary when the absorbance is above 0.06. The quenching of protein fluorescence at 340 nm was employed for K_d determination. However, at this wavelength correction for the secondary inner filter effect is necessary because here absorbance of MANT–ATP increases to a value of 1.2. Absorption at 340 nm leads to quenching of the protein fluorescence at this wavelength (process 4 in Fig. 1) and cannot be ignored. Omission of the corrections for primary and secondary inner filter effects leads to an inaccurate K_d determination and in the worst case leads to incorrect conclusions. Although in Ref. [31] the discussed points might not invalidate the conclusions of the study, the application of corrections would make the analysis more accurate.

In another example of using MANT–ATP for K_d determination, Ni and coworkers titrated PKA with MANT–ATP up to a concentration of 140 μM [4]. They reported a linear relation between MANT–ATP concentration and fluorescence over the concentration range tested (excitation at 290 nm), whereas our observations suggest that at the higher concentrations the inner filter effect causes deviations from linearity, necessitating corrections for the primary inner filter effect. The values obtained from this experiment with MANT–ATP were used to correct titrations of PKA with increasing MANT–ATP concentrations for the contribution of free MANT–ATP. The resulting values were used for the calculation of K_d. However, because the absorption of MANT–ATP at high concentrations at 340 nm is above 0.6, a significant fraction of the tryptophan fluorescence is absorbed by MANT–ATP, resulting in additional fluorescence intensity at 440 nm.

For most studies that use MANT nucleotide titrations to determine the affinity of proteins for ATP or ADP, critical assessments can be made. Only few authors take precautions to avoid the need for use of correction factors. The current analysis shows that understanding of the contributing factors provides a general correction method for commonly encountered pitfalls and improves the quality of the data. Using the appropriate corrections, the use of FRET methods can be extended to much higher concentrations of fluorophore and can accommodate the use of competing binders, including fluorescent compounds.

Conclusions

MANT nucleotides mimic the binding characteristics of ATP in ligand–protein interaction studies and are potential fluorescence acceptors in FRET experiments. The use of MANT nucleotides has been extended to study the binding properties of nucleotides to a variety of mutant proteins. We employed FRET spectroscopy to identify binding affinities for JH1 of JAK2 for MANT nucleotides and the lack of binding for MANT–AMP. We presented a detailed procedure to evaluate the correction parameters, including those to correct for primary and secondary inner filter effects that need to be taken into account for determination of correct nucleotide binding parameters, when the absorbance of the solution surpasses certain values. These corrections allow extending titrations to higher ligand concentrations.

Acknowledgments

The authors thank Paula Kosonen and Merja Lehtinen for excellent technical assistance and thank Niek de Klerk for checking details in the data analysis. This study was supported by the Sigrid Juselius Foundation, the Medical Research Council of the Academy of Finland, the EU Research Training Network ReceptEur, the Finnish Cancer Foundation, the Medical Research Fund of Tampere University Hospital, and the Tampere Tuberculosis Foundation.

Appendix A. Supplementary material

Supplementary material associated with this article can be found, in the online version, at http://dx.doi.org/10.1016/j.ab.2013.07.020.

References

[1] D.M. Jameson, J.F. Eccleston, Fluorescent nucleotide analogs: synthesis and applications, Methods Enzymol. 278 (1997) 363–390.
[2] C.R. Bagshaw, ATP analogues at a glance, J. Cell. Sci. 114 (2001) 459–460.
[3] T. Hiratsuka, Fluorescent and colored trinitrophenylated analogs of ATP and GTP, Eur. J. Biochem. 270 (2003) 3479–3485.
[4] D.Q. Ni, J. Shaffer, J.A. Adams, Insights into nucleotide binding in protein kinase A using fluorescent adenosine derivatives, Protein Sci. 9 (2000) 1818–1827.
[5] K. Tanaka, T. Kimura, S. Maruta, Synthesis of a novel fluorescent non-nucleotide ATP analogue and its interaction with myosin ATPase, J. Biochem. 149 (2011) 395–403.
[6] D. Vertommen, L. Bertrand, B. Sontag, A. Di Pietro, M.P. Louckx, H. Vidal, L. Hue, M.H. Rider, The ATP-binding site in the 2-kinase domain of liver 6-phosphofructo-2-kinase/fructose-2,6-bisphosphatase, J. Biol. Chem. 271 (1996) 17875–17880.
[7] F. Heitz, M.C. Morris, D. Fesquet, J.C. Cavadore, M. Dorée, G. Divita, Interactions of cyclins with cyclin-dependent kinases: a common interactive mechanism, Biochemistry 36 (1997) 4995–5003.
[8] M. Erdorf, R. Seifert, Pharmacological characterization of adenylyl cyclase isoforms in rabbit kidney membranes, Naunyn Schmiedebergs Arch. Pharmacol. 383 (2011) 357–372.
[9] B.A. Witthuhn, F.W. Quelle, O. Silvennoinen, T. Yi, B. Tang, O. Miura, J.N. Ihle, JAK2 associates with the erythropoietin receptor and is tyrosine phosphorylated and activated following stimulation with erythropoietin, Cell 74 (1993) 227–236.
[10] O. Silvennoinen, B.A. Witthuhn, F.W. Quelle, J.L. Cleveland, T. Yi, J.N. Ihle, Structure of the murine Jak2 protein–tyrosine kinase and its role in interleukin 3 signal transduction, Proc. Natl. Acad. Sci. U.S.A 90 (1993) 8429–8433.
[11] C. Haan, S. Kreis, C. Margue, I. Behrmann, Jaks and cytokine receptors—an intimate relationship, Biochem. Pharmacol. 72 (2006) 1538–1546.
[12] J. Boudeau, D. Miranda-Saavedra, G.J. Barton, D.R. Alessi, Emerging roles of pseudokinases, Trends Cell Biol. 16 (2006) 443–452.
[13] D. Ungureanu, J. Wu, T. Pekkala, Y. Niranjan, C. Young, O.N. Jensen, C.F. Xu, T.A. Neubert, R.C. Skoda, S.R. Hubbard, The pseudokinase domain of JAK2 is a dual-specificity protein kinase that negatively regulates cytokine signaling, Nat. Struct. Mol. Biol. 18 (2011) 971–976.
[14] P. Saharinen, K. Takaluoma, O. Silvennoinen, Regulation of the Jak2 tyrosine kinase by its pseudokinase domain, Sci. Signal. 20 (2000) 3387–3395.
[15] A. Sanz, D. Ungureanu, T. Pekkala, R. Ruijtenbeek, I.P. Touw, R. Hilhorst, O. Silvennoinen, Analysis of Jak2 catalytic function by peptide microarrays: the role of the JH2 domain and V617F mutation, PLoS One 6 (2011) e18522.
[16] P. Saharinen, M. Vihinen, O. Silvennoinen, Autoinhibition of Jak2 tyrosine kinase is dependent on specific regions in its pseudokinase domain, Mol. Biol. Cell 14 (2003) 1448–1459.
[17] J.H. Kurzer, L.S. Argetsinger, Y.J. Zhou, J.L.K. Kouadio, J.J. O'Shea, C. Carter-Su, Tyrosine 813 is a site of JAK2 autophosphorylation critical for activation of JAK2 by SH2-Bβ, Mol. Cell. Biol. 24 (2004) 4557–4570.
[18] T. Hall, T.L. Emmons, J.E. Chrencik, J.A. Gormley, R.A. Weinberg, J.W. Leone, J.L. Hirsch, M.J. Saabye, J.F. Schindler, J.E. Day, Expression, purification, characterization, and crystallization of non- and phosphorylated states of JAK2 and JAK3 kinase domain, Protein Expr. Purif. 69 (2010) 54–63.
[19] G. Divita, R. Goody, D. Gautheron, A. Di Pietro, Structural mapping of catalytic site with respect to α-subunit and noncatalytic site in yeast mitochondrial F1-ATPase using fluorescence resonance energy transfer, J. Biol. Chem. 268 (1993) 13178–13186.
[20] E. Zeqiraj, B.M. Filippi, S. Goldie, I. Navratilova, J. Boudeau, M. Deak, D.R. Alessi, D.M.F. van Aalten, ATP and MO25α regulate the conformational state of the STRADα pseudokinase and activation of the LKB1 tumour suppressor, PLoS Biol. 7 (2009) e1000126.
[21] K. Cheng, J.G. Koland, Nucleotide binding by the epidermal growth factor receptor protein–tyrosine kinase: Trinitrophenyl-ATP as a spectroscopic probe, J. Biol. Chem. 271 (1996) 311–318.
[22] A.Y. Jan, E.F. Johnson, A.J. Diamonti, K.L. Carraway III, K.S. Anderson, Insights into the HER-2 receptor tyrosine kinase mechanism and substrate specificity using a transient kinetic analysis, Biochemistry 39 (2000) 9786–9803.
[23] F. Shi, S.E. Telesco, Y. Liu, R. Radhakrishnan, M.A. Lemmon, ErbB3/HER3 intracellular domain is competent to bind ATP and catalyze autophosphorylation, Proc. Natl. Acad. Sci. U.S.A. 107 (2010) 7692–7697.

[24] M. Kubista, R. Sjöback, S. Eriksson, B. Albinsson, Experimental correction for the inner-filter effect in fluorescence spectra, Analyst 119 (1994) 417–419.
[25] M. van de Weert, Fluorescence quenching to study protein–ligand binding: common errors, J. Fluoresc. 20 (2010) 625–629.
[26] M.L. Mertens, J.H.R. Kägi, A graphical correction procedure for inner filter effect in fluorescence quenching titrations, Anal. Biochem. 96 (1979) 448–455.
[27] B. Birdsall, R.W. King, M.R. Wheeler, C.A. Lewis Jr., S.R. Goode, R.B. Dunlap, G.C.K. Roberts, Correction for light absorption in fluorescence studies of protein–ligand interactions, Anal. Biochem. 132 (1983) 353–361.
[28] N.K. Subbarao, R.C. MacDonald, Experimental method to correct fluorescence intensities for the inner filter effect, Analyst 118 (1993) 913–916.
[29] Y. Liu, W. Kati, C.M. Chen, R. Tripathi, A. Molla, W. Kohlbrenner, Use of a fluorescence plate reader for measuring kinetic parameters with inner filter effect correction, Anal. Biochem. 267 (1999) 331–335.
[30] B. Van der Meer, Kappa-squared: from nuisance to new sense, Rev. Mol. Biotechnol. 82 (2002) 181–196.
[31] J.A. Rivas-Pardo, A. Caniuguir, C.A.M. Wilson, J. Babul, V. Guixé, Divalent metal cation requirements of phosphofructokinase-2 from *E. coli:* evidence for a high affinity binding site for Mn^{2+}, Arch. Biochem. Biophys. 505 (2011) 60–66.

Elsevier Editorial System(tm) for BBA - Proteins and Proteomics
Manuscript Draft

Manuscript Number: BBAPRO-14-117

Title: The JH2 domain and SH2-JH2 linker regulate JAK2 activity: a detailed kinetic analysis of wild type and V617F mutant kinase domains

Article Type: Regular Paper

Keywords: JAK2 recombinant protein, kinetic mechanism, Km, Vmax, multiplex kinetic assay, peptide microarray

Corresponding Author: Dr. Riet Hilhorst, Ph.D.

Corresponding Author's Institution: PamGene International BV

First Author: Arturo Sanz-Sanz

Order of Authors: Arturo Sanz-Sanz; Yashavanthi Niranjan; Henrik Hammarén; Daniela Ungureanu; Rob Ruijtenbeek; Ivo P Touw; Olli Silvennoinen; Riet Hilhorst, Ph.D.

Abstract: JAK2 tyrosine kinase regulates many cellular functions. Its activity is controlled by the pseudokinase (JH2) domain by still poorly understood mechanisms. The V617F mutation in the pseudokinase domain activates JAK2 and causes myeloproliferative neoplasms. We conducted a detailed kinetic analysis of recombinant JAK2 tyrosine kinase domain (JH1) and wild-type and V617F tandem kinase (JH1JH2) domains using peptide microarrays to define the functions of the kinase domains. The results show that i) JAK2 follows a random Bi-Bi reaction mechanism ii) JH2 domain restrains the activity of the JH1 domain by reducing the affinity for ATP and ATP competitive inhibitors iii) V617F decreases affinity for ATP but increases catalytic activity compared to wild-type iv) the SH2-JH2 linker region participates in controlling activity by reducing the affinity for ATP.

Suggested Reviewers: Maarten R Egmond
Membrane Biochemistry and Biophysics, Utrecht University
m.r.egmond@uu.nl

Peter P Sayeski
Dept of Physiology and Functional genomics, University of Florida
psayeski@ufl.edu

Antonie J Visser
Emeritus professor , Biochemistry, Wageningen University
antoniejvisser@gmail.com

Jason Rawlings
jason.rawlings@furman.edu

The JH2 domain and SH2-JH2 linker regulate JAK2 activity: a detailed kinetic analysis of wild type and V617F mutant kinase domains

Arturo Sanz Sanz[1#], Yashavanthi Niranjan[2#], Henrik Hammarén[2], Daniela Ungureanu[2], Rob Ruijtenbeek[3], Ivo .P. Touw[1], Olli Silvennoinen[2,4*], Riet Hilhorst[3*]

[1]Department of Hematology, Erasmus MC, Rotterdam, Netherlands, [2]Institute of Biomedical Technology and School of Medicine, University of Tampere, 33014, Tampere, Finland, [3]PamGene International BV, 5200 BJ 's-Hertogenbosch, The Netherlands, [4]Department of Internal Medicine, Tampere University Hospital, 33520 Tampere, Finland

# Contributed equally to this work

*Corresponding address to: rhilhorst@pamgene.com or olli.silvennoinen@uta.fi

Riet Hilhorst, PamGene International BV, 5200 BJ 's-Hertogenbosch, The Netherlands. Telephone: +31 (0)73 615 8076, Fax: +31 (0)73 615 8081.

Olli Silvennoinen, Institute of Biomedical Technology, Tampere 33014, FIN, Telephone: +358 50 359 5740, Fax: + 358 33551 7332

Running title: Role of JH2 and JH2-SH2 linker in JAK2 regulation

Abstract

JAK2 tyrosine kinase regulates many cellular functions. Its activity is controlled by the pseudokinase (JH2) domain by still poorly understood mechanisms. The V617F mutation in the pseudokinase domain activates JAK2 and causes myeloproliferative neoplasms. We conducted a detailed kinetic analysis of recombinant JAK2 tyrosine kinase domain (JH1) and wild-type and V617F tandem kinase (JH1JH2) domains using peptide microarrays to define the functions of the kinase domains. The results show that i) JAK2 follows a random Bi-Bi reaction mechanism ii) JH2 domain restrains the activity of the JH1 domain by reducing the affinity for ATP and ATP competitive inhibitors iii) V617F decreases affinity for ATP but increases catalytic activity compared to wild-type iv) the SH2-JH2 linker region participates in controlling activity by reducing the affinity for ATP.

Keywords: JAK2 recombinant protein, kinetic mechanism, K_m, V_{max}, multiplex kinetic assay, peptide microarray

Highlights:

- Kinetic analysis of recombinant JAK2 proteins revealed a random Bi-Bi mechanism.
- The JH2 domain reduced V_{max} 5–20 fold in JH1JH2WT and JH1JH2V617F.
- The JH2 domain increased K_a (ATP) 4–10 fold for the 10 substrate peptides tested.
- V617F mutation increased V_{max} possibly by changing the activation loop conformation.
- The SH2-JH2 linker increased inhibition by JH2 and reduced the affinity for ATP.

1. **Introduction**

JAK2 belongs to the Janus tyrosine kinase family and functions as a central mediator of cytokine signaling. Cytokine stimulation induces hetero/homo dimerization of hematopoietic cytokine receptors and facilitates the activation of JAK2 by auto and/or trans-phosphorylation. JAK2 contains at the N-terminus a FERM (4.1/ezrin/radixin/moesin) domain which together with an SH2 (Src homology 2)-like domain encompasses JAK homology (JH3 - JH7) regions that are followed by the pseudokinase domain (JH2) and the tyrosine kinase domain (JH1) at the C terminus of the protein.

The JH2 domain negatively regulates the JH1 activation and JAK2-mediated signaling (1, 2). The JH2 domain was initially considered to be devoid of catalytic activity but was recently found to bind ATP and be able to phosphorylate two negative regulatory sites in JAK2 (3). Mutations in the JH2 domain have been shown to lead to hyperactive JAK2 (4-7), and constitutive activation of JAK2 is causing myeloproliferative diseases (8). Despite the wide interest towards JAK2 and mechanisms of its regulation, the precise function of the JH2 domain is still only partially understood.

In this study we have extended the biochemical and kinetic characterization of JAK2 kinase domains by analysing JH1, JH1JH2WT_513, JH1JH2V617F_513 and JH1JH2V617F_536 (see M&M) using peptide microarrays. The presence of JH2 domain decreased V_{max} and increased K_m for ATP (referred as K_a) which resulted in reduced affinity for ATP competitive inhibitors in the JH1JH2 constructs. Comparison of kinetic parameters between the constructs showed that the SH2-JH2 linker regulates JAK2 kinase activity by reducing the affinity for ATP.

2. **Material and Methods**

2.1 Plasmid constructs, cell lines and reagents - JAK2 (EC-2.7.10.2) C-terminal thrombin cleavable 6XHis tag proteins JH1JH2WT_513–1132 (wild type), JH1JH2V617F_536–1132, JH1JH2V617F_513–1132 and JH1_836–1132 were expressed and purified as described previously (9). PamChip® tyrosine kinase microarrays and BioNavigator software for analysis of peptide microarrays were from PamGene International BV (‘s-Hertogenbosch, The Netherlands). 10x PK kinase buffer and 100x BSA were from New England Biolabs, BSA Fraction V from Calbiochem, ATP, ADP-β-S from Sigma-Aldrich and fluorescein-labeled PY20 anti-phosphotyrosine antibody from Exalpha Biologicals. Prism 6 and SigmaPlot was obtained from GraphPad and Systat respectively.

2.2 PamChip® peptide microarrays - Custom made PamChip® Tyrosine kinase microarrays containing 21 different JAK2 substrate peptides (13–15 amino-acids long, derived from putative tyrosine-phosphorylation sites in human proteins), each at 300, 400, 600, 750, 1000 and 2000 µM spot concentration were used. Peptides were named based on UniProt knowledgebase protein identities and amino acid position numbers (www.expasy.org/sprot). A pre-tyrosine-phosphorylated peptide was used as a control for antibody binding. Spotted peptide concentrations were checked by Sypro Ruby staining. Instrumentation, array properties and quality control of arrays have been described elsewhere (9, 10). Details on peptide names and sequences are shown in Table S2.

2.3 Kinetic studies - Incubations and kinetic readings of the peptide microarrays were performed at 30ºC on a PamStation 96 instrument (PamGene International BV, 's-Hertogenbosch, The Netherlands) that allows simultaneous incubation of 96 arrays. Incubations were performed as described in Sanz *et al* (9) and in Fig.S1 with 1.13 pmoles per reaction for JH1JH2WT_513, 0.4 pmoles per reaction for JH1JH2V617F_513 and JH1JH2V617F_536 and 0.04 pmoles per reaction for JH1 in a final reaction volume of 25 µl. For JAK2JH1, the ATP concentration varied from 0–100 µM, for the other constructs from 0–400 µM while the concentration of ADP-β-S ranged from 0–1 mM. Assays without inhibitors were performed in duplicate in 2–5 independent experiments.

2.4 Signal quantification and data analysis - Signal intensities on each peptide spot were quantitated for all time series of images with BioNavigator software. The initial reaction rate (v) for each spot was determined according to *Sanz et al* (9) at the fifth cycle via $v = y_{max} * k * e^{-kc}$. Only v values that had $R^2 > 0.7$ in the fit and where y_{max} was less than 500000 were used for subsequent data interpretation. To eliminate overall differences in signal intensity between the PamChip® 96 array plates, all v-values were expressed with respect to the mean v-value at 100 µM ATP of 21 peptides present at 1000 µM. Initial velocities (v) were expressed in % relative activity per pmol protein.

2.5 Kinetic analysis - Initial reaction rates as function of ATP or peptide concentration were fitted to the equations for ordered Bi-Bi, random Bi-Bi or Ping Pong mechanisms in the Enzyme Kinetics Module of Sigma Plot. It should be noted however, that it was possible to obtain reliable values for 10 peptides out of 21 in the peptide array where the peptide concentration surpassed the K_b values. Data presented are the average of a number of experiments (3 for JH1, 4 for JH1JH2WT_513, 5 for JH1JH2V617F_513 and 2 for JH1JH2V617F_536) performed on different days. Each of these experiments comprised 2 technical replicates of the conditions without inhibitor.

For inhibitor studies, data at variable ATP or peptide concentrations and inhibitor concentrations were fitted to the equations for competitive and non-competitive inhibition in SigmaPlot.

3. Results

Histidine-tagged recombinant JAK2 JH1, JH1JH2WT and JH1JH2V617F proteins comprising amino acids (aa) 836–1132 and 513–1132 respectively were produced in Sf9 cells (9). Attempts to produce the aa 536–1132 construct of JH1JH2WT failed but JH1JH2V617F comprising aa 536–1132 (JH1JH2V617F_536) could be stably expressed and purified.

Experiments were performed at protein concentrations where the kinase activity was linear in relation to protein concentration. The reactions took place under initial rate conditions, i.e., 10% or less of the peptide was phosphorylated in the course of the reaction. Peptide phosphorylation was monitored in real time by detecting the binding of fluorescent anti-phosphotyrosine antibody. The rate limiting step in all reaction conditions was the phosphorylation of the peptide. Detection of phosphorylation by fluorescent antibody binding results in relative reaction rates that depend on e.g. lamp intensity, degree of labeling of the antibody and affinity of the antibody for the phosphopeptide. Therefore, the values can not be quantitated in moles of product formed but are presented as % relative activity per pmol of kinase (see Materials and Methods).

3.1 JAK2 follows a random Bi-Bi reaction mechanism

Initial reaction rates for JH1 catalyzed peptide phosphorylation as a function of ATP concentration were determined on PamChip® 96 array plates that enable simultaneous real time recording of phosphorylation kinetics on 96 arrays, each containing 21 different peptides at 6 concentrations each (Fig. S1). EGFR_1190_1202 peptide showed the highest catalytic activity and data for this peptide are shown. Lineweaver-Burk plots at either varying peptide concentrations or varying ATP concentrations (Fig. 1A and 1B) confirm a sequential reaction mechanism, where both substrates bind before the products are released and demonstrate that binding of ATP increases the interaction with peptide (11).

The dead end inhibitor ADP-β-S (one of the oxygen atoms of the β phosphate is replaced by a sulphur atom) was used to discriminate between the random Bi-Bi and ordered Bi-Bi reaction mechanisms. Such inhibitors, usually structural analogues of a substrate, bind to an active site without conversion to product. Plots of 1/v vs 1/[S] show a non-competitive or competitive inhibition pattern for ADP-β-S with respect to peptide and ATP respectively (Fig. 1C and 1D) which corroborates that JH1 follows a random sequential mechanism.

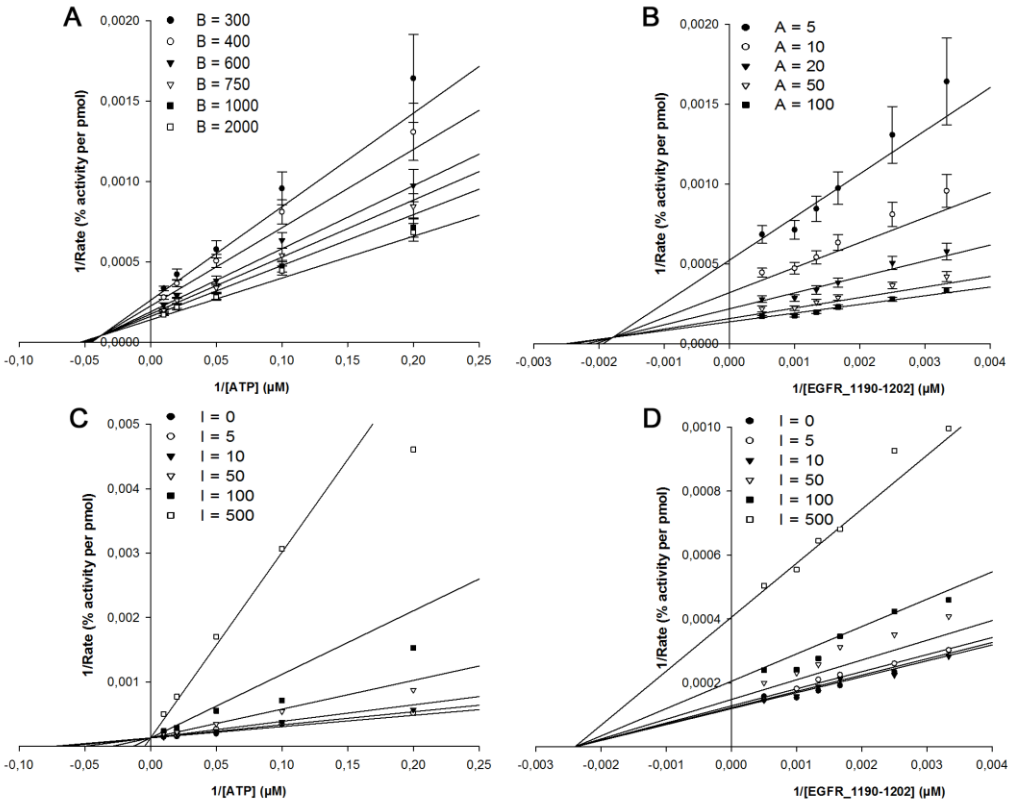

Figure 1: Two substrate steady state kinetics and inhibition by ADP-β-S for JH1.
Double reciprocal plots of initial reaction rates of JH1 as function of [ATP] with varying [EGFR_1190–1202] concentration (A) or as a function of [EGFR_1190–1202] with different ATP concentrations (B); ATP or peptide concentrations are indicated by 'A' or 'B' in the legend. Double reciprocal plots with variation of ATP at [EGFR_1190–1202] = 2000 µM (C) or variable [EGFR_1190–1202] concentrations at [ATP] = 100 µM (D). The [ADP-β-S] concentrations are indicated by 'I' as µM.

The effect of the JH2 domain on the kinetic parameters was investigated on PamChip® peptide microarrays using JH1JH2WT_513, JH1JH2V617F_513 and JH1JH2V617F_536 proteins with increasing concentrations of ATP and peptide substrates. Under the experimental conditions, the kinetic activity of the JH2 domain alone was too low to contribute to measured kinetic rates. Lineweaver-Burk plots (Fig. 2, 3 and S2 respectively) indicate that the reactions proceed via the formation of a ternary complex. Studies with the inhibitor ADP-β-S revealed that the JAK2 constructs all follow a random Bi-Bi mechanism like JH1 (Fig. 2C / 2D, 3 and S2C / S2D).

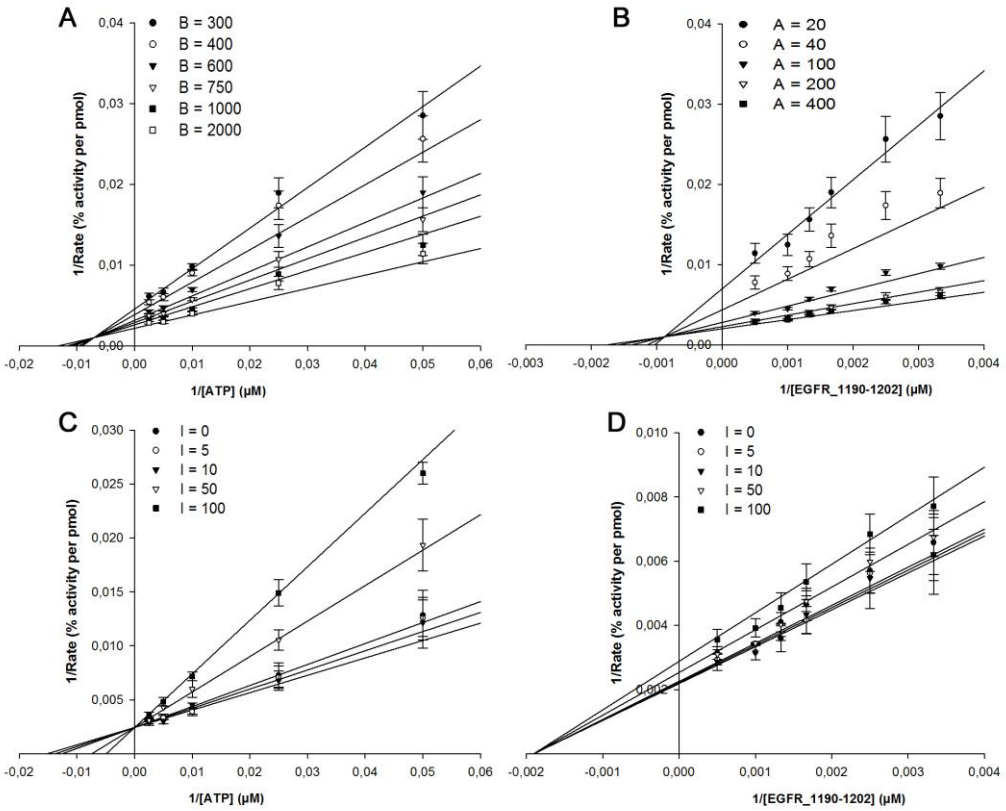

Figure 2: Two substrate steady state kinetics and inhibition by ADP-β-S for JH1JH2WT_513
Double reciprocal plots for initial reaction rates of JH1JH2WT_513 as function of [ATP] with varying [EGFR_1190–1202] concentration (A) or as function of [EGFR_1190–1202] with different ATP concentrations (B); ATP or peptide concentrations are indicated by 'A' or 'B' in the legend. Plots with ADP-β-S against ATP at fixed [EGFR_1190–1202] = 2000 μM (C) or against [EGFR_1190–1202] and fixed [ATP] = 100 μM, with [ADP-β-S] concentrations marked as 'I' in the inset of the figure as μM.

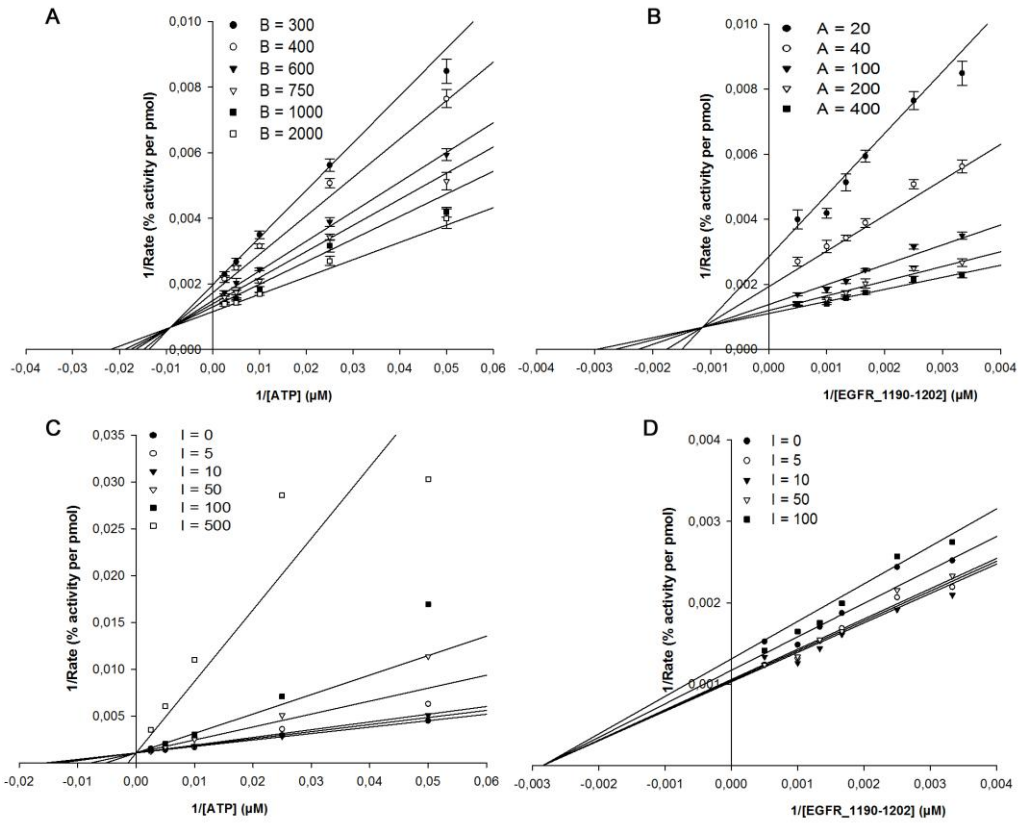

Figure 3: Two substrate steady state kinetics and inhibition by ADP-β-S inhibitor for JH1JH2V617F_536

Double reciprocal plots for initial reaction rates of JH1JH2V617F_536 as function of [ATP] with varying [EGFR_1190–1202] concentration (A) or as function of [EGFR_1190–1202] with difference ATP concentrations (B); ATP or peptide concentrations are indicated by 'A' or 'B' in the legend. Plots with ADP-β-S against ATP at fixed [EGFR_1190–1202] = 2000 µM (C) or against [EGFR_1190–1202] and fixed [ATP] = 100 µM, with [ADP-β-S] concentrations marked as 'I' in the inset of the figure as µM.

3.2 Determination of kinetic parameters

V_{max} and K_m values at infinite concentrations of both substrates for JH1, JH1JH2WT and both mutants were obtained from non-linear fits to the equation for a random Bi-Bi mechanism for 10 peptides (Table 1 and S1). For JH1JH2WT_513 the presence of the JH2 domain resulted in a 10–20 fold reduction in V_{max} compared to JH1. The V617F mutation in JH1JH2V617F_513 alleviates the inhibitory effect and shows a 4 fold reduction in V_{max}. The JH1JH2V617F (536–1132) protein lacking the SH2-JH2 linker peptide shows an 8 fold reduction in V_{max}. The K_a for the JH2 containing proteins increased 2–6 fold as compared to JH1 in the order JH1JH2V617F_536, JH1JH2WT_513 and JH1JH2V617F_513. K_m for peptide (K_b) is in the same range in JH1JH2WT_513 and JH1JH2V617F_536, but increases substantially for JAK2JH1JH2V617F_513

as compared to JH1. The data suggest that in addition to the JH2 domain, the linker domain also participates in regulation of JAK2 activity.

Table 1: Kinetic parameters extrapolated to infinite concentration of either substrate for four JAK2 constructs and three peptide substrates.
K_a and K_b are in µM, V_{max} in % relative activity per pmol protein

	JAK2JH1				JAK2JH1JH2WT_513			
Peptide Identity	**K_a ± SD**	**K_b ± SD**	**V_{max} ± SD**	**Alpha value**	**K_a ± SD**	**K_b ± SD**	**V_{max} ± SD**	**Alpha value**
EGFR_1190-1202	17 ± 3	365 ± 75	8489 ± 566	1.5 ± 0.8	60 ± 18	474 ± 109	567 ± 46	2.3 ± 1,4
JAK1_1015-1027	13 ± 4	686 ± 130	6977 ± 559	2.2 ± 1.2	35 ± 18	1541 ± 262	659 ± 63	3.16 ± 2.1
JAK2_563-577	24 ± 9	1276 ± 323	3988 ± 552	1.6 ± 0.8	78 ± 20	1200 ± 195	200 ± 20	0.81 ± 0.3
	JAK2JH1JH2V617F_513				JAK2JH1JH2V617F_536			
Peptide Identity	**K_a ± SD**	**K_b ± SD**	**V_{max} ± SD**	**Alpha value**	**K_a ± SD**	**K_b ± SD**	**V_{max} ± SD**	**Alpha value**
EGFR_1190-1202	101 ± 33	752 ± 194	1930 ± 227	1.11 ± 0.7	36 ± 5	287 ± 35	988 ± 33	3 ± 1
JAK1_1015-1027	79 ± 42	2413 ± 594	2463 ± 401	1.3 ± 1	14 ± 6	681 ± 70	1040 ± 43	8.6 ± 4.6
JAK2_563-577	103 ± 55	2367 ± 718	997 ± 202	0.7 ± 0.6	62 ± 13	966 ± 125	597 ± 38	1.4 ± 0.5

3.3 Determination of inhibition constants

K_i values for ADP-β-S were determined for the peptides JAK1_1015–1027, JAK2_563–577 and EGFR_1190–1202 at either variable ATP concentration and 2000 µM of peptide or varying peptide concentration at 100 µM ATP for JH1 and 400 µM ATP for the other constructs (Table 2). The higher ATP concentration was used to reflect the increased K_a in JH2 containing constructs. Values for K_i were obtained from fitting the reaction rates to equations for competitive or non-competitive inhibition. The presence of the JH2 domain resulted in significantly higher K_i values compared to the JH1 kinase domain. K_i for JH1JH2WT_513 was 8 times higher than for JH1. JH1JH2V617F_513 showed 4 fold increased K_i compared to JH1 and deletion of the SH2-JH2 linker in JH1JH2V617F_536 increased the K_i values to 10 fold higher than for JH1. These data confirm that both JH2 and the SH2-JH2 linker affect the affinity for ATP and the ATP competitive inhibitor ADP-β-S and that the SH2-JH2 linker harbors an inhibitory function in JAK2.

Table 2: Inhibition constants for ADP-β-S for the four JAK2 constructs and three peptide substrates.

	var ATP ([peptide] = 2000 µM)				var peptide ([ATP] = 100 (JH1) or 400 µM (JH1JH2)			
	JAK2JH1	**JAK2JH1JH2 WT_513**	**JAK2JH1JH2 V617F_513**	**JAK2JH1JH2 V617F_536**	**JAK2JH1**	**JAK2JH1JH2 WT_513**	**JAK2JH1JH2 V617F_513**	**JAK2JH1JH2 V617F_536**
Peptide name	K_i (µM)				K_i (µM)			
EGFR_1190-1202	6.5 ± 1	48 ± 6	21 ± 4	49 ± 8	42 ± 4	316 ± 34	179 ± 28	365 ± 56
JAK1_1015-1027	6 ± 1	49 ± 6	26 ± 4	47 ± 5	39 ± 5	563 ± 122	213 ± 22	352 ± 39
JAK2_563-577	6 ± 1	47 ± 10	24 ± 4	46 ± 8	31 ± 3	295 ± 38	186 ± 18	257 ± 42

4. **Discussion**

Reaction mechanism followed by JAK2 kinase domains

In this study we performed full kinetic analyses of recombinant JAK2 kinases. Variation in both ATP and peptide concentrations and of the peptide substrates showed that JAK2JH1 and JAK2JH1JH2 constructs follow a random Bi-Bi mechanism, like the majority of kinases (12-17). These results are in line with the findings from Erdmann *et al*. for JH1 and full length JAK2 (18).

Kinetic parameters for JAK2 JH1

In our kinetic studies, K_a and K_b values for all constructs were determined by extrapolation to infinite concentration of the other substrate. The K_a values of 12–24 μM for JH1 are similar to those reported previously (19, 20), but higher than the 0.68 μM that was determined at a low ATP range (0–10 μM) (18) and lower than the values at fixed peptide concentrations (11).

K_b values range from 392 μM for RON peptide to about 1276 μM for JAK2 peptide. The K_b for only STAT5A peptide has been previously reported. The K_b for STAT5A extrapolated to infinite ATP concentration (833 ± 160 μM) is higher than the K_b^{app} of 239 ± 36 μM at 100 μM ATP (10) and the K_b of 113 ± 7 μM, at 0–10 μM ATP (18). Also the K_b^{app} for the JAK2 activation loop peptide (205 ± 34 μM) is lower than our value (686 ± 130 μM) for the JAK1 activation loop peptide that shares sequence elements (21). In conclusion, the kinetic parameters determined with peptide microarrays are very similar to those obtained with other methods.

Regulation of JAK2 activity and role of V617F mutation and SH2-JH2 linker region

The JH2 domain, the V617F mutation and the SH2-JH2 linker were all found to affect the kinetic parameters. The presence of the JH2 domain lowered the catalytic activity and the affinity for ATP. The V617F mutation resulted in a lower affinity for ATP but a higher V_{max}. The increased V_{max} may involve a conformational change of the activation loop to the active conformation. Molecular dynamic simulations have suggested that in JAK2WT full activation of the kinase domain is prevented by interaction of F595 and S591 in JH2 with the activation loop of JH1 resulting in an auto-inhibited conformation (22, 23). The V617F mutation might release the inhibitory interaction formed via a π-π stacking interaction between phenylalanines 617 and 595 (24) that allow a conformational change of the activation loop (23, 25-27).

Differences in kinetics between the V617F_513 and V617F_ 536 protein suggest an important role for the 513–536 SH2-JH2 linker. In the presence of the linker, K_a is increased. Removal of the linker allowed binding of ATP with the same affinity as JH1 but reduced the V_{max}. This suggests that binding and catalysis are distinct processes that involve different parts of JH1. Molecular dynamics studies suggest that the π-π stacking interaction (that leads to an active conformation of

the activation loop) was lost in the absence of the linker (27). Apart from regulating the affinity for ATP and the conformation of the activation loop, the linker is essential for interaction with the EPO receptor (28). The poor solubility of the JH1JH2WT_536 construct further supports an important role for the linker region. Activating mutations in this linker have been reported in MPN patients (28, 29). The crystal structure of JAK1 JH2 domain includes the SH2 linker and provides structural insights into this regulation. The F575 in the linker region interacts with C helix F636 and with V658F which is the corresponding site for V617F in the JH2 β4-β5 loop (30). Recently it was also shown that FERM domain possess a regulatory role in hyperactivation of JAK2V617F (21). Thus, the regulation of JAK2 activity involves several regions of the JAK2 molecule.

The crystal structures of individual JAK2 JH1 and JH2 domains of the wild type and V617F mutant have been solved (24, 31). The structure of the tandem kinase domain has not yet been reported which may reflect the flexibility and the complex allosteric interaction between JH1 and JH2. Conformational changes ranking from movements of the activation loop to large displacements of domains have been described for several kinases, such as Abl (32). This is the first study where the effect of the JH2 domain and the SH2-JH2 linker on kinetic parameters has been reported in a full kinetic analysis.

Consequences of changes in the affinity for ATP for inhibitor design

The presence of the JH2 domain reduces the affinity for ATP and for ADP-β-S. Interestingly, K_a for JH1JH2WT_513 is higher than K_a for JH1JH2V617F_536, but K_i values are exactly the same. This could point at a different binding mode for these compounds. The reduced affinity for ATP could indicate that inhibitors designed against the JH1 domain may be less effective in the presence of all regulatory domains of JAK2. This observation might, in addition to the effect of determining IC_{50} at very low ATP concentrations, explain the discrepancy between *in vitro* and *in vivo* efficacy of JAK inhibitors (33).

In conclusion, the present study provides detailed enzymatic and kinetic analysis of the JAK2 kinase function. JH1, JH1JH2WT_513, JH1JH2V617F_513 and JH1JH2V617F_536 follow a sequential random Bi-Bi reaction mechanism. Our studies confirm the hypothesized role for the SH2-JH2 linker in reducing the activity of JH1JH2WT_513 but also indicate that this linker affects ATP binding. This study also introduces methodologies that can be implemented to screen for compounds that target JAK2 outside the tyrosine kinase domain.

Acknowledgements

The authors thank Paula Kosonen and Merja Lehtinen for excellent technical assistance. This study was supported by the Sigrid Juselius Foundation, the Medical Research Council of Academy of Finland, the EU Research Training Network ReceptEur, the Finnish Cancer Foundation, Medical Research Fund of Tampere University Hospital, Tampere Tuberculosis Foundation.

References

1. Saharinen P, Takaluoma K, Silvennoinen O. Regulation of the Jak2 tyrosine kinase by its pseudokinase domain. Mol Cell Biol. 2000;20(10):3387-95.

2. Saharinen P, Vihinen M, Silvennoinen O. Autoinhibition of Jak2 tyrosine kinase is dependent on specific regions in its pseudokinase domain. Mol Biol Cell. 2003;14(4):1448-59.

3. Ungureanu D, Wu J, Pekkala T, Niranjan Y, Young C, Jensen ON, et al. The pseudokinase domain of JAK2 is a dual-specificity protein kinase that negatively regulates cytokine signaling. Nature structural & molecular biology. 2011;18(9):971-6.

4. Baxter EJ, Scott LM, Campbell PJ, East C, Fourouclas N, Swanton S, et al. Acquired mutation of the tyrosine kinase JAK2 in human myeloproliferative disorders. The Lancet. 2005;365(9464):1054-61.

5. James C, Ugo V, Le Couédic J, Staerk J, Delhommeau F, Lacout C, et al. A unique clonal JAK2 mutation leading to constitutive signalling causes polycythaemia vera. Nature. 2005;434(7037):1144-8.

6. Kralovics R, Passamonti F, Buser AS, Teo S, Tiedt R, Passweg JR, et al. A gain-of-function mutation of JAK2 in myeloproliferative disorders. N Engl J Med. 2005;352(17):1779-90.

7. Levine RL, Wadleigh M, Cools J, Ebert BL, Wernig G, Huntly BJ, et al. Activating mutation in the tyrosine kinase JAK2 in polycythemia vera, essential thrombocythemia, and myeloid metaplasia with myelofibrosis. Cancer cell. 2005;7(4):387-97.

8. Spivak JL, Barosi G, Tognoni G, Barbui T, Finazzi G, Marchioli R, et al. Chronic myeloproliferative disorders. ASH Education Program Book. 2003;2003(1):200-24.

9. Sanz A, Ungureanu D, Pekkala T, Ruijtenbeek R, Touw IP, Hilhorst R, et al. Analysis of Jak2 catalytic function by peptide microarrays: The role of the JH2 domain and V617F mutation. PloS one. 2011;6(4):e18522.

10. Hilhorst R, Houkes L, van den Berg A, Ruijtenbeek R. Peptide microarrays for detailed, high-throughput substrate identification, kinetic characterization, and inhibition studies on protein kinase A. Anal Biochem. 2009;387(2):150-61.

11. Segel I. Steady-state kinetics of multireactant enzymes. Enzyme kinetics. 1975:505-15.

12. Trauger JW, Lin F, Turner MS, Stephens J, LoGrasso PV. Kinetic mechanism for human rho-kinase II (ROCK-II). Biochemistry (N Y). 2002;41(28):8948-53.

13. Whitehouse S, Feramisco J, Casnellie J, Krebs E, Walsh D. Studies on the kinetic mechanism of the catalytic subunit of the cAMP-dependent protein kinase. J Biol Chem. 1983;258(6):3693-701.

14. LoGrasso PV, Frantz B, Rolando AM, O'Keefe SJ, Hermes JD, O'Neill EA. Kinetic mechanism for p38 MAP kinase. Biochemistry (N Y). 1997;36(34):10422-7.

15. Keshwani MM, Harris TK. Kinetic mechanism of fully activated S6K1 protein kinase. J Biol Chem. 2008;283(18):11972-80.

16. Chène P. Challenges in design of biochemical assays for the identification of small molecules to target multiple conformations of protein kinases. Drug Discov Today. 2008;13(11):522-9.

17. Parast CV, Mroczkowski B, Pinko C, Misialek S, Khambatta G, Appelt K. Characterization and kinetic mechanism of catalytic domain of human vascular endothelial growth factor receptor-2 tyrosine kinase (VEGFR2 TK), a key enzyme in angiogenesis. Biochemistry (N Y). 1998;37(47):16788-801.

18. Erdmann D, Allard B, Bohn J, De Pover A, Floersheimer A, Fontana P, et al. Kinetic study of human full-length wild-type JAK2 and V617F mutant proteins. Open Enzyme Inhibition Journal. 2008;1:80-4.

19. Hall T, Emmons TL, Chrencik JE, Gormley JA, Weinberg RA, Leone JW, et al. Expression, purification, characterization and crystallization of non-and phosphorylated states of JAK2 and JAK3 kinase domain. Protein Expr Purif. 2010;69(1):54-63.

20. Hedvat M, Huszar D, Herrmann A, Gozgit JM, Schroeder A, Sheehy A, et al. The JAK2 inhibitor AZD1480 potently blocks Stat3 signaling and oncogenesis in solid tumors. Cancer cell. 2009;16(6):487-97.

21. Zhao L, Ma Y, Seemann J, Huang L. A regulating role of the JAK2 FERM domain in hyperactivation of JAK2 (V617F). Biochem J. 2010;426:91-8.

22. Kaushansky K. On the molecular origins of the chronic myeloproliferative disorders: It all makes sense. Blood. 2005;105(11):4187-90.

23. Lee T, Ma W, Zhang X, Giles F, Kantarjian H, Albitar M. Mechanisms of constitutive activation of janus kinase 2-V617F revealed at the atomic level through molecular dynamics simulations. Cancer. 2009;115(8):1692-700.

24. Bandaranayake RM, Ungureanu D, Shan Y, Shaw DE, Silvennoinen O, Hubbard SR. Crystal structures of the JAK2 pseudokinase domain and the pathogenic mutant V617F. Nature structural & molecular biology. 2012.

25. Gnanasambandan K, Magis A, Sayeski PP. The constitutive activation of Jak2-V617F is mediated by a π stacking mechanism involving phenylalanines 595 and 617. Biochemistry (N Y). 2010;49(46):9972-84.

26. Dusa A, Mouton C, Pecquet C, Herman M, Constantinescu SN. JAK2 V617F constitutive activation requires JH2 residue F595: A pseudokinase domain target for specific inhibitors. PLoS One. 2010;5(6):e11157.

27. Wan X, Ma Y, McClendon CL, Huang LJ, Huang N. Ab initio modeling and experimental assessment of janus kinase 2 (JAK2) kinase-pseudokinase complex structure. PLoS computational biology. 2013;9(4):e1003022.

28. Zhao L, Dong H, Zhang CC, Kinch L, Osawa M, Iacovino M, et al. A JAK2 interdomain linker relays epo receptor engagement signals to kinase activation. J Biol Chem. 2009;284(39):26988-98.

29. Scott LM, Tong W, Levine RL, Scott MA, Beer PA, Stratton MR, et al. JAK2 exon 12 mutations in polycythemia vera and idiopathic erythrocytosis. N Engl J Med. 2007;356(5):459-68.

30. Toms AV, Deshpande A, McNally R, Jeong Y, Rogers JM, Kim CU, et al. Structure of a pseudokinase-domain switch that controls oncogenic activation of jak kinases. Nature structural & molecular biology. 2013;20(10):1221-3.

31. Lucet IS, Fantino E, Styles M, Bamert R, Patel O, Broughton SE, et al. The structural basis of janus kinase 2 inhibition by a potent and specific pan-janus kinase inhibitor. Blood. 2006;107(1):176-83.

32. Hantschel O. Structure, regulation, signaling, and targeting of abl kinases in cancer. Genes & cancer. 2012;3(5-6):436-46.

33. Yu V, Pistillo J, Archibeque I, Han Lee J, Sun B, Schenkel LB, et al. Differential selectivity of JAK2 inhibitors in enzymatic and cellular settings. Exp Hematol. 2013.

Legend to supplementary figures

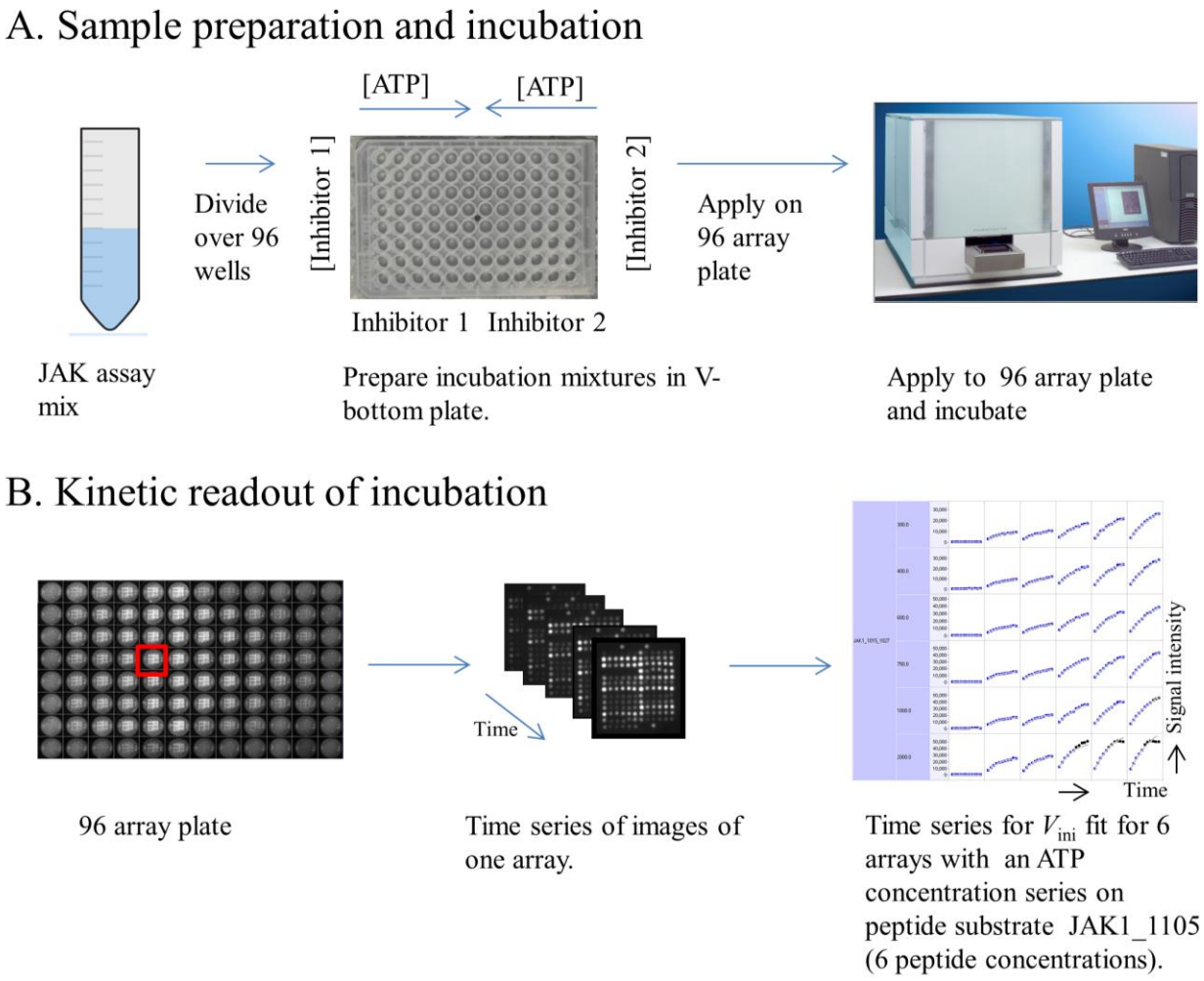

Figure S1: Schematic representation of assay setup

A: Sample preparation and incubation – Prior to incubation with protein kinases, arrays were blocked with 2% BSA (w/v),) in water for 30 cycles and washed three times with PK assay buffer (50 mM Tris–HCl (pH-7.5), 10 mM $MgCl_2$, 1 mM EGTA, 2 mM DTT, and 0.01% Brij-35). JAK2 proteins with kinase assay buffer (Protein Kinase buffer, JAK proteins at indicated concentration, 0.01 % w/v BSA, 12.5 µg/ml fluorescein-labelled PY20 antibody, 0.5 % DMSO) with varying

[ATP] and [Inhibitor] concentrations were pipetted onto the 96 arrays and incubated. B: The kinase reactions were performed for 60 cycles of pumping up and down through the pores of the microarrays at a rate of 2 cycles per minute. Arrays were imaged every minute by an integrated CCD-based optical system. The signal intensity as a function of time was used to calculate the initial rate of reaction. C. To eliminate differences between 96 array plates, data of each 96 array plate were normalized to the mean of the peptides at 1000 µM concentration in the absence of inhibitor. The resulting normalized initial reaction rates were used as input for kinetic analysis.

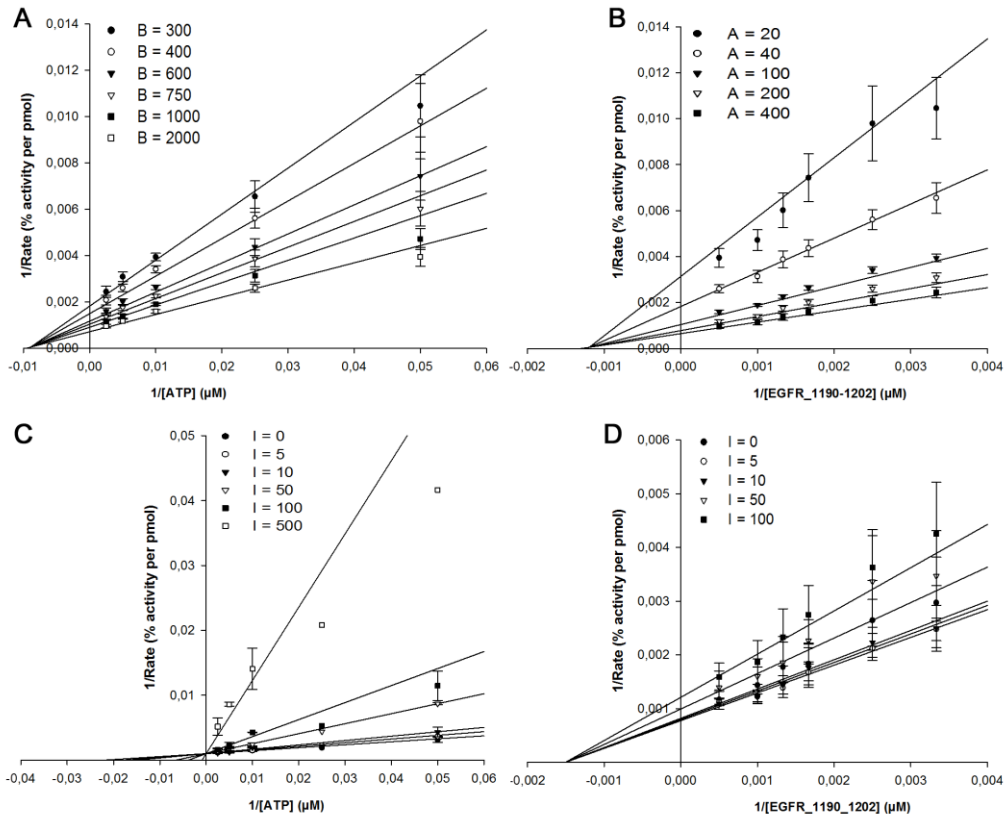

Figure S2: Two substrate steady state kinetics and inhibition by ADP-β-S for JH1JH2V617F_513

Double reciprocal plots of initial reaction rates of JH1JH2V617F_513 as function of [ATP] with varying [EGFR_1190–1202] concentration (A) or as a function of [EGFR_1190–1202] with different ATP concentrations (B); ATP or peptide concentrations are indicated by 'A' or 'B' in the legend. Double reciprocal plots with variation of ATP at [EGFR_1190–1202] = 2000 µM (C) or variable [EGFR_1190–1202] concentrations at [ATP] = 100 µM (D). The [ADP-β-S] concentrations are indicated by 'I' as µM.

Table S1

Kinetic parameters extrapolated to infinite concentration of either substrate for four JAK2 constructs and seven peptide substrates. For comparison, all 10 peptides are shown.
K_a and K_b are expressed in µM, V_{max} in % relative activity per pmol protein

	JAK2JH1				JAK2JH1JH2WT_513				JAK2JH1JH2V617F_513				JAK2JH1JH2V617F_536			
Peptide Identity	**K_a ± SD**	**K_b ± SD**	**V_{max} ± SD**	**Alpha value**	**K_a ± SD**	**K_b ± SD**	**V_{max} ± SD**	**Alpha value**	**K_a ± SD**	**K_b ± SD**	**V_{max} ± SD**	**Alpha value**	**K_a ± SD**	**K_b ± SD**	**V_{max} ± SD**	**Alpha value**
EGFR_1190-1202	17 ± 3	365 ± 75	8489 ± 566	1.5 ± 0.8	60 ± 18	474 ± 109	567 ± 46	2.3 ± 1,4	101 ± 33	752 ± 194	1930 ± 227	1.11 ± 0.7	36 ± 5	287 ± 35	988 ± 33	3 ± 1
JAK1_1015-1027	13 ± 4	686 ± 130	6977 ± 559	2.2 ± 1.2	35 ± 18	1541 ± 262	659 ± 63	3.16 ± 2.1	79 ± 42	2413 ± 594	2463 ± 401	1.3 ± 1	14 ± 6	681 ± 70	1040 ± 43	8.6 ± 4.6
JAK2_563-577	24 ± 9	1276 ± 323	3988 ± 552	1.6 ± 0.8	78 ± 20	1200 ± 195	200 ± 20	0.81 ± 0.3	103 ± 55	2367 ± 718	997 ± 202	0.7 ± 0.6	62 ± 13	966 ± 125	597 ± 38	1.4 ± 0.5
EGFR_1103-1115	18 ± 14	979 ± 421	1359 ± 269	3.6 ± 4.3	156 ± 125	3830 ± 1876	100 ± 37	0.57 ± 0.6	124 ± 75	2559 ± 921	264 ± 65	0.71 ± 0.6	48 ± 60	2903 ± 1175	203 ± 56	2 ± 3.2
ERBB2_1241-1253	13.3 ± 3	623 ± 105	8209 ± 585	1.1 ± 0.5	75 ± 17	619 ± 107	491 ± 35	1.32 ± 0.6	86 ± 25	944 ± 185	1908 ± 183	1.31 ± 0.7	38 ± 11	406 ± 76	993 ± 61	3 ± 1.6
INSR_992-1004	14 ± 6	1118 ± 249	4506 ± 521	1.7 ± 1.1	79 ± 36	2216 ± 539	298 ± 47	1 ± 0.7	88 ± 33	2461 ± 523	1038 ± 149	0.8 ± 0.5	54 ± 20	1927 ± 297	846 ± 81	1.7 ± 0.9
PGFRB_1014-1028	12 ± 3	579 ± 103	7628 ± 553	1.4 ± 0.8	75 ± 19	621 ± 124	493 ± 42	1.1 ± 0.6	117 ± 38	1375 ± 320	2403 ± 1766	0.6 ± 0.4	29 ± 5	304 ± 40	987 ± 36	4.2 ± 1.6
RON_1346-1358	18.3 ± 5	392 ± 94	6253 ± 495	1.9 ± 1.1	53 ± 20	1115 ± 201	651 ± 60	2.3 ± 1.3	156 ± 62	764 ± 282	1499 ± 269	0.4 ± 0.5	30 ± 5	504 ± 45	1061 ± 34	4.3 ± 1.2
RON_1353-1365	15 ± 6	901 ± 223	9576 ± 1110	2.4 ± 1.7	79 ± 26	1407 ± 265	647 ± 69	1.2 ± 0.7	88 ± 26	1315 ± 248	1966 ± 206	1.1 ± 0.6	48 ± 9	833 ± 82	1129 ± 52	2 ± 0.6
STAT5A_687-699	14 ± 5	833 ± 160	6372 ± 536	3.6 ± 2.1	93 ± 33	2143 ± 427	448 ± 58	0.9 ± 0.5	135 ± 66	1706 ± 567	1531 ± 3121	0.7 ± 0.6	57 ± 13	1202 ± 146	892 ± 57	1.6 ± 0.6

Table S2

Peptide Identity	Sequence	Tyrosine	UniProt Accession	Description
EGFR_1103-1115	GSVQNPV**Y**HNQPL	[1110]	P00533	Epidermal growth factor receptor
EGFR_1190-1202	STAENAE**Y**LRVAP	[1197]	P00533	Epidermal growth factor receptor
ERBB2_1241-1253	PTAENPE**Y**LGLDV	[1248]	P04626	Receptor tyrosine-protein kinase erbB-2
INSR_992-1004	**Y**ASSNPE**Y**LSASD	[992, 999]	P06213	Insulin receptor
JAK1_1015-1027	AIETDKE**Y**Y**Y**TVKD	[1022, 1023]	P23458	Tyrosine kinase JAK1
JAK2_563-577	VRREVGD**Y**GQLHETE	[570]	O60674	Tyrosine kinase JAK2
PGFRB_1014-1028	PNEGDND**Y**IIPLPDP	[1021]	P09619	Beta-type platelet-derived growth factor receptor
RON_1346-1358	SALLGDH**Y**VQLPA	[1353]	Q04912	Macrophage-stimulating protein receptor RON
RON_1353-1365	**Y**VQLPAT**Y**MNLGP	[1353, 1360]	Q04912	Macrophage-stimulating protein receptor RON
STAT5A_687-699	LAKAVDG**Y**VKPQI	[694]	P42229	Signal transducer and activator of transcription 5A

Peptide details: Peptide names, sequences, Uniprot identities and description for the peptides used in this study are shown. Peptide names are based on UniProt Knowledgebase (human proteins). Tyrosine residues involved in phosphorylation reactions are shown in bold.